"EFFECT OF POOR CURING CONDITIONS AND REMEDIES ON THE DURABILITY OF STEEL IN CONCRETE"

MAJID MALEKI-TOYSERKANI

Doctor of Philosophy

THE UNIVERSITY OF ASTON IN BIRMINGHAM

September 1987

THE UNIVERSITY OF ASTON IN BIRMINGHAM

"EFFECT OF POOR CURING CONDITIONS AND REMEDIES ON THE DURABILITY OF STEEL IN CONCRETE"

Majid MALEKI-TOYSERKANI Doctor of Philosophy 1987

SUMMARY

An investigation was undertaken to study the effect of poor curing simulating hot climatic conditions and remedies on the durabilty of steel in concrete. Three different curing environments were used i.e. (1) Saturated $Ca(OH)_2$ solution at 20^oC, (2) Saturated $Ca(OH)_2$ solution at 50^oC and (3) Air at 50^oC at 30% relative humidity. The third curing condition corresponding to the temperature and relative humidity typical of Middle Eastern Countries.

The nature of the hardened cement paste matrix, cured under the above conditions was studied by means of Mercury Intrusion Porosimetry for measuring pore size distribution. The results were represented as total pore volume and initial pore entry diameter. The Scanning Electron Microscope was used to look at morphological changes during hydration, which were compared to the Mercury Intrusion Porosimetry results. X-ray diffraction and Differential Thermal Analysis techniques were also employed for looking at any phase transformations.

Polymer impregnation was used to reduce the porosity of the hardened cement pastes, especially in the case of the poorly cured samples.

Carbonation rates of unimpregnated and impregnated cements were determined. Chloride diffusion studies were also undertaken to establish the effect of polymer impregnation and blending of the cements.

Finally the corrosion behaviour of embedded steel bars was determined by the technique of Linear Polarisation. The steel was embedded in both untreated and polymer impregnated hardened cement pastes placed in either a solution containing NaCl or an environmental cabinet which provided carbonation at 40^oC and 50% relative humidity.

KEY WORDS cements, porosity, polymer impregnation, carbonation, corrosion.

To my wife Sheila and my

beautiful daughter Sheiva

My Mother and Father

my sister Monier and brother Hamid

ACKNOWLEDGEMENT

I would like to thank Dr N R Short Lecturer in the Department of Civil Engineering and Consrtuction for his help, valuable guidance and excellent supervision throughout this work.

I would also like to thank Mr C J Thompson for his technical assistance.

Thanks are also due to my friends in the department of Civil Engineering and Construction for their continual encouragement, especially Dr G Sergi.

I also wish to thank all my friends who helped in any way they could.

I am deeply indebted to all the members of my family, especially my parents and my brother Hamid for their moral and financial support.

Finally, I would like to thank my wife Sheila for her excellent typing of this work and a very special thank you for her endless support, understanding and encouragement, which made all this possible.

LIST OF CONTENTS

LIST OF FIGURES

Figures in appendices

LIST OF TABLES

LIST OF APPENDICES

CHAPTER 1 INTRODUCTION AND LITERATURE SURVEY

1.1 INTRODUCTION

Reinforced and prestressed concrete structures are used widely and generally give satisfactory performance showing excellent durability in service (1). However, a small proportion of structures do undergo significant deterioration, the most common cause being corrosion of the embedded steel (2) which may result in cracking, spalling or in extreme cases loss of serviceability and structural integrity.

In good quality concrete, steel is normally passive as a result of the high alkalinity of the associated pore solution, which may have a pH value in excess of 13. Corrosion problems which do occur are as a result of depassivation of the embedded steel owing to either excessive carbonation of the concrete cover or the presence of an agressive environment, especially chloride ions which can promote corrosion even in highly alkaline conditions (3).

The presence of chloride ions in concrete may have been added as an original constituent of the mix e.g. admixtures containing calcium chloride, or as contaminants in the aggregate and mixing water. Alternatively they may result from exposure to marine environments or the use of deicing salts.

There are many reports (4-10) suggesting that concrete structures in hot arid environments tend to deteriorate more rapidly than those in temperate parts of the world. The reasons for this, in the first instance, are related to the climatic conditions. Solar radiation can lead to very high surface and air temperatures. Rapid daily temperature variations of 20-30^{o}C and relative humidity fluctuations of 70%, are not uncommon. Rapid evaporation of moisture may occur and is even more pronounced with increase in wind velocity. The effects of hot weather are most critical during periods of rising temperature and falling humidity.

These climatic conditions can have a pronounced effect on the mixing, placing and curing characteristics of fresh concrete and the properties of hardened concrete. Rapid evaporation of mixing water can lead to large and rapid slump loss causing a high water demand. Evaporation of moisture from the surface may be greater than internal moisture movement, leading to plastic shrinkage cracks and surface crazing. Increased drying shrinkage resulting from greater water demand and subsequent cooling from a high temperature at which the concrete hardens, both increase the cracking tendency of the concrete.

Concretes placed and cured at elevated temperatures normally develops higher early strengths than concrete produced and cured at normal temperatures, but later strengths are generally lower. The higher temperatures can give rise to more rapid hydration and accelerated setting with resultant lower strength due to the establishment of a less uniform framework of gel.

Admixtures such as retarders plus water reducers and superplasticizers are often used to offset some of these undesirable aspects, particularly in relation to the placing of concrete, but require careful control. Poor mixing, placing and curing of concrete giving rise to reduced strength, increased porosity and cracking leads to increased permeability and subsequent reduced durability of the concrete. Other factors often associated with these problems, include poor quality and contaminated aggregate, contaminated mixing water, variable cement quality and poor workmanship which aggravates the problem. Coatings on the reinforcement, inhibitors in the concrete, surface barrier coatings and polymer impregnation have been suggested to reduce the problem. However there is little information available on their use in hot weather environments.

This thesis covers various aspects of the effect of hot weather curing conditions on the durability of reinforced concrete.

1.2 Literature Survey

1.2.1 Effect of Time and Temperature on Workability

Freshly mixed concrete stiffens with time. Some water from the mix is absorbed by the aggregate, some is lost by evaporation, particularly if the concrete is exposed to sun or wind, and some is removed by the initial chemical reaction. The exact value of the loss in workability varies with the richness of the mix, the type of cement, the temperature of the concrete and the initial workability (11-15). Also workability depends on the moisture content of the aggregate, the loss in workability being greater with dry aggregate owing to the absorption of water, as would be expected. The workability of a mix is also affected by the ambient temperature; it is apparent that on a hot day the water content of the mix would have to be increased for a constant workability to be maintained. Up to a temperature of $40^{o}C$ and with a relative humidity within the range 20-70%, no effect of temperature on slump has been observed; only above $50^{o}C$ or with humidity lower than 20% does the slump fall off rapidly.

Moreover, it seems that the loss of slump in hot and dry air is greater than the decrease in ease of placing. There is therefore no corresponding large increase in the water requirement. These findings apply within 20 minutes of mixing, but over longer periods there is an unmistakable loss of slump, so that for instance, with a long haul of ready-mixed concrete, high temperature would increase the water requirement for a given workability.

Admixtures such as retarding, or water reducing and retarding, as recommended by A.C.I (II), have been found to be beneficial in offsetting some of the undesirable characteristics of concrete placed during periods of high temperatures. Admixtures may be used in varying proportions, so that, as temperature increases, higher dosages of the mixture may be used to obtain a uniform setting

time (16-18).

In order to obtain good concrete, the placing of an appropriate mix must be followed by curing in a suitable environment, especially at early ages. Good control of temperature and of moisture movement from and into the concrete is required (19-21). During curing the concrete should be kept saturated, or as nearly saturated as possible, until the original water filled space in the fresh cement paste has been filled to the desired extent by the products of hydration of cement. Hydration at a maximum rate can proceed only under conditions of saturation.

It must be stressed that for a satisfactory development of strength it is not necessary for all the cement to hydrate, and indeed this is rarely achieved in practice. The quality of concrete depends on the gel/space ratio of the paste. If however the water-filled space in fresh concrete is greater than the volume that can be filled by the products of hydration, greater hydration will lead to a higher strength and a lower permeability. Evaporation of water from concrete soon after placing depends on the air temperature, relative humidity and wind velocities.

The method of curing, depends on the site condition and the size, shape, and position of the concrete section. In the case of concrete sections with a small surface/volume ratio, curing may be aided by oiling and wetting the forms before casting, the forms may be wetted during hardening, and after stripping the concrete should be sprayed and wrapped with polythene sheets.

Large surfaces of concrete, such as road slabs, present a more serious problem. In order to prevent crazing of the surface on drying-out loss of water must be prevented even prior to setting. As the concrete at that time is mechanically weak, it is necessary to suspend a covering above the concrete. Once the concrete has set, wet curing can be provided by keeping the concrete in contact with a source of water. This may be achieved by spraying or flooding, or by covering the concrete with wet sand, earth, or periodically wetted hessian or cotton mats. Another means

of curing is to use an impermeable membrane or water proof paper.

The period of curing cannot be simply prescribed, but it is usual to specify a minimum of seven days for ordinary portland cement concrete. With slower hardening cements such as OPC/BFS a longer curing period is desirable (22).

It is clear that a rise in the curing temperature speeds up the chemical reaction of hydration and benefits the early strength of concrete.

However, later strengths from about 7 days onwards may well be adversely affected. The explanation is that a rapid initial hydration appears to form products of a poorer physical structure, probably more porous, so that a large proportion of the pores will always remain unfilled. It follows from the gel/space ratio rule that this will lead to a lower strength, compared with a less porous, through slowly hydrating paste in which a high gel/space ratio will eventually be reached. Verbeck and Helmuth (23) suggested that rapid rates of hydration produce a non-uniform distribution of products within the paste. The reason for this is that at high rates of hydration there is insufficient time available for the diffusion of the products of hydration away from the cement grains, for uniform precipitation in the interstitial space. As a result, a high concentration of the products of hydration is built up in the vicinity of the hydrating grains, and this retards subsequent hydration and adversely affects long-term strength. In addition, the non-uniform distribution of the products of hydration adversely effects the strength because the gel/space ratio in the interstices is lower than would be otherwise the case for an equal degree of hydration.

1.2.2 Durability of Concrete

It is essential that concrete should withstand the conditions for which it has been designed without deterioration, over a long period of time. Durability may be affected either by the environment to which the concrete is exposed or by causes

within the concrete itself. The external factors may be physical, chemical or mechanical. They may be due to weathering, occurrence of extreme temperature, abrasion, and attack by natural or industrial liquids and gases. The extent of damage mainly depends on the quality of the concrete especially its permeability (24). Internal causes are alkali-aggregate reaction and volume changes due to differences in thermal properties of aggregate and cement paste.

Penetration of concrete by materials in solution may adversely effect its durability e.g. when $Ca(OH)_2$ is leached out or an attack by an aggressive liquid takes place. This penetration depends on the permeability of the concrete (25).

The permeability of concrete is not a simple function of its porosity, but depends also on the size, size distribution, and continuity of the pores. Also in a mature paste, permeability depends on the size, shape, and concentration of the gel and on whether or not the capillaries have become discontinuous (26).

1.2.3 Carbonation

Carbonation is regarded as the neutralisation of a porous cementitious material by acidic gases such as CO_2, which diffuse into the structure. The action of CO_2 takes place even at small concentrations such as are present in rural air, when the CO_2 content is about 0.03% by volume. As carbon dioxide reacts with hydrated cement compounds in the presence of moisture, the greater the concentration of CO_2 the greater the rate of carbonation (27-30). In the presence of $Ca(OH)_2$, NaOH and KOH which are products of hydration, the pore solution may have pH values in excess of 13.5. The CO_2 will react with and decompose these compounds; i.e.

$$Ca(OH)_2 + CO_2 \longrightarrow CaCO_3 + H_2O$$

$$2KOH + CO_2 \longrightarrow K_2CO_3 + H_2O$$

$$2NaOH + CO_2 \longrightarrow Na_2CO_3 + H_2O$$

As carbonation proceeds, other products such as calcium silicates, aluminates and aluminoferrites are attacked resulting in the formation of calcium carbonate. Calcium carbonate may exist in three mineralogical forms, calcite, vaterite and sometimes aragonite as reported in the literature (31,32). Vaterite is the most unstable form of $CaCO_3$ and is the first product of carbonation especially if the cement or concrete is subjected to accelerated carbonation and it will eventually convert to a stable form of calcite (33).

Work by Kondo et al (34) showed that by carbonating mortar prisms through one surface only, some variation of the $CaCO_3$ modifications with increasing depth was observed. Since the carbonation had been relatively fresh at deeper parts of the specimens, the more amorphous vaterite was found. As the depth decreases i.e. nearer the surface, calcite was formed. They have also pointed out that hydrated C_3S tends to produce calcite, but the unhydrated form produces vaterite. As for physical aspects, the depth of carbonation depends upon the transport of CO_2 through the pores of cement. Good quality cement paste with very low porosity, or kept at very high relative humidity conditions reduces the carbonation reaction. For the carbonation reaction to carry on, the humidity within the pores must not be too high or too low e.g. (100%, 30%) see figure 1.1. (35). At a high relative humidity most pores are full of water and the diffusion of CO_2 into the paste becomes restricted, conversly, for a low relative humidity there is insufficient water in the pores for CO_2 to form carbonic acid. The rate of carbonation depends on the moisture content of the concrete or cement and the relative humidity of the ambient medium

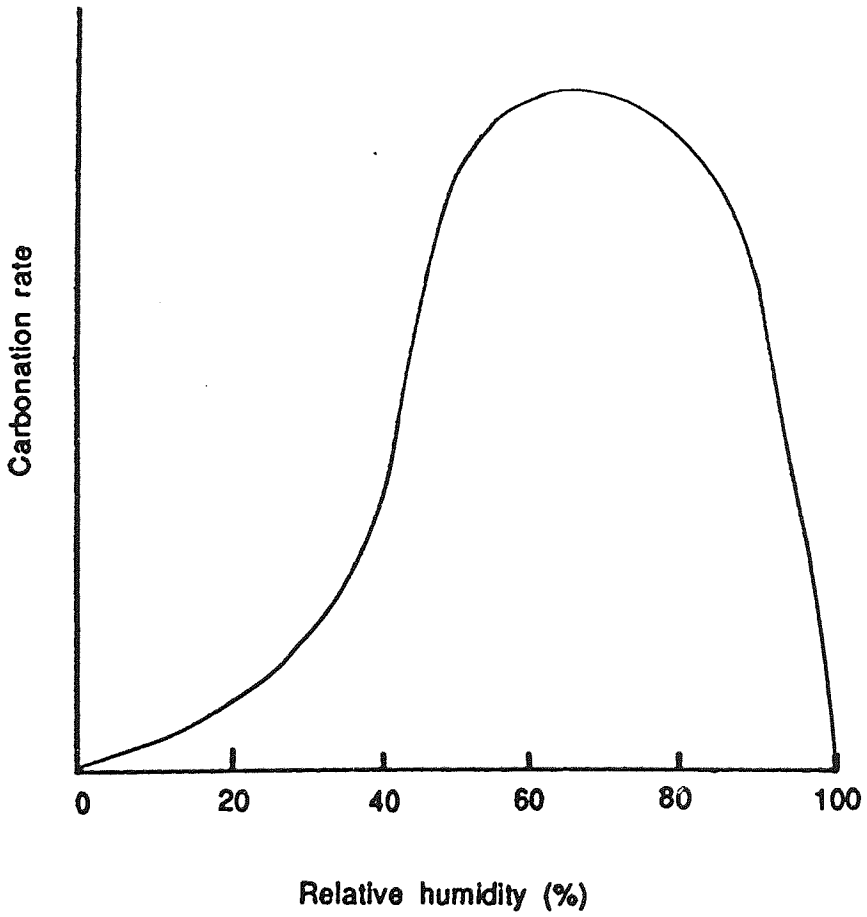

Figure 1.1 Rate of carbonation of hardened cement paste as a function of relative humidity (after Tuutti).

(27). There is an optimum for rapid carbonation at around 65%.

Carbonation of cement or concrete results in increasing strength (27,36), shrinkage increases, probably due to the dissolving of crystals of $Ca(OH)_2$ while under a compressive stress and depositing of $CaCO_3$ in spaces free from stress.

Powers (37), showed that at intermediate relative humidities shrinkage will accompany carbonation. His explanation of this was that partial drying of the cement paste causes a compressive stress on the calcium hydroxide crystals. Therefore in the pore solution as the dissolved $Ca(OH)_2$ carbonates, this leads to more dissolution of stressed crystals, which slowly releases the compressive stresses, followed by the deposition of $CaCO_3$ in stress free regions. The newly formed $CaCO_3$ will nucleate and grow in the pores so even though there will be an increase in mass, it would not necessarily prevent shrinkage. The calcium silicate hydrate gel, carbonates later by topochemical reaction therefore shrinkage would not occur.

Skalny and Bajza (38) showed that the real effect would then be a decrease in porosity leading to a more compact structure. Furthermore higher strength is obtained as a result of higher compaction.

Such a strength increase was observed by Manns and Weshe (39) for some carbonated cement pastes, but a decrease was found in others. There is a general agreement in published literature on the effect of carbonation on porosity (34,40,41) work by Rozental and Alekseev (40), with the aid of mercury intrusion porosimetry had shown that pores in the range of 0.01-1mm diameter in carbonated mortars of 0.5 and 0.6 water/cement ratios, had decreased by about half the volume.

Finally since carbonation results in a reduced pH value of the cement (27), it therefore has an undesirable influence on the protection of the embedded steel, in the presence of oxygen and moisture. The drop in pH will destroy the normally passivating medium and also the higher pH buffering capacity offered to steel by soluble phases such as $Ca(OH)_2$. This is therefore the most significant aspect of carbonation.

It is normal to explain the resistance of cement to carbonation in terms of the increase of the carbonation depth with time; e.g. according to Alexander (42) the rate of carbonation depends on the hydration of the concrete, on storage conditions (relative humidity chiefly) and compactness factors (water/cement ratio, cement content, compaction etc.).

Several formulae have been proposed by other researchers in this field for determining a constant for the rate of carbonation; e.g. Page (43) suggested that for a uniform concrete with the simple unidirectional diffusion of CO_2 into it can be shown that the rate of increase of the carbonation front if there is no variation of the diffusion coefficient D, with time t, or depth, x, would be:

$$\frac{dx}{dt} = \frac{DC}{Ax}$$

A, represents the quantity of alkaline substances reacting per unit volume of concrete, providing the temperature, relative humidity and CO_2 concentration, C, are constant.

On integration this yields a parabolic relationship,

$$x^2 = \frac{2DCt}{A}$$

$$\text{or } x = k\sqrt{t}$$

where k is a constant

Efes and Schubert (44) have found a similar relationship for the rate of carbonation of concrete cubes stored at 20°C in a 65% RH environment which were subjected to either air or 10% CO_2 and their formula was:

$$d_k = k_0 + v_k \sqrt{t}$$

where,

v_k : the rate of carbonation ($mm/day^{1/2}$)

k_0 : is a constant for a particular condition

t : is the time for carbonation (days)

d_k : is the depth of carbonation (mm)

For air cured samples typical values of v_k ranged from less than 1, for CO_2 cured prisms up to 8. As they observed higher water/cement ratios of the original mix meant higher carbonation rates. Mayer (36) had observed a similar relationship for the carbonation of the mortars after an induction period where carbonation appeared to commence a certain time after exposure. His comment was that for long carbonation times, such an induction period is negligible.

Alekseev and Rozental (45) in similar experiments also showed that the relationship between carbonation depth and the square root of time under natural

conditions was linear for short term studies. They also found deviations between the rates for longer as opposed to shorter periods of exposure, which they explained by the following reasons.

1) A continuing hydration of cement resulting in a higher density concrete and a reduction on CO_2 penetration.

2) A reduction of concrete permeability with an increasing carbonation layer.

3) A counter diffusion of $Ca(OH)_2$ so that when the flow of $Ca(OH)_2$ gets close in its magnitude to the CO_2 flow, displacement of the chemical reaction zone slows down or stops altogether. Smolczyk (31,46) worked on a long term study on the rate of carbonation where his aim was to produce a formula which could predict carbonation rates of most types of concrete. His work involved the statistical calculation of 16 cements, 3 water/cement ratios for 8 years of carbonation.

The outcome were two formulae with correlation coefficients of 0.97. They were of the general form.

$$x = a\left(\frac{w/c}{\sqrt{N_T}} - b\right)\sqrt{t}$$

x : depth of carbonation

t : time of carbonation

w/c : water/cement ratio of the concrete

a & b : constants which depend on carbonation conditions

N_T : is the compresive strength of the cement at T days

At first approximation, T is the age of the concrete when the carbonation began i.e. 7

days. For times greater than 7 days, T was not taken as a constant value in order to take into account the influence of later hardening of the cement. It appeared that the reference time T is a very slightly increasing function of the carbonation time t. He assumed the value T to increase at the rate of 1 day per year. To support the above formula theoretically he turned to Verbeck and Helmuth (47) who showed that compressive strength is inversely proportional to its capillary porosity. Mills (48) also showed that there is an increase in capillary porosity with increasing CaO/SiO_2 ratio at constant strength so Smolczyk developed the expression:

$$\text{strength} = \frac{f'(CaO)}{f''(\text{Capillary porosity})}$$

From

$$\text{carbonation} \simeq \sqrt{\frac{f'(\text{capillary porosity})}{f''(CaO)}}$$

he arrived at,

$$\text{carbonation} \simeq \frac{1}{\sqrt{\text{strength}}}$$

Mayer (36) and Hamada (49) in their experiments looked at the BFS or Pozzolanic addition on the rate of carbonation of cements.

Mayer had illustrated that slag cements containing varying amounts of BFS had carbonated faster as the amount of BFS was increased. As already shown,

$$\text{carbonation} \simeq \frac{1}{\sqrt{f(CaO)}}$$

So the carbonation rate increases with the decreasing CaO content of the slag cements.

1.2.4 Penetration of Chlorides

Transport phenomena in a hardened cement paste are very important not only to its hydration and durability but also in applications such as the use of cementitious materials in the isolation of hazardous waste materials.Regarding the durability of concrete especially corrosion of steel by carbonation or contamination from Cl^- ion have become serious problems. The Cl^- diffusion in a given cement may be influenced by many factors and is affected by many properties, such as chemical composition of cement, pore size distribution, texture, species of codiffusing ion, concentration and temperature (50-55).

When sufficient amounts of Cl^- ion reach the surface of steel embedded in cement or concrete, depassivation of the steel may occur, normally in the form of pitting, (56,57). There is also evidence that pitting is related to the ratio $[Cl^-]/[OH^-]$ and not simply on the Cl^- level (58). The levels of free chloride and hydroxyl ions in the pore solution are governed by several factors. The concentration of hydroxyl ions would be expected to increase with the alkalinity of the cement, although several processes have been suggested which may tend to reduce particularly high alkalinities (59). There is considerable evidence that C_3A content of the cement is important since it is known that C_3A may form an insoluble complex, calcium chloroaluminate hydrate (Friedel's salt) thus reducing the concentration of chloride in the pore solution (60,61). The presence of sulphate ions may result in liberation of Cl^- owing to preferential formation of calcium sulpho-aluminate of hydrates (62). Other factors such as temperature, crystallographic form of C_3A and the decomposition of calcium chloroaluminate hydrate by carbonation may also be important in determining the extent of chloride complexation. Furthermore, it has been suggested that chloride, present on mixing is complexed to a greater extent than chloride penetrating hardened concrete from an external environment (63).

This process by which chloride ions penetrate the structure from the external source is normally one of diffusion. The passivity of the embedded steel is only affected provided the chloride ions are moving freely around the interface between the steel and cement and concrete (64). Provided this process of Cl^- ions migration is diffusion controlled, it is therefore possible to say that for a given temperature, the mobility of the Cl^- ions in cement or concrete is directly proportional to the diffusion coefficient (65) as stated by the Nernst - Einstein relationship

$$D = UKT$$

where,

D = the coefficient of diffusion

U = the mobility of the ions

K = the Boltzmann constant

T = the temperature

so calculated values of the diffusion coefficient D, would be representative of the Cl^- ions mobilities. Fick in the middle of the last century developed the laws of diffusion to allow the determination of diffusion kinetics from measurable quantities.

Fick's first law states that the flux is proportional to the concentration gradient, the diffusion coefficient D, being the constant of proportionality in the relationship

$$J = -D \frac{dc}{dx}$$

where,

J = Flux or diffusion current density - the amount of material diffusing in a unit time per unit area perpendicular to the x-axis

D = Diffusion Coefficient

c = Volume concentration

x = Distance along direction of diffusion under steady-state conditions

As the units of flux are mass over area by time and those of concentration are mass over volume then the diffusion coefficient has units of area over time and may be expressed in terms of square centimetres per second (66).

There are mainly two different methods to determine the diffusion kinetics of chlorides in cement successfully (67). One was that used by Page et al (68) and was applied on fault free cement paste cylinders. After an initial curing of 60 days in lime water such cylinders were cut into discs of around 3 millimeters in thickness from the centre portions of the cylinders with a diamond saw. In a specially designed glass cell the discs were then exposed to chloride solution. This glass cell consists of two compartments with the cement discs fitted in between. Both compartments were filled with saturated calcium hydroxide solution while in one of the compartments one molar sodium chloride was also added. The effective diffusion coefficients were then determined from the measuring of the level of chloride ion in the low concentration side solution with time. This was possible by using Flick's first law as applied to quasi - steady - state diffusion.

From the slope of the rectilinear plot of the chloride ion concentration in the low side against time the value of D was calculated. The technique is described in detail in chapter 2 section (2.6). Similar work has been carried out (53,69,70) on a number of ionic species such as (D_{Cl^-}, D_{K^+}, D_{Na^+}, D_{Li^+},) to determine the effective diffusion coefficients and all were in the order of 10^{-7} -10^{-8} cm^2 s^{-1}.

Takagi et al (53) used the same method on different cements to measure diffusion coefficients for Na^+ and I^-. They suggested that because of the existence of the electric double layer the cation diffused slower than the anion. This they claimed

was caused by the adsorption of Ca^{++} ions on the surface of cement hydrates which become positively charged (71).

The anions are then attracted towards the surface enabling them to enter the micro-pores and hence diffuse easier, whereas the repelled cations are reluctant to do so.

Collepardi et al (72-74) used an alternative technique for measuring effective diffusivities. After exposing the end faces of cement cylinders, cast under vacuum to eliminate air bubbles, to 3% calcium chloride solution (74) the specimens were sliced into discs at increasing depths which were then subjected to specific chemical analysis to determine the total chloride ion concentration. A solution to Fick's 2nd law was then applied to steady-state condition for a semi-infinite solid to determine the value of D.

$$Cx = Cs \left[1 - \operatorname{erf} \frac{x}{2\sqrt{Dt}} \right]$$

for the boundary conditions

$$Cx = 0 \text{ at } t = 0$$

$$0 < x < \infty$$

$$Cx = Cs \text{ at } x = 0$$

$$0 < t < \infty$$

where,

Cx = chloride ion concentration of slice (M cm^{-3})

Cs = chloride ion concentration of external solution (M cm^{-3})

x = thickness of disc (cm)

t = time of exposure (sec.)

D = diffusion coefficient (cm^2 s^{-1})

Diffusion coefficients for chloride ions did not depend on the concentration of the

solution and were in the range of 10^{-8} cm^2 s^{-1}.

Spinks et al had used this method even earlier 1952 (75) by using solutions labelled with radioactive isotopes (^{45}Ca, ^{35}S, ^{131}I or ^{22}Na). After exposing the one side of cylindrical OPC pastes for a length of time. They measured the radiation at different depths of the pastes and translated their readings into concentration of the particular ion under investigation. They used the above solution to Fick's second law of diffusion into a semi-infinite solid, so they were able to calculate diffusion coefficients for each of the ions, which ranged in the order of 10^{-11} to 10^{-9} cm^2s^{-1}.

1.2.5 Corrosion as an Electrochemical Process

Corrosion is an electrochemical process. In other words, it is a chemical reaction involving the transfer of charge (electrons) from one species to another (56,76). Exposed steel will corrode in moist atmospheres due to differences in the electrical potential on the steel surface forming anodic and cathodic sites. The metal oxidises at the anode where corrosion occurs according to

$$Fe\ (metal) \rightleftharpoons Fe^{2+}(aq.) + 2e^- \qquad (1)$$

At the cathodic site the excess free electrons in the metal are consumed reducing dissolved oxygen to form OH^- ions or by liberation of hydrogen gas according to:

$$^1/_2\ O_2 + H_2O + 2e^- \rightleftharpoons 2OH^-\ (aq.) \qquad (2)$$

$$2H^+\ (aq.) + 2e^- \rightleftharpoons H_2\ (gas) \qquad (3)$$

The electrons produced during this process are conducted through the metal whilst the ions formed are transported via the electrolyte (77).

In non-acidic environments the oxygen reduction reaction predominates so the overall reaction is:

$$Fe + H_2O + {}^1/_2\, O_2 \longrightarrow Fe^{++} + 2(OH^-) \longrightarrow Fe(OH)_2$$

Ferrous hydroxide

In neutral solution, ferrous hydroxide is unstable and combines further with oxygen by the reaction:

$$2\, Fe^{2+} + 4OH^- + {}^1/_2\, O_2 \longrightarrow 2Fe\ 0.0H + H_2O$$

Brown deposit (rust)

Normally the presence of the hydroxides of sodium, potassium and calcium in good quality concrete provide an alkaline environment to the iron (78). This high degree of alkalinity is normally sufficient to induce passivation of embedded steel (79-81).

The bulk of surrounding concrete acts as a physical barrier to many of the steel's aggressors. Corrosion problems that arise in concrete structures are therefore associated with conditions leading to depassivation of the embedded steel and these circumstances are commonly brought about either by excessive carbonation of the concrete or by the presence of chlorides (82).

The transformation of the protective alkaline pore solution in concrete to a corrosive condition may be caused by reaction with acidic substances i.e. (CO_2) or depassivating anions such as chloride, as is illustrated by the Pourbaix diagrams (83) figures 1.2 and 1.3.

Until recently, corrosion of steel in concrete was most frequently studied by exposing samples to known environments for long peroids of time, then removing the concrete cover and either weighing or measuring the steel to determine the amount of material corroded. Such experiments take many years to complete and are, obviously destructive in nature. It is generally only used as a source of secondary information when the main sequence of corrosion monitoring has been completed.

As an alternative electrochemical techniques have come to be used in the study of reinforcing steel, particular the linear polarization technique. This method is quick and easy to carry out, and non-destructive in nature (84-86). Andrade and Gonzalez (87) have shown a good correlation in the determination of corrosion rates between gravimetric weight loss measurements and the linear polarization technique.

The other method which is widely used due to gain quickness in testing and is non-destructive in nature is Rest Potentials which can be measured instantaneously without the need to know the area of the steel electrode (88). It is the most simple to carry out, the only equipment required being a reference electrode and a high impedance voltmeter.

The main disadvantage of potential measurements is that they only indicate the balance between the anodic and cathodic area of the steel and cannot be used to determine actual corrosion rates.

For this work however linear polarisation technique was used and is described in detail in Chapter 2, section 2.7.1.

1.2.6 Protection

To protect concrete from chemical or general external attack such as carbonation or penetration of chloride ions a number of protective methods have been suggested and assessed (79).

Polymer Impregnation, which involves impregnating concrete with a liquid monomer, and subsequently polymerising by thermal means results in filling or partial filling of the pores. Such a process improves the structural and durability properties of cement or concrete . As a result of these superior properties, Polymer Impregnated Concrete (PIC) has been considered for applications requiring high strength (89 , low permeability and water absorption, (90) the reduction in diffusion of CO_2, and Cl^- (91) and subsequently increasing the corrosion resistance (92). Application uses of PIC in bridge decks structural elements, and pipes have been examined. Unfortunately, the impregnation process is complex and the costs of monomers are very high. Therefore, most current uses are in applications where the gain in service life is believed to compensate for the high cost.

Other methods, like surface coating of concrete have been applied in order to reduce diffusion of oxygen and chloride ions to the metal surface (93-95). The coatings should be alkali resistant, able to cure at low temperatures and cover damp surfaces. A wide range of coatings including paints, asphalts, coal tar, linseed oil, epoxy and bituminous systems have been tried with variable success. They may however do more harm than good since they have a tendency to maintain high moisture contents within the concrete. Reinforced vinyl - elastomers and PVC membranes have gained some acceptance for protecting foundations, repairing walls, banks and pipes (96). Cathodic protection has been applied successfully in

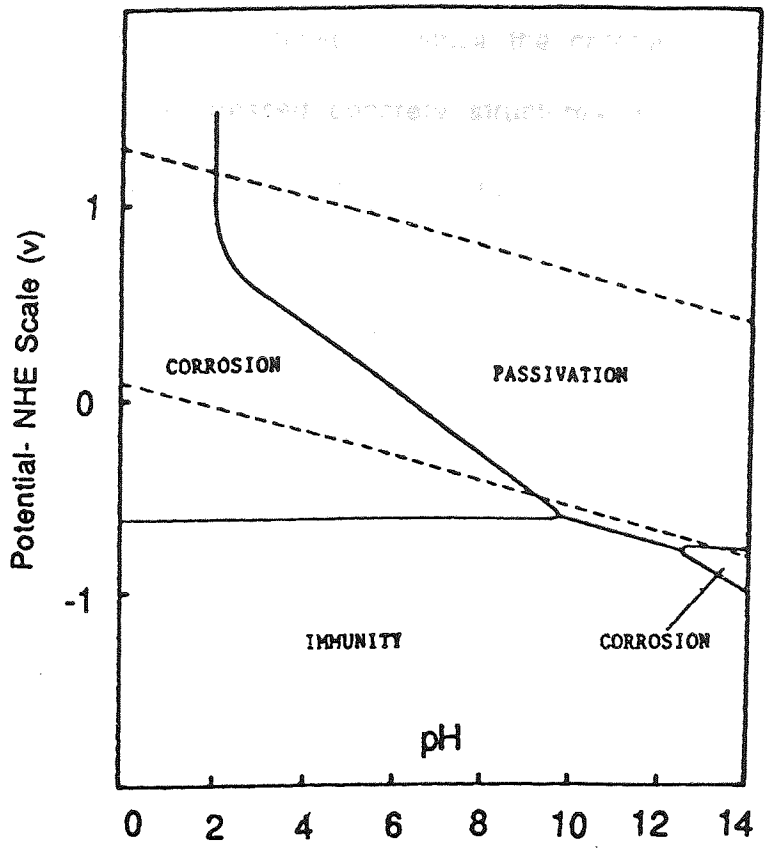

Figure 1.2 A simplified form of the Pourbaix diagram for Iron.

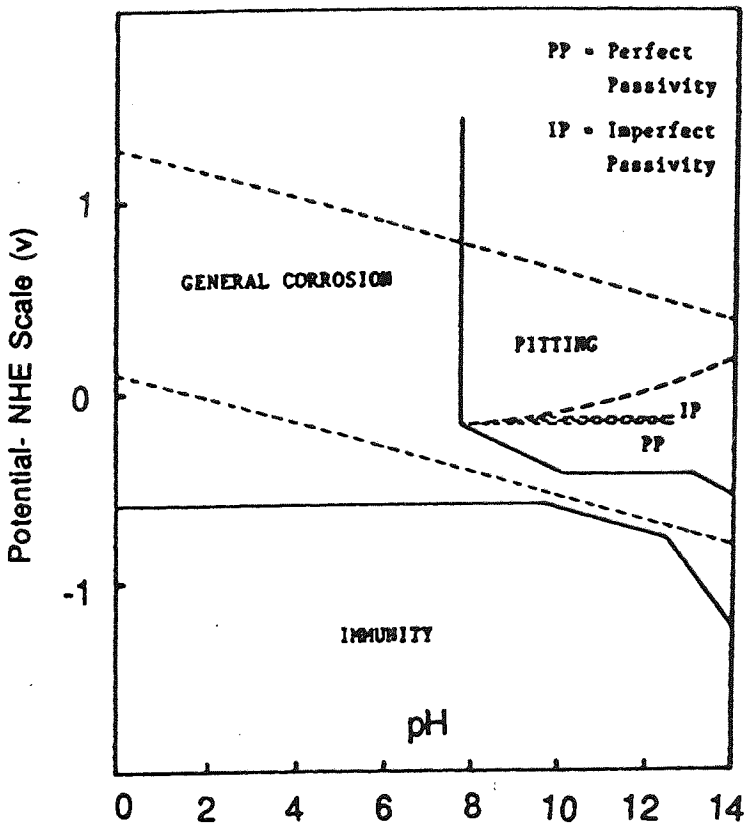

Figure 1.3 Plot of potential against pH for Iron in a rapidly stirred 1 M NaCl solution

some cases (97). Care is required, however, since the criteria for cathodic protection of reinforced and prestressed concrete structures are different to comparable steel structures. The main problem from a practical point of veiw is obtaining a close control of potential and current densities over the entire reinforcements.

Anodic inhibitors such as chromates, nitrites and benzoates have been found to be effective (98,99). They are, however, only effective in high concentrations otherwise corrosion may be intensified locally. Conversely high concentrations may adversly affect the properties of the concrete. Mixtures of nitrite and benzoate seem to offer best solution, although more complete and fundamental investigations are needed.

The most widely used forms of protection include organic and inorganic coating over the reinforcement themselves. Varieties of non-metallic coatings have been applied to reinforcing steel including dense cement mortar, asphalt, chlorinated rubber, vinyl and epoxy systems (100,101). These are barrier coatings in that they keep corrosive agents away from the steel. However, this gives rise to possible accelerated local corrosion at breaks in the coating. Metal coatings which have been investigated for use as protective coatings on steel reinforcement include Zn, Cd, Ni, Sn, Pb, Cu (101,102).

1.3 Aims Of The Project

An investigation was undertaken to elucidate relevant factors affecting the durability of steel in concrete subjected to poor curing conditions, which for example, may be found in hot climates.

Studies were carried out in order to investigate the effect of poor curing conditions on the following;

1. Microstructure, mineralogy, pore size distribution, in relation to durabilities.
2. The rate of carbonation.
3. Chloride penetration through cement paste.
4. Electrochemical behaviour of mild steel embedded in cement paste.
5. To investigate the introduction of Polymer Impregnation of concrete as a means of resolving the above mentioned poor curing.

1.4 Plan of Presentation

After an introduction to the work, in Chapter 1 the relevant literature is reviewed on the topics of Durability, Carbonation, Penetration of chlorides, Corrosion and Protection of cement pastes. This is followed by a description of the scope of this research.

The materials used were Ordinary Portland Cement (OPC), Sulphate Resisting Portland Cement (SRPC), Ordinary Portland Cement/Blast Furnace Slag (OPC/BFS) and Ordinary Portland Cement/Pulverised Fuel Ash (OPC/PFA) these, together with

Chapter 3 describes the effect of curing conditions on porosity and pore size distribution and measurements of total pore volume by both Mercury Intrusion Porosimetry (MIP) and Pycnometer techniques.

Chapter 4 describes studies using Scanning Electron Microscope to look at microstructural features of the OPC and OPC/BFS using different curing conditions. Also X-ray diffraction and DTA were used to analyse the different phases.

In Chapter 5, polymer impregnation was introduced to combat cement pastes weaknesses occurring as a result of poor curing.

Chapter 6 and 7 describe carbonation studies and chloride penetration in both plain and impregnated cement pastes

In Chapter 8 the corrosion behaviour of steel embedded in hardened cement paste again for untreated and polymer impregnated cement pastes is described.

Chapter 9 contains the general discussion and conclusions and recommendations for further work.

CHAPTER 2 MATERIALS AND EXPERIMENTAL TECHNIQUES

In this chapter the materials used, the sample preparation and the experimental techniques, are explained in detail.

2.1 MATERIALS AND PREPARATION OF SAMPLES

2.1.1 MATERIALS

All of the specimens used in this research have been prepared from four different types of cement.

A) Aston ordinary Portland cement (OPC) from a single batch of research grade.

B) Sulphate resisting Portland cement, (SRPC) 'Ketton'.

C) A blended cement prepared from 70% OPC and 30% pulverised fuel ash (PFA) as prescribed by BS 3892: 1965 (OPC/PFA)

D) A blended cement prepared from 35% OPC and 65% ground granulated blast furnace slag (GGBFS) as prescribed by BS 146: 1973 (OPC/BFS)

All the above mentioned cements were stored in airtight drums until required and before use passed through a 150μm seive. The compositions of the various materials expressed in percentages by weight of the constituent oxides are shown in Table 2.1. Four compounds are usually regarded as the major constituents of cement: They are listed in Table 2.2 together with their abbreviated symbols. Using the Bogue's formula (103) the composition of OPC and SRPC cements can be determined.

Material	CaO	SiO_2	Al_2O_3	Fe_2O_3	SO_3	MgO	Na_2O	K_2O	Ignition Loss
OPC	63.0	20.3	7.1	2.7	3.3	1.3	0.47	0.60	0.8
SRPC	64.0	20.2	4.1	5.3	2.6	1.4	0.28	0.39	1.1
GGBFS	42.37	33.30	10.77	0.33	-	8.74	0.37	0.50	-
PFA	2.9	46.6	24.0	9.5	0.9	2.1	2.0	3.8	3.3

Table 2.1 Chemical analysis of cements and blending agents (wt %)

Name of Compound	Oxide Composition	Abbreviation
Tricalcium Silicate	$3CaO\ SiO_2$	C_3S
Dicalcium Silicate	$2CaO\ SiO_2$	C_2S
Tricalcium Aluminate	$3CaO\ Al_2O_3$	C_3A
Tetracalcium Alumino-Ferrite	$4CaO\ Al_2O_3\ Fe_2O_3$	C_4AF

Table 2.2 Main compounds of Portland cement

For the OPC and SRPC used in the present work the percentages of main compounds are given below.

OPC: $C_3S = 41.15$, $C_2S = 27.23$, $C_3A = 14.25$, $C_4AF = 8.21$.

SRPC: $C_3S = 64.42$, $C_2S = 9.40$, $C_3A = 1.91$, $C_4AF = 16.11$.

SPECIAL CEMENTS

SRPC

Sulphates which may exist in the environment surrounding the concrete, tend to penetrate the concrete or cement paste structure, and eventually attack the calcium aluminate hydrates. The C_3A hydrates can react with the sulphate salts, such as magnesium and sodium sulphates, to form fresh expansive calcium sulphoaluminates. This reaction can cause a gradual disintegration of concrete. The remedy lies in the use of cement with a low C_3A content, and such a cement is

known as sulphate-resisting Portland cement.

PULVERISED FUEL ASH

Pulverised fuel ash, is ash precipated electrostatically from the exhaust fumes of coal-fired power stations, and is the most common artificial pozzolana. A pozzolana is a natural or artificial material, containing silica in a reactive form. The ASTM specification C618-78 describes it as "A siliceous or siliceous and aluminous material, which in itself possesses little or no cementitious value but will, in finely divided form and in the presence of moisture, chemically react with calcium hydroxide at ordinary temperatures, to form components possessing cementitious properties".

Portland cements can be mixed with pozzolanas, such as PFA, to provide the necessary $Ca(OH)_2$ as it liberates during its hydration.

BLAST FURNACE SLAG

Blast furnace slag is a waste product in the manufacture of pig iron. The slag is a mixture of iron ore with the limestone flux, that is the same oxides that make up OPC, namely lime, silica and alumina, but in different proportions.

Blast furnace slag can make a cementitious material in different ways, i.e. can be mixed with a suitable proportion of limestone, as a raw material for the conventional manufacture of Portland cement, or straight with a Portland cement. As in the case of OPC/PFA, the blast furnace slag tends to react with the $Ca(OH)_2$ formed. However in the case of a high substitution of OPC by blending agents such as BFS, the chemical reactions occurring during hydration, tends to leave little or

no free $Ca(OH)_2$ (104). This may have the effect of diminishing the protection of the steel on the reinforced concrete.

STEEL

Mild steel bars of diameter 4.64mm were embedded in cement for corrosion experiments. The analysis of the steel is given in Table 2.3.

MONOMER (METHYL METHACRYLATE)

Methyl methacrylate was used to impregnate the cement pastes. Its properties were stated as:-

Minimum assay 99.5%

Weight per ml at 20°C 0.941 to 0.943 g

Refractive index 1.413 to 1.415,

Maximum limits of impurities, free acid 1 ml N%, water 0.1% and stabilised with 0.01% quinol.

2.1.2 Sample Preparation

The cements used for making the specimens were first passed through a 150µm sieve. De-ionised water was added to the cements to give a water/cement ratio of 0.4 or 0.6. The cement pastes were mixed thoroughly and cast into cylindrical PVC moulds, 47mm diameter, 74mm length, and vibrated for 2 minutes to remove trapped air and bring about good compaction. The layer of bubble-laden

Carbon	0.38
Silicon	0.21
Manganese	0.74
Phosphorous	0.018
Sulphur	0.12
Chromium	0.04
Molybdenum	0.06
Nickel	0.04
Iron	Balance

Table 2.3 Chemical analysis of mild steel (%)

cement on the surface of the specimen was removed and the mould topped up with fresh paste, and vibrated for another 2 minutes.

The completely filled moulds were tightly sealed and subjected to continuous rotation at 10rpm about a horizontal axis. This served to prevent significant segregation within the pastes, whilst their condition remained fluid.

The specimens were demoulded after 24 hours and cured in three different environments:

(1) Saturated $Ca(OH)_2$ solution at 20^oC referred to as cc(1)

(2) Saturated $Ca(OH)_2$ solution at 50^oC referred to as cc(2)

(3) Air at 50^oC and 30% relative humidity referred to as cc(3)

The environment for curing condition 3 was maintained with the use of a "FISONS" environmental cabinet.

Steel

Steel bars for corrosion studies were grit blasted, degreased with AR grade acetone and kept in a desiccator containing silica gel for a period of two weeks, in order to produce a uniform oxide film on the surface of each bar.

2.2 Measurment of Pore Size Distribution and Total Porosity

2.2.1 Introduction

It is widely recognized that the porosity of a material exerts an enormous influence on its physical and chemical properties. This is especially true for hydraulic materials such as Portland cement, where a large volume of porosity is inherent in the set structure (105-108). This porosity is derived mainly from the excess water which is required to lubricate the powder particles so that the plastic mass may be placed. The pores that exist within the structure of set cements are present in two main forms, capillary pores and gel pores. The capillary pores represent that part of the gross volume which has not been filled by the products of hydration (109,110). Because these products occupy more than twice the volume of the original solid cement paste alone, the volume of the capillary system is reduced with the progress of hydration.

Initially, all the pores are capillary pores and as hydration proceeds the capillary volume is reduced since the capillary space becomes filled with hydration products and the gel porosity increases. This leads to a net reduction in total porosity. According to Powers (111) in a fully hydrated cement paste, at a critical water/cement ratio of about 0.38, only gel pores would be present, which account for about 28% of the gel volume. The gel pores are in fact interconnected interstitial spaces between the gel particles. In the Powers model the gel itself consists of colloidal C-S-H particles of up to two or three layers, arranged randomly and bonded together by surface forces, as in clay, with occasional strong ionic-covalent bonds linking adjacent particles (112) figure 2.1(i). There is not sufficient long-range order to consider the material crystalline. The pores of these interstitial spaces are orders of magnitude finer than capillary pores being

between 15 and 20 Å in diameter (111-113). For this reason, the vapour pressure and mobility of adsorbed water are different to the corresponding properties of free water.

In the Feldman-Sereda model see figure 2.1(ii) (114) the C-S-H structure is present as an irregular array of single layers which may come together randomly to create interlayer space, as is observed in clay minerals, but in no regular ordered way. Bonding between layers is considered to be through solid-solid contacts which are visualised as bonds intermediate in character between weak Van der Waals' and strong ionic-covalent bonds. The solid-solid contacts form on drying but are disrupted by wetting. Interlayer bonding is a special kind of chemical bonding and cannot be considered as resulting from interactions between free surfaces. Water can move reversibly in and out of the interlayer space.

Daimon et al (115) further modified the Feldman-Sereda model see figure 2.1(iii) because, according to them, only then was the true pore structure revealed. Adsorption measurements indicated the existance of two kinds of pores: a wider inter gel-particle pore which can be seen even in the inner C-S-H by SEM, and a smaller intragel pore existing within the gel particles which cannot be observed by SEM. The intragel pores are further classified into an intercrystallite pore similar to the micropore reported by Brunauer et al (116), but which may enlarge in the presence of water, and intracrystallite pores corresponding to the interlayer space mentioned by Feldman (117) . Alford and Rahman (118,119) see figure 2.1(iii) concluded that closed spherical voids, or macropores, that cannot be intruded by mercury, contribute significantly to the total porosity of hardened cement paste, affect the pore size distribution, modify surface area determined by mercury intrusion porosity (MIP) and thus contribute to "lost" porosity.

If the water/cement ratio is sufficiently high (i.e according to Powers higher than

0.38) the volume of the gel after full hydration is not sufficient to fill all the space available, so that there will be some volume of capillary pores left even after the process of hydration has been completed. According to Verbeck and Helmuth (23) the size of capillary pores can vary between 50 and 350 nm and is dependant on water/cement ratio. They vary also in shape and may exist as an interconnected system if the water/cement ratio is sufficiently high or if hydration is incomplete, and are randomly distributed through the cement paste. These capillary pores are mainly responsible for the permeability of hardened cement paste. Such pores have a very complex geometry but to facillitate some understanding of their properties they are considered as having more simple shapes such as (those shown in figure 2.1(iv)a,b,c,d (119).

Figure 2.1(iv)a shows a system where low-pressure porosimetry would produce reliable results. Figure b, c and d show systems where low-pressure porosimetry would produce erronius results. Figure 2.1(iv)b shows a system where porosimetry would only "see" the first large opening and interpret the second opening as the diameter of the connecting channel i.e. the pore entry diameter. In figure 2.1(iv)c the large spherical pore is connected by pore channels which are available to admit mercury under the maximum pressure available. Figure 2.1(iv)d shows a large spherical void surrounded by hydration products which are too fine and closely-packed to be intruded by mercury.

2.2.2 Determination of Pore Size Distribution

There are many methods for determining pore size distribution including Mercury Intrusion Porosimetry (MIP), Sorption Isotherms, Optical and Electron Microscopy (120,121). MIP is mostly used to determine the sizes of

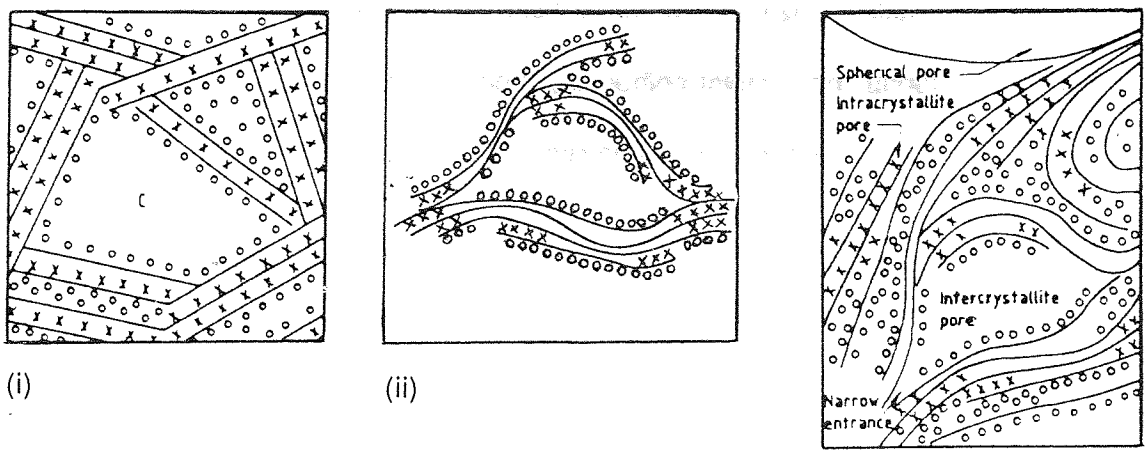

(i) (ii) (iii)

Figure 2.1 (i,ii,and iii) Schematic presentation of various models of C-S-H-gel (i) Powers and Brunauer adapted from (112), (ii) Feldman and Sereda (114),(iii) Feldman and Sereda, Successively modified by Daimon et al (115) and Rahman (118).

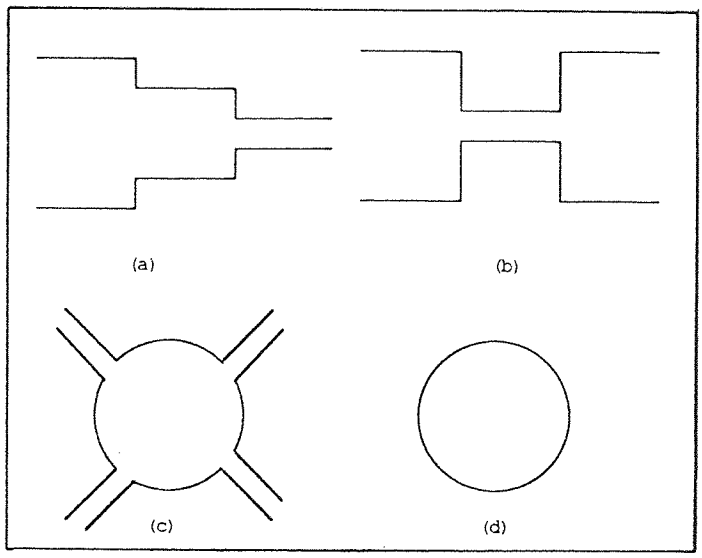

(iv)

Figure 2.1(iv) Schematic representation of variation in pore geometry (after Alford).

relatively large pores, or macro pores > 30 nm whilst sorption isotherms are best suited in the case of smaller pores, including micro and ultramicro pores < 30 nm. Optical means may be used to analyse sections of the sample in the range of $\geq\mu$. Most complete information on pore size distribution may be obtained by using MIP jointly with optical or electron microscopy methods (122,123).

MIP is the most commonly used technique and is effective in directing evaluating porosity and pore size distrbution.

As the main area of interest in this work is the macroporous region of cement paste and since MIP is the technique most commonly used in evaluation of cement macroporosity, considerable attention has been devoted to this method and its limitations.

2.2.3 Mercury Intrusion Porosimetry (MIP)

The theory of Mercury Porosimetry is now widely reported (124,129), and is used commercially for a growing number of porous materials. The principle of the instrument is to determine the quantity of a nonwetting liquid, mercury, which will penetrate a porous material under pressure.

The system is first evacuated to remove adsorbed gases and vapours. By applying pressure, mercury will be forced into the evacuated pores. If the pores are assumed to have a simple shape, e.g. cylindrical, the relationship between pressure and diameter of pores is given by the Washburn displacement equation (130):-

$$P = \frac{-4\,\gamma \cos\theta}{d}$$

where,

P = the applied pressure (N/mm^2)

d = the pore diameter filled at the pressure P (nm)

γ = the surface tension of the liquid = dynes/cm (474 mJ/ m)

θ = the contact angle between the liquid and solid, (degrees)

The mercury porosimetry method enables the widest range of pore-size distribution to be measured. The lower limit can be as small as 30 nm, depending on the pressure and the contact angle used in the calculation.

The mercury porosimeter used in the present work was a Micromeritics model 900/910 series, capable of producing a pressure of 50,000 psi (351 N/mm^2) figure (2.2). It should be noted that, because of the operational characteristics of the intrusion measurement system, the term "diameter" may be better defined as "pore entry diameter". This is because at the outset of a mercury intrusion determination, the sample is surrounded by mercury. As pressurisation proceeds, mercury is forced from the surface of the sample towards its centre, through whatever pores are available to it. If the path the mercury must follow to reach a particular internal pore is smaller in diameter than the internal pore itself, that internal pore will be intruded only after sufficient pressure is applied to intrude the narrower pathway (109).

Finally isolated pores having no communication with the exterior of the sample cannot be measured in any event, regardless of the pressure used. Corrections have to be made for the compressibility of the mercury.

Figure 2.2 Mercury Intrusion Porosimeter Model 900/910 series.

In general, mercury porosimetery has left open the question of the contact angle (θ) formed by mercury on the interior surface of porous solids. Despite the evident need, it has not been possible to obtain measurements of these contact angles. Measurements on macroscopic surfaces of a solid cannot be relied upon, because an internal surface will, in general be rough and in the case of cement paste, heterogeneous.

Good (131) has suggested that on account of roughness and void area, the contact angle of mercury on macroscopic samples of hardened portland cement paste was at least 170^{o}. Winslow and Diamond (109) have on the other hand reported the contact angle of mercury on simulated pores in hardened portland cement paste to be 117^{o}, this value was obtained by drilling small holes in hardened cement paste and measuring the pressure required to intrude mercury into them. The problem remains of determining which value, if either, is correct. The surface of a drilled hole can be expected to have a higher surface energy (131) than that of a crystal formed by a growth process, such as occurs in the hydration of portland cement, which would lead to a lower contact angle. If a value of contact angle is to be assumed rather than measured the experience of other workers would suggest that 117^{o} is most suitable for oven dried specimens (109,129) while 130^{o} should be assumed where vacuum drying has been employed (109,129). The value used for surface tension (γ) of mercury is 474 mJ/m, and the proof of the Washburn equation and also an example calculation of pore size distribution is given in Appendix 1.

2.2.4 Samples Used

In these experiments samples of OPC and OPC/BFS, SRPC and OPC/PFA were made with water/cement ratio of 0.4 and 0.6. After the samples were demoulded

they were cured in three different environments curing conditions cc(1), cc(2) and cc(3).

The preparation of the samples and conditions of each environment have been explained in this chapter, section 2.1.2. The curing times of 7, 28 and 60 days were considered for this test. After curing thin sections were sliced from the mid-section of the cylindrical samples using a diamond cutting wheel. Care was also taken to use the area close to the centre of the sliced disc. The samples were then broken by hand into small pieces, approximately 8mm wide and 15mm long. The specimens were then oven dried at 105 ^{o}C until a constant weight was obtained, in order to remove the evaporable water. The dried specimens were then stored in a desiccator containing silica gel and "Carbosorb" until needed for test.

2.2.5 Determination of Total Porosity

The determination of total porosity involved the measurement of the bulk (or apparent) density and the true density of the dry cement paste.

The bulk density may be calculated from the mass of dry specimen and its external volume obtained by the displacement of a non-wetting liquid (i.e. Mercury). A specially designed 'bottle and top' (pycnometer) was used, which was capable of reproducing a fixed volume of mercury. The top was levelled with a glass slide, figure 2.3, the 'bottle' was filled with mercury, and the 'top' inserted and the meniscus of mercury levelled with the glass slide. The outside was carefully cleaned with a brush, and weighed. The 'top' was opened and the weighed oven dried sample inserted. The 'top' was replaced and the exuded mercury carefully removed and the bottle re-weighed.

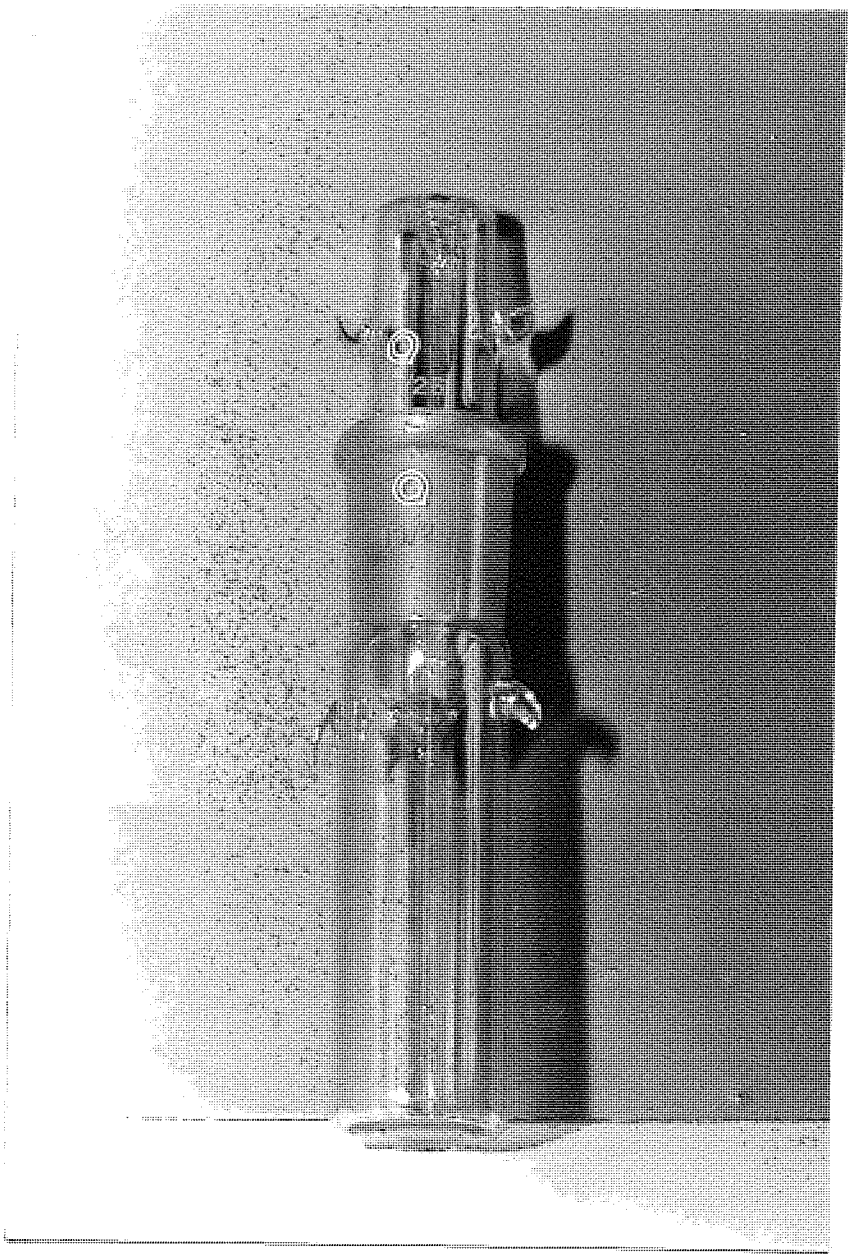

Figure 2.3 Pycnometer.

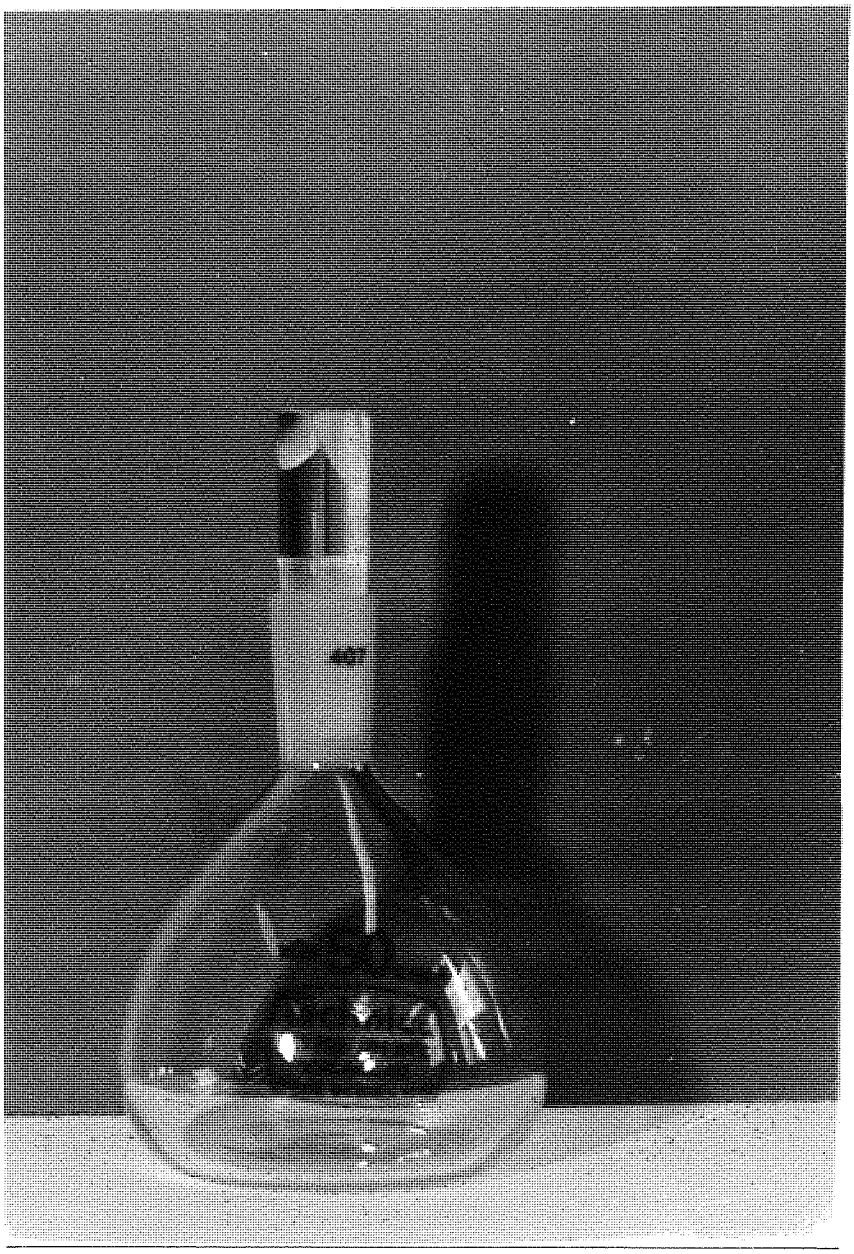

Figure 2.4 Density bottle.

The true density was determined using a density bottle. The paste was ground to powder, whose volume was determined by the mass difference between the density bottle filled with a wetting liquid (paraffin) Figure 2.4 and the same density bottle with the powder in it, filled up with paraffin. The filling operation was done under vacuum to ensure that the liquid completely wetted the powder.

An example calculation of total porosity of cement paste is given in Appendix 2.

2.3 MORPHOLOGICAL STUDIES

2.3.1 Scanning Electron Microscopy

The Scanning Electron Microscope (SEM) has been used in studies of the hydration of cements. Fracture surfaces of cement specimens are relatively easy to prepare and the high resolution and excellent field depth allow hardened cement paste microstructures to be examined in detail (121,123,132-134).

Prior to observation, the specimens were cut and then dried by means of vacuum drying. This was carried out as follows. After cutting, the specimens were quickly transferred to a small glass cell and evacuated with use of a vacuum pump until the pressure dropped to $2x10^{3}$mm Hg which was maintained at that level for at least 4 days. The samples were then kept in a desiccator containing silica gel and carbosorb for as short a time as possible. The specimens were finally mounted on aluminium stubs and coated with a thin conducting film of gold to carry the incident electrons from the SEM away to earth. The thickness of gold layer was about 250 nm.

2.3.2 X-Ray Diffraction Analysis

Samples were ground to a fine powder and placed in the specimen holder of a Philips X-ray Diffractometer (figure 2.5) with proportional counter and a copper tube with a Ni K_β filter.

The number of counts per second for OPC powder was chosen to be $4x10^2$ and for OPC/BFS powder $1x10^2$. The OPC has a higher count rate than the OPC/BFS, since it is much more crystalline. However the conditions that must be satisfied for the reflection of rays of a specific wave length are given by Bragg's law (135) which states that

$$n \lambda = 2d \sin \theta$$

where

n = the order of reflection (1,2,3 etc)

λ = the wave length of the X-rays

θ = the angle of the incidence or reflection of X-ray beam

d = the spacing of the crystal planes

Hence for a given wave length and angle of incidence where reflection occurs, the atom spacing may be calculated. The analysis of powder specimens has been carried out with an electronic counter tube to measure the intensity of the X-ray reflections.

The counter and specimen are both rotated in the X-ray beam. The counter tube is moved at twice the speed of the specimen so as to maintain the correct angle for each Bragg reflection. The output from the spectrometer is a trace of intensity against Bragg angle from which the 'd'- values may be determined and compared with standard data (136).

An example of identification of XRD trace is given in Appendix 3.

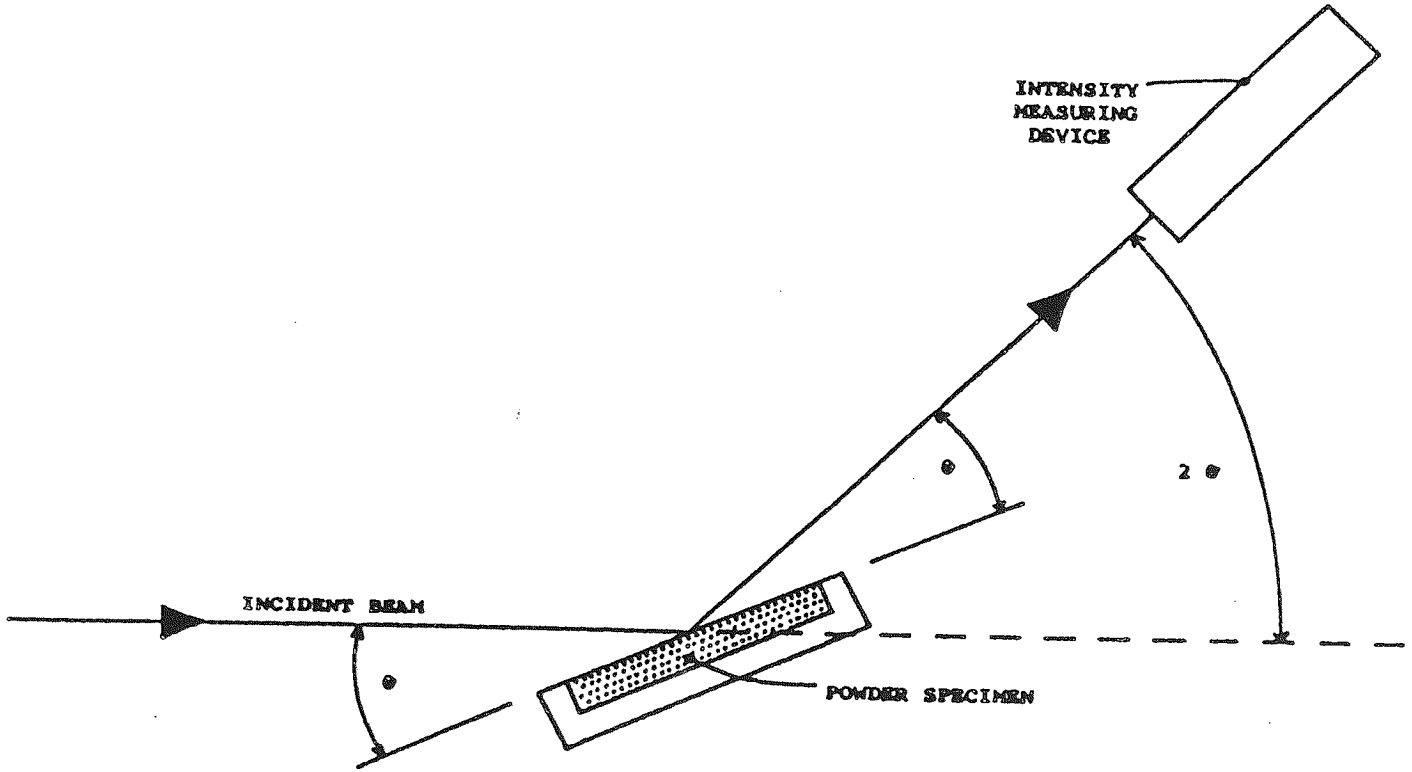

Figure 2.5 Geometric arrangement of X-ray Diffractometer.

2.3.3 Differential Thermal Analysis

Differential Thermal Analysis, provides a convenient method of measuring the physicochemical changes in a hardened cement paste, while it is being heated or cooled at a controlled rate (137). Prior to testing, the cement paste samples were ground by hand using a pestle and mortar until passing through a 150μm seive. The ground specimens were dried over silica gel in a CO_2-free system at ambient temperature. A small portion of the sample to be tested was then packed into a platinum/rhodium crucible and placed in the furnace of the analyser next to a similar crucible packed with a thermally inert substance (alumina). At a rate of 20^oC/min, the furnace raises the temperatures of the crucibles from ambient to 950^oC. Thermocouples measure the difference in temperature between the two crucibles and this was plotted against furnace temperature on a pen recorder. Position of the peaks on the chart are characteristics of the compounds present and the peak heights proportional to the amount of a specific compound.

Thus the effect of environment and time on curings of certain compounds, may therefore be compared between specimens, and the traces produced checked against standard data, see Appendix 4. Also figures 2.6 and 2.7 show schematic diagrams of its analyser layout and analyser.

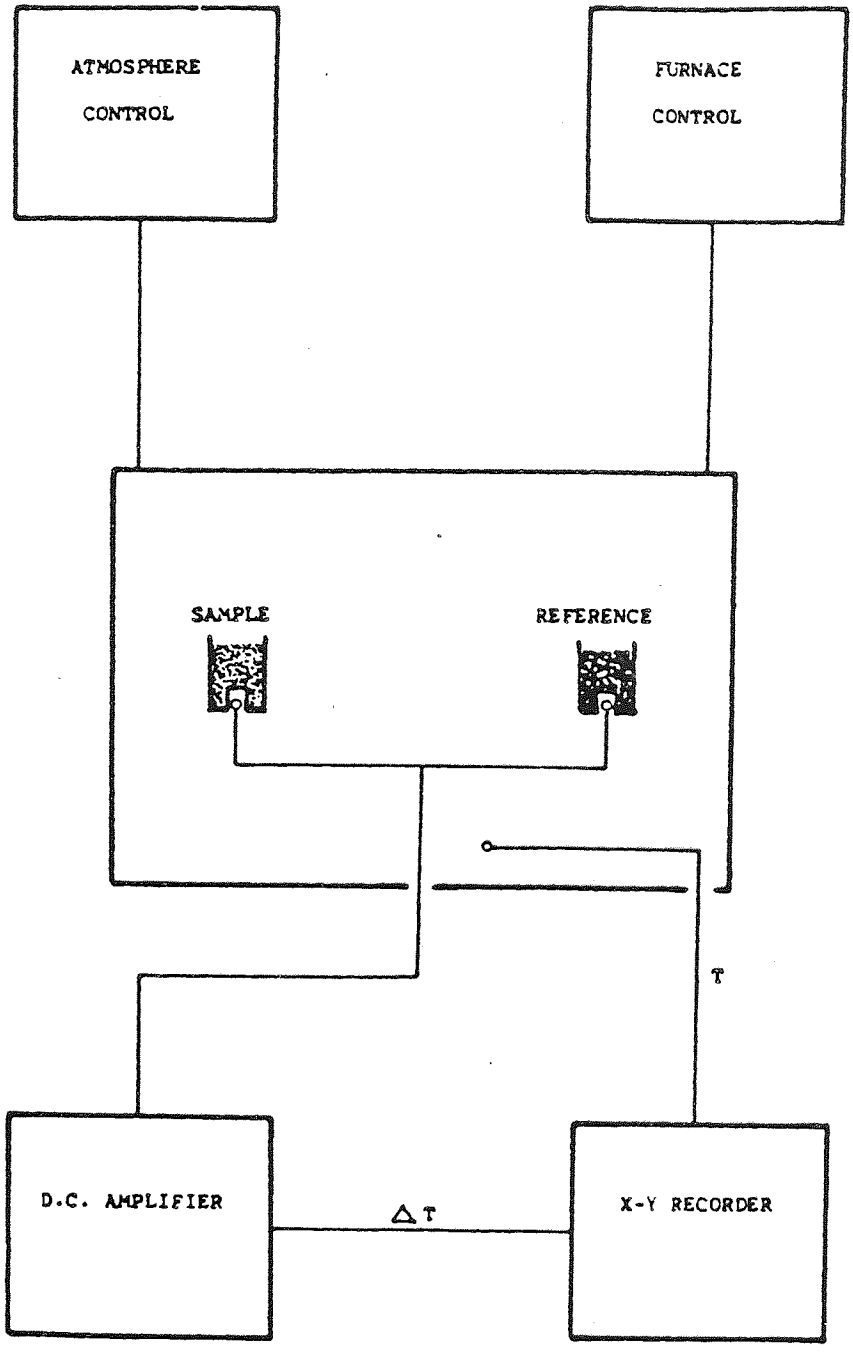

Figure 2.6 Schematic diagram of Differential Thermal Analyser (DTA).

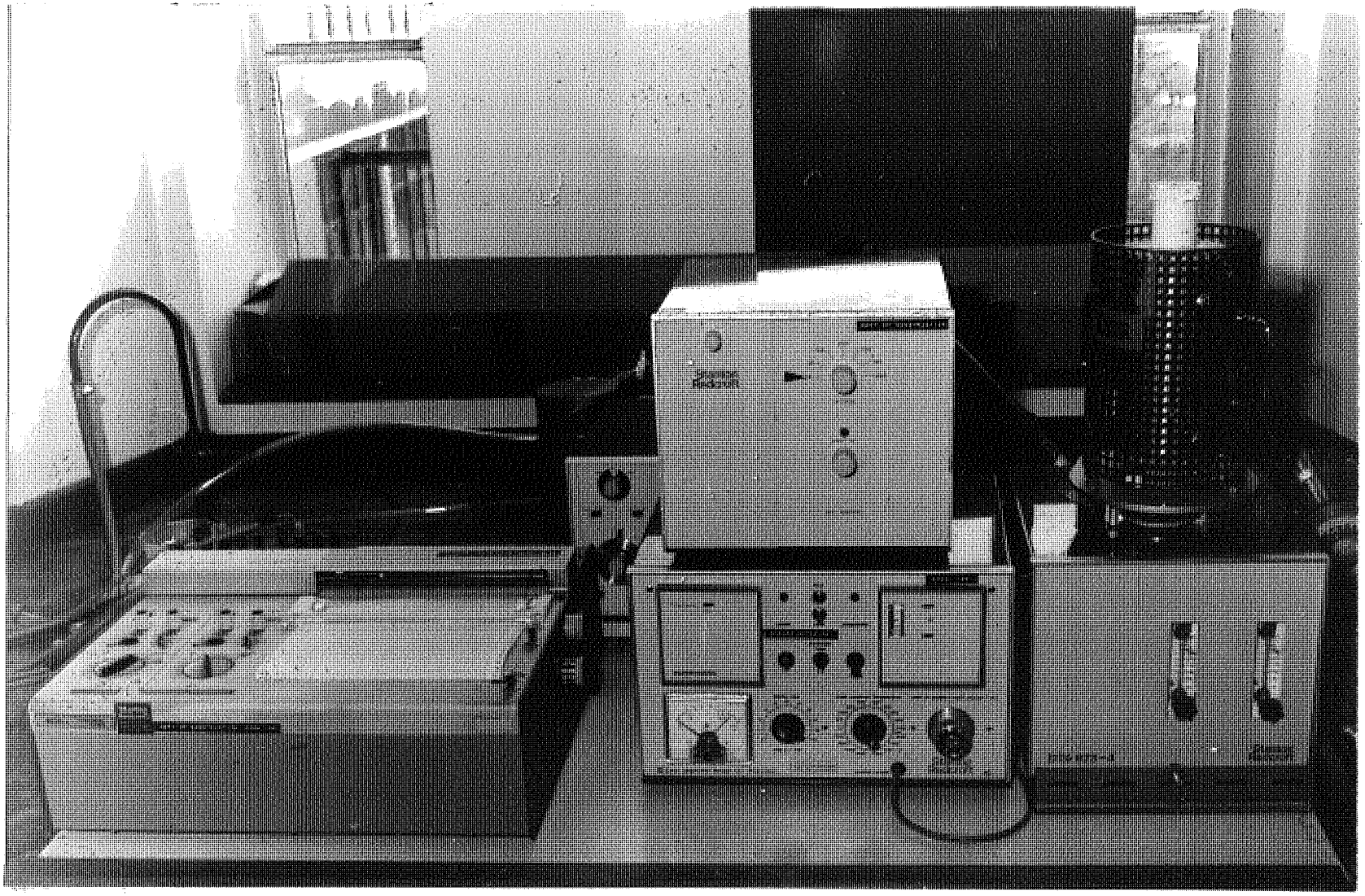

Figure 2.7 Differential Thermal Analyser

2.4 POLYMER IMPREGNATION

International interest in the use of polymers in concrete, dates back to the early 1950's. This work expanded into large scale research in the 1960's and early 1970's. Since then many attempts have been made to incorporate polymers into concrete, to improve the ultimate properties of it. This is normally achieved by filling a percentage of pores of the cement paste with a liquid monomer, which can undergo polymerisation and hence provide a composite material with superior properties, compared to ordinary concrete, (96,138-146).

As previously mentioned, there could be an increase in strengh (89), durability (91,146), corrosion resistance (92,96) and a reduction in permeability (140), water absorption (92), and gaseous transfer.This would suggest that polymer impregnated concrete may have many practical applications.

The effect of the diffusion of gases such as (CO_2,SO_2) and ions like Cl^- through unimpregnated cement paste are well known.

However these effects are reduced when polymer impregnated samples were used (92,96). In the late 1960's, several exploratory experiments were carried out on impregnation of concrete with monomers such as Styrene, Methyl Methacrylate, and other vinyl monomers. Liquid monomers were found to be generally easy to handle, as most of them have fairly low vapour pressures and low viscosity, which in this case is slightly lower than water, thereby facilitating the easy impregnation into the well dried hardened cement paste. There are several polymerisation techniques after impregnation of the monomers into cements or concretes (138,139), but normally, three types have been employed:-

(1) Thermal-catalytic, (2) Promoted-catalytic, and (3) Radiation.

Thermal-catalytic which is the most popular, and the simplest method of polymerisation is through the addition of small amounts of a compound which will generate free radicals on heating. Several of the commercially available compounds such as Benzoyl Peroxide, Azobis (isobutyronitrile) can be used in forming polymer impregnated cement or concrete. These compounds decompose at different rates over a range of temperatures to generate free radicals. The selection of type and concentration of initiator and the optimum polymerisation temperature were seen to be the important factors in the production of a uniformly good quality polymer impregnated cement or concrete. Benzoyl Peroxide catalyst is well suited for most vinyl monomers, in this case Methyl Methacrylate, because it decomposes well below its boiling points. The chemical reaction between Benzoyl Peroxide and Methyl Methacrylate is discussed later. However, there has been some concern expressed in the literature about the use of Benzoyl Peroxide in polymer impregnated cement or concrete, due to its easy susceptability to induced chemical decomposition, thus increasing the risk of an accidental bulk polymerisation, if the catalyzed monomer is stored. For this method a higher temperature at $85^{o}C$ is required for polymerisation and the associated potential hazard of explosion, due to the presence of catalytic agents constitute positive disadvantages.

However the conversion of the monomer Methyl Methacrylate to Polymethyl Methacrylate is normally via radical chain polymerisation, which involves three stages viz; initiation, propagation and termination.

Initiation is normally achieved by addition of activating agents, such as Benzoyl Peroxide (or Azobisisobutyronitrile) which form free radicals by thermal decomposition, thus:-

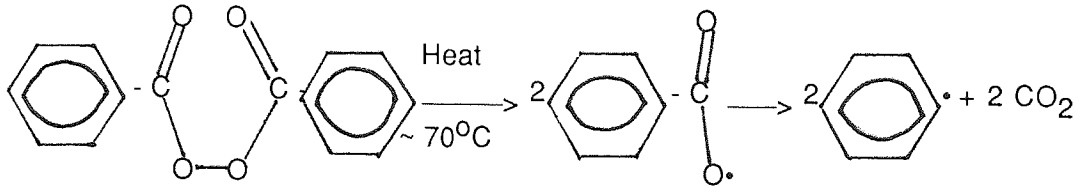

Initiation is produced when the free radical adds to the double bond of the Methyl Methacrylate monomer to produce another radical.

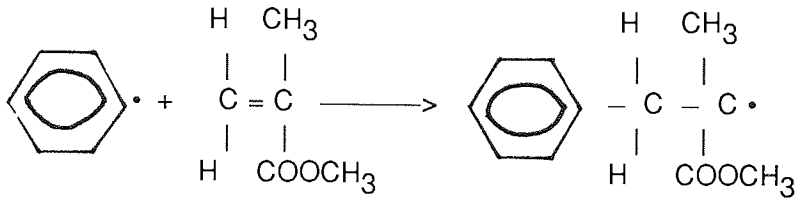

Methyl Methacrylate

The chain radical thus produced in the above step is then capable of adding succesive monomers to propagate the chain. Propagation would continue until the supply of monomer had been exhausted, were it not for the fact that radicals tend to react with each other with consequent loss of activity. This does, however, tend to be compensated for, by the fact that the concentration of radical is small compared to the concentration of monomers.

Termination can take place by combination ∴.

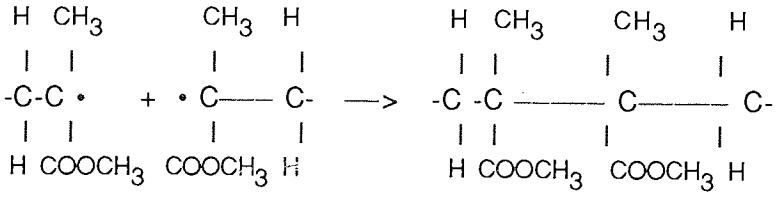

or by disproportionation ∴.

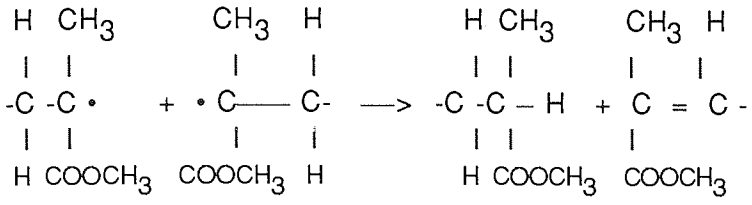

Termination is normally by disportionation at temperatures above 60°C and partly by each mechanism at lower temperatures.

2.4.1 The Impregnation Technique

The hydrated cement paste specimens after the original curing regime and their particular drying, were submerged in methyl methacrylate containing 3% by weight benzoyl peroxide. After a duration of 24 hours the samples were gently removed from the methyl methacrylate, since after 20 hours, there was no further increase in weight. The specimens were then carefully removed from the liquid monomer and covered in aluminium foil and placed in an oven at 85°C for a duration of 5 hours, (144) at which polymerization was completed.

A film of polymer which deposited on the surface due to evaporation was then carefully removed. Finally the samples were checked for any possible defects or cracks.

However it is important to mention that in some cases, a double impregnation technique was undertaken to improve the percentage of polymer loading.

2.5 CARBONATION STUDIES

A study of measuring the rate of carbonation through samples of hardened cement paste, originaly cured under two different conditions cc(1) and cc(3) for the duration of 28 days, was carried out.

Four different types of cement were used,

(a) OPC (b) SRPC (c) OPC/BFS and (d) OPC/PFA .

Each type of cement was made up at 0.6 and 0.4 water/cement ratio, into cylindrical specimens, as described in Para 2.1.2. Six specimens were made for each condition i.e. 4 cements specimens which were exposed to two curing conditions. After the duration of the original curing period, as mentioned above, each set of cylinders (three) were cut into 2cm thick discs using a hacksaw. Then each of the discs were cut into three sections of 4.7cm length and 1.8cm width.

About half of the test specimens were impregnated with methyl methacrylate and the remaining samples were kept in their original environment. Finally all the samples were placed in an environmental condition of $40^{o}C$ and 50% RH, which was taken to simulate harsh conditions in parts of the Middle East, and speed up carbonation. The depth of carbonation was measured at different time intervals, until about 15 readings were collected.

Various methods can be undertaken to detect or demonstrate the reaction of CO_2 in cement. Optical Microscopy may be used to show accurately the border between newly formed $CaCO_3$ and unaffected hydrated cement phases, in thin sections . An indicator like a 2% solution of phenolphttalein in ethyl-alcohol can show the modification on the cement paste by carbonation, but does not allow the determination of the exact pH of the concrete.

As for the colouring effect, the uncarbonated cement, after applying phenolphthalein, shows a pink colour, where as the carbonated region, due to the reduction in pH level from about 13.5 to approximately 9-8 remains colourless. Apart from phenolphthalein, thymolphthalein and alizarin yellow are used by other workers as indicators (36). Phenolphthalein was used as the indicator in this work as it shows a more distinct colouring. Figure (2.8) shows the depth of carbonation as determined by the phenolphthalein method.

To carry out the carbonation measurements the test pieces were split into a further three parts to give required fracture surfaces, onto which phenolphthalein was applied. The carbonation measurements were based on the average of different fracture surface readings, and from each surface minimum and maximum readings were taken, where the difference between the readings in most cases was 0.5mm. The carbonation lines in almost all cases were straight or nearly parallel to the surface except in the case of OPC/BFS cc(1) for both water/cement ratios, where initially, readings were eratic but as the time proceded they tended to improve. Figure (2.9) shows the definition of the depth of carbonation.

In order however to show the carbonation reaction for unimpregnated samples with a different method, and also to ensure and support the method used earlier for measurements of depth of carbonation with phenolphthalein, X-ray diffraction and D.T.A was undertaken, to verify and identify the carbonation products.

Figure 2.8 Schematic diagram of the carbonated test specimen

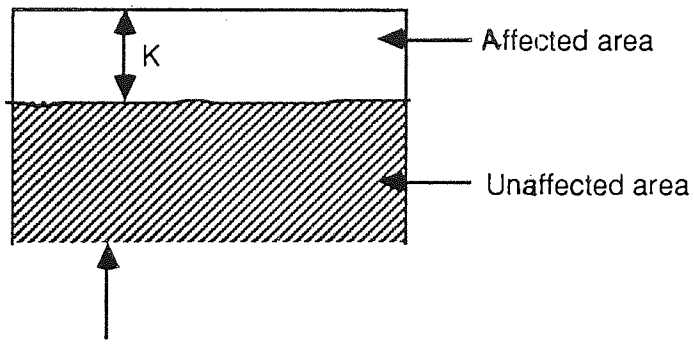

(Form a) for OPC,SRPC,OPC/PFA

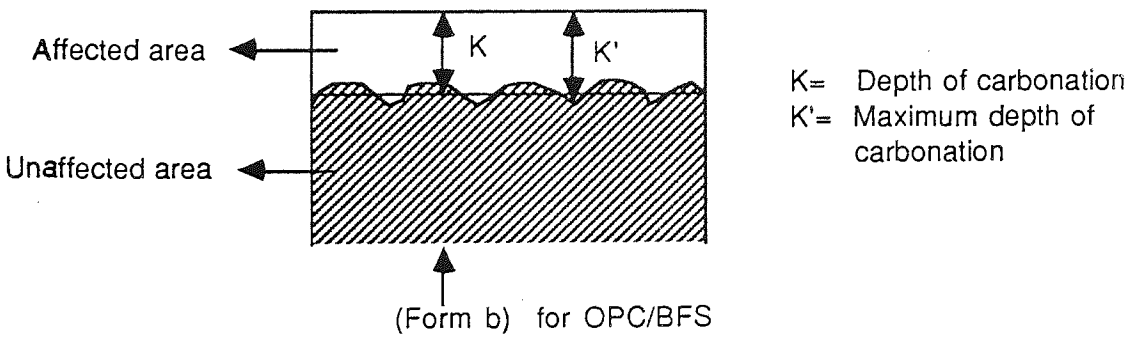

(Form b) for OPC/BFS

Figure 2.9 Schematic diagram of the definition of the depth of carbonation (after Mayer).

2.6 CHLORIDE DIFFUSION STUDIES

In these experiments, samples of OPC and OPC/BFS were made, with water/cement ratio 0.4 and 0.6 cured under cc(1) and cc(3) for a duration of 28 days.

Samples were cut by means of a micro slicer to provide discs of ~3mm thickness, which were then lightly ground until both surfaces became parallel. Half the discs were oven dried for 24 hours at 85^{o}C and then impregnated with methyl methacrylate (as described in section 2.4.1). From weight measurements made before and after impregnation, the degree of impregnation could be calculated. It was found that discs of 3mm thickness could not be impregnated satisfactorily and the thickness had to be increased to 6mm.

The experimental procedure follows closely that of earlier work (68) and has been used at Aston University for some years.

Each disc was mounted between the ground flanges of two half cells as shown in figure (2.10). Lightly greased rubber gaskets were placed between the discs and flanges, and the cells held together with elastic bands. The joints were further supported with P.T.F.E. tape. The gaskets ensured a leak tight fit and allowed a known area of the disc to be exposed. The high concentration side of each cell was filled with 1M/l Sodium Chloride solution, saturated with calcium hydroxide, while the low concentration side was filled with saturated calcium hydroxide. The cells were then sealed with stoppers to prevent evaporation and atmospheric carbon dioxide from reacting with the solution and supported in water baths at the experimental temperature (25^{o}C), by plastic cradles.

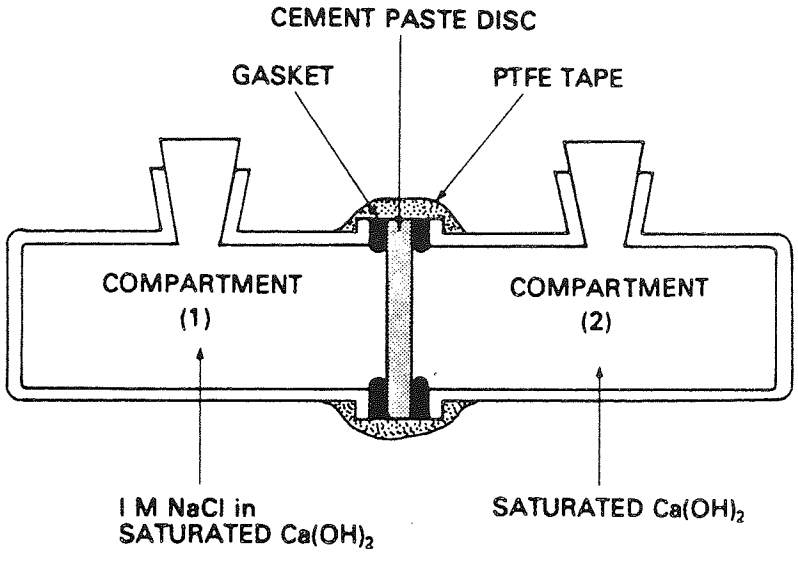

Figure 2.10 Diffusion cell (68).

After an initial period of time, over which the diffusion through the disc became established, 0.1ml aliquots of solution were taken from the low concentration side of each cell and analysed for chloride ion content by a standard spectrophotometric technique (147). Each 0.1ml aliquot of solution containing Cl^- ions was made up to 10ml with distilled water in a test tube. Added to these were 2ml of 0.25 M/l ferric ammonium sulphate ($Fe\ (NH_4)\ (SO_4)_2,\ 12H_2O$) in 9M nitric acid and 2ml of saturated mercuric thiocyanate in ethanol. Chloride ions displace thiocyanate ions and these combine with ferric ions to produce a highly coloured complex:

$$2\ Cl^- + Hg\ (SCN)_2 + 2\ Fe^{3+} \longrightarrow Hg\ Cl_2 + 2\ [\ Fe\ (SCN)\ ]^{2+} \qquad (147)$$

This solution is placed in a glass cell, in a spectrophotometer along side another cell containing a blank solution as reference.

The selected wave length of light used in this analysis is 460nm. The amount of chloride ion present, is proportional to the difference in absorption between the blank and test solution and may be found in terms of molarity by constructing a calibration curve of standard chloride solutions against absorption. See Appendix 5.

The Beer - Lambert equation, describes the relationship between concentration and intensities.

$$I_t = I_0 \exp(-\varepsilon c x)$$

where

I_t = intensity of transmitted light

I_0 = intensity of incident light

ε = molecular extinction coefficient

c = concentration of solution

x = optical path length through solution

Therefore for a constant path length, the intensity of beam of monochromatic light is inversely proportional to the concentration of the absorbing substance it passes through (148). The spectrophotometer optics are shown in figure (2.11).

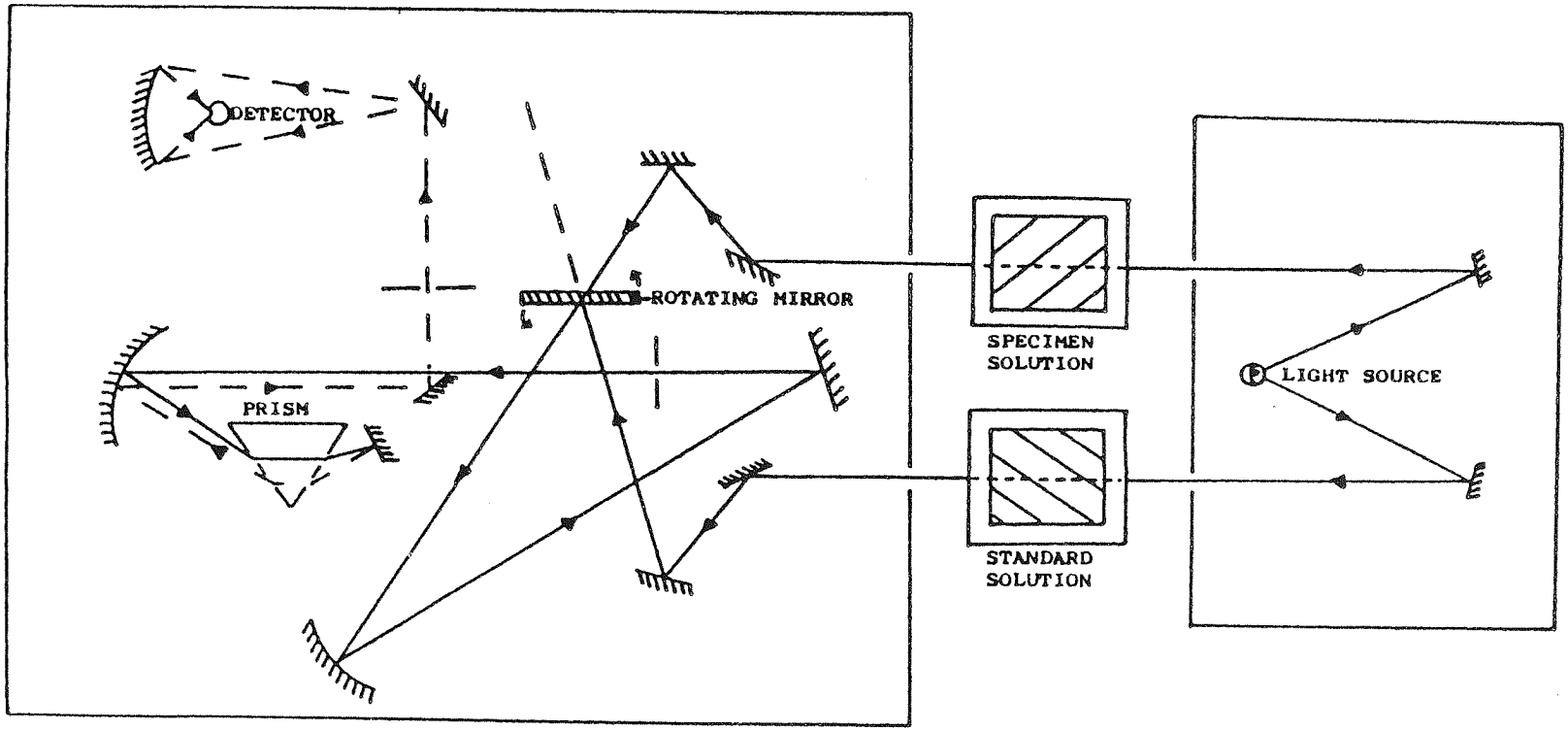

Figure 2.11 Schematic diagram of a twin beam Spectrophotometer.

2.7 CORROSION STUDIES

Mild steel bars of 4.64mm diameter were cut into lengths of 70mm and the cut ends, finished on 600 grade emery paper. All the specimens were then grit blasted and degreased with AR grade acetone, so as to produce a consistent surface condition.

In an attempt to avoid problems of crevice attack, specimens were masked in the form of a collar around the top 20mm of each bar, this was made out of a mixture of 50% Styrene-Butadiene rubber (SBR) + 50% water added to a volume of cement making a convenient paste. The thickness of this added paste was maintained at around 2mm. Once the cement paste was hardened, a covering of PTFE tape was applied, so as to seal totally the top of the steel specimen. Care was taken to ensure that the tape did not come into contact with the bottom edge of the paste collar. In such a manner that the paste collar ensured that no crevice existed at the interface with the cement. The bars were then placed in a desiccator containing silica gel for a period of two weeks, in order to produce a uniform oxide film on the surface of each bar. Meanwhile the tops to the PVC cylinders which were used for casting the cements, were geometrically designed in such a way that two steel bars and also a carbon counter electrode bar were inserted parallel to each other, into the three previously punched equidistant holes, figure 2.12, at a distance of 10mm from the circumference of the cylinder. As steel bars were inserted the top 5mm of masked ends were left protruding from the surface of the cylinder cap, together with the top 10mm of the 7mm diameter of carbon rod, and they were introduced in a way that after the cylinder cap was resealed with molten wax, the bars were parallel to one another. The cements were OPC and OPC/BFS at 0.6 water/cement ratio. The procedures employed for sieving, mixing, casting and vibrating are given in this chapter, section 2.1.2. The cement pastes were

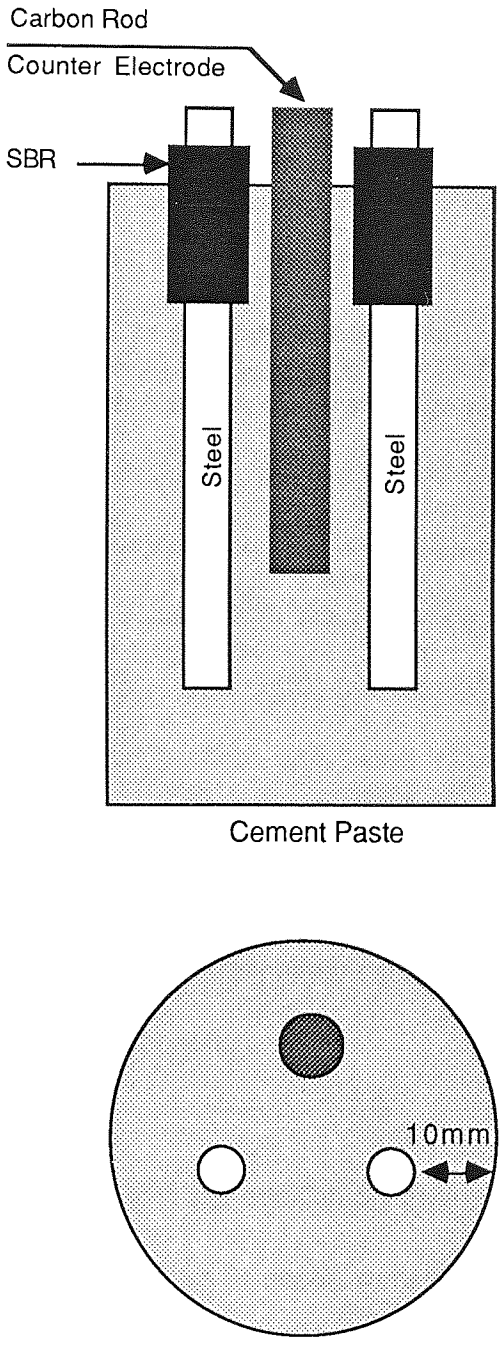

Figure 2.12 Schematic diagram of the arrangement of the corrosion specimens.

cast in cylindrical PVC moulds of 49mm diameter, by 74mm length. Then the already prepared cap was placed carefully onto the cylinder; it was then placed in a ball mill for a period of 24 hours, which as explained in chapter 2, section 2.1.2 was rotating continually. After removing the samples from the ball mill, they were then demoulded and some were placed in cc(1) and the rest in cc(3) for a period of 28 days.

After this original curing regime, half of the samples from each of the curing conditions were then subjected to polymer impregnation. For samples of OPC taken from cc(1) after being subjected to single impregnation, the polymerisation of monomer to polymer was not complete, due to constant evaporation of monomer, therefore these samples were subjected to double impregnation. This is explained fully in chapter 5. In order to proceed with the corrosion test, for each type of cement and curing condition, cc(1) and cc(3), four samples either impregnated or unimpregnated each containing steel bars were placed in three different environments.

(a) The samples were placed in the environmental cabinet at 40^{o}C and 50% relative humidity, i.e. fast carbonation.

(b) Saturated $Ca(OH)_2$ solution with the addition of 1M/l of sodium chloride. These samples each being 7.4 cm in depth, were immersed into the solution to a depth of 6cm. There were two reasons for this, firstly to prevent the solution from directly being in contact with the steel bars and secondly to encourage availability of oxygen from the top surface.

(c) The samples were placed at 100% relative humidity.

From the samples placed in environments (a) and (b), rest potential readings

were taken after 10 days and then every 3-4 weeks versus a saturated calomel reference electrode. All the samples from environment condition (a) were removed from that environment 24 hours previous to the potential reading and were placed in a saturated $Ca(OH)_2$ solution the reason for using in $Ca(OH)_2$ is explained in chapter 8 . After recording the potential reading they were placed back into environment (a).

Two of each type of specimen from each environment were opened after 6 months and their appearance compared with the I_{corr} and E_{corr} data.

2.7.1 Polarisation Resistance Measurement

Polarisation resistance or linear polarisation is an electrochemical method, which can be used for determining the corrosion rates of steel reinforcement. The technique is carried out by applying a potential scan over a small range, i.e. 20 mv either side of the rest potential. The current produced per unit area (current density) is plotted against the potential and the polarisation resistance is obtained from the slope, figure 2.13.

This is translated into corrosion intensity (I_{corr}) by the Stearn and Geary relationship (149).

$$\frac{\Delta E}{\Delta I} = \frac{\beta_a \beta_c}{(2.3)\ (I_{corr})\ (\beta_a + \beta_c)}$$

where,

$\frac{\Delta E}{\Delta I}$ = the polarisation resistance or slope of the plot.

I_{corr} = the corrosion current

$\beta a \beta c$ = the anodic and cathodic Tafel constants.

This relationship only applies when ΔE is small. The Tafel constants are the gradients of the anodic and cathodic polarisation curves. They were assumed to be equal to 0.12 volts/decade enabling the calculation of I_{corr}.

Andrade et al found that by making these assumptions the values of I_{corr} obtained correlated well with weight loss measurements (87). The polarisation resistance measurements have been carried out on an EG and G/PAR model 350 microprocessor controlled corrosion measurement console equiped with an IR compensation module which compensates for the IR drop between the working electrode and the reference electrode. The corrosion measurement console was capable of carrying out a preprogrammed scan over a range of 20 mv either side of the rest potential (E_{corr}) and presenting the results by means of an integral 'X-Y' plotter.

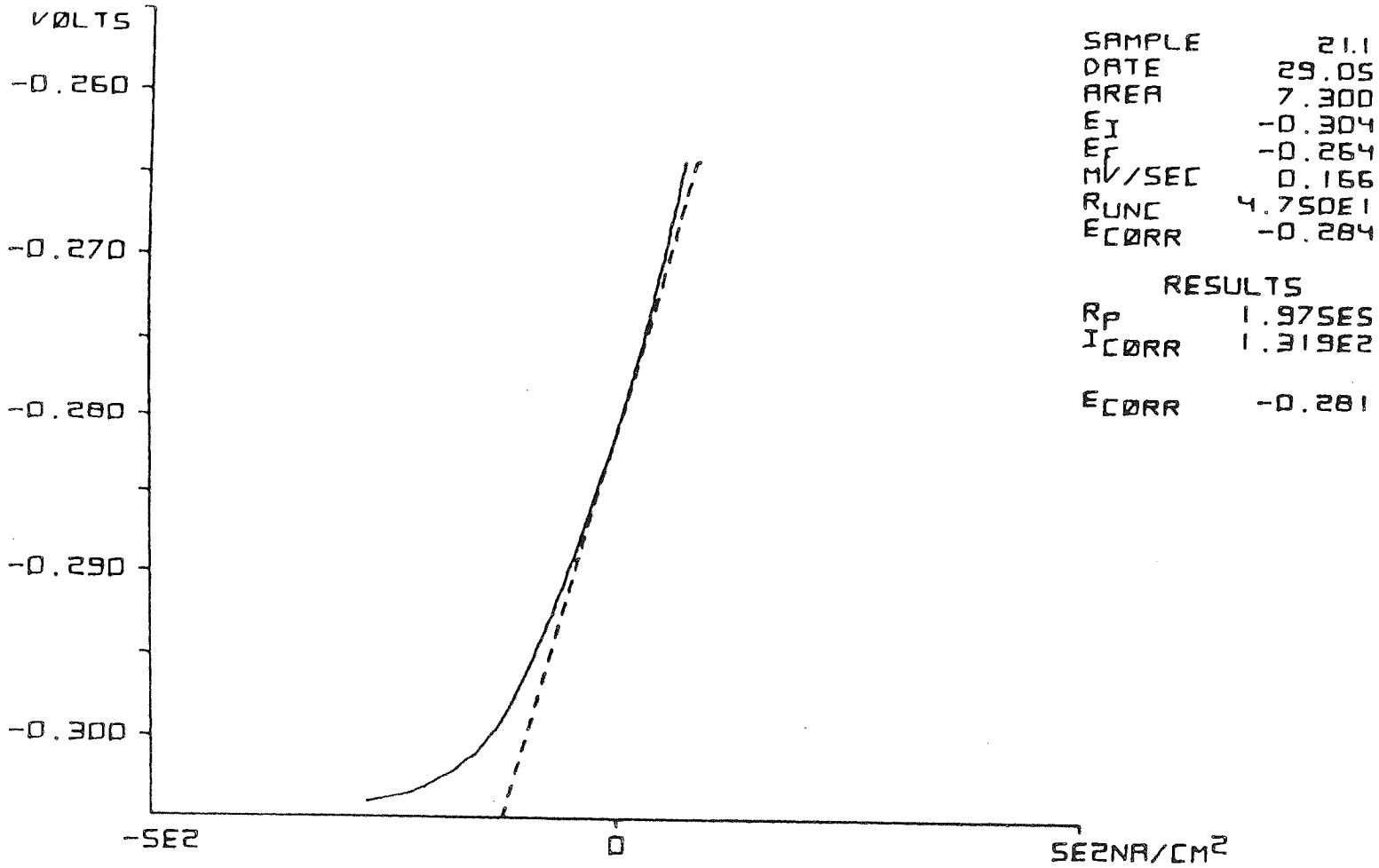

Figure 2.13 Typical Linear polarisation plot of the "PAR" Microprocessor.

CHAPTER 3 EFFECT OF CURING CONDITIONS ON POROSITY AND PORE SIZE DISTRIBUTION

As previously discussed in chapter 2 section 2.2, the porosity and pore size distribution of a hydrated cementitious material depends upon the water/cement ratio and degree of hydration. This is especially true at early ages.

During hydration, voids become partly filled with gel and micro crystalline hydrate particles. The manner of filling depends on the particle size distribution of the cement, the original water/cement ratio, availability of water during hydration and the temperature at which hydration takes place. Rapid evaporation of mix water will alter the hydration reactions and hence the porosity and pore size distribution.

3.1 MERCURY INTRUSION POROSIMETRY (MIP)

3.1.1 Presentation of Results

Values of penetration volume versus pore diameter do not usually fit a simple functional relationship. Data may be expressed as plots of the cumulative intruded pore volume or the change in intruded pore volume versus pore diameter. The latter case produces a plot which is the differential of the cumulative plot. If a differential volume axis is selected, and the pore diameters span more than an order of magnitude, then the slope must be calculated on the basis of changes in the logarithm of the pore size (Δ volume per Δ log size). Failure to do this will greatly distort a differential plot (125). There are several other difficulties with the use of differential plots. Since the distribution will rarely fit a mathematical

function, its differential cannot be evaluated continuously and approximate numerical methods are required. Another, and major disadvantage is that the total intruded pore volume is not readily apparent from the plot. Differences in total volume between plots for different materials are likewise obscured. To summarise, the differential plot is subject to distortion in appearance, and may obscure important aspects of the pore size distribution. It does not convey any information that is not also available on the cumulative plot. A peak of the differential plot is, after all, a steep region on the cumulative plot. Therefore, in this work as in many others (108,109), a cumulative type of plot has been used.

3.1.2 Results and Discussion

Typical cumulative curves are shown in figures 3.1 and 3.2. These show extreme cases for the effect of temperature and relative humidity. Further traces are presented in Appendix 6. Due to the large number of plots obtained, direct comparison between different cements and curing conditions, is facilitated by plotting histograms of maximum penetration volume (which represent total porosity) and initial pore entry diameter (which indicates the coarseness of the pores). These plots can be seen in figures 3.3 to 3.6, and values of maximum penetration volume and initial pore entry diameter are given in tables 3.1 and 3.2. Figures 3.3 and 3.4 compare the effect of temperature on curing different cements at water/cement ratio 0.4 and 0.6, whilst figure 3.5 and 3.6 compare the combined effect of temperature and relative humidity.

It was evident from the literature (68) that total porosity and pore size distribution are very significant with regards to durability, since they effect the rate of ingress of aggressive agencies.

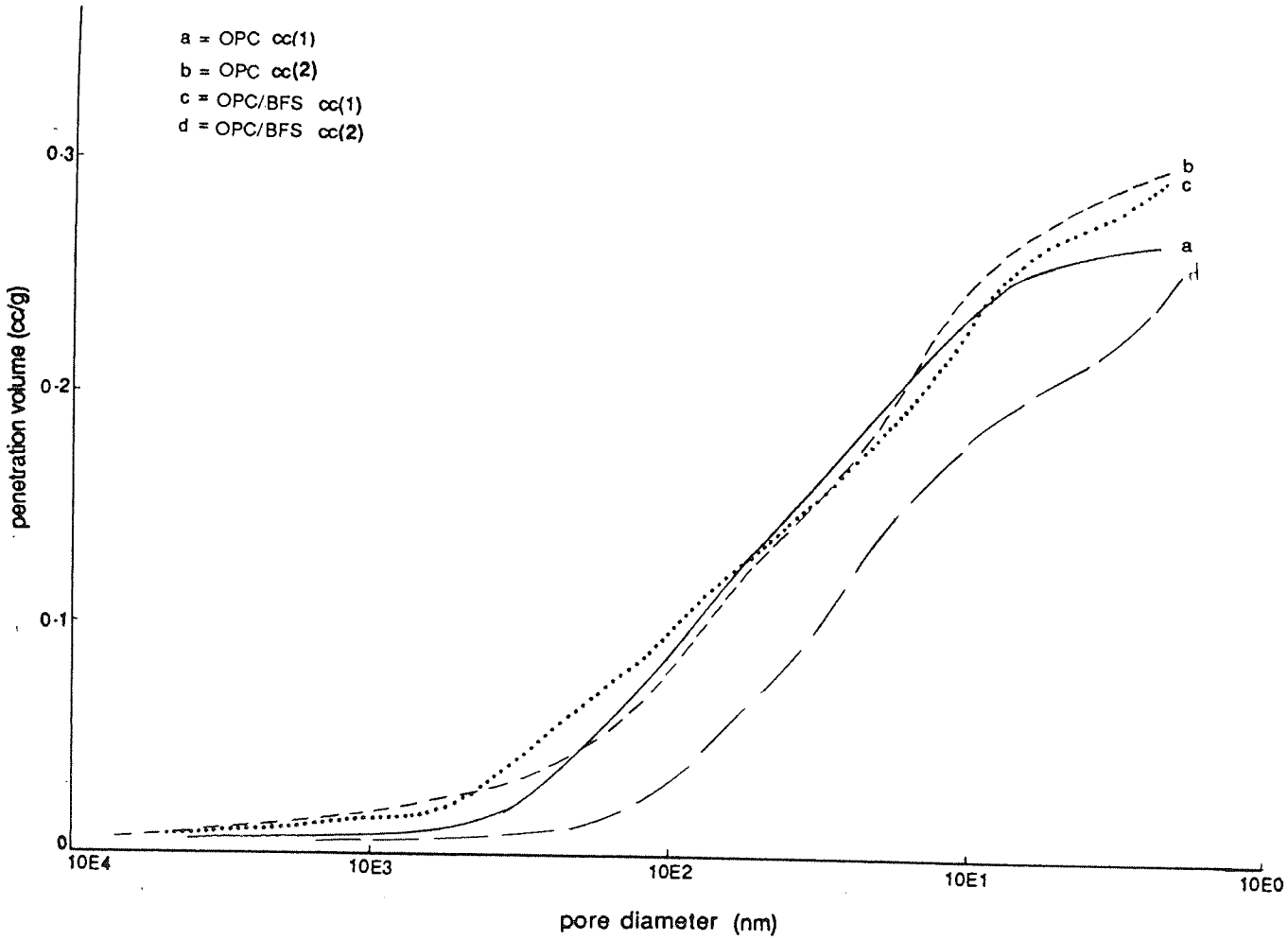

Figure 3.1 Pore size distribution curves of OPC and OPC/BFS pastes of 0.6 water/cement ratio cured for 28 days at cc(1) and cc(2).

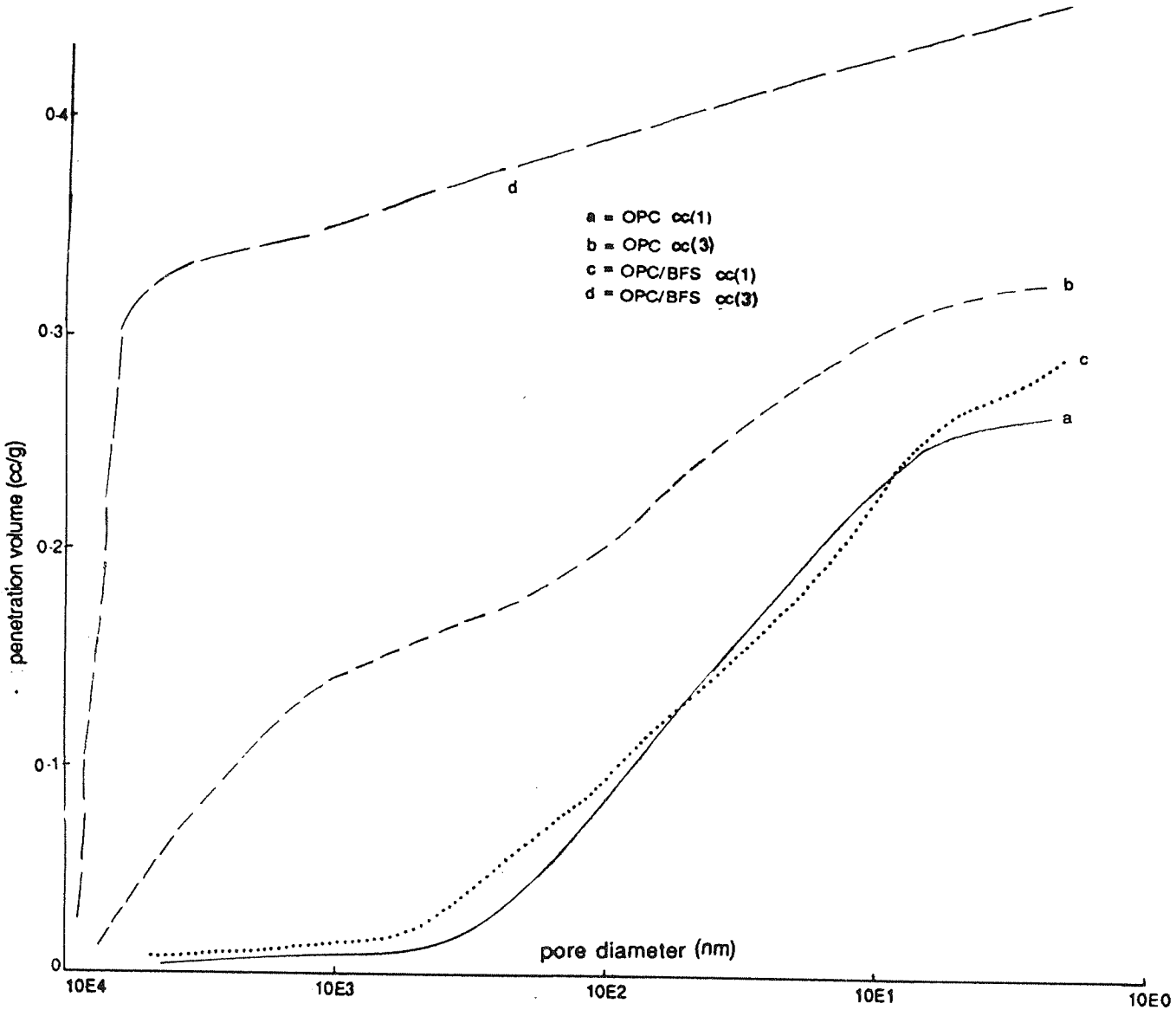

Figure 3.2 Pore size distribution curves of OPC and OPC/BFS pastes at 0.6 water/cement ratio cured for 28 days at cc(1) and cc(3).

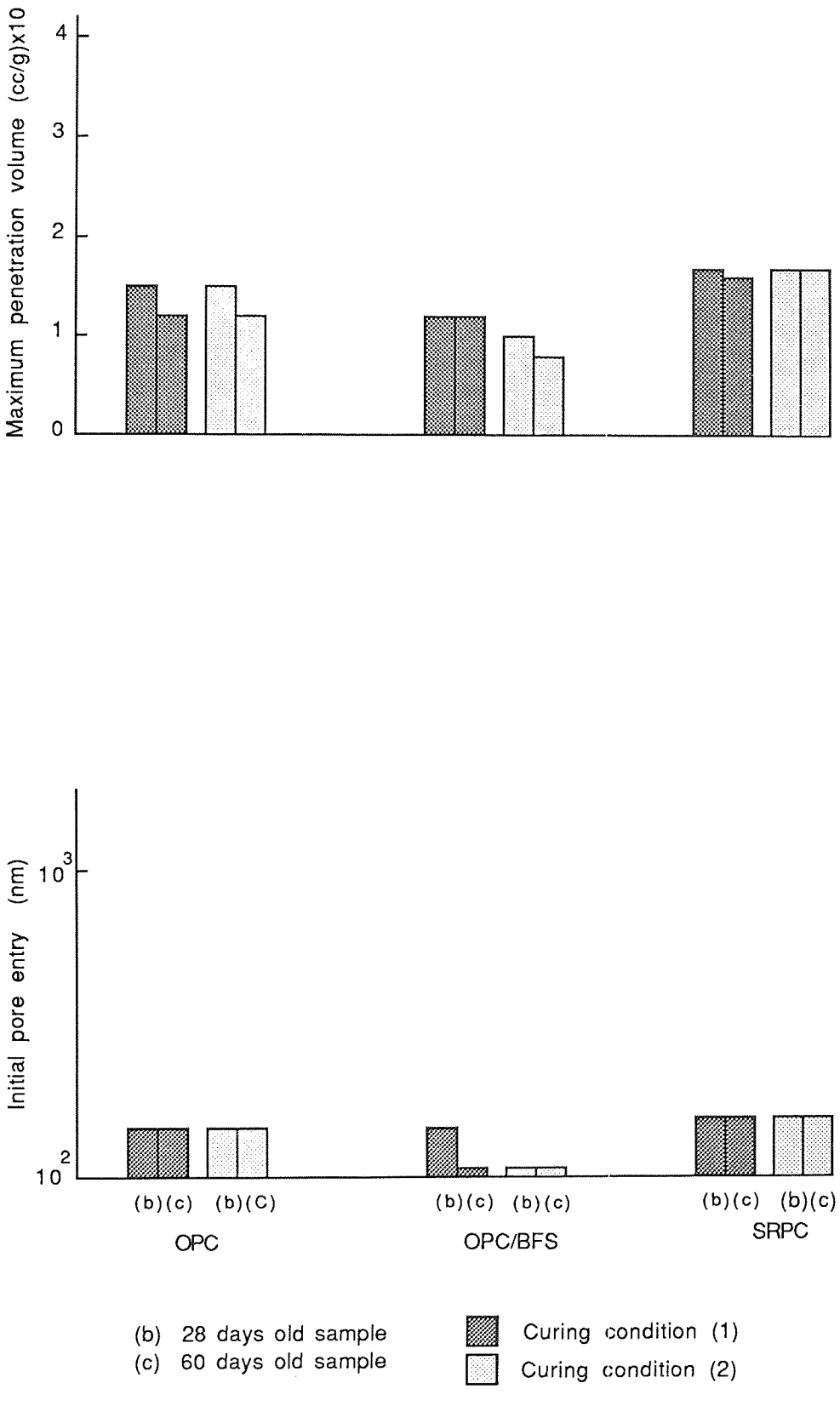

Figure 3.3 Histograms showing maximum penetration volume and initial pore entry of 0.4 W/C ratio cement pastes, comparing cc(1) and cc(2).

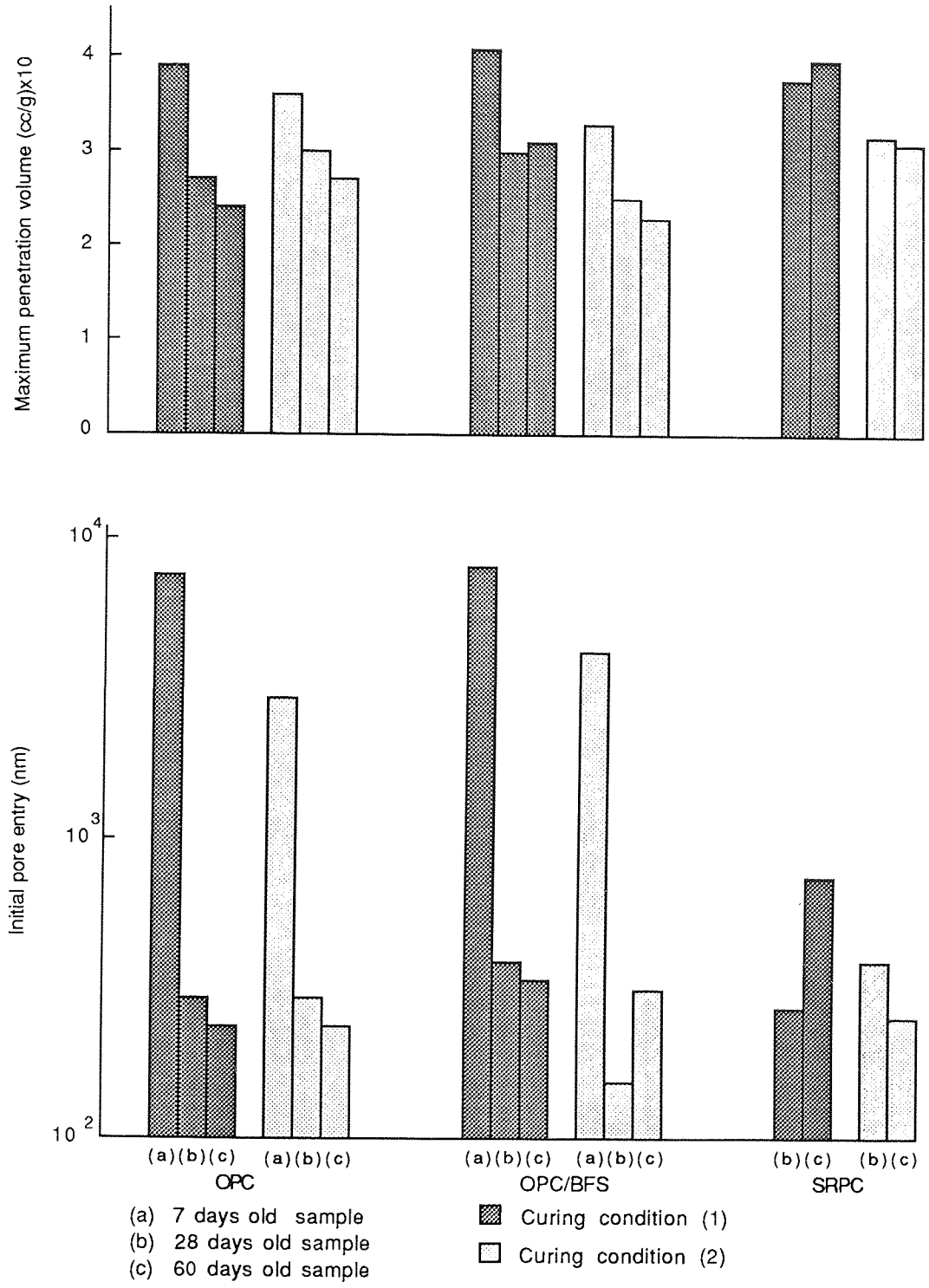

Figure 3.4 Histograms showing maximum penetration volume and initial pore entry of 0.6 W/C ratio cement pastes, comparing cc(1) and cc(2).

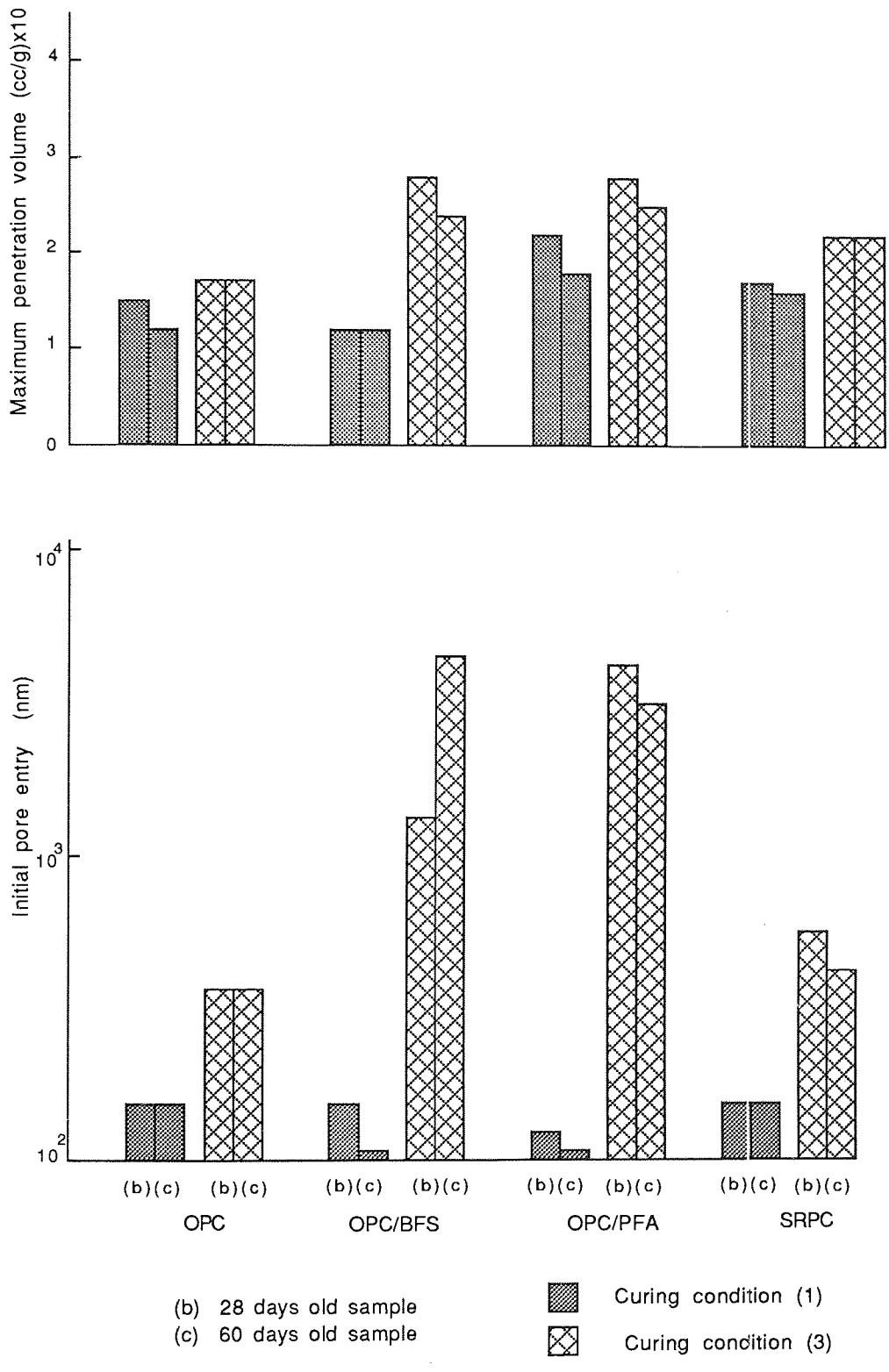

Figure 3.5 Histograms showing maximum penetration volume and initial pore entry of 0.4 W/C ratio cement pastes, comparing cc(1) and cc(3).

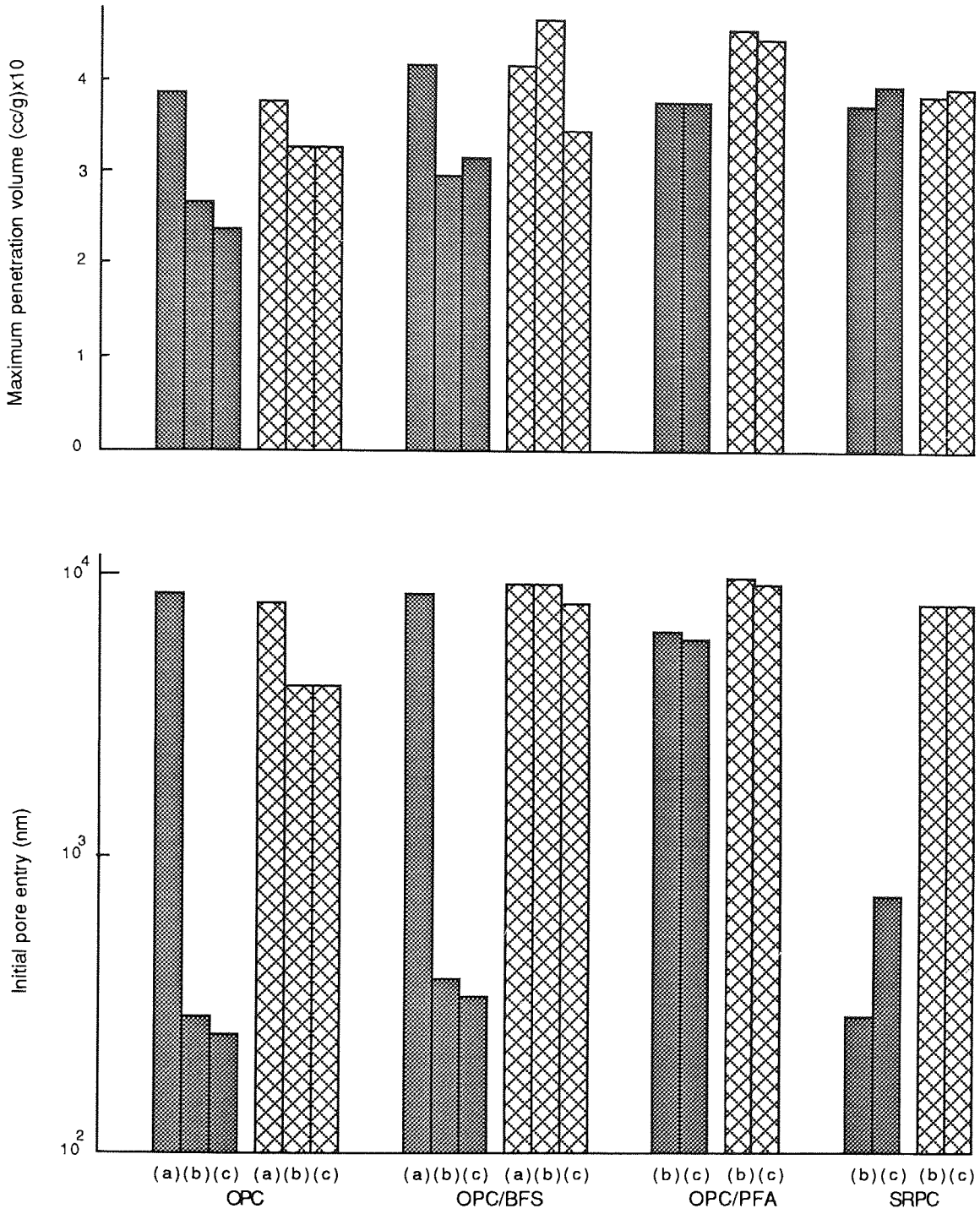

Figure 3.6 Histograms showing maximum penetration volume and initial pore entry of 0.6 W/C ratio cement pastes, comparing cc(1) and cc(3).

Cement	Days	0.4 w/c ratio			0.6 w/c ratio		
		cc(1)	cc(2)	cc(3)	cc(1)	cc(2)	cc(3)
OPC	7				0.39	0.36	0.38
	28	0.15	0.15	0.17	0.27	0.30	0.33
	60	0.12	0.12	0.17	0.24	0.27	0.33
OPC/BFS	7				0.41	0.33	0.42
	28	o.12	0.10	0.28	0.30	0.25	0.47
	60	0.12	0.08	0.24	0.31	0.23	0.35
OPC/PFA	28	0.22		0.27	0.38		0.46
	60	0.18		0.25	0.38		0.45
SRPC	28	0.17	0.17	0.22	0.38	0.32	0.39
	60	0.16	0.17	0.22	0.40	0.31	0.40

Table 3.1 Maximum penetration volume (cc/g) for different cement pastes at two water/cement ratios and variable curing conditions.

Cement	Days	0.4 w/c ratio			0.6 w/c ratio		
		cc(1)	cc(2)	cc(3)	cc(1)	cc(2)	cc(3)
OPC	7				8500	3000	8100
	28	150	150	250	300	300	6000
	60	150	150	250	250	250	6000
OPC/BFS	7				8500	4400	9000
	28	150	100	2000	400	150	9000
	60	100	100	7000	350	300	8000
OPC/PFA	28	120		6400	7000		9200
	60	105		3800	6800		9000
SRPC	28	150	150	450	300	400	8000
	60	150	150	400	800	250	8000

Table 3.2 Initial pore entry diameter (nm) for different cement pastes at two water/cement ratios and variable curing conditions.

Figure 3.3 shows values of total pore volume (TPV) and initial pore entry diameter (IPD) for three types of cement, OPC, OPC/BFS and SRPC 0.4 water/cement ratio, cc(1)and cc(2) and after 28 and 60 days curing.

Consider first the case of OPC. For both cc(1)and cc(2) there is little difference between the two specimens at 28 and 60 days. When the curing time increases from 28 to 60 days the total pore volume is only marginally reduced. The results for the initial pore entry for the above samples show no difference between the values obtained. Thus little effect of increased temperature is noticeable after 28 days curing.

For the slag blended cement, total pore volume is slightly less than OPC particularly so after curing at the higher temperature. With regards to initial pore entry at 28 days cc(1) values are the same as with OPC. However at longer curing times and higher temperature it is somewhat reduced.

In the case of SRPC the total pore volume is slightly greater than OPC and initial pore entry is about the same. The effect of temperature is not noticeable after 28 days.

Results for the same range of cements and curing conditions at 0.6 water/cement ratio are shown in figure 3.4. At this water/cement ratio samples for OPC and OPC/BFS were examined at 7, as well as 28 and 60 days. As would be expected the total porosity and coarseness of the pores is greater than that for water/cement ratio 0.4 for a given cement, time and curing condition, (compare figures 3.3 and 3.4)

For the OPC it can be seen that total pore volume diminished appreciably between

7 and 28 days and then slightly between 28 and 60 days, as was the case with the 0.4 water/cement ratio samples. Similar trends are found for initial pore entry but particularly marked, is the change between 7 and 28 days, especially as results are plotted on a log scale. This is probably due to insufficient hydration products at an early age of curing, i.e. 7 days, but as the time of curing increases to 28 days, the larger amount of these products produced will cause segmentation of capillary pores. It would seem that the effect of temperature is greatest at early ages, and at low temperature, the reactions "catch up" as it were. Similar values and trends in results were found for the OPC/BFS blend.

In the case of SRPC as with water/cement ratio 0.4, there is again a slightly higher value of total pore volume compared to the other cements. Effect of time, is not as clearly defined since there are no 7 day results. Values of initial pore entry are similar to those for the OPC, the value of cc(1) at 60 days, being considered somewhat spurious.

It seems from the above mentioned results that the temperature used for this work i.e.($50^{o}C$) did not significantly affect the pore structure of OPC, OPC/BFS and SRPC. A similar observation was made by Parker and Roy (150) for 60/40 slag cements, in an investigation of the affect of water/cement ratio and curing temperature on the porosity and the critical pore radius of the pastes. Curing temperatures up to $60^{o}C$ did not significantly increase the coarseness of the pore structure at water/cement ratios <0.5. At higher temperatures they observed an increase in the coarseness of the cements. This may be attributed to the suggestion by Roy and Idorn (151) that the solubility of calcium hydroxide is suppressed at higher temperatures so its ability to activate slag hydration is reduced.

Pratt et al (152) studied the influence of curing temperature on OPC pore

structure. They discoverd that an increase in temperature to 40°C will accelerate the hydration of OPC pastes, but the mechanism of hydration does not appear to be altered greatly, with similar microstructures appearing at equivalent times as judged by calorimeter curves . On the other hand Helmuth (23) suggested that the rapid initial rate of hydration at higher temperatures retards the subsequent hydration and produces a nonuniform distribution of the products of hydration within the paste. The reason for this is that at the high initial rate of hydration there is insufficient time available for the diffusion of the products of hydration away from the cement grain and for a uniform precipitation in the interstitial space (as in the case at lower temperatures). As a result, a high concentration of the products of hydration is built up in the vicinity of the hydrating grains, and this retards the subsequent hydration and adversely affects the long-term strength.

The effects of relative humidity as well as those of temperature, for cc(1)and cc(3) on total pore volume and initial pore entry can be seen in figures 3.5 and 3.6. The cements used were OPC, OPC/BFS, OPC/PFA and SRPC at 0.4 and 0.6 water/cement ratio and examined in all cases at 28 and 60 days but also in a few cases at 7 days.

Considering first, the case of samples made with water/cement ratio 0.4, figure 3.5. Generally, for a given cement and curing condition, there is little difference between samples cured at 28 and 60 days. That the initial pore entry diameter for the OPC/BFS specimen at 60 days is greater than at 28 days indicates scatter in the results obtained using cc(3) (as was noted earlier). With the OPC, bad curing results in only a slightly higher total pore volume but there is a noticeable increase in initial pore entry, which indicates that although total porosity does not increase there is a coarser pore structure. This may be caused by the

segmentation of the larger pores leading to a reduced initial pore entry, but the total porosity in effect remains the same.

In the case of the OPC/BFS blended cements poor curing leads to an increase in both total pore volume and initial pore entry. This may however be due to slow rate of hydration reaction for BFS based cement, kept at cc(3).

Results for the samples of OPC/PFA are very similar to those found for OPC/BFS blended cements. The trends in results for SRPC are very similar to those for OPC, and show only slight increase in total pore volume and initial pore entry when compared to the OPC.

In the case of the samples made with water/cement ratio 0.6, there were a few extra samples examined after 7 days. The effect of time on these, has already been discussed for cc(1).

The values of total pore volume and initial pore entry for all the cement types that have been badly cured, are very similar and show only small changes with time of curing. In the case of the OPC and SRPC these results are significantly greater than at water/cement ratio 0.4.

The combination of the higher water/cement ratio (i.e 0.6) and poor curing, has substantial effect on total pore volume and in particular the initial pore entry for the OPC and SRPC specimens (comparing figures 3.5 to 3.6).

In the case of the blended cements OPC/BFS and OPC/PFA, the total pore volumes are greater than at water/cement ratio 0.4, but the initial pore entries are very similar.

In the case of the 0.6 water/cement ratio cc(1) PFA specimens, cured at 28 and 60 days, hydration occurs more slowly as the pozzolanic reaction only becomes significant at later ages (153). Porosity remains, therefore, high even after 60 days of hydration. This is evident from the results of the initial pore entry and total porosity measurements figure 3.6. Initial pore entry for the 0.4 water/cement ratio OPC/PFA specimens does not appear to be influenced in the same way, however, suggesting that the retardation of the hydration process is more prominent at higher water/cement ratios.

3.2 RESULTS AND DISCUSSION FOR TOTAL POROSITY MEASUREMENTS

In this set of experiments, the aim was to cross-check the total porosity measurements carried out by the MIP using a different method. This was achieved by determining the bulk or (apparent) density of the hydrated pastes, cured for 28 days, under two different curing conditions cc(1)and cc(3) both at 0.4 and 0.6 water/cement ratios for four different cements. The total porosity data has been derived from calculations of true density and bulk (or apparent) density measurements, which are presented in appendix 2. However, total porosity, as a function of water/cement ratio for all different cements, are shown in table 3.3 (in combined) and compared with total porosity obtained by the MIP method. The main objective of using the total porosity measurements as a technique, were simply to compare the results obtained by this method to those found by the MIP. These data showed apart from one condition, that there was no significant difference between the results obtained by both methods as can be seen from table 3.3.

The one condition was slag cement cured under curing condition (3) which showed

a higher total pore volume when subjected to MIP (0.47 cc/g) compared to the pycnometeric technique (0.40 cc/g). One explanation for this is that put forward by Feldman (154) and supported by Marsh and Day (155). Feldman subjected a number of ordinary and blended cement pastes to MIP and found, in many cases, higher total pore volumes for blended cements compared to results obtained by helium pycnometery. They concluded that pore size distributions of hydrated cement blends measured by mercury intrusion appear to be incorrect owing to structural damage that occurs at high intrusion pressures during measurement. Day and Marsh carried out similar studies comparing porosities of PFA and silica fume pastes obtained by either MIP or alchohol resaturation (155). They too observed that for the blended cement porosities were higher when determined by MIP. They explained it as follows:

Hydration products by pozzolanic reactions block off pores making them inaccessible to alchohol. As the walls of these pores are relatively weak, the intrusion of mercury at high pressures breaks through the blocked regions. Pores which exist behind the blockages are then filled and are correspondingly assigned to a smaller pore radius than they may actually possess. The net result is that an inaccurate assessment of the pore size distribution is obtained. Of particular significance is their observation that the tendency of the pore size distributions of these cements is to become convex towards the radius axis in the high-pressure region (below 10nm pore radius). A number of cements in this study had shown such a tendency (see page 260 for cc(1) and cc(2) in appendix 3). This effect did not however appear to significantly alter the measured total porosity and, as already mentioned, the porosities determines by the two techniques were in the main comparable (table 3.3).

Total porosity (cc/g)								
Cement	0.4 w/c ratio				0.6 w/c ratio			
	cc(1) pycno	cc(1) MIP	cc(3) pycno	cc(3) MIP	cc(1) pycno	cc(1) MIP	cc(3) pycno	cc(3) MIP
OPC	0.16	0.15	0.17	0.17	0.30	0.27	0.34	0.33
OPC/BFS	0.15	0.12	0.26	0.28	0.32	0.30	0.40	0.47
OPC/PFA	0.23	0.22	0.27	0.27	0.38	0.38	0.45	0.46
SRPC	0.18	0.17	0.23	0.22	0.33	0.38	0.38	0.39

Table 3.3 Total porosity (cc/g) for different cement pastes and curing conditions, cured for 28 days obtained by both the pycnometric and MIP methods.

3.3 CONCLUSIONS

As expected for the cements studied, curing at higher temperature with 0.6 water/cement ratio, reduces porosity, which suggests that the rate of hydration is increased, particularly at early ages (<28 days). In the case of OPC and SRPC, temperature has little effect on total pore volume and initial pore entry after 28 days although with OPC/BFS blend, the effect is noticeable up to at least 60 days.

Compared to OPC at 60 days, the OPC/BFS blend exhibits a slightly lower total pore volume and less coarse pore structure, whilst the opposite is true for SRPC.

For the temperatures studied in this work the effect of temperature on its own, is likely to have little effect on durability from the point of view of altering pore structure, (although it may well speed up ingress of aggressive agencies and degradation reactions).

Combined high temperature and low relative humidity results in a slightly coarser pore structure for OPC and SRPC of water/cement ratio 0.4, but has little effect on total pore volume. There is a much more dramatic effect with the OPC/BFS and OPC/PFA blends, there being a significant increase in total pore volume and a much greater increase in coarseness of pores. At 0.6 water/cement ratio, all cements exhibit high total porosity and coarse pore structure.

It would appear that relative humidity is more important than temperature, and that blended cements are more likely to become prone to poor curing than OPC and SRPC, although even these will be affected at higher water/cement ratio.

The total pore volume values obtained by both the MIP and the TP technique, suggest that there is no significant difference between the two methods.

CHAPTER 4 MORPHOLOGICAL STUDIES

4.1 INTRODUCTION

In this work an attempt was made to explain the morphology of the cement paste and to relate and compare this to the results obtained by Mercury Intrusion Porosimetry (MIP). Examination of the individual products of hydration of different cement pastes, OPC and OPC/BFS, required the study of fracture surfaces of cement pastes, with different times of curing. The work concentrates on the extent of major phase changes during the hydration of the above named cements in two curing conditions, which can be detected by X-ray diffraction and D.T.A. Results were related to the hydration behaviour of the cements and to pore size distribution. As previously mentioned, little effect on porosity was observed during high temperature curing so cc(2) ($50^{o}C$ in $Ca(OH)_2$) was eliminated for this chapter. Only cc(1) and cc(3) were therefore studied. Time considerations and the fact that the change in curing condition had least effect on the 0.4 water/cement ratio specimens resulted in the decision to use only 0.6 water/cement ratio specimens for the work described in this chapter.

4.2 RESULTS AND DISCUSSION

Figures 4.1 and 4.2 show SEM micrographs of the fracture surfaces of OPC cc(1) 2 and 8 days after casting. It can be seen that clusters of individual cement grains have become covered with a shell of hydrous, gel like material. A network of intertwinning fibres can be seen to have grown radially from the cement paste particles, which are most probably C-S-H gel. There is little difference between the 2 and 8 day samples. Figure 4.3, shows the sample at 29 days, where further hydration has led to the outgrowing fibres interlocking with one another, leading to the development of a denser structure. Figure 4.4, shows the structure at 61 days. It is now evident that there is a more solid

structure and platelets of $Ca(OH)_2$ can now be observed. The results of X-ray diffraction for the above samples, at 2 , 8 , 28 and 61 days are shown in figure 4.10. It is apparent that the relative height of the $Ca(OH)_2$ peak increases with time, due to the formation of $Ca(OH)_2$ as cement grains react with water leading to the precipitation of $Ca(OH)_2$ (Portlandite) (156). The C_3A peak virtually disappears after 2 days, whilst C_3S and C_2S peaks gradually decrease with time, as would be expected .

Figures 4.5 - 4.8 show SEM micrographs of samples of OPC cc(3) at 2 , 8 , 29 and 61 days. At two days, figure 4.5, the fracture surface is granular, consisting essentially of the original unbonded grains, which are only sparsely covered with a network of fibres, unlike in the case of cc(1) figure 4.1.

At 8 days, more fibres are present, figure 4.6. The reason for this would appear to be the unavailability of moisture during the confinement of samples in cc(3). As a result, partial drying occurs, leading to the lack of hydration products, which can normally be seen as in the case of cc(1) figure 4.2.

At 29 days, figure 4.7, there is very little change in the fracture surface of the cements, as compared to the 8 day samples.

At 61 days, figure 4.8, it is evident that the fracture surface was not as compact as for the samples of OPC cc(1) at the same age, figure 4.4, and that the hydration reaction was retarded. Generally the hydration behaviour of the cc(3) samples was, however, somewhat erratic, making it difficult to compare with those of cc(1) at different times (see for example the 8 day samples, figure 4.6).

The X-ray diffraction results for OPC cc(3) at 2,8,29 and 61 days, are shown in figure 4.11. In comparing the 2 day hydrated samples with the results of unhydrated OPC, as shown in figure 4.9, it is evident that some hydration has

already taken place. There is still however a large amount of C_3A remaining, figure 4.11, which is less evident in the sample cured in cc(1) for the same age, figure 4.10.

Furthermore the decrease in the unhydrated cement constituents for cc(3) (i.e. C_3A, C_2S and C_3S), with hydration time is not as marked as for cc(1) which can be clearly seen by comparing figures 4.10 and 4.11. This indicates a retardation in the hydration process, caused by the harshness of cc(3). The results of DTA on OPC paste for cc(1)and cc(3) as shown in figures 4.12 and 4.13, which are typical for the materials. In the case of OPC cured under cc(1) the peaks at 190^{o}C, and ~500^{o}C, representing the gel and $Ca(OH)_2$ respectively indicate that OPC is normally hydrated.

For OPC cured at 50^{o}C and 30% relative humidity, figure 4.13, these peaks are again present, but with an additional small peak at 900^{o}C, indicating the presence of some $CaCO_3$. The main difference however between the two, is the amount of C-S-H gel and $Ca(OH)_2$. If it is assumed that the area under the DTA peaks represent the quantity of the appropriate phase and that the mass of each of the specimens is constant, then it is possible to compare two DTA thermographs, by the size of their peaks. In this case, both the peaks representing the gel and the calcium hydroxide phases are larger for the cc(1) specimens revealing a more complete hydration.

Figure 4.14 and 4.15 shows the fracture surface of OPC/BFS cc(1) for 2 and 8 days, where it can be seen that at this stage of the hydration reaction the cement particles are thinly covered with a spongy film of hydration product i.e. C-S-H gel on the top surface. In hydration of the BFS added cement, OPC is the first to hydrate and produce C-S-H gel and $Ca(OH)_2$. The gel covers the cement particles (157).

In comparing the fracture surface micrographs of the BFS based cement to OPC,

figure 4.1, 4.2 - 4.14, 4.15, in cc(1) at the same age, there is little sign of clusters of fibres outgrowing from the top surface of hydrated particles of the blended cement as is the case for OPC, but in both cases there is some C-S-H gel and $Ca(OH)_2$. During the hydration of OPC $Ca(OH)_2$ is liberated out, which will later act as an activating agent and will encourage BFS to hydrate (22,157-159).

There is little difference in appearance between the 2 and 9 day samples of OPC/BFS cured in cc(1). Figure 4.16 forOPC/BFS after 29 days. Shows a different texture of the fracture surface. The hydration reaction at this age for blended cements is relativly active, and more C-S-H gel formation which surrounds the remaining BFS grains. In comparing the blended cement to OPC at this stage, both show that hydration is well in progress. Figure 4.17 shows that 61 days, is, for the BFS based cement sample a compact and continuous structure, which compares well with OPC. Results generally confirm the slower rate of hydration of OPC/BFS at an early stage of curing compared to OPC.

The X-ray diffraction for the above samples of OPC/BFS using cc(1) at 2 , 8, 29 and 61 days, can be seen in figure 4.22. In comparing the X-ray diffraction traces for the 2 day samples, to unhydrated blended cements, figure 4.9, a clear difference can be seen between the two set of peaks, indicating that hydration has taken place even after 2 days of curing. For the hydrated blended cements at the different ages, apart from the normal sharp peaks there is also a distinct broad line, which represents the glassy phases of the slag (157).

During hydration under cc(1) the $Ca(OH)_2$ peaks are evident after 2 days, and thereafter remain almost constant, presumably as a result of the interaction between the phases of the slag and $Ca(OH)_2$. The C_3A peak eventually disappears but takes longer than for the OPC, similarly there is some decrease in the C_3S and C_2S peaks, but in comparison to OPC, it is much less.

The DTA for the above samples, as shown in figure 4.24 indicate the different characteristics of the two types of cement, when subjected to cc(1). Calcium hydroxide is evidently reduced by blending the OPC with BFS. Furthermore an exothermic peak appears at about 950^{o}C for the OPC/BFS cement, which is due to the devitrification of the glassy phase (160).

The fracture surface for OPC/BFS at 2 , 9, 29 and 61 days for cc(3), are as shown in figures 4.18 - 4.21. At 2 days, the surface texture was similar to cc(1). There was also little change in the structure after 8 days, under cc(3). The structure of the surface texture at 29 and 61 days was still very porous and there was little difference between them, suggesting that hydration had slowed down considerably.

Results for X-ray diffraction for the same samples are shown in figure 4.23. There is little difference between the relative height of the peaks at 2 , 8 , 29 and 61 days, which indicates that there was little change in the degree of hydration, even after 61 days, as was previously observed in the SEM study.

Comparing the DTA thermographs, figures 4.24 and 4.25, there appears to be only a minimal difference between cc(1) and cc(3), except for the presence of the carbonation peak at 800^{o}C, which is more prominent for cc(3), suggesting a minor carbonation reaction.

The results of the SEM and X-ray diffraction for cc(1) at 8 , 29 and 61 days for both OPC and OPC/BFS compare favourably with the results of the MIP experiment discussed in chapter 3. For example after 28 days of hydration the total volume of pores as determined by the MIP is lower for both cement types, than after 7 days as hydration progresses. In the case of cc(3) for both cement types at 7 , 28 and 60 days, the total volume of pores were all equally high, which indicates that the hydration reaction has slowed down considerably, as compared to cc(1).

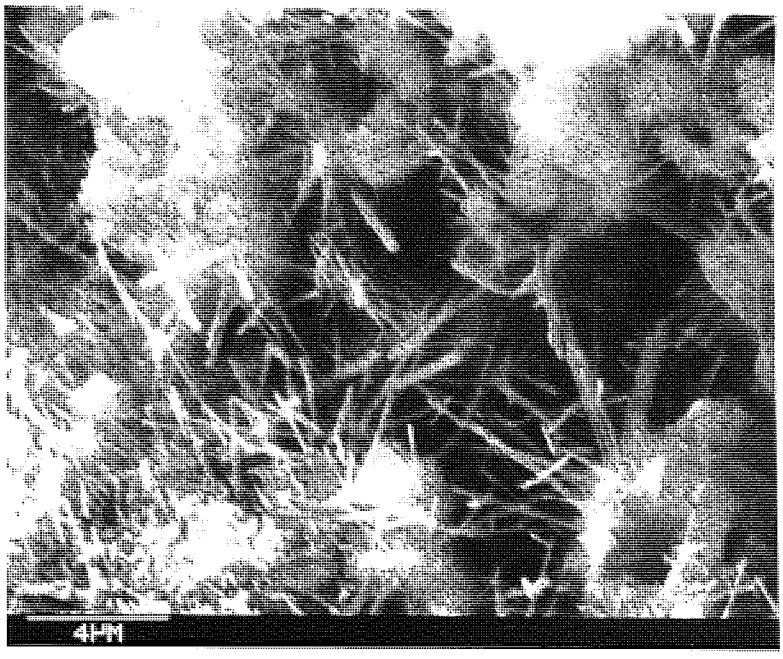

Figure 4.1 SEM micrograph of the fracture of OPC paste after 48 hours hydration under cc(1).

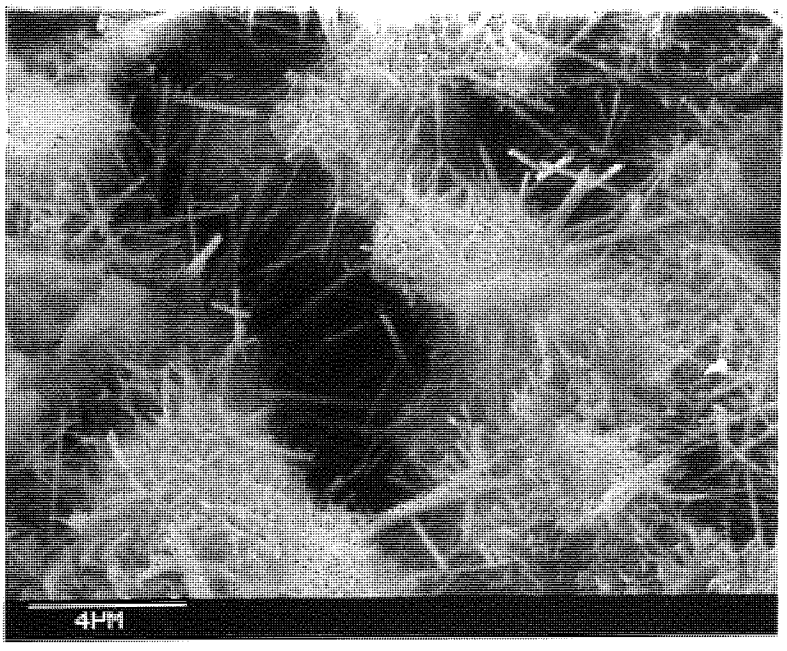

Figure 4.2 SEM micrograph of the fracture surface of OPC after 8 days hydration under cc(1).

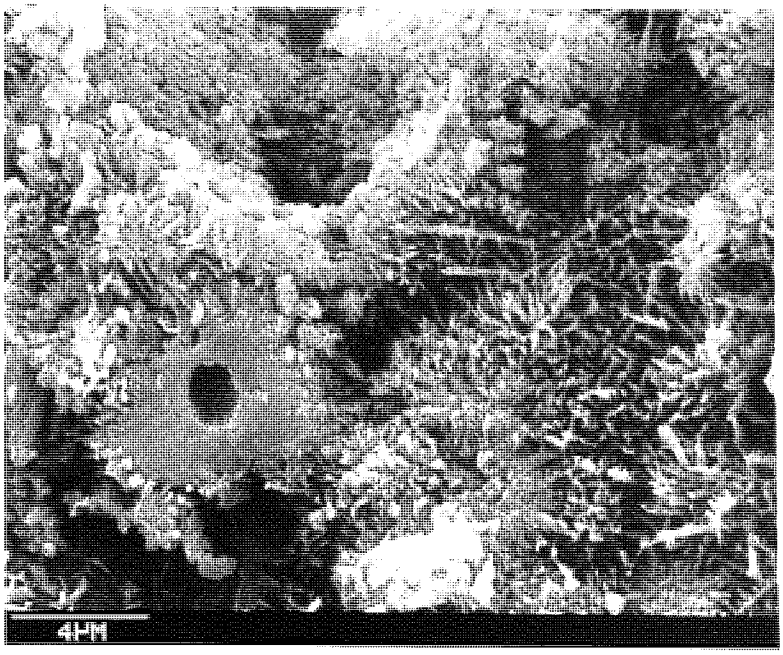

Figure 4.3 SEM micrograph of the fracture surface of OPC after 29 days hydration under cc(1).

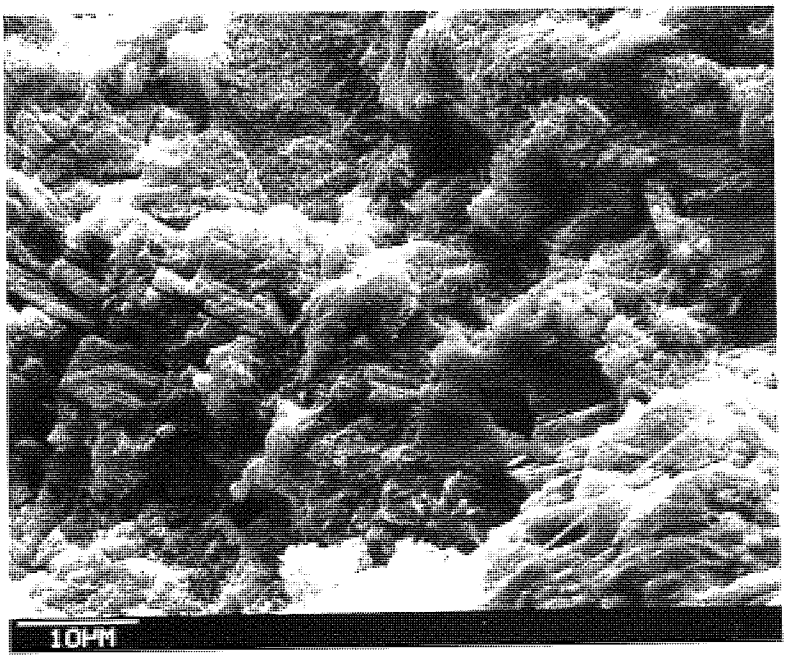

Figure 4.4 SEM micrograph of the fracture surface of OPC after 61 days hydration under cc(1).

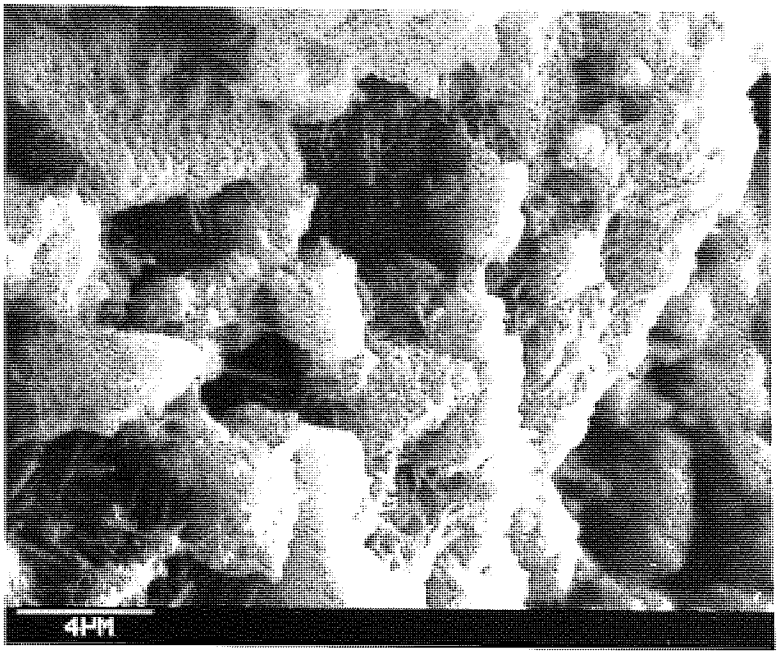

Figure 4.5 SEM micrograph of the fracture surface of OPC after 48 hours hydration under cc(3).

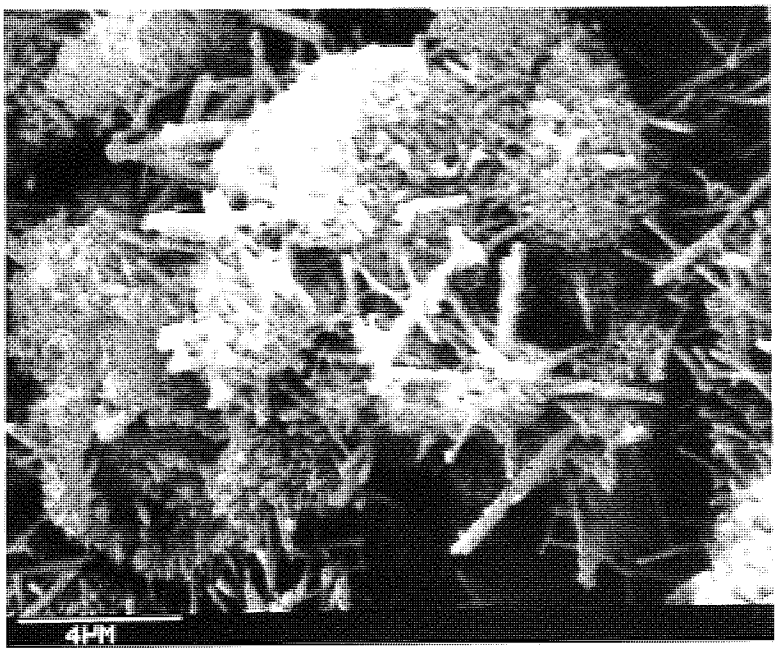

Figure 4.6 SEM micrograph of the fracture surface of OPC after 8 days hydration under cc(3).

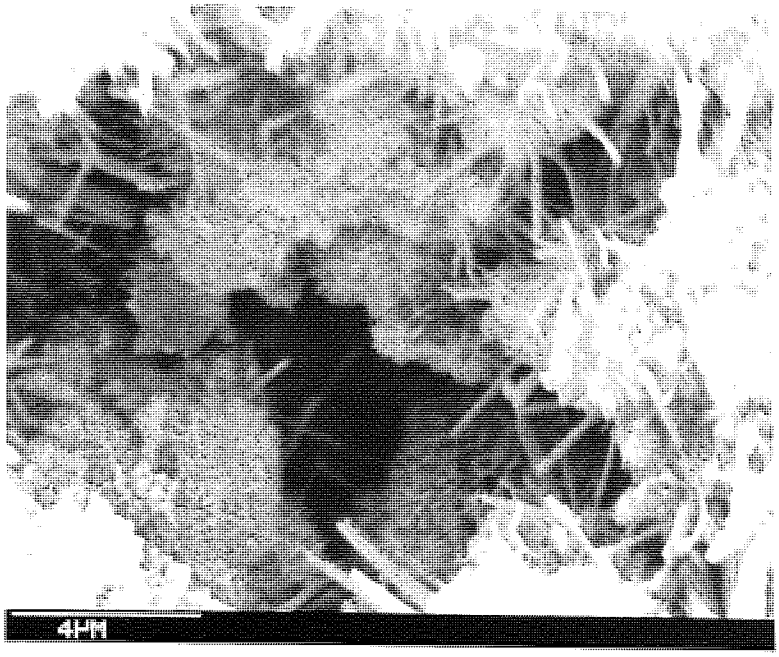

Figure 4.7 SEM micrograph of the fracture surface of OPC after 29 days hydration under cc(3).

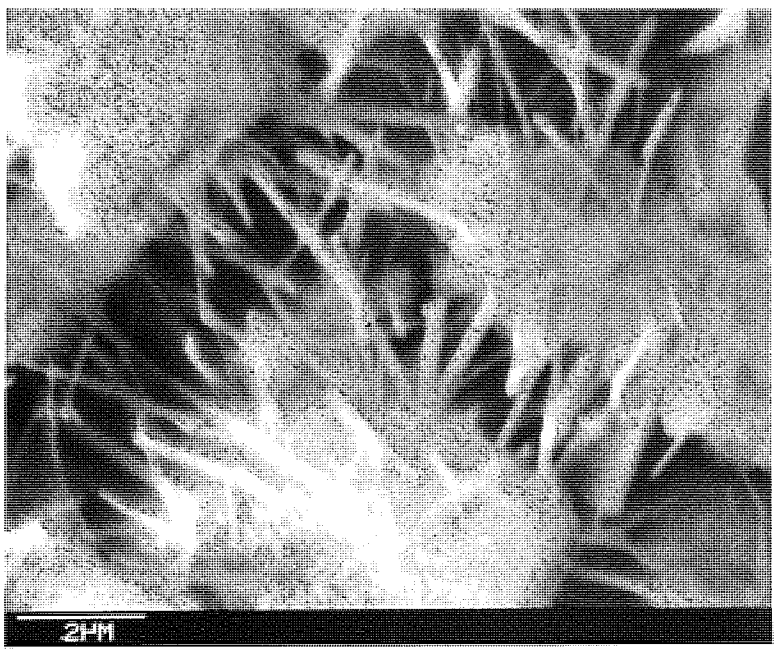

Figure 4.8 SEM micrograph of the fracture surface of OPC after 61 days hydration under cc(3).

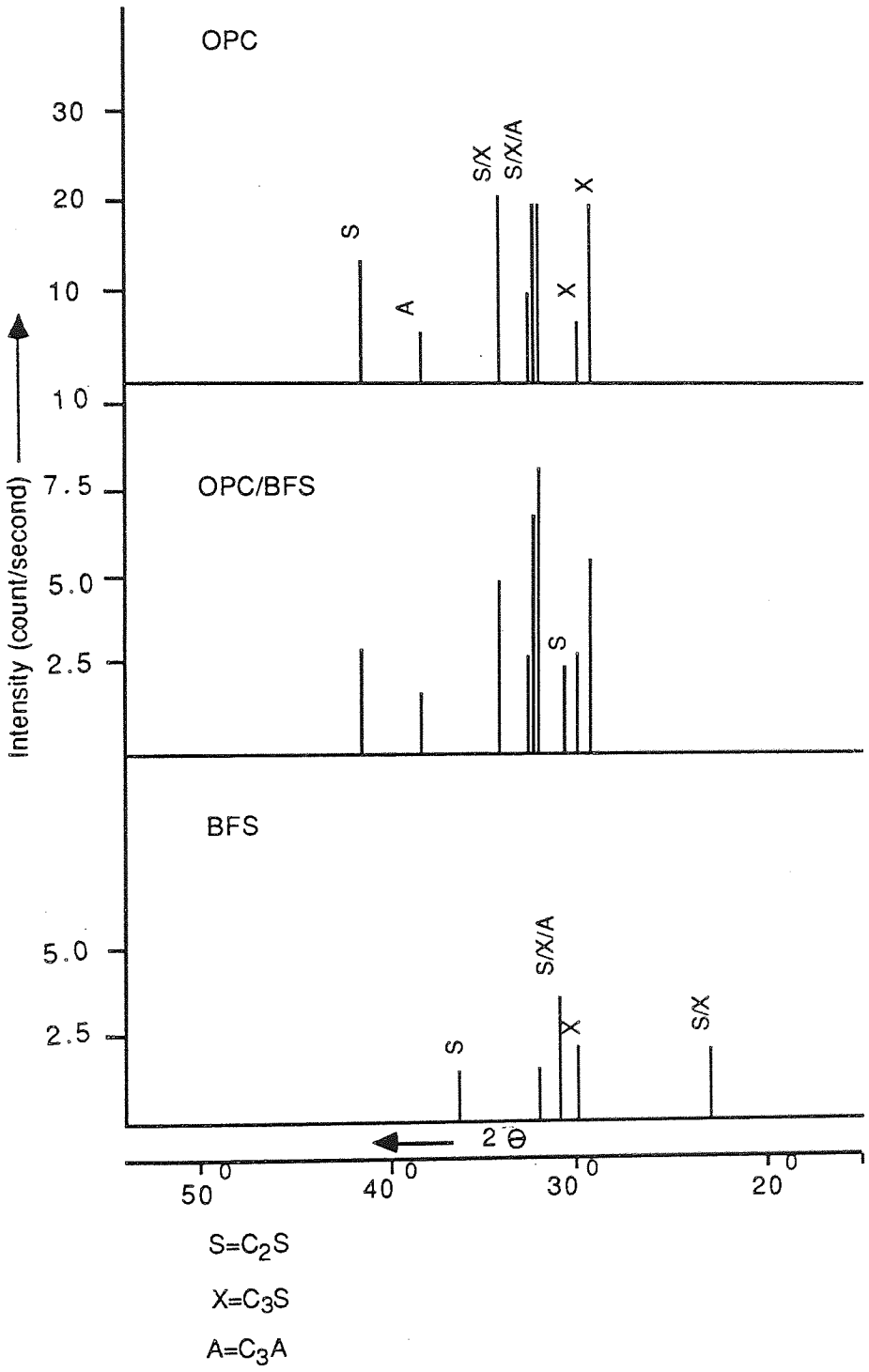

Figure 4.9 XRD traces of unhydrated OPC, OPC/BFS and BFS.

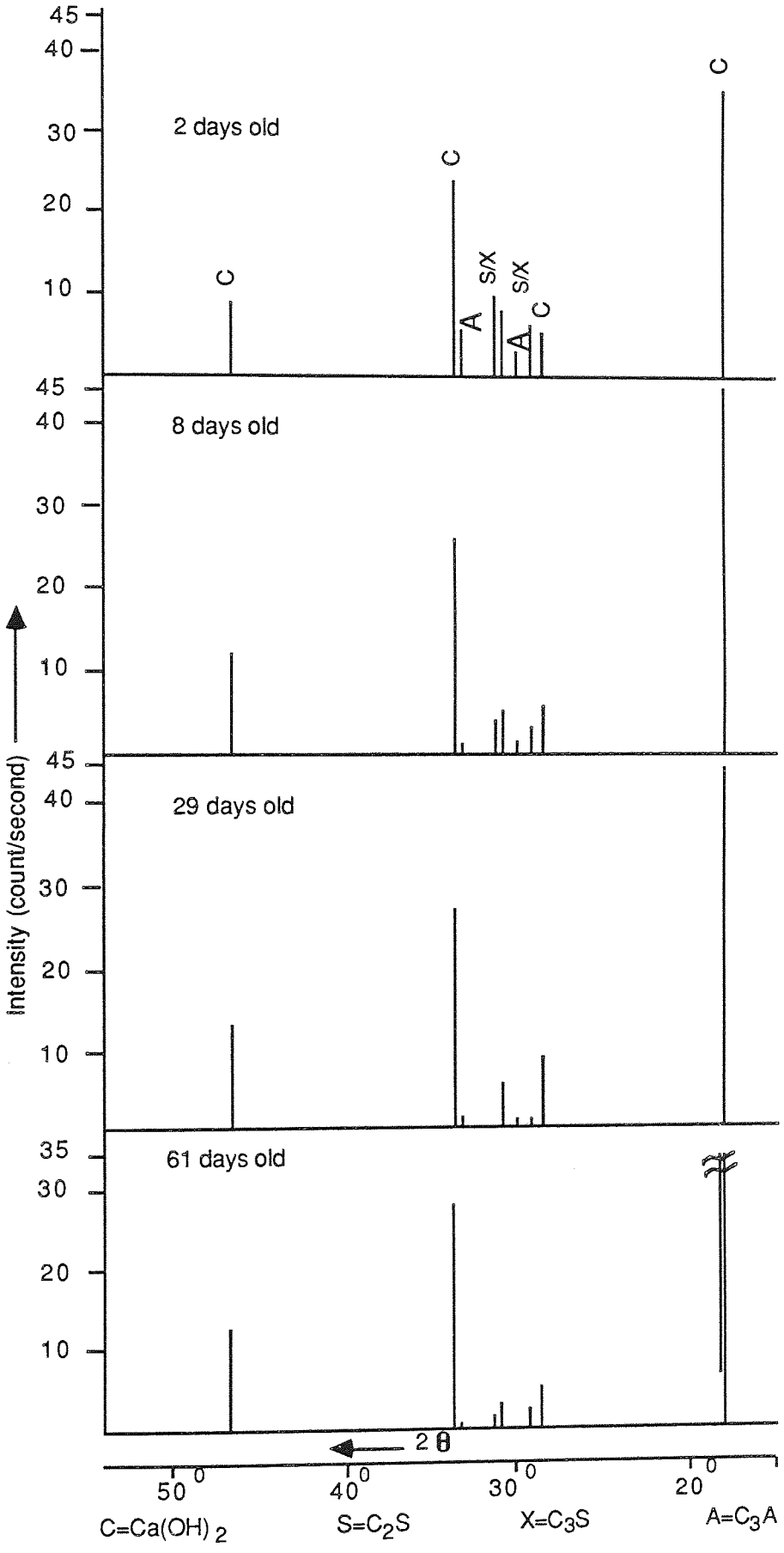

Figure 4.10 XRD traces of OPC samples cured under cc(1) for different times.

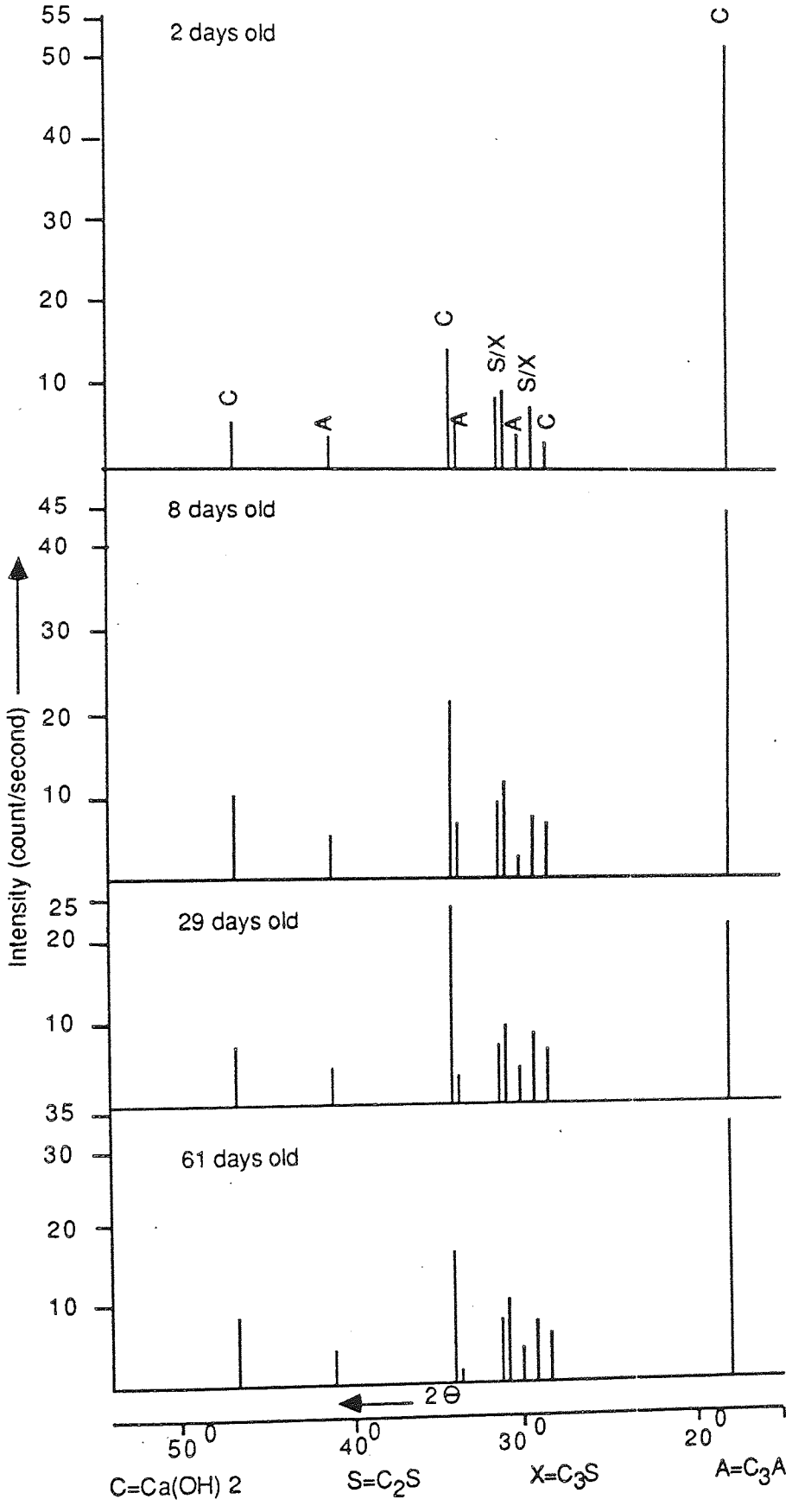

Figure 4.11 XRD traces of OPC samples cured under cc(3) for different times.

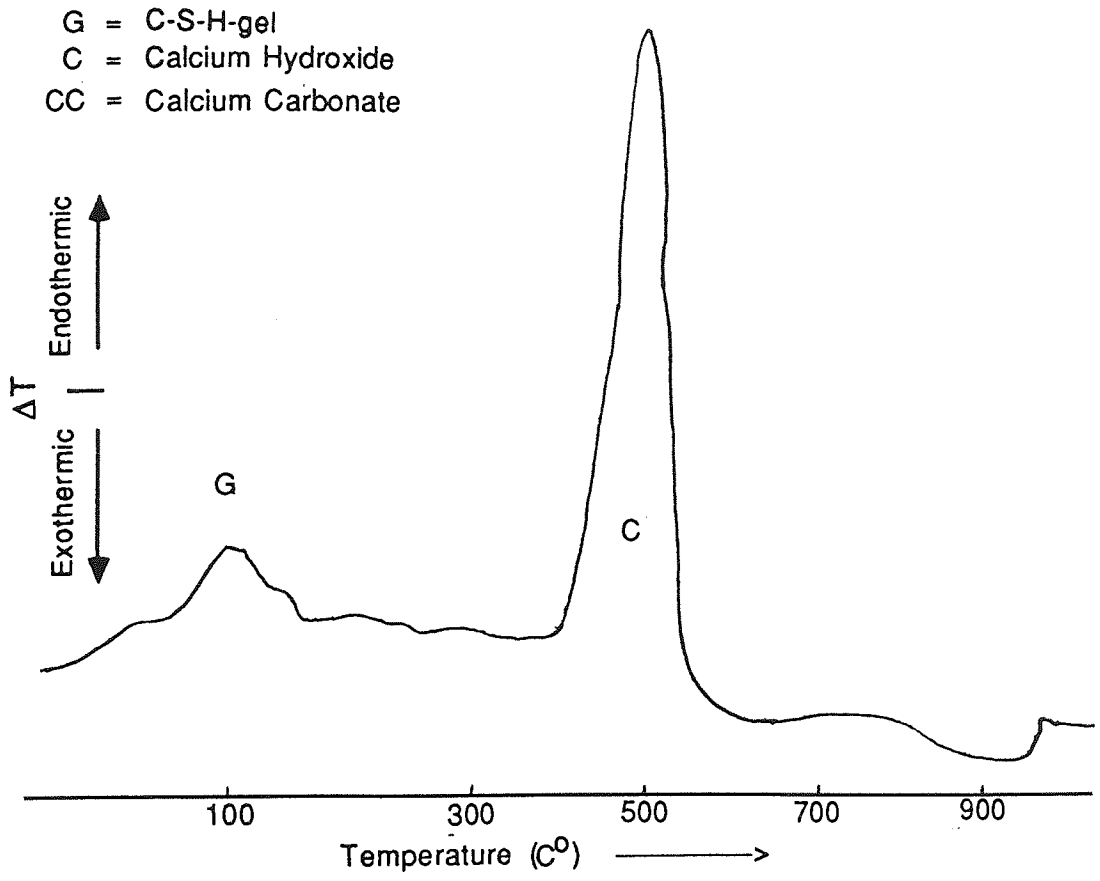

Figure 4.12 DTA thermograph of OPC cement paste cured under cc(1).

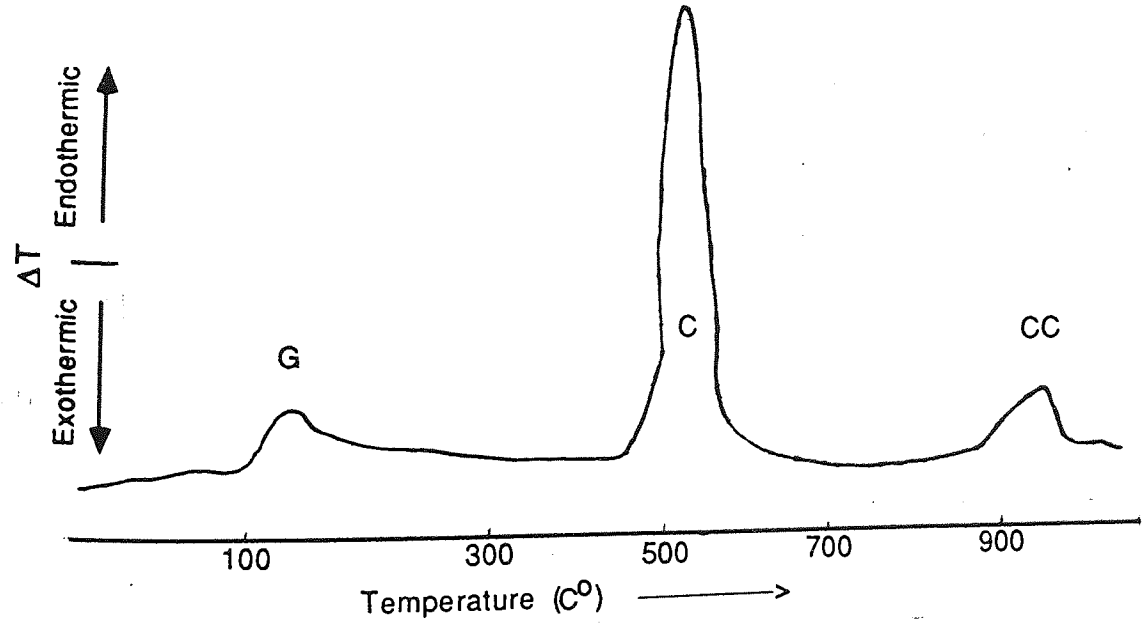

Figure 4.13 DTA thermograph of OPC cement paste cured under cc(3).

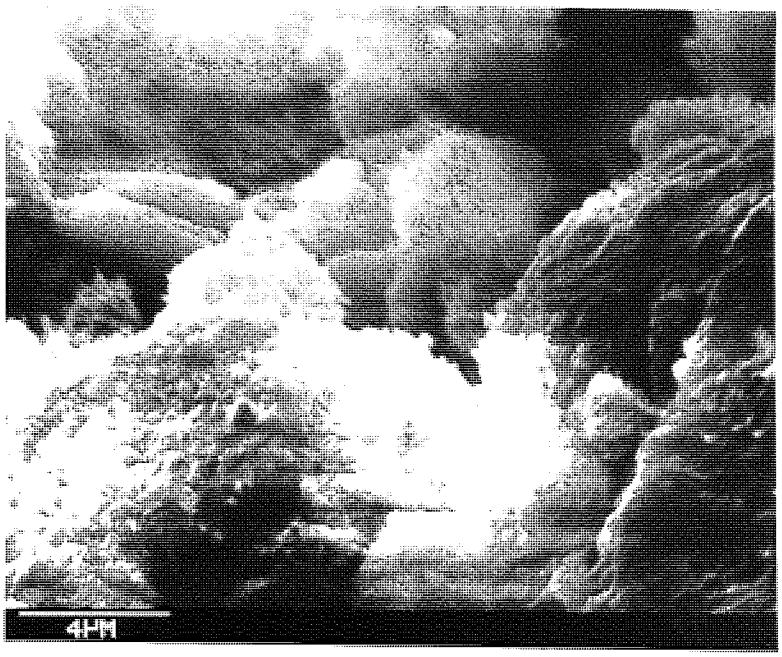

Figure 4.14 SEM micrograph of the fracture surface of OPC/BFS after 48 hours hydration under cc(1).

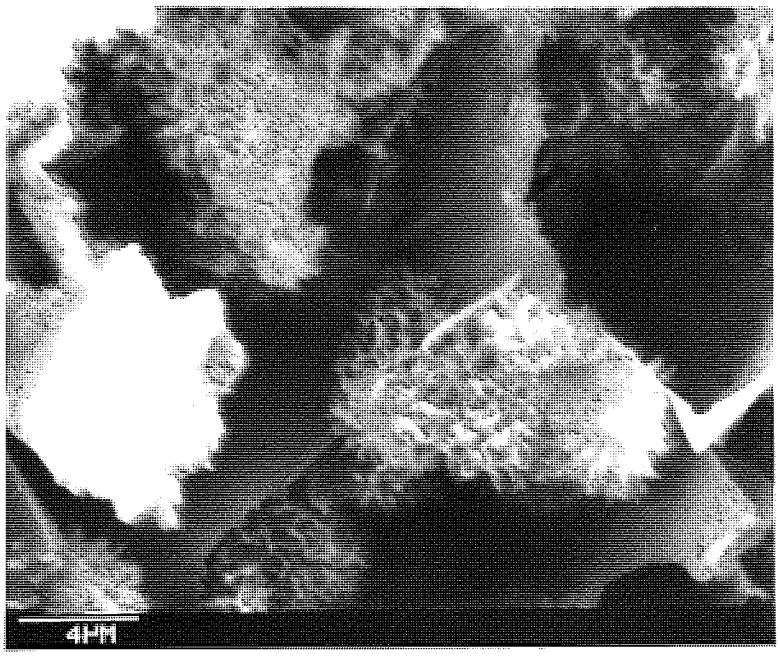

Figure 4.15 SEM micrograph of the fracture surface of OPC/BFS after 8 days hydration under cc(1).

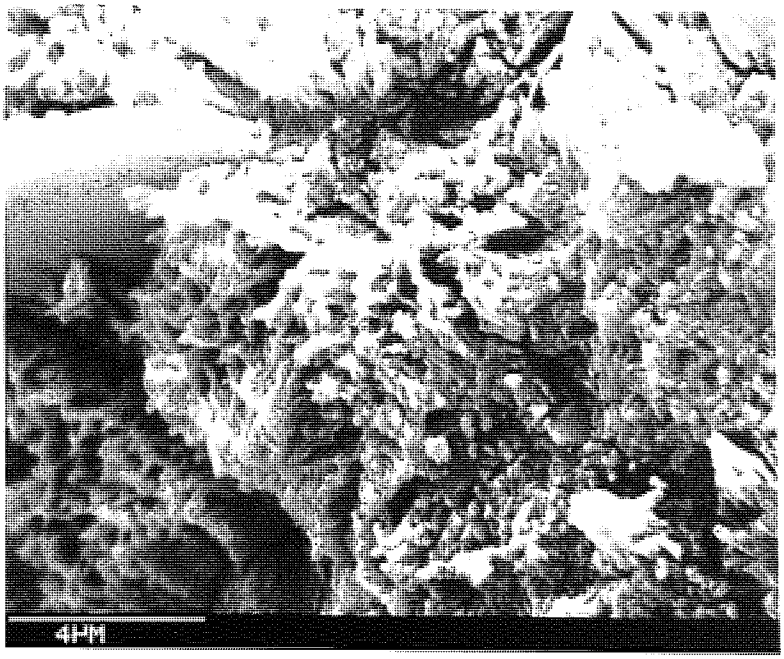

Figure 4.16 SEM micrograph of the fracture surface of OPC/BFS after 29 days hydration under cc(1).

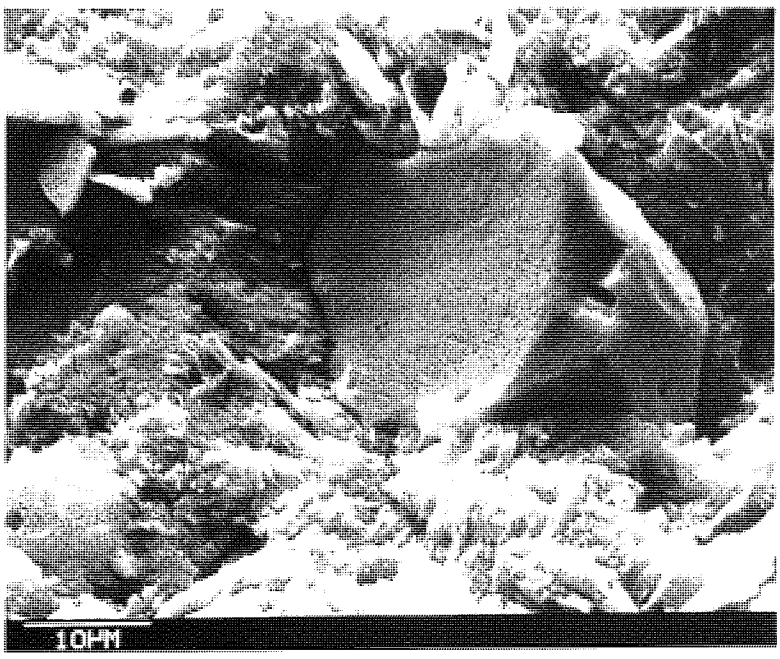

Figure 4.17 SEM micrograph of the fracture surface of OPC/BFS after 61 days hydration under cc(1).

Figure 4.18 SEM micrograph of the fracture surface of OPC/BFS after 48 hours hydration under cc(3).

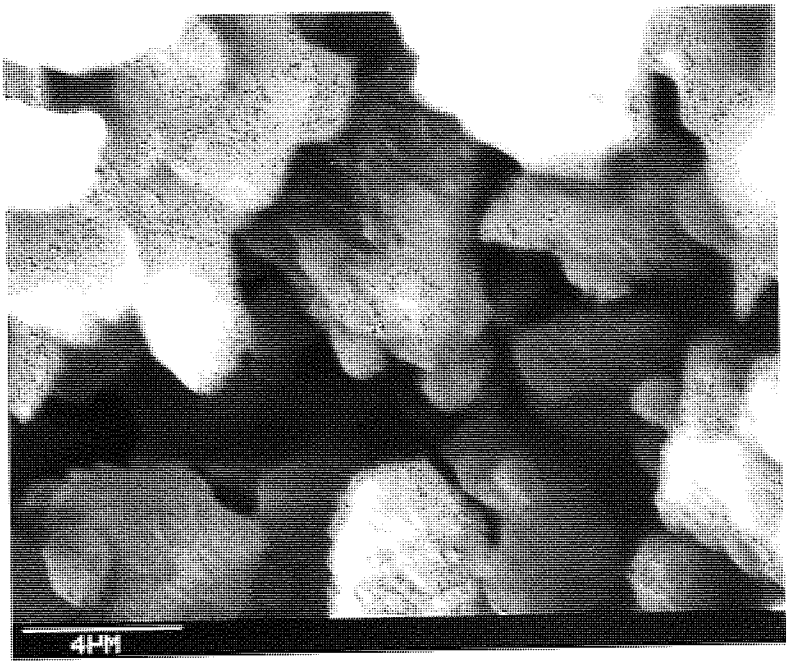

Figure 4.19 SEM micrograph of the fracture surface of OPC/BFS after 8 days hydration under cc(3).

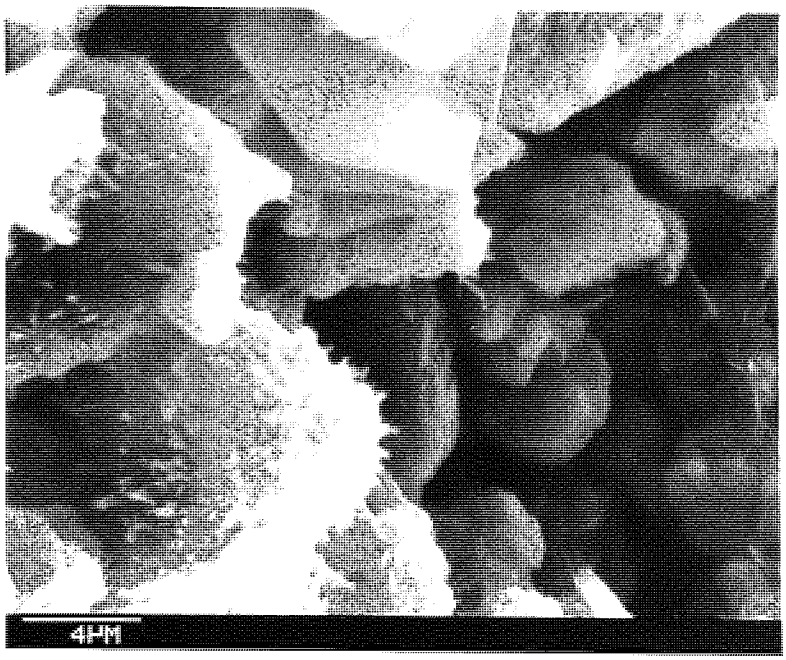

Figure 4.20 SEM micrograph of the fracture surface of OPC/BFS after 29 days hydration under cc(3).

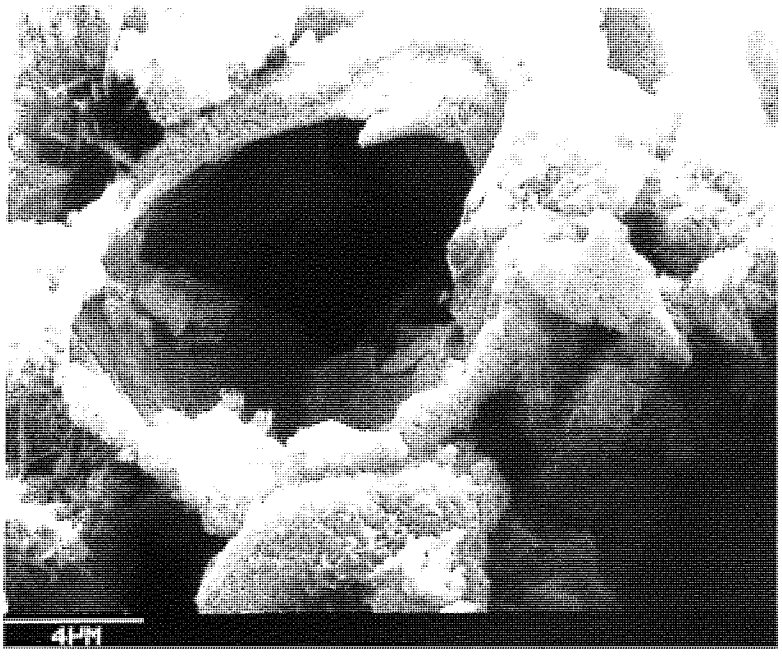

Figure 4.21 SEM micrograph of the fracture surface of OPC/BFS after 61 days hydration under cc(3).

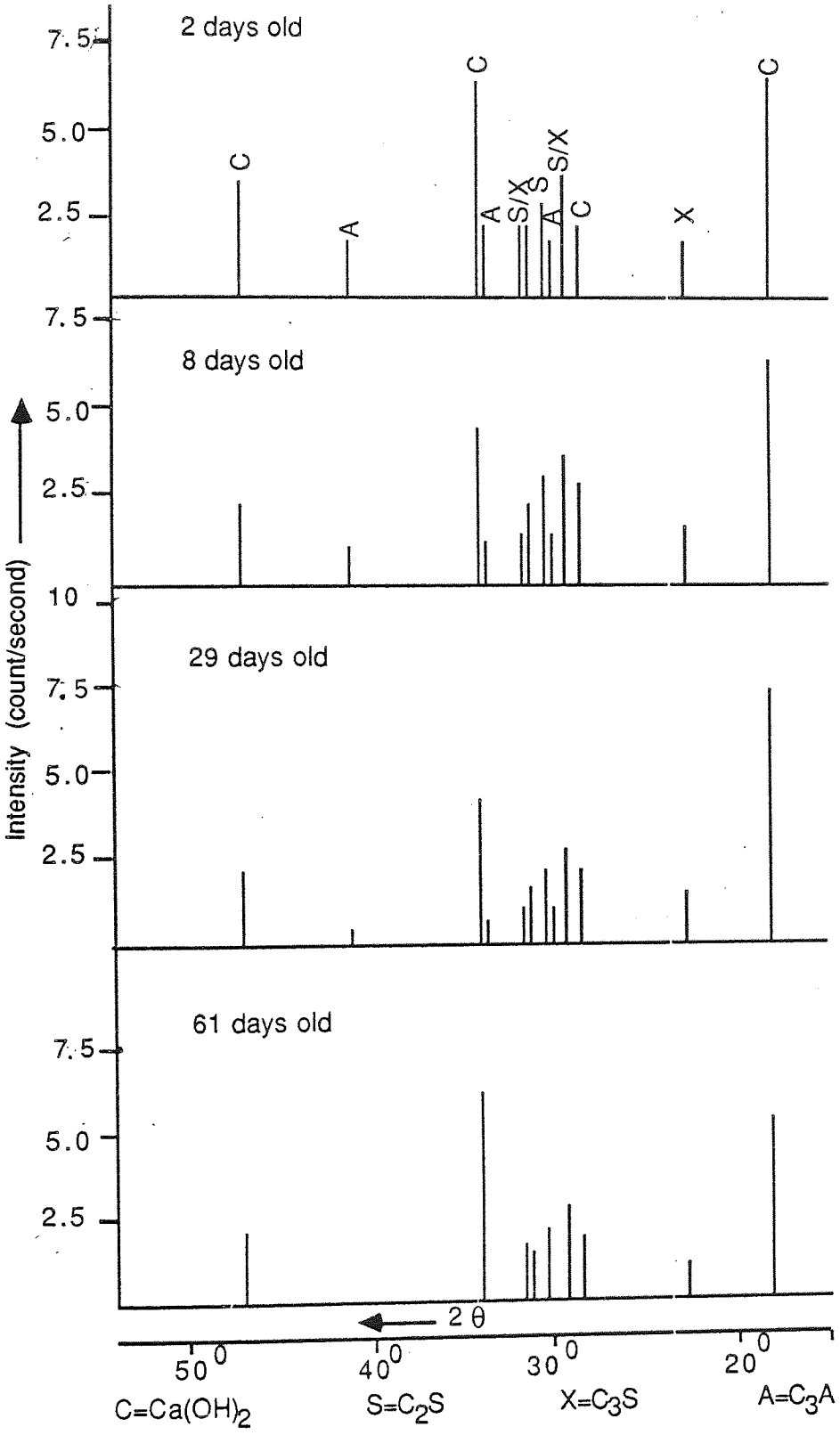

Figure 4.22 XRD traces of OPC/BFS samples cured under cc(1) for different times

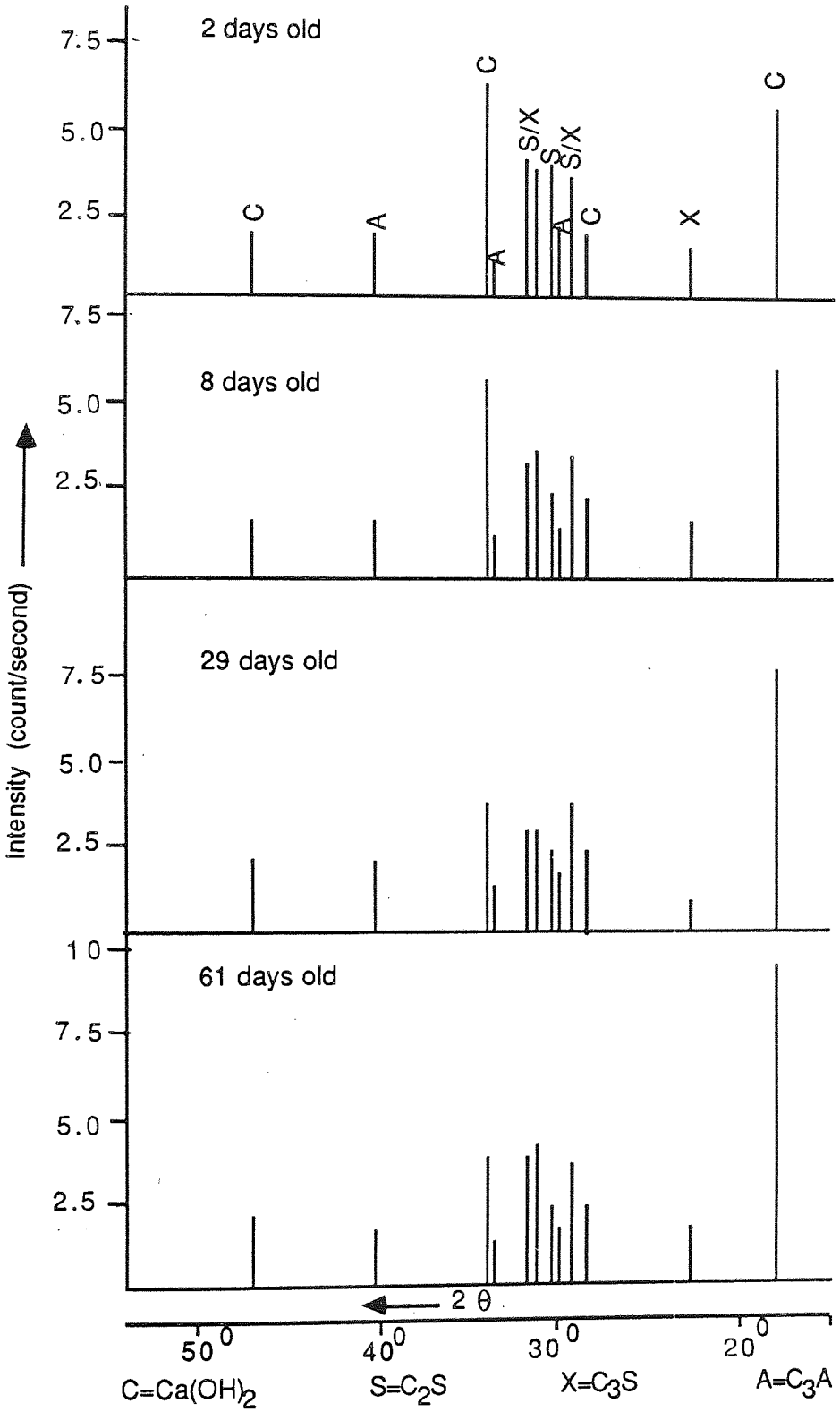

Figure 4.23 XRD traces of OPC/BFS samples cured under cc(3) for different times.

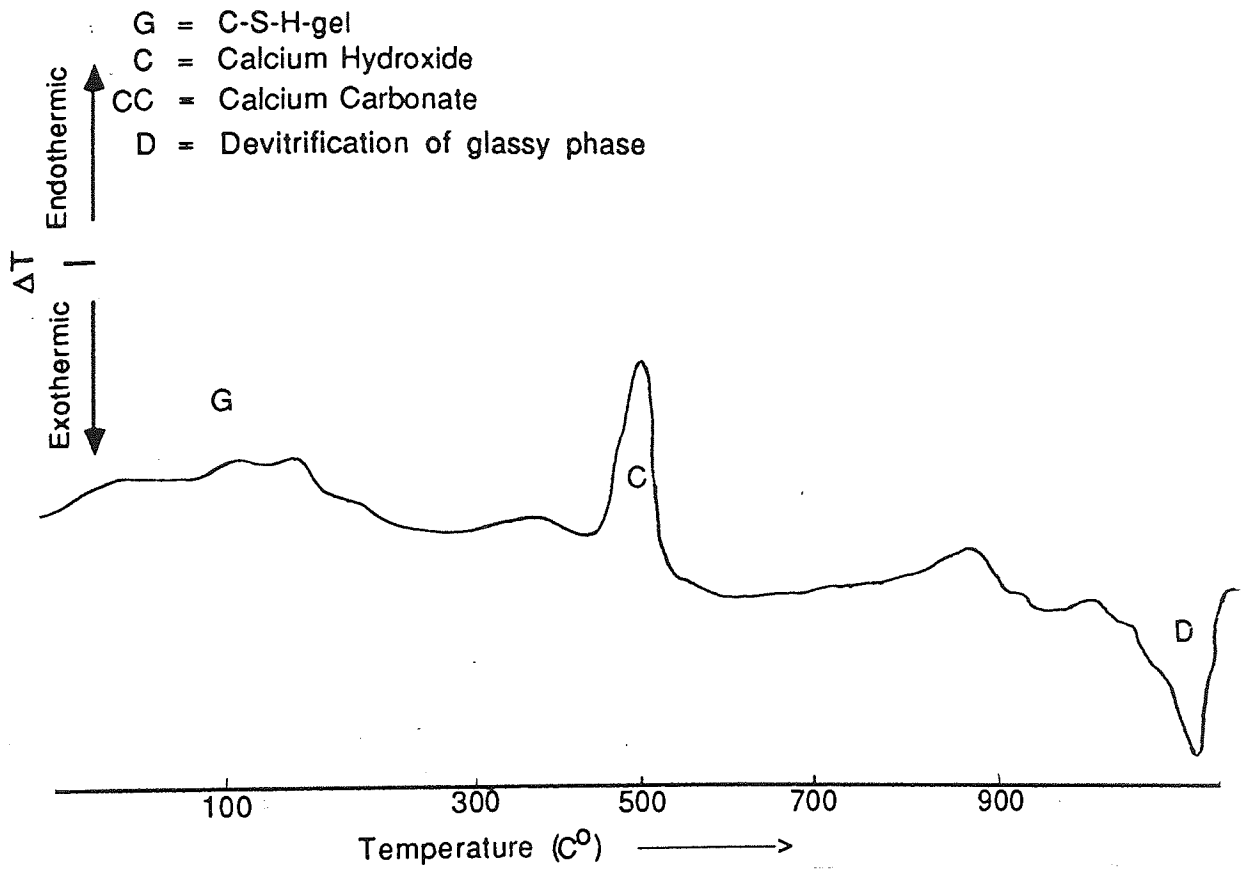

Figure 4.24 DTA thermograph of OPC/BFS cement paste cured under cc(1).

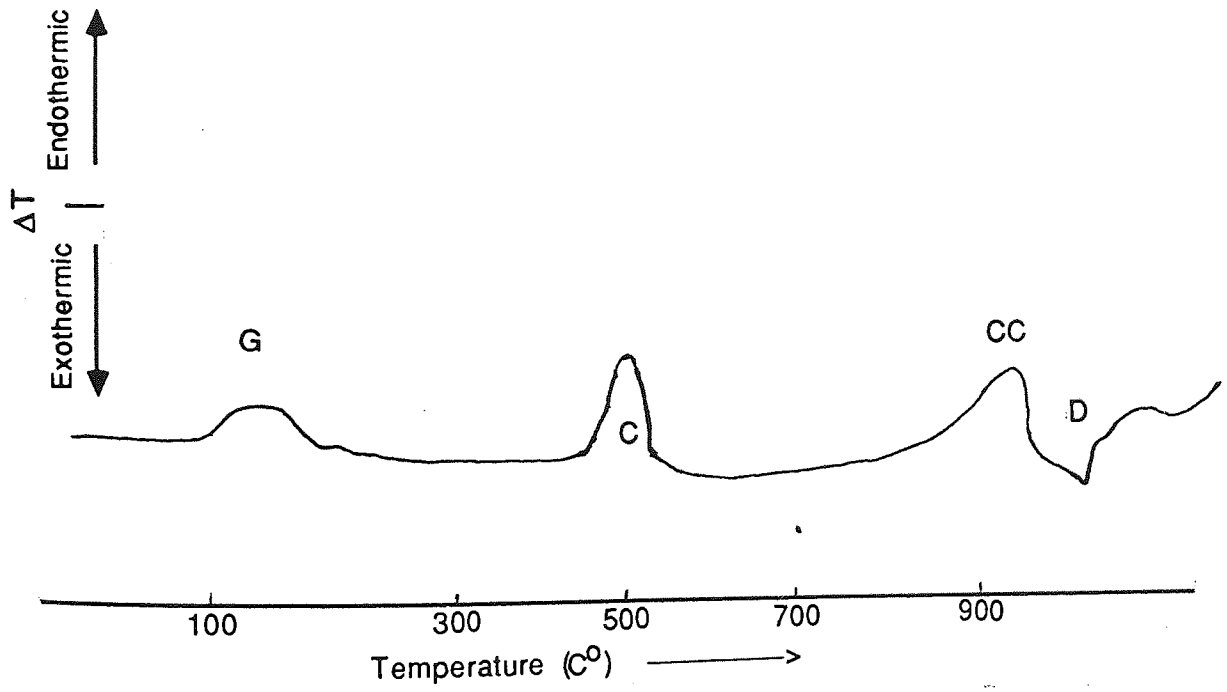

Figure 4.25 DTA thermograph of OPC/BFS cement paste cured under cc(3).

4.3 CONCLUSIONS

a) For well cured samples of OPC, it was shown that a relatively long network of C-S-H fibres, grows radially from the top surface of the calcium silicates, this being observed at an early age of hydration, i.e. 2 days to 29 days. These fibres interlock with neighbouring particles to form eventually a compact continuous structure. Hexagonal plate-shape crystals of $Ca(OH)_2$ are also present in the matrix. Calcium silicate hydrate and calcium hydrate result from the hydration of calcium silicates.

b) For the blended cement OPC/BFS the needle-shaped fibres are shorter figures (4.1 , 4.14). This is because the granulated BFS reacts at a slower rate than the OPC constituents.The hydration of the BFS is activated by $Ca(OH)_2$ produced during the hydration of OPC. This was evident from the DTA results, which indicated that $Ca(OH)_2$ peak intensity for OPC were nearly three to four times as much as for blended cements.

c) XRD for the above cements and same curing conditions showed there are major phase changes occuring, even after 48 hours of hydration, i.e. C_3A peak for OPC disappears at this age, but in the case of blended cements since the hydration is slower, this peak can still be seen but not as much as for unhydrated samples.

d) For badly cured samples of OPC and OPC/BFS, it is clear that because of the fast evaporation of the moisture when samples are subjected to cc(3) the hydration reactions are almost immediately terminated. From the results obtained it is evident that a very loose structure, where the particles are independent of one another exists. This observation agrees with the MIP results where higher porosities and coarser pore structure were obtained for these conditions (see chapter 3).

e) XRD for the poor curing condition, shows that C_3A is normally the first compound to hydrate. However after 61 days this can still be detected, for both OPC and OPC/BFS and is more so for blended cement.

5.1 RESULTS AND DISCUSSION

5.1.1 Changes in Properties of Polymer Impregnated Cement

The samples used in this part of the work were cylinders of 47mm diameter and 74mm length. Preparation of the cement paste has already been explained in chapter 2. section 2.1.2. The cements used were OPC, OPC/BFS, OPC/PFA and SRPC, at 0.4 and 0.6 water/cement ratio, both at cc(1) and cc(3). Initially polymer impregnation was confined to OPC and OPC/BFS of water/cement ratio 0.6 cured under curing condition 3, for 28 days.

Physical Changes

Table 5.1 shows the percentage of polymer loading by weight, from which it is possible to calculate the volume of polymer within the pores of the samples. Using volume of total porosity determined in chapter 3. it is then possible to calculate the % of pores filled by polymer, (an example calculation can be seen in appendix 7). These results show that for OPC pastes up to 70% of the total pore volume of the samples are filled or blocked with polymer, this figure being 62% for OPC/BFS cement. Thus there is a reduction in total pore volume, which is reflected in the pore size distribution. This can be seen from MIP cumulative pore size distribution curves shown in figure 5.1, where curve (a) is for an unimpregnated sample and curve (b) for a similar impregnated sample. The difference between the two curves can be explained as follows.

It is evident that there is a substantial drop in total pore volume, a large

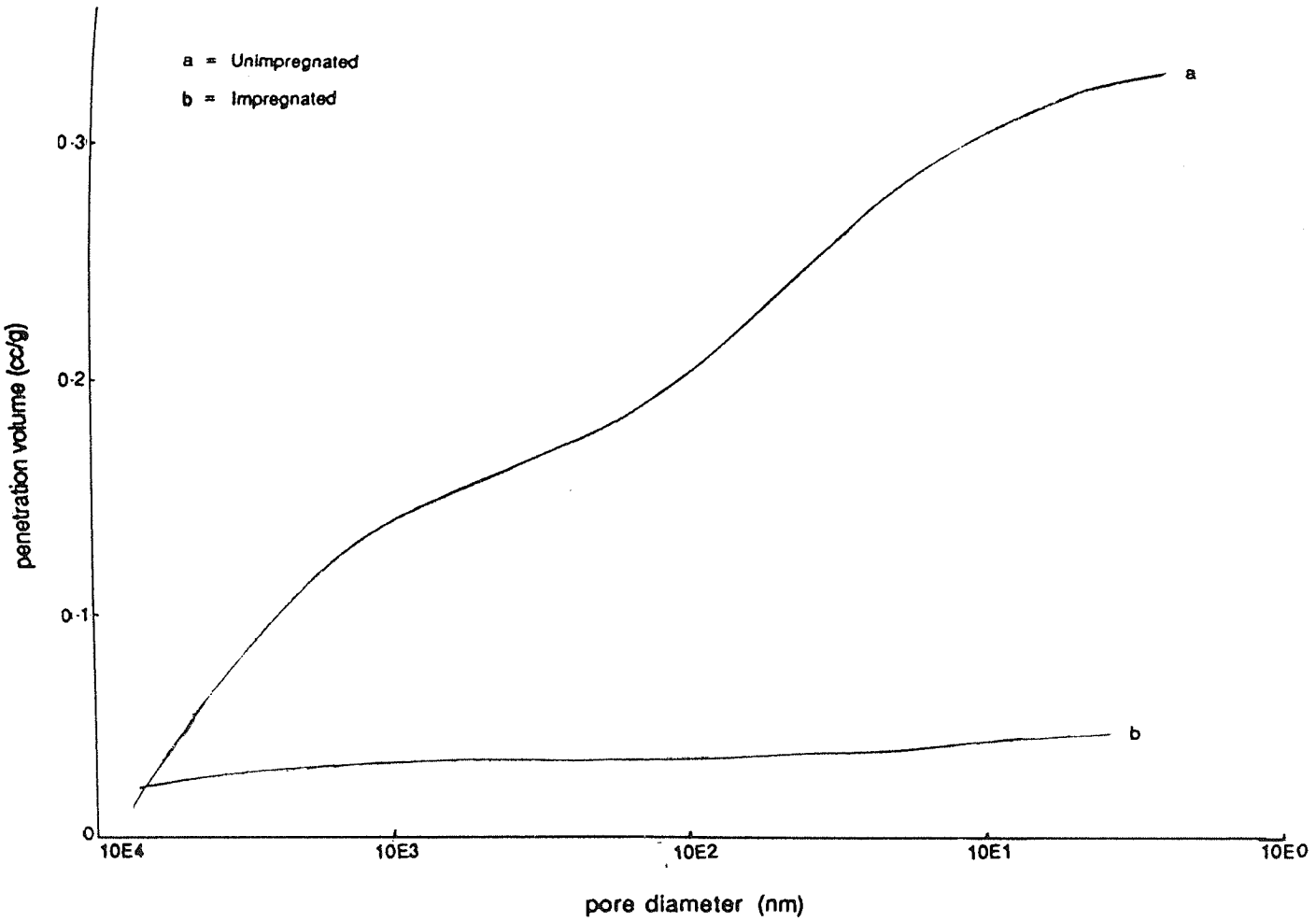

Figure 5.1 Pore size distribution curves of polymer impregnated and unimpregnated OPC pastes of 0.6 water/cement ratio cured under cc(3).

number of pores having been filled with polymer. Monomer penetration takes place within the samples during the soaking period and eventually converts to polymer at a temperature of 85^{o}C for a duration of 5 hours. The monomer that has formerly filled the pores will shrink to a smaller volume and may vacate part of the pores. The MIP curves show that there are still some pores which are not polymer filled and into which mercury can still be intruded.

The MIP results for OPC/BFS, figure 5.2, show a similar pattern to the OPC results, except that the total pore volumes for both impregnated and unimpregnated samples are greater than for OPC.

Fracture surfaces of the samples were examined in the SEM at two different depths (a) outer layer (area of the sample close to the circumference of the cylinder) and (b) inner layer (from the core of the cylinder, about 23mm in from the circumference). Figure 5.3a,b, shows OPC samples from depth (a). By comparing the SEM photomicrographs of the impregnated sample with those of unimpregnated material, figure 4.7a, chapter 4. cured under the same condition and water/cement ratio, a clear difference in their appearance is visible.

Figure 5.4a,b, shows OPC samples for depth (b). By comparing these micrographs with others for unimpregnated samples, figure 4.7, Chapter 4. of the same age and curing condition, it can be seen that polymerisation has taken place even at this depth, the normally fairly clear structure of the unimpregnated samples is no longer evident as it appears to be coated by the polymer. It is not clear however from the micrograph, whether the amount of polymer is the same as for the specimens from the outer layer of the cylinder.

SEM photomicrographs for the OPC/BFS sample are shown in figure 5.5a,b, for

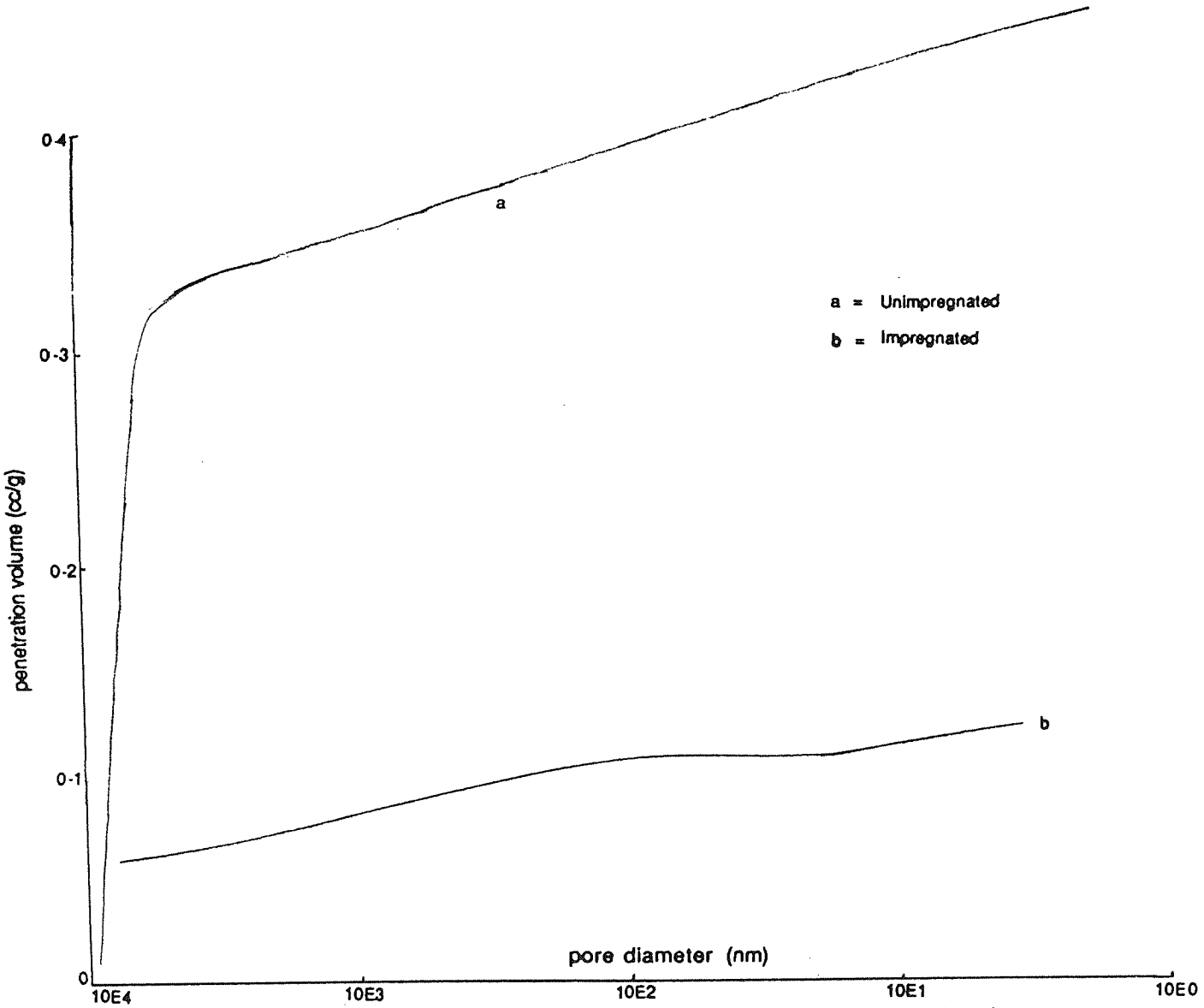

Figure 5.2 Pore size distribution curves of polymer impregnated and unimpregnated OPC/BFS pastes of 0.6 water/cement ratio cured under cc(3).

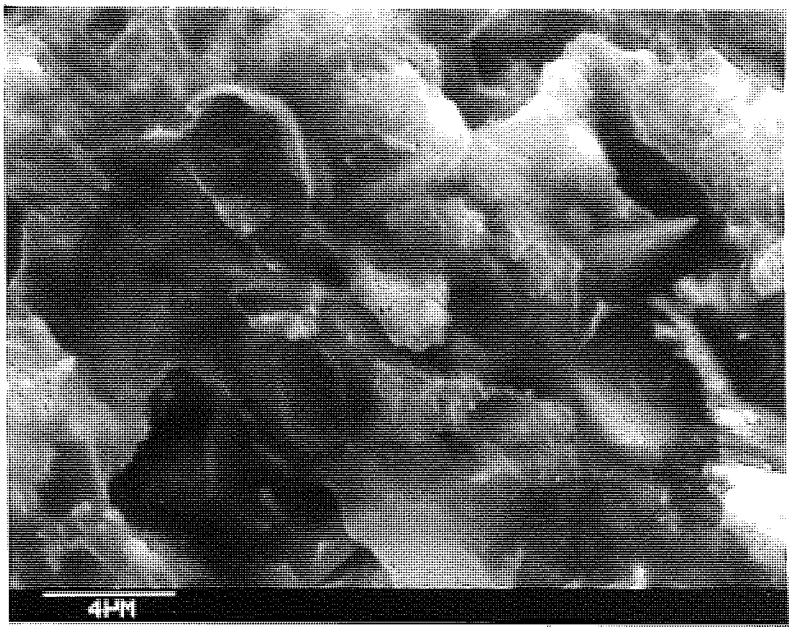

Figure 5.3a

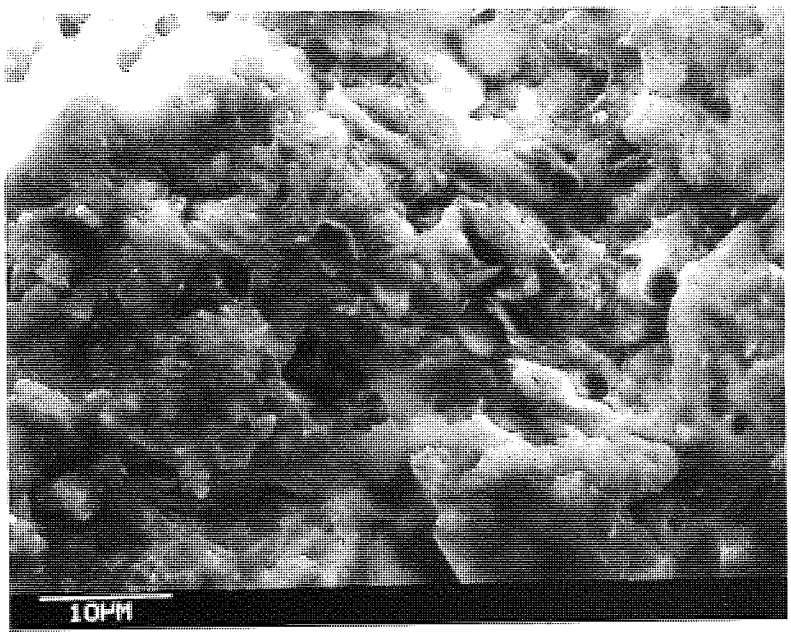

Figure 5.3b

SEM micrographs of different magnification of the fracture surface of the (outer layer) of polymer impregnated OPC of 0.6 water/cement ratio cured under cc(3).

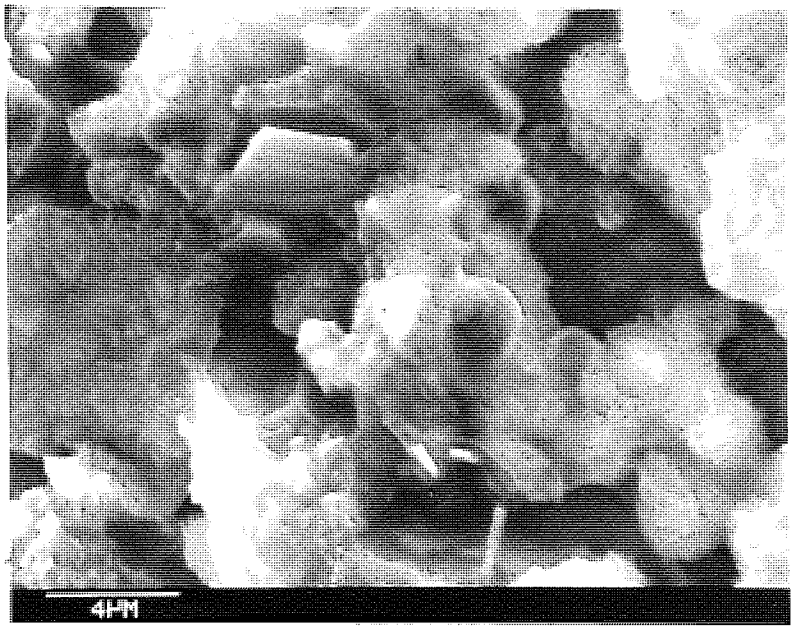

Figure 5.4a

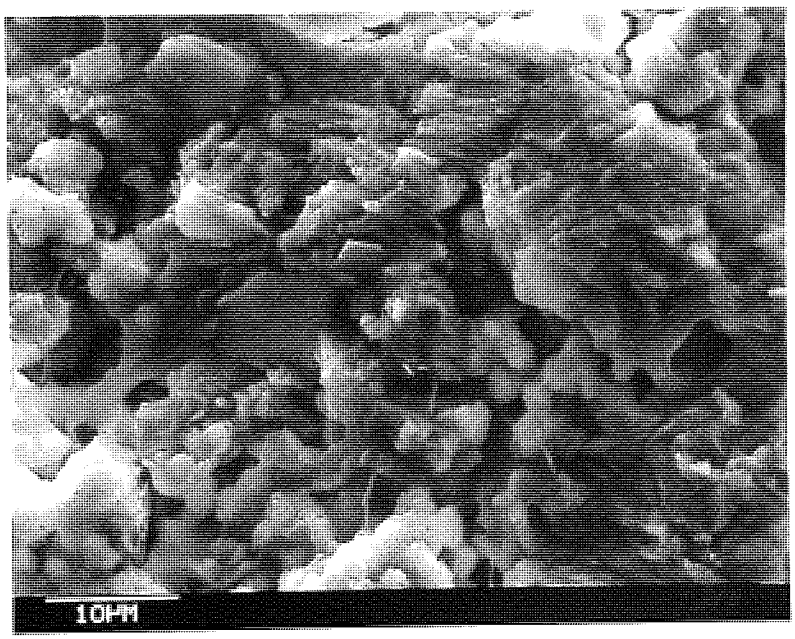

Figure 5.4b

SEM micrographs of different magnification of the fracture surface of the (inner layer) of polymer impregnated OPC of 0.6 water/cement ratio cured under cc(3).

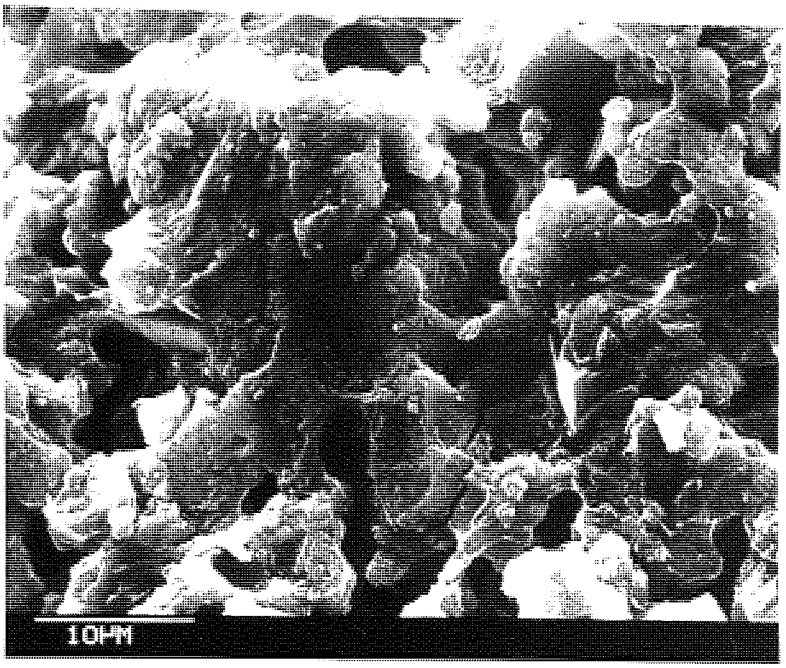

Figure 5.5a

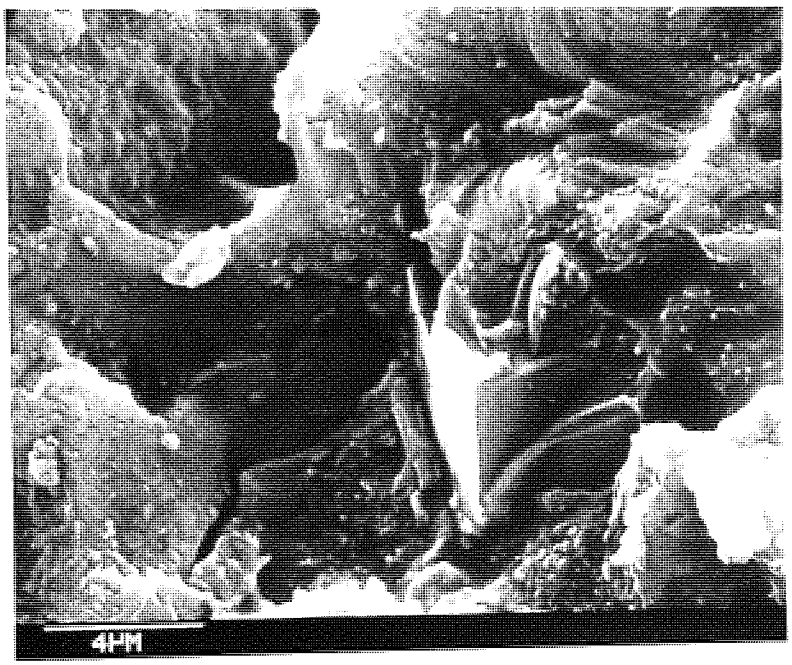

Figure 5.5b

SEM micrographs of different magnification of the fracture surface of the (outer layer) of polymer impregnated OPC/BFS of 0.6 water/cement ratio cured under cc(3).

the outer layer of the samples (depths a). As in the case of the OPC samples, polymerisation has taken place in this region and polymer has converted the hydrated cement into a very compact mass.

By comparing photos 5.3(a) and 5.5(a) to ones of untreated OPC/BFS, figure 4.20, Chapter 4., a clear difference on the fracture surface can be seen. (b) figure 5.6a,b, are of the same samples but taken from the core. The existence of polymer at this depth can be seen. In comparison to an untreated sample figure 4.20, Chapter 4., shows how great this difference is.

Chemical Changes

X-ray diffraction was carried out on pastes of 0.6 water/cement ratio, cc(1) and cc(3) both for impregnated and unimpregnated samples of 28 days curing. These are represented by figure 5.7a and b. For the impregnated and badly impregnated samples, the intensity of the $Ca(OH)_2$ peaks have been reduced drastically, even though there is a general reduction of the C_3S, C_2S, C_3A, peaks as well. Apart from these differences there was no sign of any other peaks corresponding to the formation of any new compound, such as $CaCO_3$.

It is interesting also to note that for the one condition where no polymerisation had actually taken place due to the evaporation of the monomer (i.e. 0.6 water/cement ratio cc(1) the same reduction in the relative intensity of the XRD peaks was observed figure 5.7a,(impregnated).

The intensity of the $Ca(OH)_2$ peaks of the OPC impregnated sample (of figures 5.7 a and b) were found to be consistantly lower than the value of the unimpregnated sample. As an example the peak at 18^o had a relative intensity

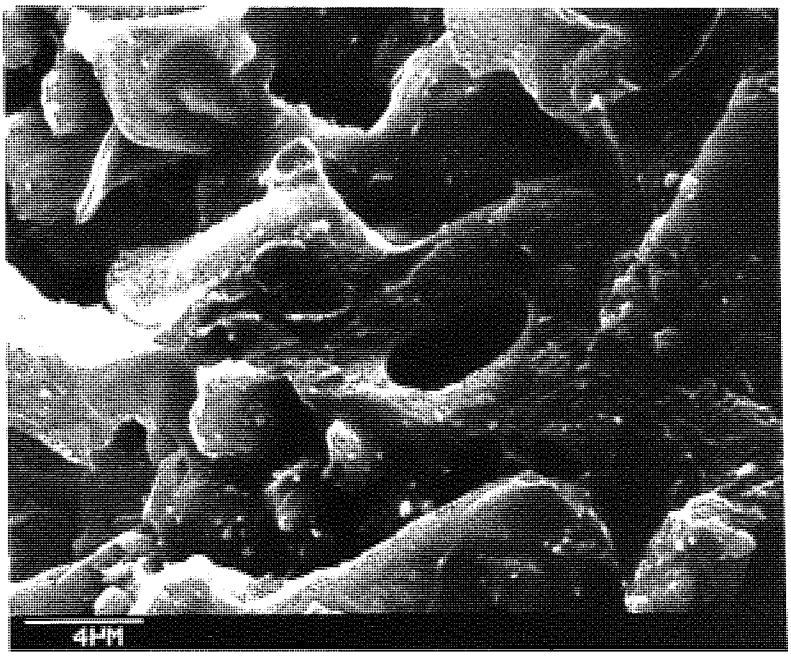

Figure 5.6a

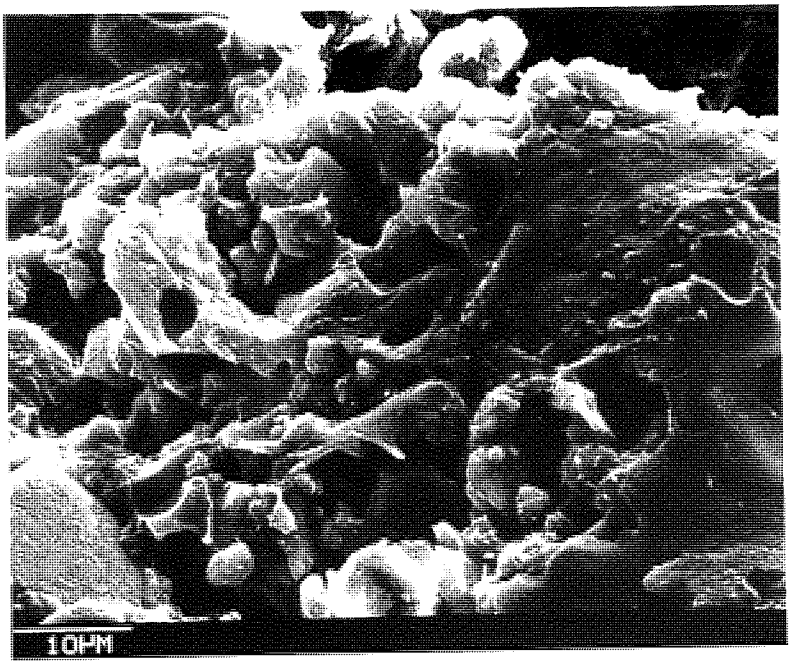

Figure 5.6b

SEM micrographs of different magnification of the fracture surface of the (inner layer) of polymer impregnated OPC/BFS of 0.6 water/cement ratio cured under cc(3).

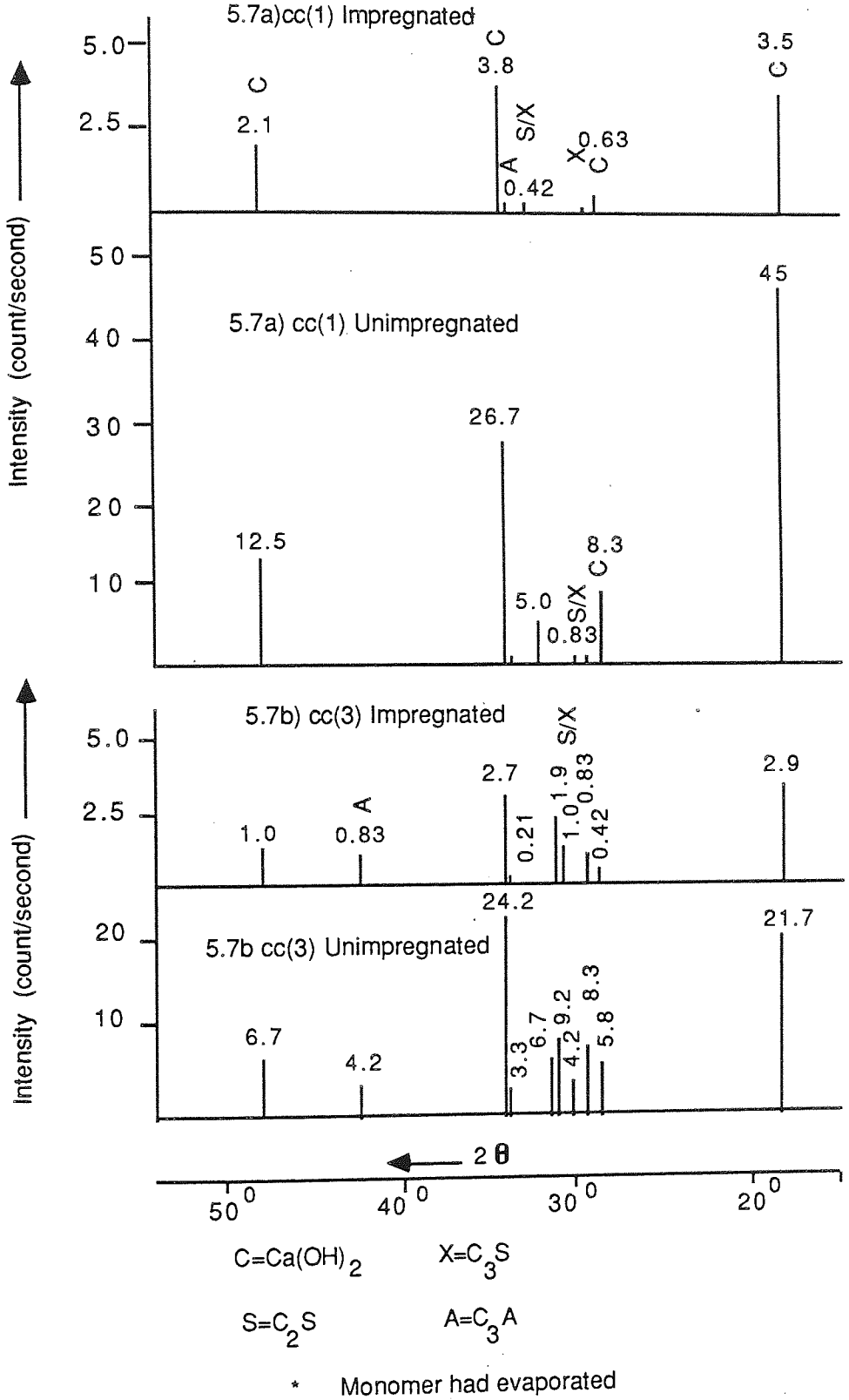

Figure5.7a & b XRD traces of OPC cured originally for 28 days both for polymer impregnated and unimpregnated samples.

of 45 for the unimpregnated sample compared to 3.5 for the impregnated sample (see figure 5.7a). This would suggest that substantial amount of $Ca(OH)_2$ was consumed by chemical interaction with the monomer. A similar reduction of peak intensity was found for the other calcium bearing phases of the sample.

Ramachandran (161) using a different technique e.g. (DTA) has also found that the intensity of the $Ca(OH)_2$ peak in impregnated specimens was reduced, but he related this finding to a reaction between methyl methacrylate and $Ca(OH)_2$ during heating in the DTA furnace, a suggestion which cannot apply in this work, since X-ray diffraction did not involve any heating. However he did not rule out the possibility of some reaction at the interface between polymer and cement paste, a fact suggested also by Gebauer and Cougglin (162), but the amount so reacted would be small and be undetected by DTA.

The conversion of the monomer to a polymer with a catalyst agent such as Benzoyl peroxide, which is an unstable chemical, produces active species, which attack the monomer, resulting in the chemical reaction described in chapter 2. section 2.4. It may be possible therefore that some kind of a reaction may take place with the hydrate phases, which may produce some non-crystalline or very fine crystalline compound, which was not detected by the X-ray diffraction method. Clearly there is a need for further work in this area to identify any chemical changes that may be occuring and how they may be influencing the properties of the hydrated cements.

5.1.2 Effect of Sample Shape and Size, Geometry, Water/Cement Ratio and Curing Condition on Polymer Impregnation of Cement Pastes

As it was necessary to use a variety of geometrical shapes and sizes for the different experiments, it was necessary to determine the effect of sample geometry on the extent of polymer loading. There were three shapes of specimens used throughout the investigation which required polymer impregnation, and these are summarized in table 5.2. The kind of experiments carried out on each type of specimen is also shown in the same table as are the variety of cements, water/cement ratios and curing conditions. In some cases double impregnation was carried out, as indicated in table 5.2. The results are represented in terms of percentage of polymer loading by weight of cement and percentage of total volume of pores filled with polymer. These are summarised in tables 5.3, 5.4,and 5.5, and figures 5.8 and 5.9.

Single impregnation was not always successful as some of the monomer did not convert to the hardened mass of polymer within the cement matrix leading to its eventual evaporation. Re-impregnation of the samples with polymer resulted in a higher volume of pores filled with polymer.

In some of the earlier polymer impregnation attempts, the volume of pores filled with polymer appeared to be somewhat higher (compare tables 5.1 and 5.5). The reason for this was the difficulty in removing excess polymer that had deposited on the surface of the samples during impregnation which led to an overestimation of the final mass. As the technique was perfected, more care was taken in removing this excess polymer so the results were more reliable. For a large number of samples reproducibility of polymer loading involved an

error of ± 9% for any one set of specimens.

Thickness Of Discs

The thickness of the disc appears to play a major role in the degree of polymer loading as far as 0.4 water/cement ratio, OPC discs cured under curing condition (3) are concerned. Polymer loading has more than doubled when the thickness of the disc was increased from 3mm to 6mm, figure 5.9. As will be shown later in Chapter 7., such a difference in polymer loading had a considerable influence on the diffusivity of chloride ions through the discs.

The 6mm discs for all the other conditions compared well with the other geometrical shapes in terms of polymer loading. Tables 5.3, 5.4, 5.5.

Effect Of Water/Cement Ratio

Samples with a relatively higher water/cement ratio always showed greater % of polymer loading by weight of cement. This is due to increased porosity as a result of the higher water/cement ratio. This effect can be seen for different types of cement on table 5.3. and histogram figure 5.8.

Effect Of Curing Condition

Regardless of the type of cement used curing in two different environments i.e. cc(1) and cc(3) showed the following effects:-

a) Samples originally cured under cc(1) and then subjected to single impregnation, almost in all cases were not successful. A second

Cement	Curing condition	% of polymer loading by wt	Volume of the polymer within the sample (cc/g)	Total porosity of the sample by (pycno) (cc/g)	% of volume of pores filled with polymer
OPC	3	28.6	0.238	0.34	70.1
OPC/BFS	3	29.6	0.247	0.40	61.7

Table 5.1 Percentage of polymer loading by weight of the sample and percentage of volume of pores filled with polymer for cement pastes of 0.6 water/cement ratio.

Cylindrical (7 4 x 47 mm) used for SEM , MIP , corrosion studies

Cement	OPC	OPC/BFS
W/C	0.6	0.6
CC	1 *& 3	1 & 3

Prisms (47 x 18 x 18 mm) used for carbonation studies

Cement	OPC		OPC/BFS		OPC/PFA		SRPC	
W/C	0.4	0.6	0.4	0.6	0.4	0.6	0.4	0.6
CC	1&3	1&3	1&3	1&3	1&3	1&3	1&3	1&3

Disc 3-6 mm thick used for diffusion studies

Cement	OPC		OPC/BFS
W/C	0.4	0.6	0.6
CC	3	1*&3	3

* Include those which are double impregnated

Table 5.2 Summary of the different geometry of specimens used for the polymer impregnation test.

Cement	W/C ratio	Curing condition	% of polymer loading by wt	Volume of the polymer within the sample (cc/g)	Total porosity of the sample measured by(pycno) (cc/g)	% of volume of pores filled with polymer
OPC	0.4	1	6.3	0.053	0.16	33.1
	0.4	3	10.5	0.088	0.17	51.8
	0.6	1	8.6	0.072	0.30	24.0
	0.6	3	24.0	0.200	0.34	58.8
SRPC	0.4	1	5.3	0.044	0.18	24.4
	0.4	3	11.8	0.098	0.23	42.6
	0.6	1	7.0	0.058	0.33	17.6
	0.6	3	32.4	0.270	0.38	71.1
OPC/BFS	0.4	1	5.7	0.048	0.15	32.0
	0.4	3	21.2	0.177	0.26	68.1
	0.6	1	10.2	0.085	0.32	26.6
	0.6	3	31.0	0.258	0.40	64.5
OPC/PFA	0.4	1	6.0	0.050	0.23	21.7
	0.4	3	11.6	0.097	0.27	35.9
	0.6	1	11.4	0.095	0.38	25.0
	0.6	3	27.6	0.230	0.45	51.1

NOTE: Values are average of 9 prism shaped specimens

Table 5.3 Percentage of polymer loading by weight of the sample and percentage of volume of pores filled with polymer for cement pastes at two water/cement ratios and curing conditions.

Cement	W/C ratio	Impregnation	Curing condition	value of thickness of the disc (mm)	% of polymer loading by wt	Volume of the polymer within the sample (cc/g)	Total porosity of the sample by (pycno) (cc/g)	% of volume of pores filled with polymer
OPC	0.4	single	3	5.88	14.6	0.122	0.17	71.7
OPC	0.6	double	1	5.32	28.1	0.234	0.30	78.1
OPC	0.6	double	3	6.12	26.8	0.223	0.34	65.7
OPC/BFS	0.6	single	3	0.516	25.9	0.216	0.40	54.0

NOTE: Values are average of 5 disc specimens

Table 5.4 Percentage of polymer loading by weight of the sample and percentage of volume of pores filled with polymer for cement pastes of two different water/cement ratios and curing conditions subjected to single or double impregnation.

Cement	W/C ratio	Impregnation	Curing condition	% of polymer loading by wt	Volume of the polymer within the sample (cc/g)	Total porosity of the sample by (pycno) (cc/g)	% of volume of pores filled with polymer
OPC	0.6	double	1	27.3	0.228	0.30	75.9
OPC	0.6	single	3	24.1	0.201	0.34	59.1
OPC/BFS	0.6	single	1	15.5	0.129	0.32	40.3
OPC/BFS	0.6	single	3	25.6	0.213	0.40	53.3

NOTE: Values are average of 8 cylinder shaped specimens.

Table 5.5 Percentage of polymer loading by weight of the sample and percentage of volume of pores filled with polymer for cement pastes of 0.6 water/cement ratio and cc(1) and cc(3) subjected to single or double impregnation.

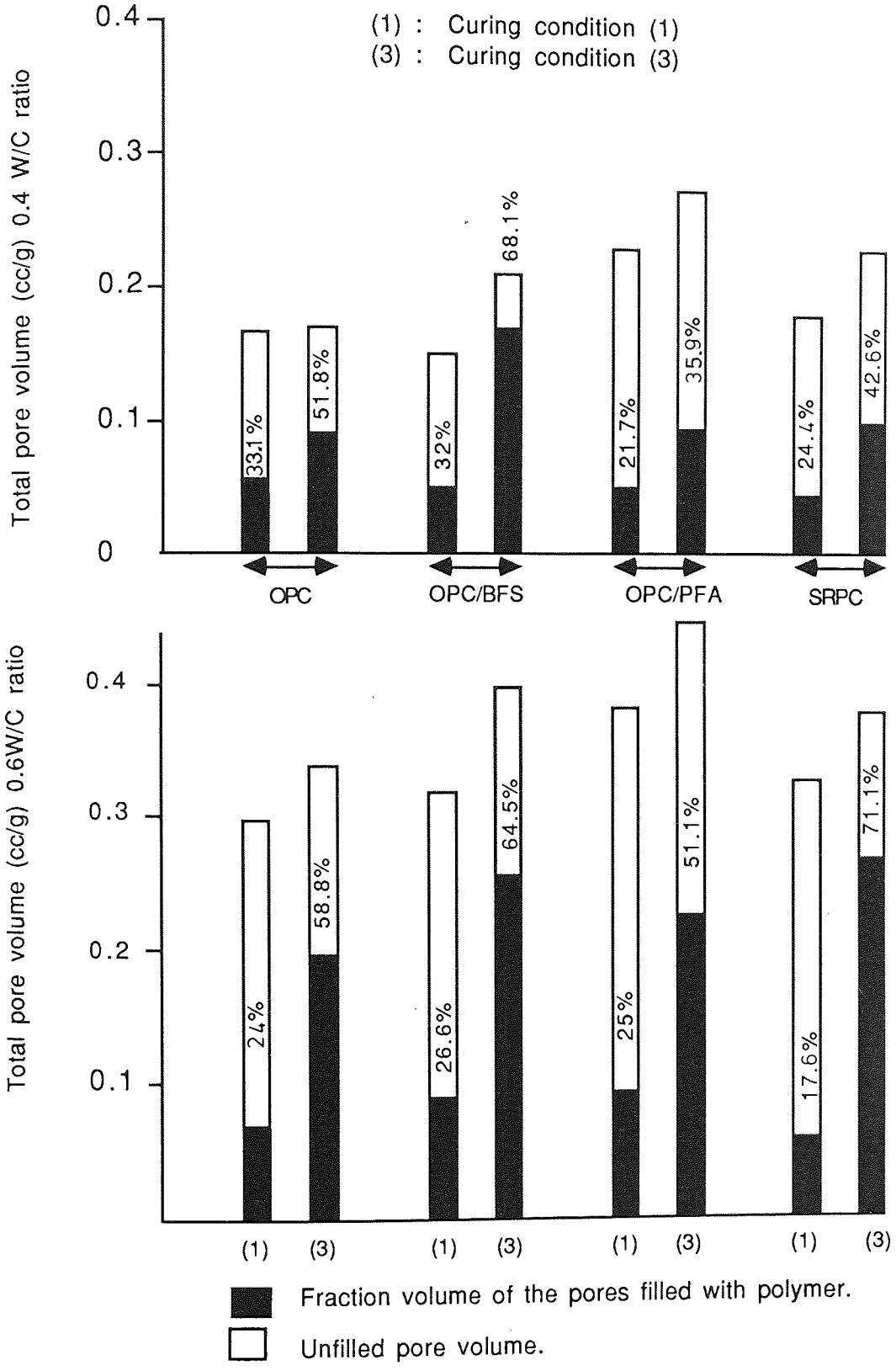

Figure 5.8 Histograms showing the total pore volume measured by the pycnometric method and the pore volume remaining empty after cement pastes were polymer impregnated.

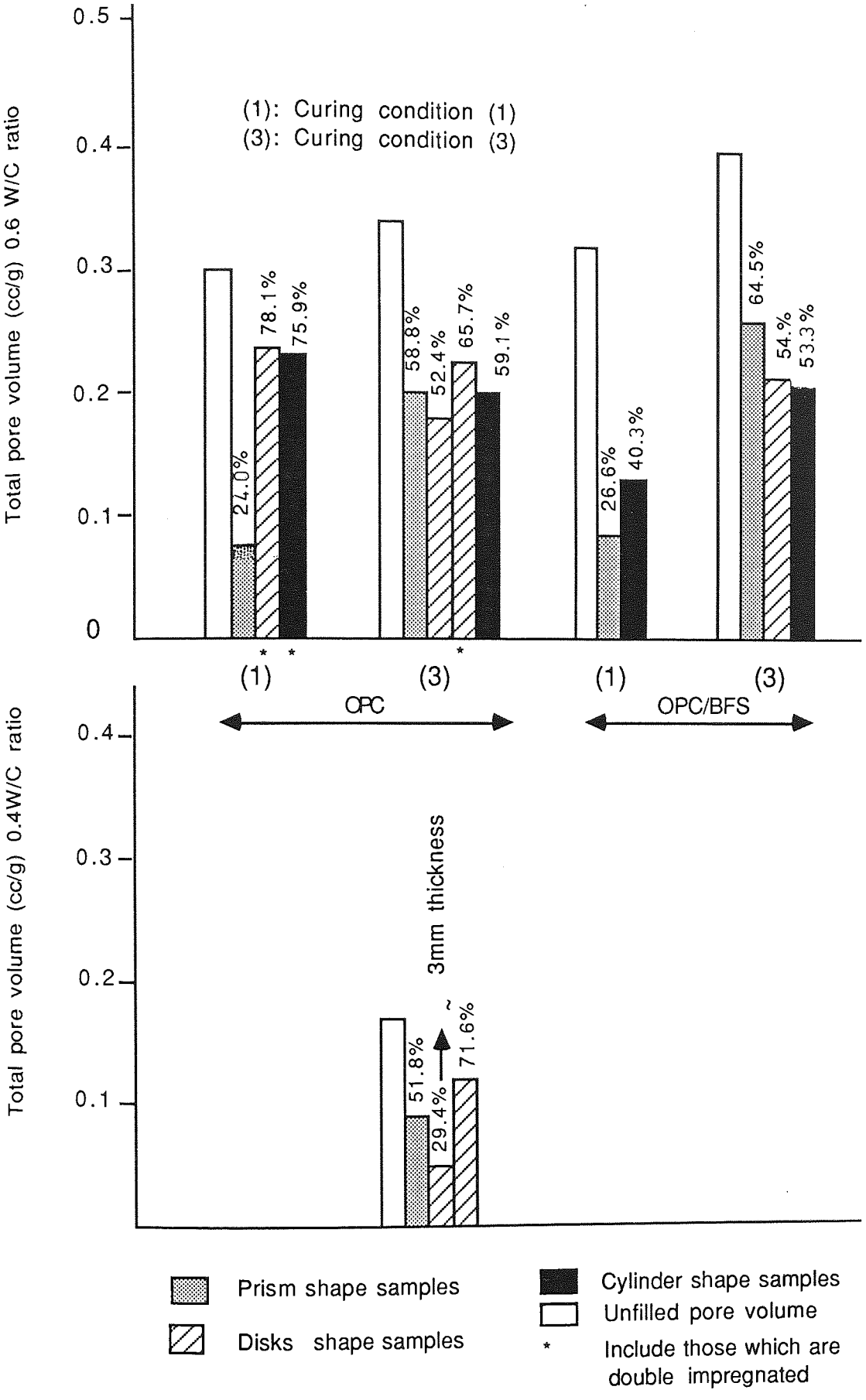

Figure 5.9 Histograms showing the total pore volume measured by the pycnometric method and the fraction of pores filled with polymer for different shapes of sample.

impregnation was required to improve the degree of polymer loading of the curing condition. The reason for this was explained in an earlier part of this chapter.

b) Samples cured under cc(3) always showed a good polymer loading and required no further impregnation.

5.2 CONCLUSIONS

a) The introduction of liquid monomer (methylmethacrylate) containing 3% (by weight) benzoyl peroxide as a dissolved initiator into samples of hydrated cement paste and the subsequent polymerisation of the monomer at 85^{o}C for 5 hours, produces a polymer impregnated cement (PIC) which in extreme cases i.e. poorly cured cement, can have up to 70% of the total pore volume filled with the polymer.

b) Fracture surfaces from polymer impregnation cements have been examined by means of the SEM. The resulting micrographs showed the presence of hardened polymer matrix surrounding the cement hydration products, both near to the surface of the specimens and in the centre.

c) Mercury intrusion porosimetry has been carried out on impregnated and unimpregnated samples of hydrated OPC and OPC/BFS blended cement pastes. It has shown that polymer impregnation results in substantial reduction but not complete elimination of the total pore volumes of the cement. However, it may be that polymer blocks the entrances of pores and prevents complete penetration of pores.

d) The results obtained by X-ray diffraction for cement paste samples both before and after impregnation, has showed that the measured intensity for

the peaks relating to $Ca(OH)_2$, C_3S,C_2S and C_3A have diminished drastically, following polymer impregnation. The actual mechanism is not clear, but it may involve some chemical reaction with the hydrated phases, resulting in non-crystalline compounds.

e) The degree of polymer loading exhibited by a hydrated cement paste is greatly affected by the initial water/cement ratio of the pastes; higher water/cement ratio leading to greater amounts of polymer loading for a particular mix. Polymer loading is also greatly influenced by the regime adopted for curing the cement pastes, poorly cured pastes i.e. cc(3), showed far higher levels of polymer loading than well cured ones, i.e. cc(1). For well cured samples, pastes of both water/cement ratio examined, required a second impregnation to be carried out for maximum loading to be achieved. This may be in some part due to the possible reaction between $Ca(OH)_2$ and the CO_2 released during polymerisation. Alternatively there may be a molecular sieve effect where the larger molecules of the benzoyl peroxide may be restricted in entering the finer pore network of some specimens

f) The geometry of the hydrated cement paste samples has been shown to greatly influence the level of polymer loading that may be achieved. In particular samples with a high surface area to volume ratio, i.e. thin discs, tend to lose a greater amount of monomer due to evaporation during the polymerisation process. This effect may be of significance when considering the suitability of polymer impregnation for pre-cast concrete units, such as cladding panels, where the surface area to volume ratio is likely to be high.

CHAPTER 6 CARBONATION STUDIES OF PLAIN AND IMPREGNATED CEMENT PASTES

6.1 INTRODUCTION

A typical plot of depth of carbonation versus time is depicted in figure 6.1; this shows that the rate of carbonation decreases with time, as was shown in chapter 1 section 1.4. The increase in the depth of carbonation with time is normally parabolic, so more information can therefore be drawn from a plot of depth of carbonation versus √time as shown by figure 6.2. In the present work an induction period t_o when carbonation is first detected is followed by a fast and approximately linear increase in the depth of carbonation up to time t_1 where the change in depth of carbonation with the square root of time, Ko (the rate of carbonation) is given by:-

$$K_o = \frac{L_o}{\sqrt{t_1} - \sqrt{t_o}} \quad \text{where } t_1 > t_o \qquad (6.1)$$

Lo = Depth of carbonation at t_1 (mm)

At t_1 the carbonation rate, as will be explained later, is reduced, but still remains approximately parabolic producing a second distinct line. The new value of rate of carbonation K is given by :-

$$K = \frac{L - L_o}{\sqrt{t} - \sqrt{t_1}} \quad \text{where } t > t_1 \qquad (6.2)$$

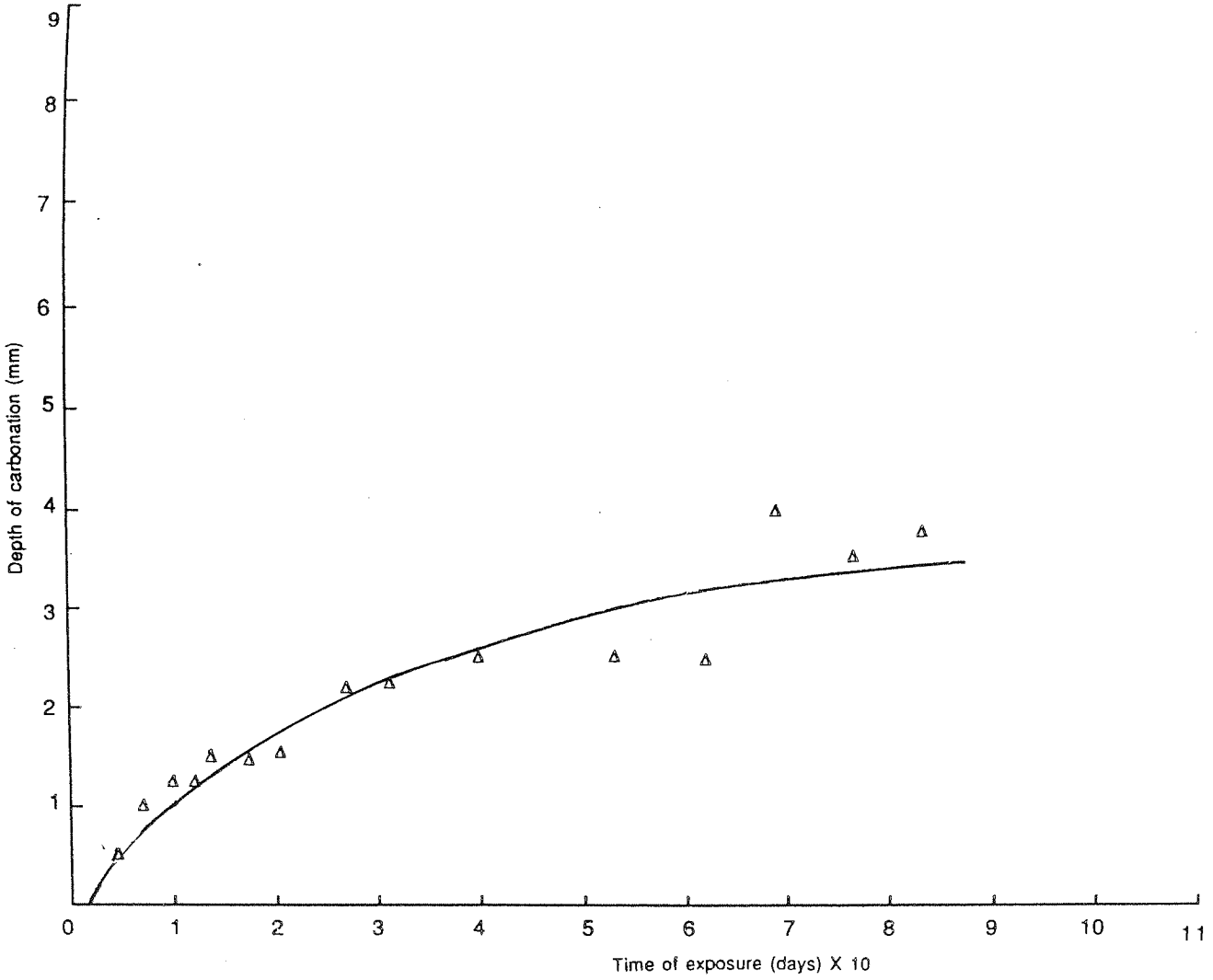

Figure 6.1 Typical plot of carbonation depth versus time for OPC paste 0.6 water/cement ratio cured under cc(1).

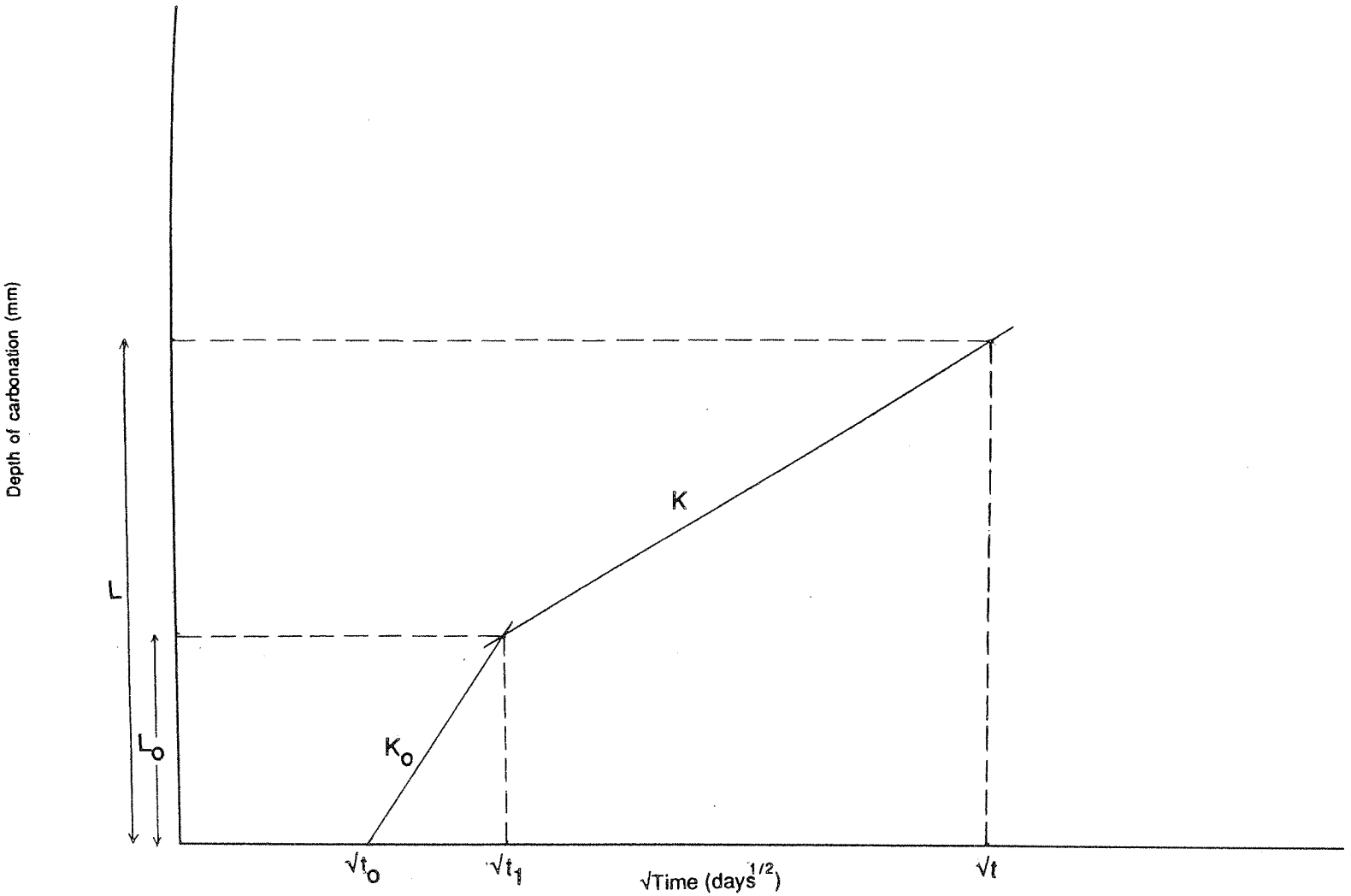

Figure 6.2 Plot of carbonation depth versus square root of time.

Showing the variables used in the equation.

An overall formula for representing the depth of carbonation, L, can therefore be written as follows:-

$$L = K_o (\sqrt{t_1} - \sqrt{t_o}) + K(\sqrt{t} - \sqrt{t_1}) \qquad (6.3)$$

where,

L = depth of carbonation (mm)

K_o and K = rate constant mm/day $^{1/2}$

t_o, t_1 and t = time of carbonation (days)

In many cases however, the first faster rate of carbonation K_o is absent so, one single straight line is observed and formula of :-

$$L = k(\sqrt{t} - \sqrt{t_1}) \qquad (6.4)$$

can be used directly for determining the carbonation rate, as the first term of the overall formula is eliminated.

6.2 RESULTS FOR PLAIN CEMENT PASTES

Figures 6.3 to 6.10 represent the change in carbonation depth with the square root of time for all the studied conditions (see chapter 2 section 2.5) values of the K_o, first faster rate of carbonation, L_o, the depth of carbonation due to K_o (where applicable) and K normal rate of carbonation and L_{100} the theoretically calculated depth of carbonation at 100 days, as shown in appendix 8, are tabulated in tables

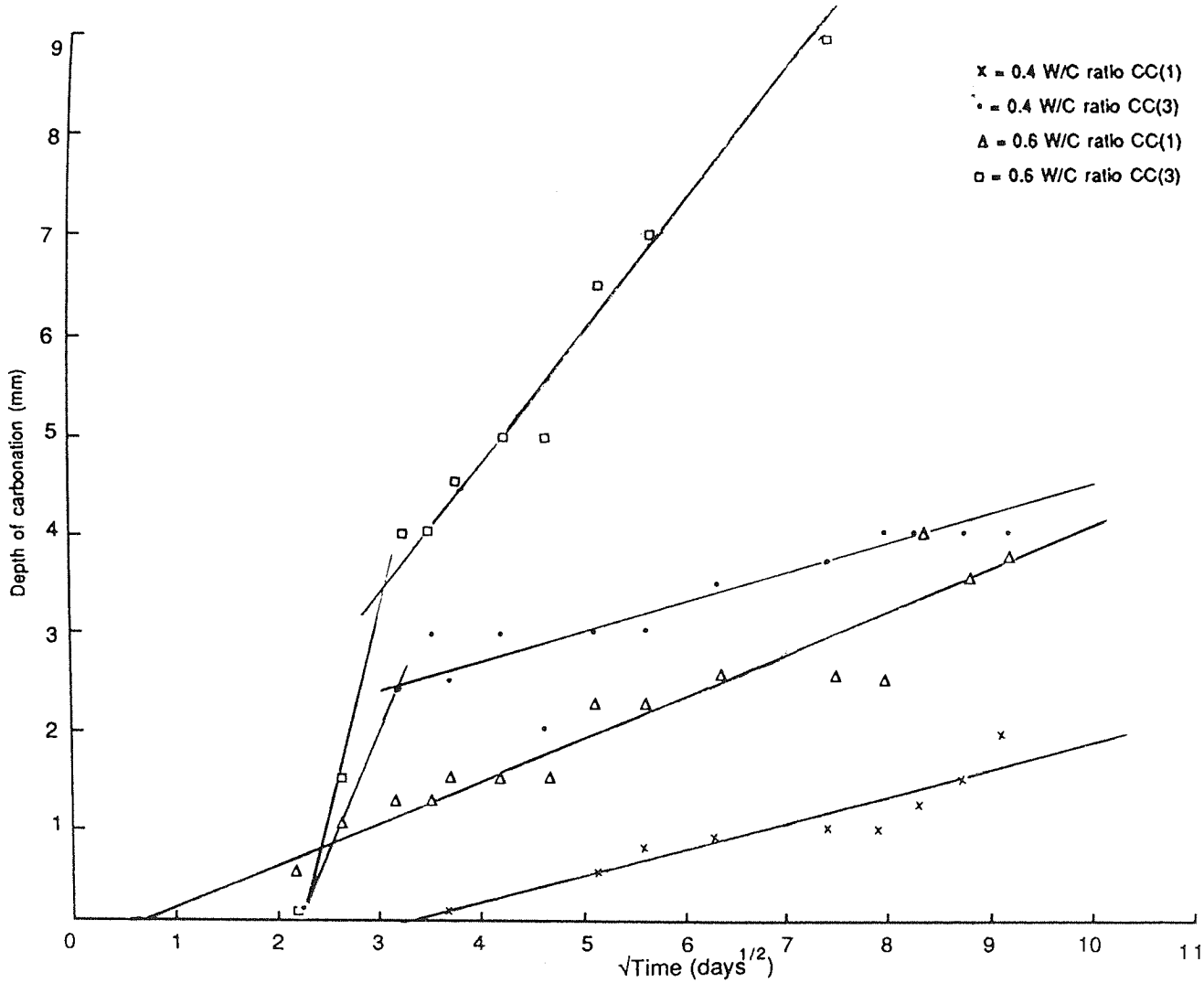

Figure 6.3 Plots of carbonation depth versus the square root of time of exposure for OPC cement pastes of different water/cement ratios and curing conditions.

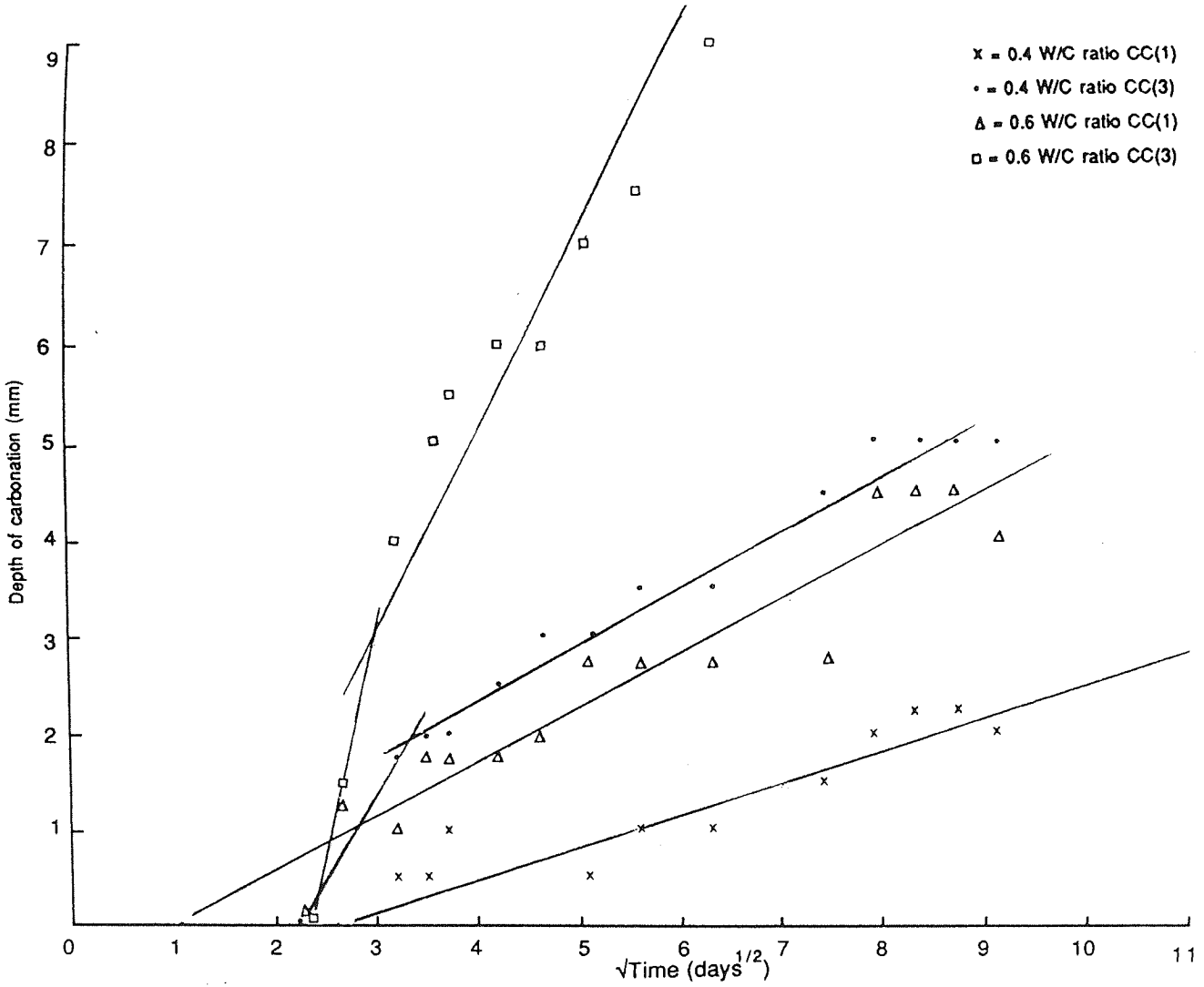

Figure 6.4 Plots of carbonation depth versus the square root of time of exposure for SRPC cement pastes of different water/cement ratios and curing conditions.

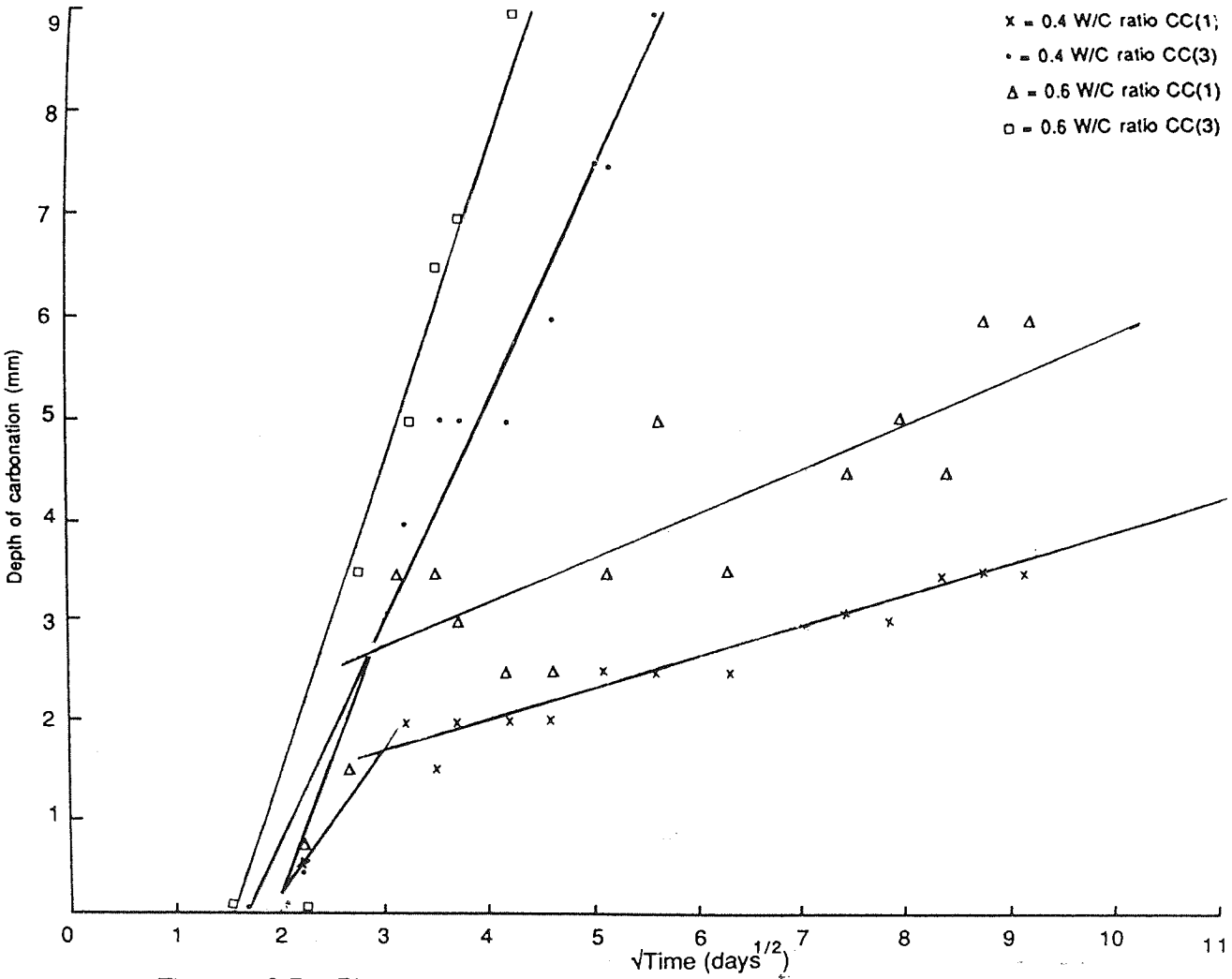

Figure 6.5 Plots of carbonation depth versus the square root of time of exposure for OPC/BFS cement pastes of different water/cement ratios and curing conditions.

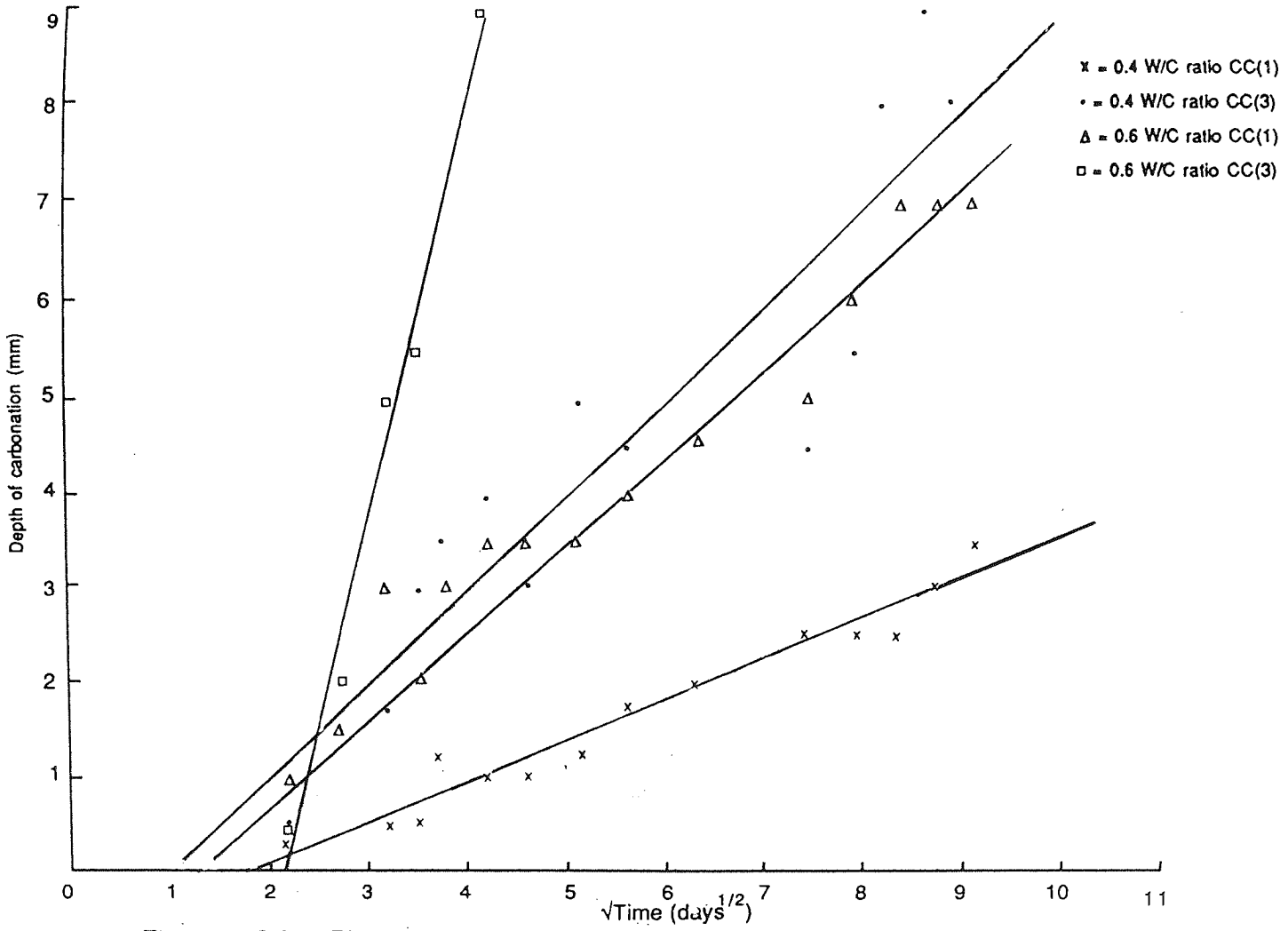

Figure 6.6 Plots of carbonation depth versus the square root of time of exposure for OPC/PFA cement pastes of different water/cement ratios and curing conditions.

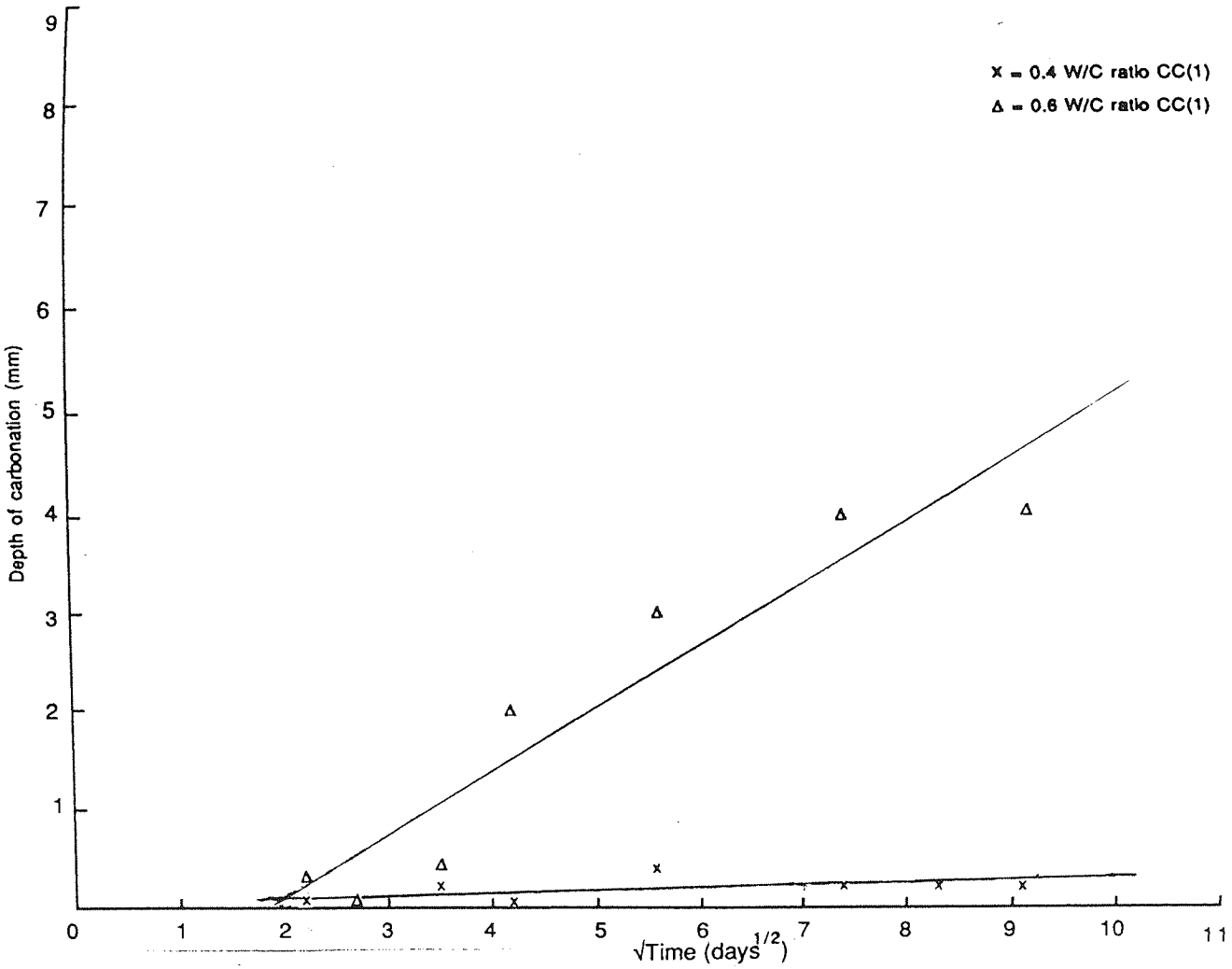

Figure 6.7 Plots of carbonation depth versus the square root of time of exposure for polymer impregnated OPC cement pastes of different water/cement ratio cured using cc(1).

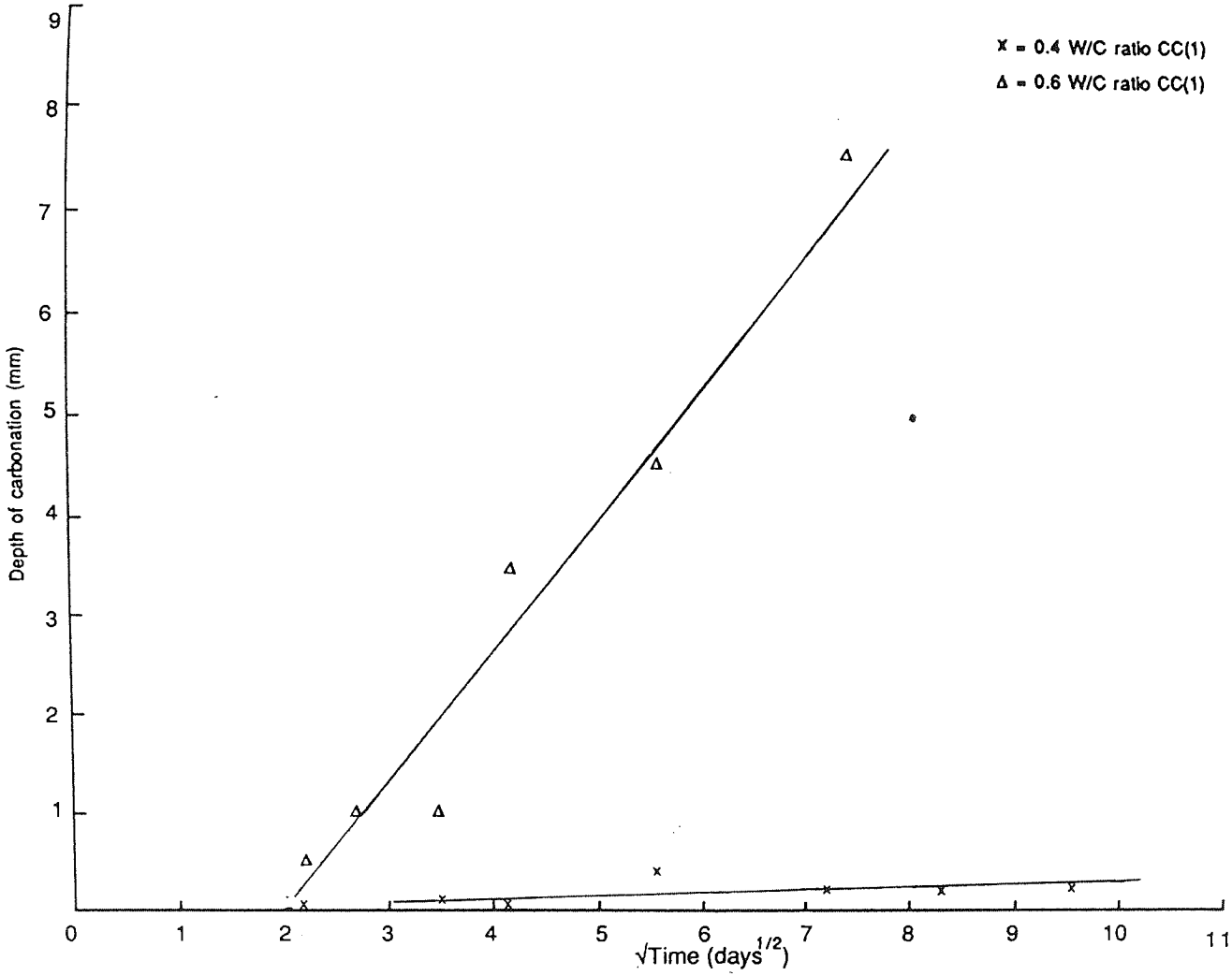

Figure 6.8 Plots of carbonation depth versus the square root of time of exposure for polymer impregnated SRPC cement pastes of different water/cement ratio cured using cc(1).

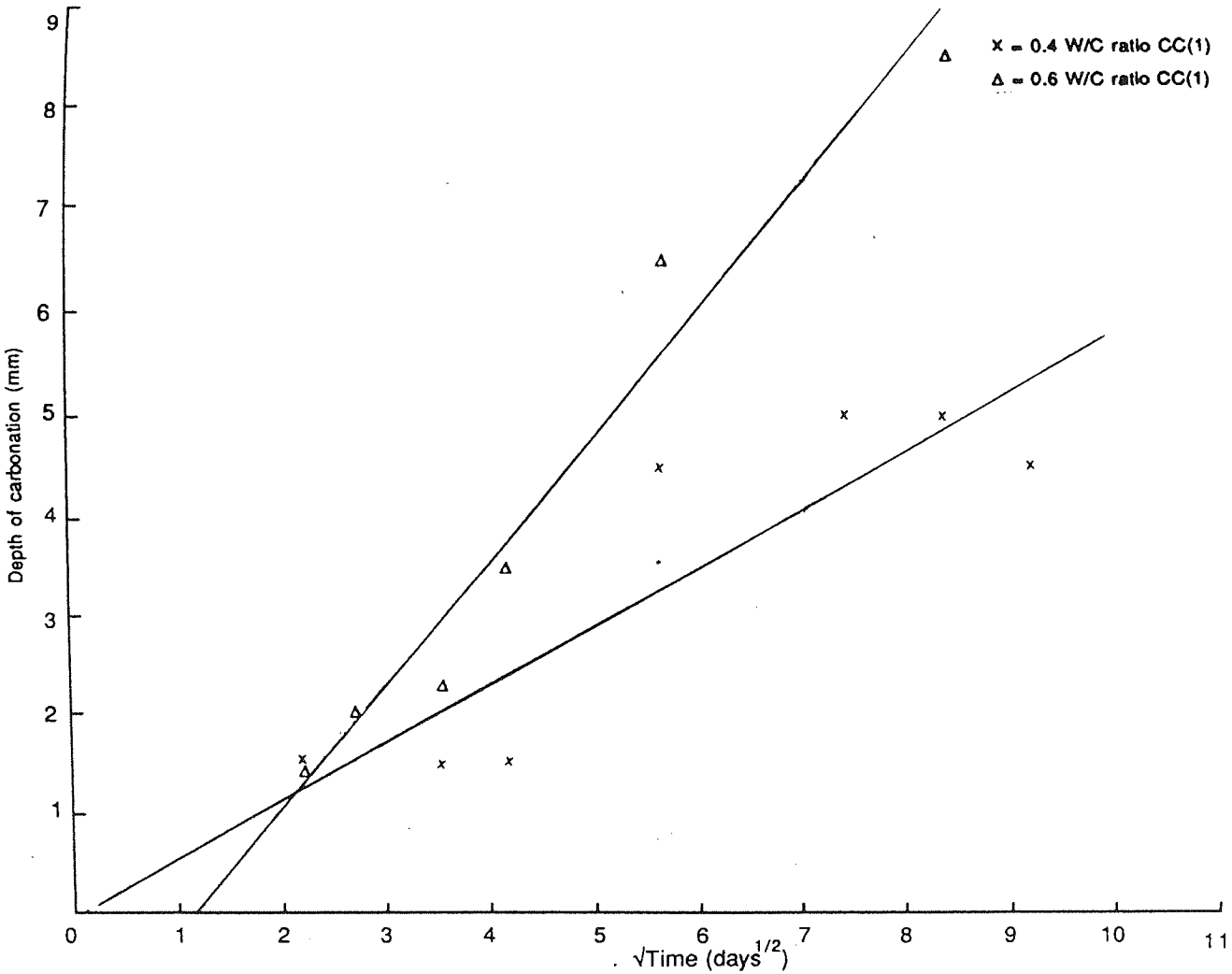

Figure 6.9 Plots of carbonation depth versus the square root of time of exposure for polymer impregnated OPC/BFS cement pastes of different water/cement ratio cured using cc(1).

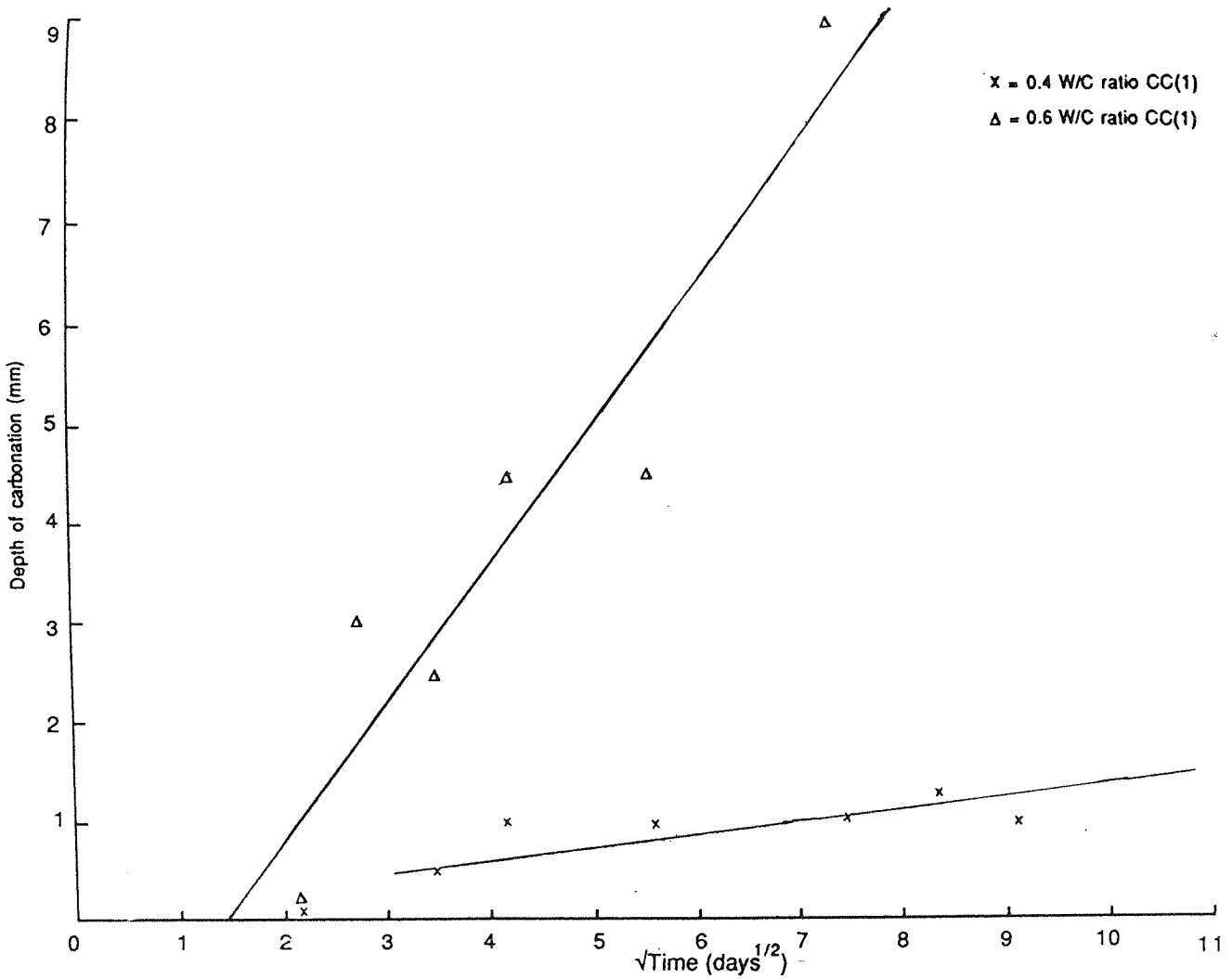

Figure 6.10 Plots of carbonation depth versus the square root of time of exposure for polymer impregnated OPC/PFA cement pastes of different water/cement ratio cured using cc(1).

(6.1 and 6.2). A high correlation coefficient was obtained for each plot of depth of carbonation against square root of time (days). The histograms in figure 6.11, show the complete results of the calculated depth of carbonation at 100 day (L_{100}) for both impregnated and unimpregnated samples. In the case of impregnated samples the % of polymer loading by weight for each indiviual cement at different water/cement ratio is also shown. The calculation of polymer loading was described in Chapter 5.

6.2.1 The Depth of Carbonation Lo, for Plain Cement Pastes

The first rapid carbonation rate K_o, observed for some conditions, led to a depth of carbonation L_o, the values of which are tabulated in table 6.1. It is interesting that this occurred only for specific conditions. In the case of the portland cements (OPC and SRPC) K_0 values were recorded only when the specimens were badly cured. The reason may be associated with further hydration of the specimens as they were subjected to a somewhat higher relative humidity (i.e. 50% RH as opposed to the original 30% during the curing period). This may not be the complete explanation since hydration at 50% RH is considered to be very low (163-165). Alternatively the carbonation products formed during carbonation may have altered the pore structure near the surface in such a way as to reduce the subsequent diffusion of CO_2. Well cured OPC/BFS specimens also exhibited a variable carbonation rate which is difficult to explain since the rate of hydration of this type of cement is slower than OPC (see chapter 4.) it may again be caused by continued hydration during their carbonation, or by alteration of the pore structure near the surface [as is the case for the above mentioned portland cements cc(3)].

Cement	W/C Ratio	Curing condit -ion	mm/day $^1/_2$		Value of L_o (mm)	L_{100} depth of carbonation at 100 days (mm)	Correlation coefficient
			K_0	K			
OPC	o.4	1	—	0.28	—	1.89	0.94
	0.4	3	2.50	0.29	2.40	4.42	0.88
	0.6	1	—	0.43	—	4.06	0.96
	0.6	3	4.16	1.28	3.65	12.46	0.99
SRPC	o.4	1	—	0.34	—	2.51	0.96
	0.4	3	1.82	0.56	2.04	5.75	0.95
	0.6	1	—	0.57	—	5.08	0.95
	0.6	3	4.18	1.99	2.83	16.89	0.95
OPC/BFS	o.4	1	1.56	0.32	1.60	3.91	0.95
	0.4	3	—	2.26	—	18.77	0.97
	0.6	1	2.90	0.45	2.74	5.92	0.80
	0.6	3	—	4.38	—	34.46	0.99
OPC/PFA	o.4	1	—	0.44	—	3.56	0.98
	0.4	3	—	0.99	—	8.88	0.93
	0.6	1	—	0.83	—	7.85	0.98
	0.6	3	—	4.37	—	34.24	0.99

Table 6.1 Values of the calculated constants K_0, K and L_{100} and the depth of carbonation at 100 days for a range of cement pastes of two water/cement ratios and two curing conditions.

Cement	W/C Ratio	Curing Conditon	K mm/day $^{1}/_{2}$	L_{100} depth of carbonation at 100 days (mm)	Correlation coefficient
OPC	0.4	1	0.025	0.28	0.46
	0.6	1	0.65	5.26	0.99
SRPC	0.4	1	0.03	0.28	0.46
	0.6	1	1.32	10.59	0.99
OPC/BFS	0.4	1	0.60	5.91	0.89
	0.6	1	1.25	11.03	0.98
OPC/PFA	0.4	1	0.12	1.36	0.80
	0.6	1	1.44	12.31	0.94

Note : For 0.4 and 0.6 W/C ratio cc(3) no carbonation took place

Table 6.2 Values of the calculated constant K and L_{100} and the depth of carbonation at 100 days for a range of polymer impregnated cement pastes of two water/cement ratios.

This was not the case however for poorly cured samples where carbonation rate were so fast that the effect of the initial rate of carbonation K_0 was simply not detected.

The OPC/PFA blend did not show this effect under any of the curing conditions used and more experimental work using a wide range of curing conditions is required for further elucidation.

The importance of L_o, the depth of carbonation due to K_0, is that for two specimens exibiting similar rates of carbonation (K) the depth of carbonation will be higher for the specimen with the faster original carbonation rate by a value related to L_o, as will be shown later.

6.2.2 The Rate Of Carbonation K Calculated

Table (6.1) shows K the rate of carbonation values for the four types of plain cement pastes OPC, OPC/BFS, OPC/PFA and SRPC at both 0.4 and 0.6 water/cement ratio after an original curing period of 28 days, in either curing condition (1) and (3), but not subjected to impregnation. Carbonation rates for the 0.4 water/cement ratio cements were in an increasing order of OPC, BFS/OPC, SRPC, OPC/PFA, but all values, except for OPC/PFA, were fairly low. As will be shown later, however the combination of the rate of carbonation, K, and the early faster carbonation rate K_o represented in table 6.1 by L_o the depth of carbonation due to K_o caused an overall increase in the depth of carbonation. In this case, although the OPC/BFS cement had a lower rate of carbonation K, the value of L_o had caused the actual depth of carbonation at 100 days to be even higher than that of OPC/PFA (see table 6.1). This concept will be discussed

further in a later section. The increased water/cement ratio (0.6) resulted in higher carbonation rates for all the cements but particularly so for the OPC/PFA cement.

Poor curing cc(3) of the 0.4 water/cement ratio specimens increased the rate of carbonation of the portland cements, but not as drastically as those of the blended cements; such a curing for the 0.6 water/cement ratio had a more dramatic effect, however, for all the cement types leading to significantly higher carbonation rates. This effect was still more pronounced for the blended cements where carbonation rates were an order of magnitude higher, compared to the 0.6 water/cement ratio pastes under cc(1).

6.2.3 Depth Of Carbonation For Samples At 100 Days

The calculated depths of carbonation, for the plain cement pastes at 0.4 and 0.6 water/cement ratio cc(1) and cc(3) can be seen in table 6.1 and in the form of histograms in figure 6.11. It was thought that such values could represent better, the ability of a cement paste to carbonate, as it takes into account the early faster carbonation rate of some cements.

It can be seen that at 0.4 water/cement ratio cc(1) all four types of cement pastes have fairly low carbonation depths, with a general trend of , OPC < SRPC < OPC/PFA < OPC/BFS.

For 0.4 water/cement ratio cc(3) in all cases the depth of carbonation has risen, compared with samples kept under cc(1), the effect being more pronounced for the blended cements and in particular for OPC/BFS.

It is evident that for 0.6 water/cement ratio cc(1) in all cases the depth of carbonation was greater than for 0.4 water/cement ratio cc(1), most values increasing roughly by a factor of two. For 0.6 water/cement ratio cc(3) the depth of carbonation was much greater when compared to 0.6 water/cement ratio cc(1). Comparing the different cements at this water/cement ratio, it can be seen that OPC resulted in the lowest carbonation depth, but is only marginally smaller than SRPC, whereas both OPC/BFS and OPC/PFA resulted in far greater values than OPC.

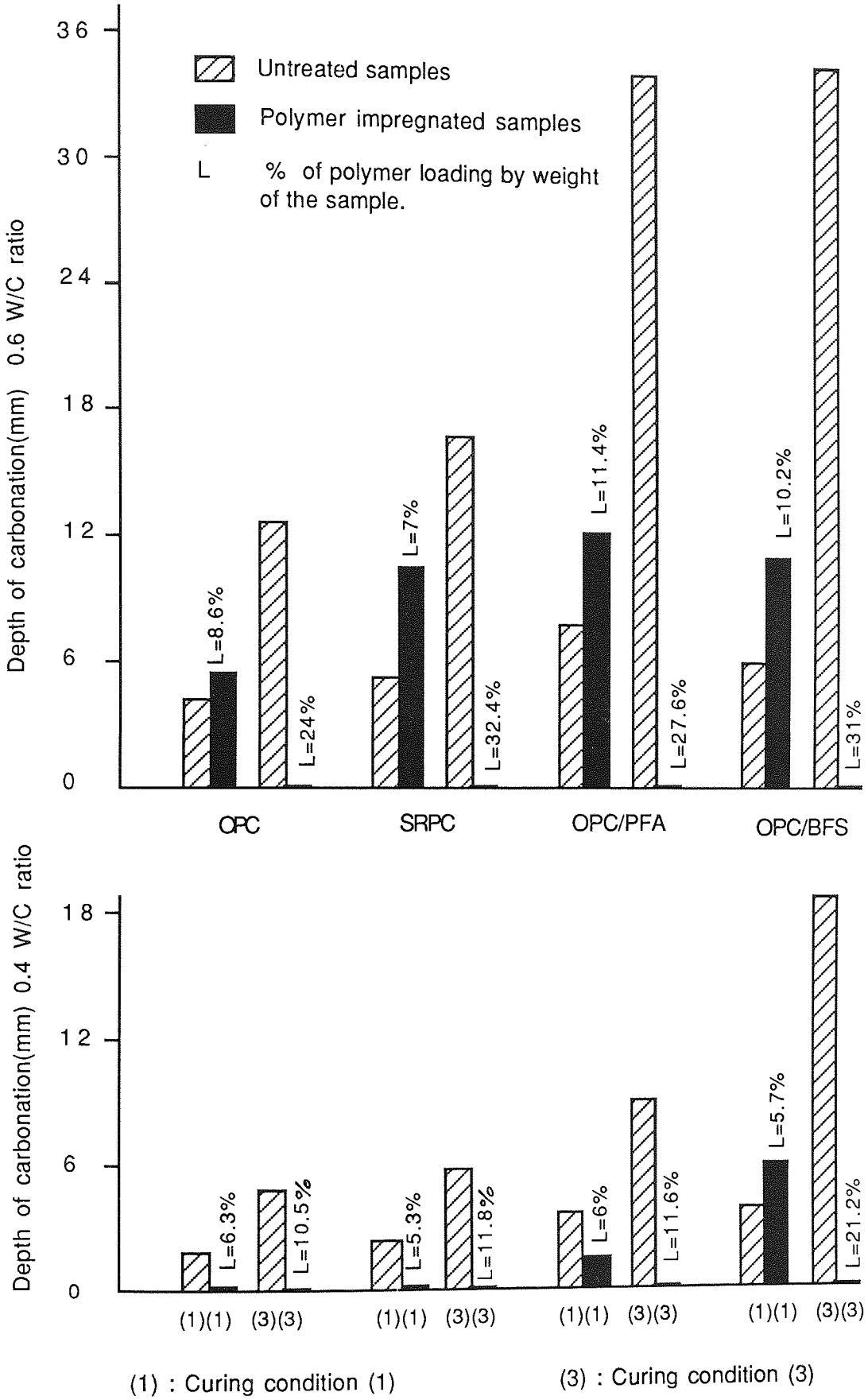

Figure 6.11 Histograms showing the calculated depth of carbonation at 100 days for polymer impregnated and unimpregnated of the different cement pastes.

6.3 RESULTS OF X-RAY DIFFRACTION OF PLAIN CEMENT PASTES

Figure 6.12(a-d) represent the X-ray diffraction traces for OPC, O.6 water/cement ratio for the carbonated and uncarbonated samples, for both curing conditions.

With cc(1), a noticeable drop in the height of the $Ca(OH)_2$ peak (at 18.1, 28.7, 34.1 and 47^o) occurs following carbonation. The formation of new peaks are observed at 23, 29.5, 31.5 and 45^o which are normally associated with calcite, one of the three mineralogical forms of $CaCO_3$ (31-33). This phase is stable and mainly forms when a well cured sample is subjected to "natural" carbonation. Vaterite, one of the other forms of $CaCO_3$ is also observed at 25, 27 and 43.8^o, which is the first to form and does not have a regular crystal pattern (31). The vaterite is unstable, but as the time proceeds will convert to calcite.

The XRD traces for OPC 0.4 water/cement ratio cc(1) figure 6.13a also show similar results. XRD traces of uncarbonated 0.6 water/cement ratio OPC cc(3) when compared with X-ray traces of carbonated samples figure 6.12c,d, indicate once more the obvious phase change occurring on carbonation. Poor curing has resulted in a different proportion of the two $CaCO_3$ phases figures 6.12b,d. Although the peaks at 25, 27 and 43.8^o representing vaterite, are present in both cases, for 0.6 water/cement ratio cc(3) figure 6.12b, the peak intensity is relatively greater. On the other hand, the peaks representing calcite are smaller. This means for samples cured under cc(3), because of the high porosity and slow rate of hydration, an ideal condition for fast carbonation was provided, which resulted in the production of vaterite. However, it is important to observe that for 0.4 water/cement ratio cc(3) the X-ray trace for the carbonated sample was

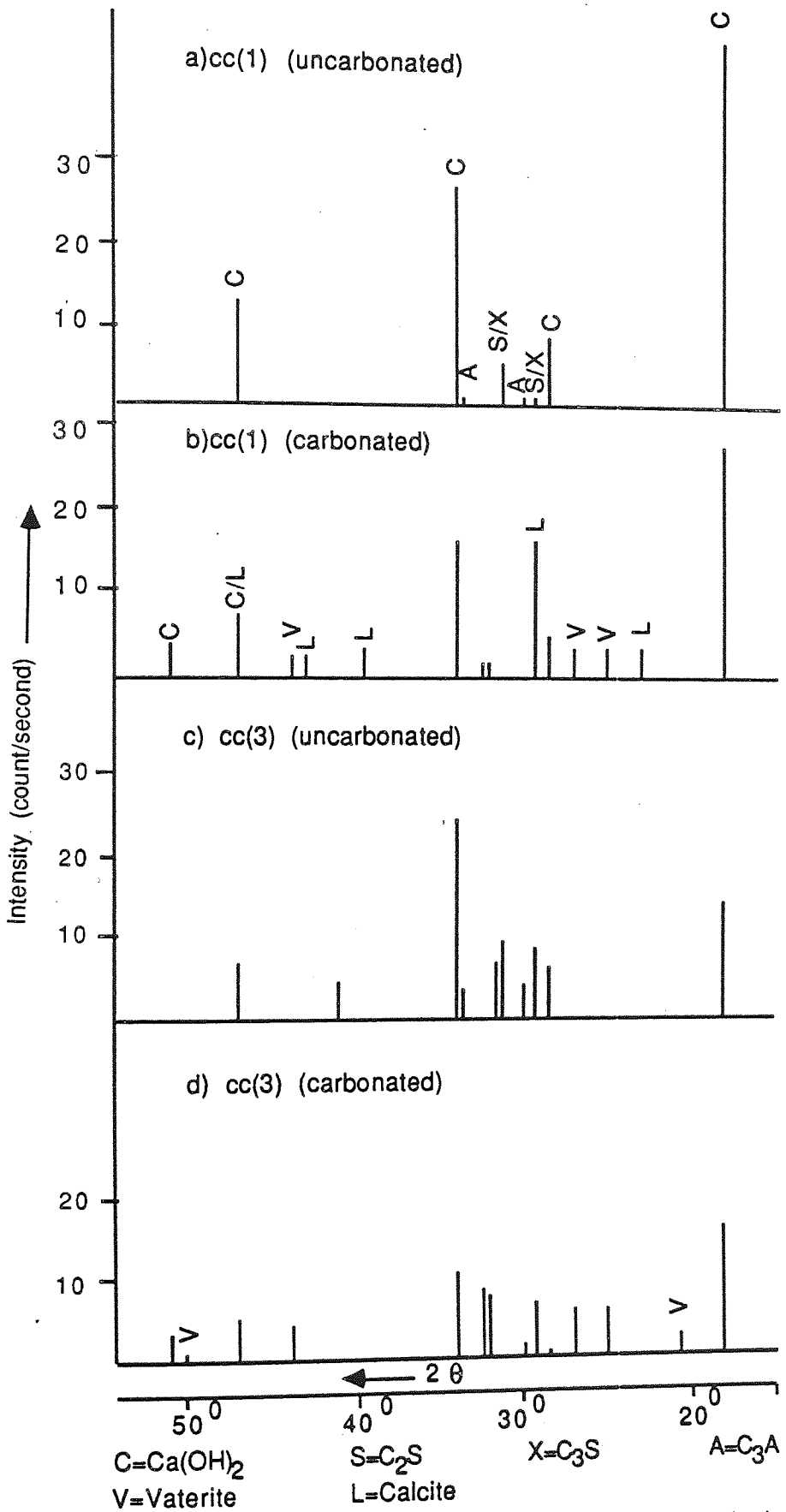

Figure 6.12 XRD traces of OPC of 0.6 W/C ratio for both carbonated and uncarbonated samples originally cured for 29 days.

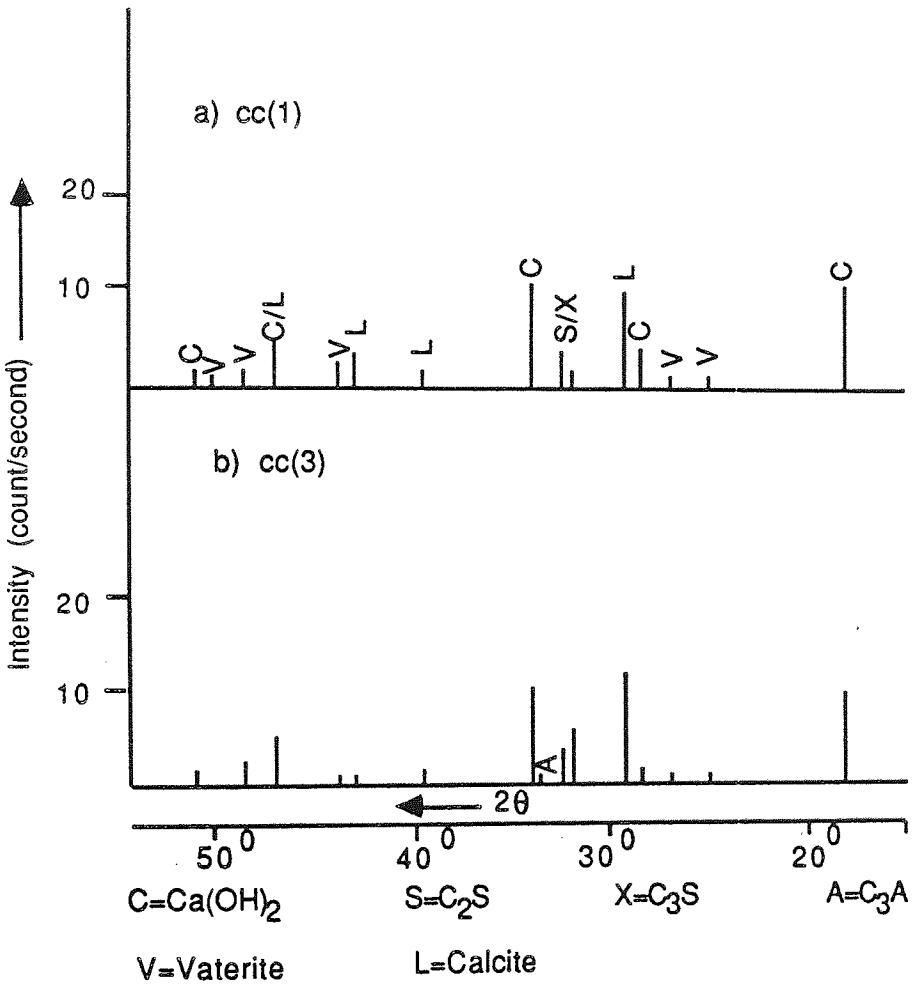

Figure6.13 XRD traces of OPC of 0.4 W/C ratio for carbonated samples originally cured for 29 days.

similar to 0.4 and 0.6 cc(1) figure 6.13b, largely because of the relatively low porosity.

In the case of OPC/BFS, the XRD trace for the 0.6 water/cement ratio cc(1) sample, shows a greater decrease in peak intensity of $Ca(OH)_2$ after carbonation (compare figures 6.12b with 6.14b). At the same time the formation of the $CaCO_3$ peaks in the form of vaterite and calcite were detected, but there was not as great a proportion of calcite as for the OPC cement at the same curing condition. This suggests that because of the faster rate of carbonation for OPC/BFS the vaterite is first to form. There is also not much difference between the X-ray traces of cc(1) at 0.4 and 0.6 water/cement ratio figure (6.14b and 6.15a). The results of the carbonated and uncarbonated OPC/BFS samples at 0.6 water/cement ratio cc(3) figure 6.14c,d, show similar results to the cc(1) 0.6 water/cement ratio samples. In general there is little difference between the X-ray traces for all carbonated OPC/BFS samples, regardless of water/cement ratio and curing condition. With SRPC, the XRD traces obtained for the carbonated samples were not too dissimilar to the ones found for OPC figure 6.16a-d, similarly, the traces in the case of OPC/PFA were almost the same as for OPC/BFS figure 6.17a-d.

6.4 RESULTS OF DTA

The results of DTA analysis for the four different types of plain cement pastes at 0.6 water/cement ratio after an initial 28 day curing period in cc(3) which were then fully carbonated, are shown in figures 6.18a,b,c,d. In all cases, the peak for the gel at 150^{o}C has broadend cosiderably as compared to the DTA results of uncarbonated samples, Chapter 4. figure 4a-d.

For all the cement pastes the intensity of the peak at 500^{o}C was reduced greatly following carbonation, whereas a peak at 850-900^{o}C indicating calcite was now

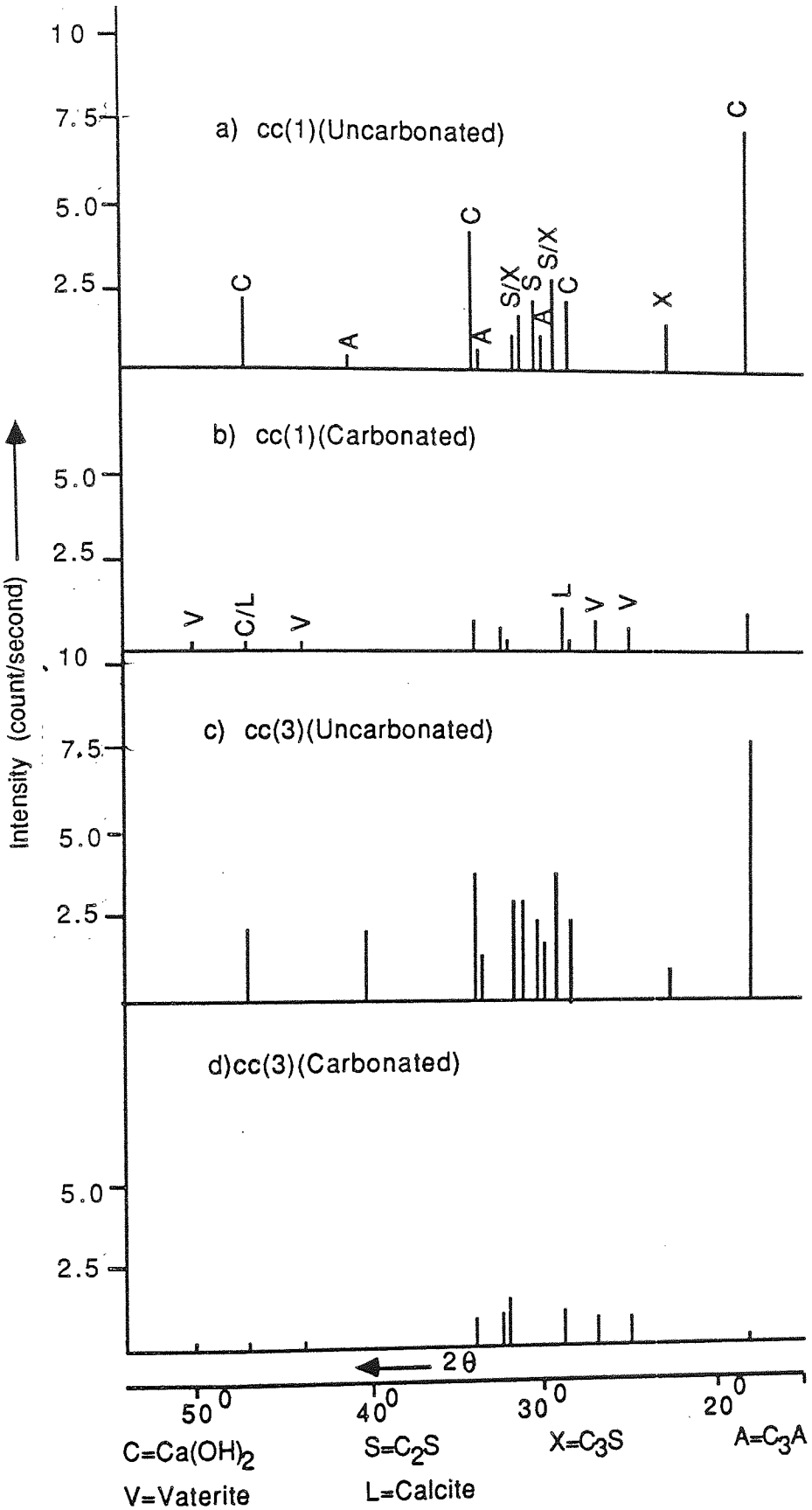

Figure 6.14 XRD traces of OPC/BFS of 0.6 W/C ratio for both carbonated and uncarbonated samples originally cured for 29 days

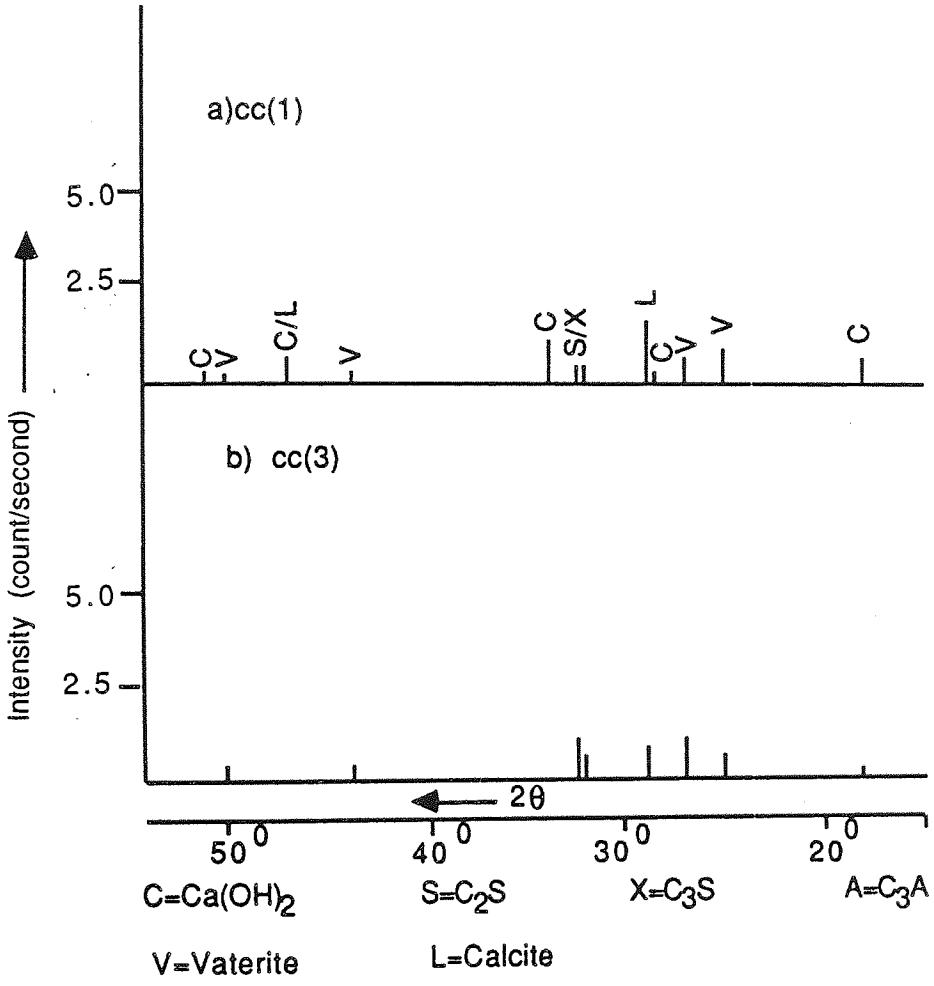

Figure 6.15 XRD traces of OPC/BFS of 0.4 W/C ratio for carbonated samples originally cured for 29 days.

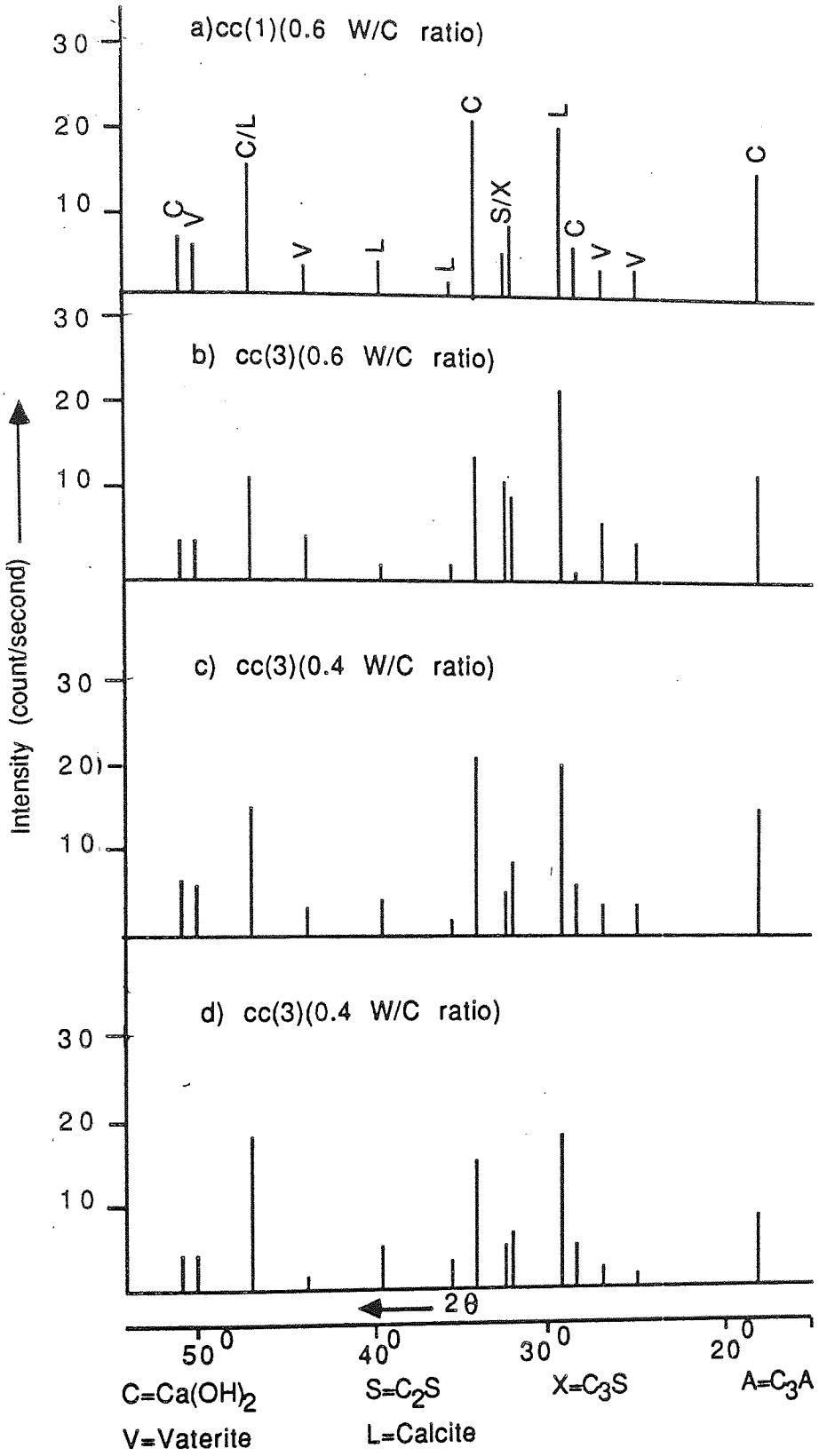

Figure 6.16 XRD traces of SRPC for carbonated samples originally cured for 29 days.

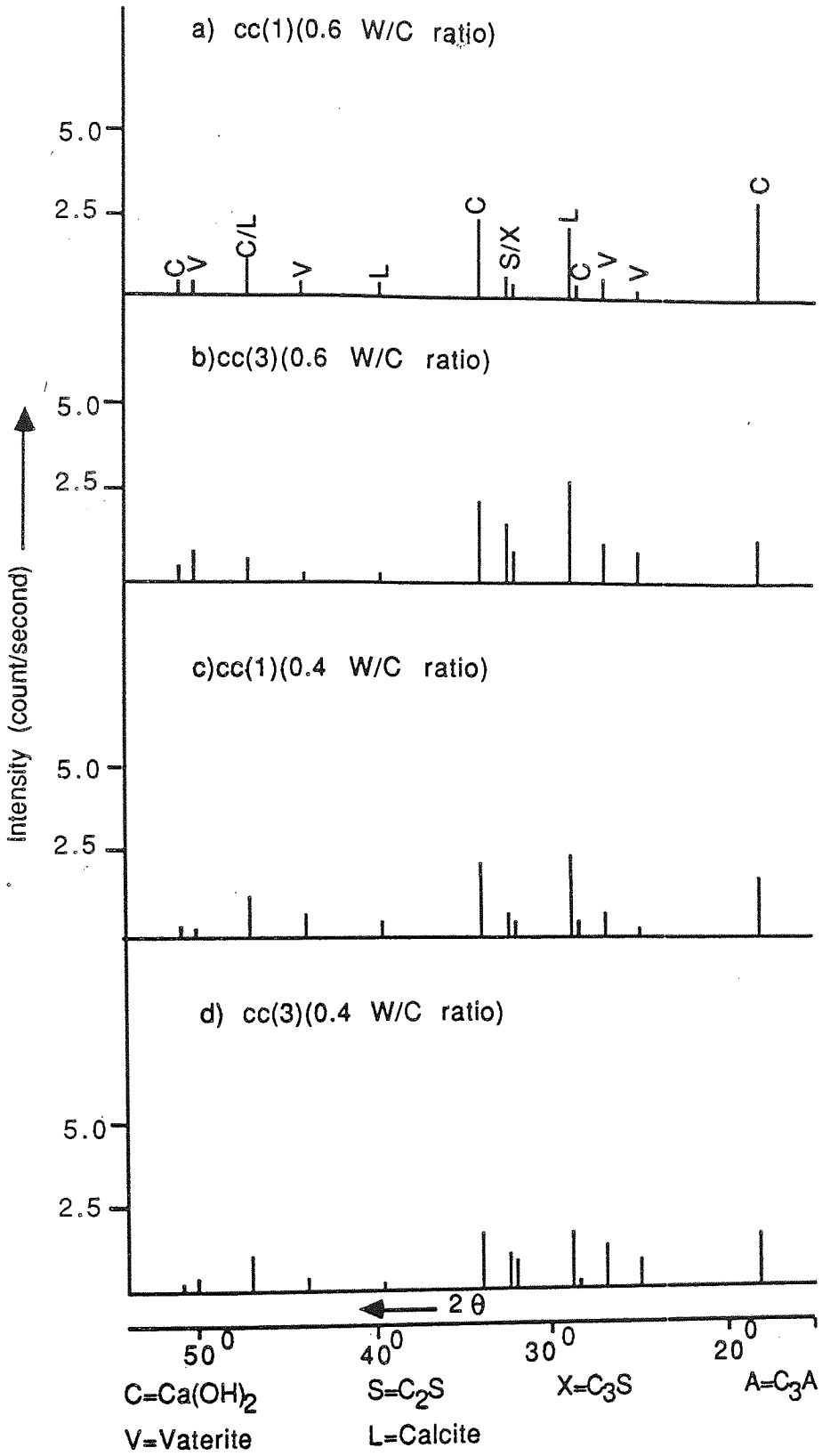

Figure 6.17 XRD traces of OPC/ PFA for carbonated samples originally cured for 29 days.

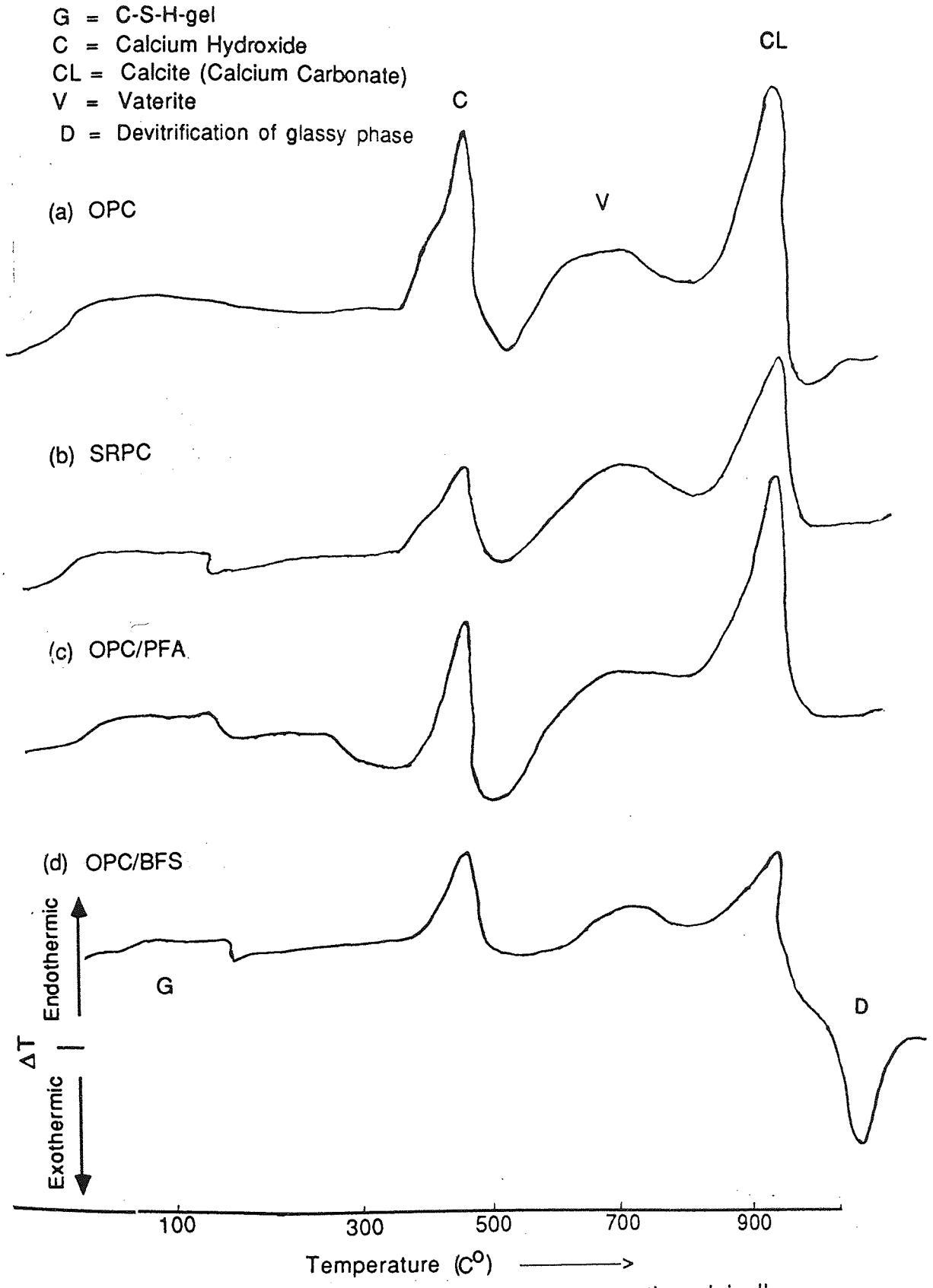

Figure 6.18 DTA thermographs of 0.6 water/cement ratio originally cured under cc(3) for 28 days and then carbonated.

evident. A broad shallow peak at about 700^{o}C was observed , which is normally related to the amount of vaterite present (32).

6.5 RESULTS FOR POLYMER IMPREGNATED CEMENT PASTES

6.5.1 The Rate Of Carbonation K For Impregnated Samples

Table 6.2 shows the carbonation rates (K value) for the same cement pastes, at 0.4 and 0.6 water/cement ratio, following polymer impregnation after curing under condition (1) and (3). Samples of cc(3) both at 0.4 and 0.6 water/cement ratio did not show any sign of carbonation, therefore these results are not shown in table 6.2. The reason for this will be refered to later.

The results for OPC,SRPC and OPC/PFA 0.4 water/cement ratio cc(1) indicate that the K rate of carbonation value was reduced compared with the unimpregnated samples, but for OPC/BFS cement K the rate of carbonation has actually increased.

6.5.2 Calculated Depth Of Carbonation For Impregnated Samples At 100 Days

The calculated depths of carbonation at 100 days for the above cements at 0.4 and 0.6 water/cement ratio[cc(1) and cc(3) can be seen in table 6.2. These are also represented in the form of histograms in figure 6.11. For 0.4 water/cement ratio cc(1) the results show that for polymer impregnated samples of OPC, SRPC and OPC/PFA with a polymer loading value of between 5.3% and 6.6% by weight of cement paste, the depth of carbonation compared to the unimpregnated samples was reduced considerably. This was not true however for OPC/BFS where the

depth of carbonation has actually increased by a small margin. The 0.6 water/cement ratio cc(1) polymer impregnated samples, had a polymer loading value of between 7% and 11.5% by weight. It is clear however, from the results that depth of carbonation for all types of cement, has increased.

This may be related to the subsequent evaporation of the monomer. As was shown in chapter 5. When a cement paste is polymer impregnated its porosity decreases sharply. This was not the case however for the 0.6 water/cement ratio cement pastes subjected to curing condition 1. Figure 6.19. representing OPC before and after impregnation, shows clearly that the pore size distribution has remained virtually the same. This would suggest therefore, that full impregnation has not taken place but this phenomenon will be discussed more fully later.

With regards to the results of % of polymer loading for 0.4 water/cement ratio cc(3) as indicated in figure 6.11 the percentage of polymer loading for OPC, SRPC, OPC/PFA increased by twice as much. Because of the high degree of loading, the depth of carbonation for all cements was reduced to zero. Similarly for 0.6 water/cement ratio cc(3) the % of polymer loading by weight, figure 6.11, increased to between 25% and 32% for all cements, and because of this there was no sign of carbonation.

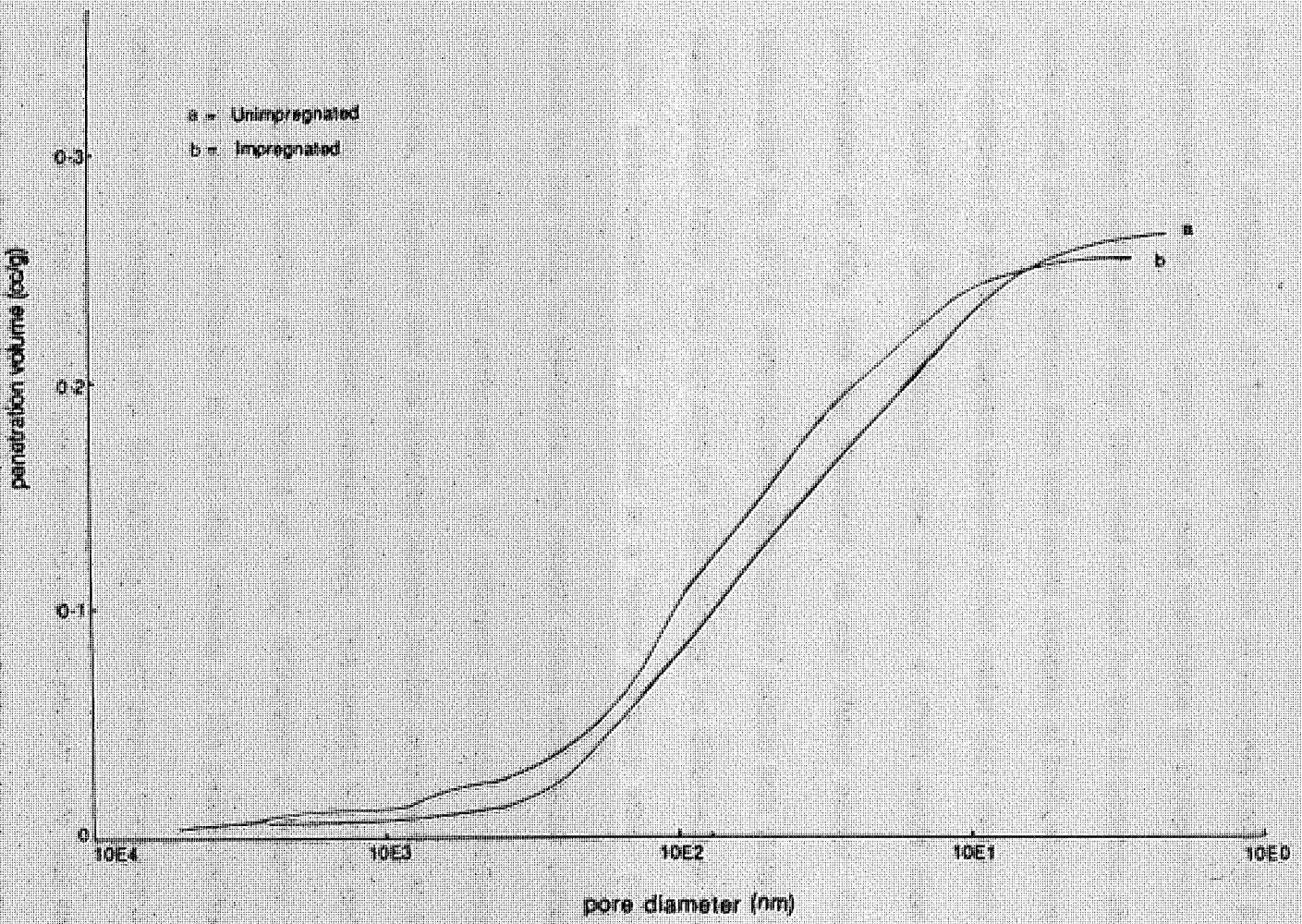

Figure 6.19 Pore size distribution curves of badly polymer impregnated and unimpregnated OPC paste of 0.6 water/cement ratio cured under cc(1).

6.6 DISCUSSION OF THE RESULTS

6.6.1 Unimpregnated Plain Cement Pastes

Well cured samples of all the different kinds of cements used at 0.4 and 0.6 water/cement ratio cc(1) show very good resistance to carbonation, compared with samples kept under cc(3). The chief reason for this is because samples kept under cc(3) are more porous than well cured samples at both water/cement ratio. As mentioned in earlier chapters samples cured under cc(1) eventually develop a very sound and dense structure, see chapter 4 which would slow down the penetration of CO_2 into the structure. As was shown earlier, the speed of carbonation for all 0.6 water/cement ratio cement pastes was faster than for 0.4 water/cement ratio. This can also be explained by the difference in porosity. The higher water/cement ratio resulted in a higher porosity which provides easy access for the CO_2 to penetrate the cement paste and cause carbonation. By comparing the rate of carbonation for different cements regardless of curing conditions, it appears that the blended cement pastes carbonated at a somewhat faster rate than the portland cement pastes. The reason for this can be partly explained by looking at the results of X-ray diffraction in chapter 4. For the different cements subjected to cc(1) the intensity of the peaks representing the calcium bearing phases in OPC for $Ca(OH)_2$ is much greater than that of the peaks for OPC/BFS. This indicates that blended cement pastes offer less resistance to carbonation than the OPC based cement paste owing to their lower content of carbonatable material, a fact supported also by the results of DTA in Chapter 4.(36).

Conversely, well cured blended cements, and in particular OPC/BFS of 0.4

water/cement ratio have a somewhat tighter pore structure than the portland cements, figure 3.3, so the resultant carbonation rates are not as high as might be expected. For samples subjected to cc(3) however, as the pore structure of the blended cements is considerably coarser, particularly at 0.6 water/cement ratio, (see also chapters 3 and 4) the carbonation rates are much higher. Curing condition appears to have a lesser effect on the porosity of portland cements, therefore the increase in the rate of carbonation is not as marked as for the blended cements.

6.6.2 Impregnated Cement Pastes

Badly cured samples i.e cc(3) of all types of impregnated cement pastes, regardless of water/cement ratio resulted in little or no carbonation. This was true also for OPC, SRPC and to some extent for the OPC/PFA blend samples of 0.4 water/cement ratio cc(1). The reason for this is mainly due to the coating of polymer which will block most pores within the cement pastes matrix. Therefore the CO_2 has to overcome this physical barrier in order to penetrate the structure and neutralize the cement matrix, figure 6.11.

For 0.6 water/cement ratio cc(1) for all types of cements, carbonation after impregnation was greater than those samples without impregnation. This appears to be contrary to the expected results. By studying table 5.3 (page 144). Some suggestions can be made. One observation is that the percentage of pore volume filled polymer after impregnation was low for all the 0.6 water/cement ratio well cured samples cc(1) (between 18 and 27% compared to 51 -71% for the badly cured samples cc(3). Polymerisation did not therefore appear to reduce porosity to a desired level. Nevertheless any reduction in porosity should still have been beneficial in reducing the carbonation rate. The fact that in all cases an increase in

carbonation was observed points to a phenomenon other than it was suggested earlier (chapter 5, section5.1) that a chemical reaction may have taken place during polymerisation which affected hydration products such as $Ca(OH)_2$. This may have reduced the total amount of carbonatable material to such a level so that even with a lower porosity the carbonation rate increased.

In the case of the badly cured samples cc(3) even though some chemical reactions may still have accured, the better polymer loading would have reduced porosity to a low enough level so that the physical barrier to CO_2 penetration would have been more important.

Even though the percentage of pores filled with polymer of the 0.4 water/cement ratio well cured samples cc(1) was still low (21 to 32%) in most cases it appears to have been sufficient to reduce the rate of carbonation as the porosity of these samples was already low. The one exception in this group is the OPC/BFS samples. As was the case with well cured 0.6 water/cement ratio cc(1) samples, carbonation was actually faster after impregnation of the samples, this may be related to the lower carbonatable material content of this particular cement, thus making somewhat easier to carbonate, see figures 4.10 and 4.22.

6.7 CONCLUSIONS

1. Some conditions produce a fast initial carbonation rate followed by a second slower rate, which make direct comparisons between conditions difficult, therefore only the rate of carbonation K is considered. A more representative value was thought to be the depth of carbonation of 100 days.

2. The rate of carbonation was found to be related to the water/cement ratio,

where 0.6 water/cement ratio pastes had showed a greater tendency to carbonate. This was thought to be due to the coarser pore structure of the 0.6 water/cement ratio cement pastes, allowing easier penetration of CO_2.

3. Curing condition also had a marked effect on the rate of carbonation, "badly-cured" specimens always resulting in much higher depth of carbonation attributed to the pore structure, where curing condition (3) had always produced higher porosities for all cement pastes.

4. Blended cements had showed a somewhat higher tendency to carbonate than portland cements, a fact which could not be attributed wholly on porosity. It appears that the lower amount of carbonatable material contained in such cements may have been responsible for the observation.

5. Polymer impregnation of cement pastes subjected to cc(3) had, in all cases, reduced carbonation to a minimum, as pores were fully or partly blocked producing a physical barrier which the CO_2 could not penetrate. Cement pastes subjected to cc(1) were not however always successful in reducing carbonation. All the 0.6 water/cement ratio cement pastes and that of OPC/BFS 0.4 water/cement ratio, had actually allowed faster carbonation to occur, which suggests a possible reduction of the carbonatable material of the cement. The reason for this is unclear but some form of reaction between the cement hydration products and the monomer cannot be ruled out. As was discussed in chapter 5., however, it may be possible to eliminate this difficulty by double impregnation of the samples

CHAPTER 7 DIFFUSION OF CHLORIDE IONS THROUGH HARDENED CEMENT PASTE DISCS

7.1 RESULTS

Values of chloride ion concentration, as measured in compartment (2) of each diffusion cell, described in chapter 2.6, were plotted against time. Typical plots are shown in figures 7.1 - 7.3.

Over the period of experiments the chloride concentration in the diffusion cell compartment (1) figure 2.10 which is the high concentration side, remains effectively constant. This is assumed with conditions of quasi - steady - state diffusion across the disc and therefore the chloride ion flux and activity are constant throughout all sections of the discs. The flux (J) in mole $cm^{-2}s^{-1}$ of chloride ion entering compartment (2) is then given by Fick's first law.

$$J = \frac{V}{A} \cdot \frac{dC_2}{dt} = \frac{D}{l} (C_1 - C_2)$$

where

D = effective diffusivity of chloride ion through the disc ($cm^2 s^{-1}$)

V = is the volume of solution in compartment 2 (cm^3)

A = is the cross - sectional area (cm^2)

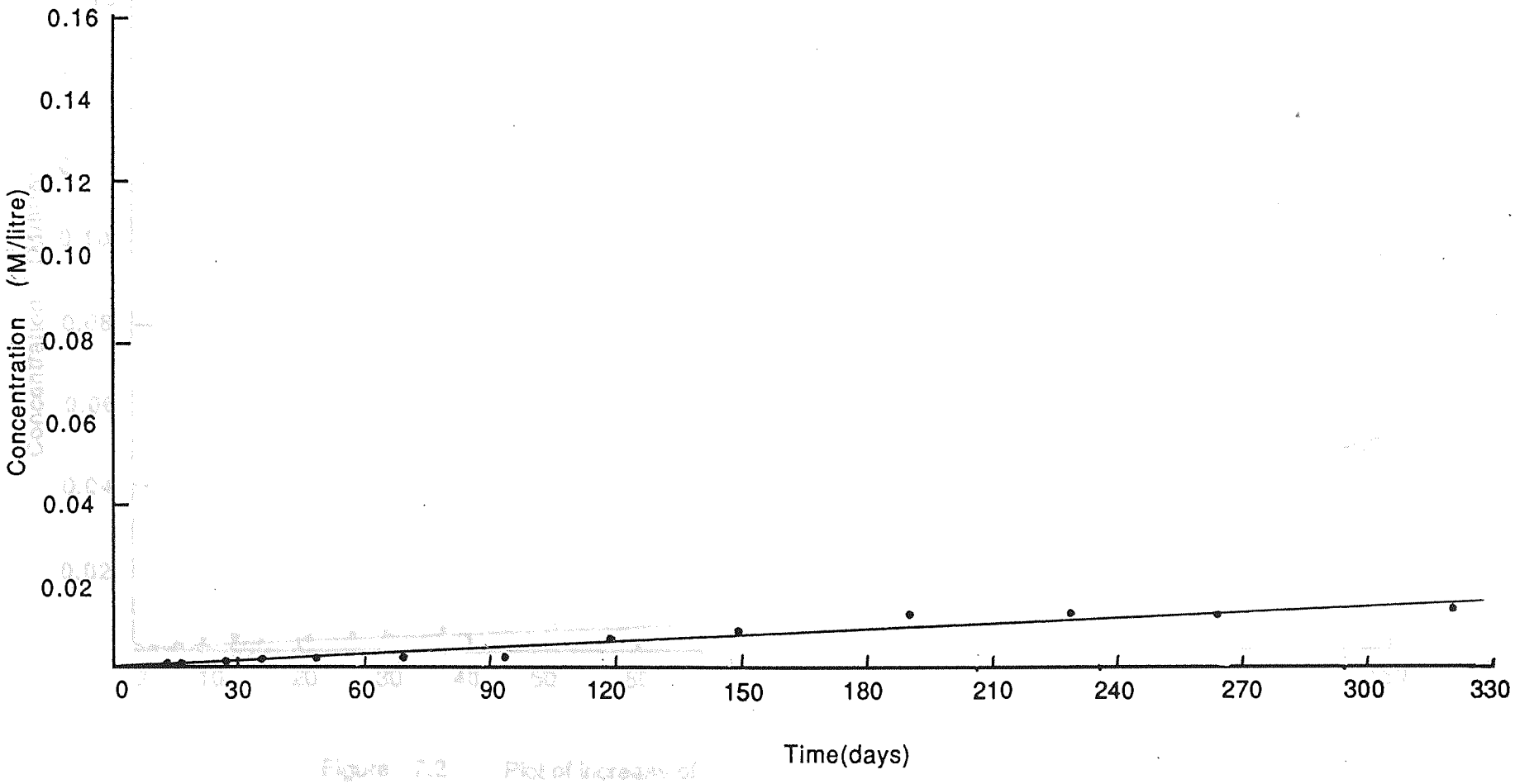

Figure 7.1 Plot of increase of ionic concentration in compartment 2 of the diffusion cell with time for polymer impregnated OPC discs of 0.6 water/cement ratio cured under cc(3).

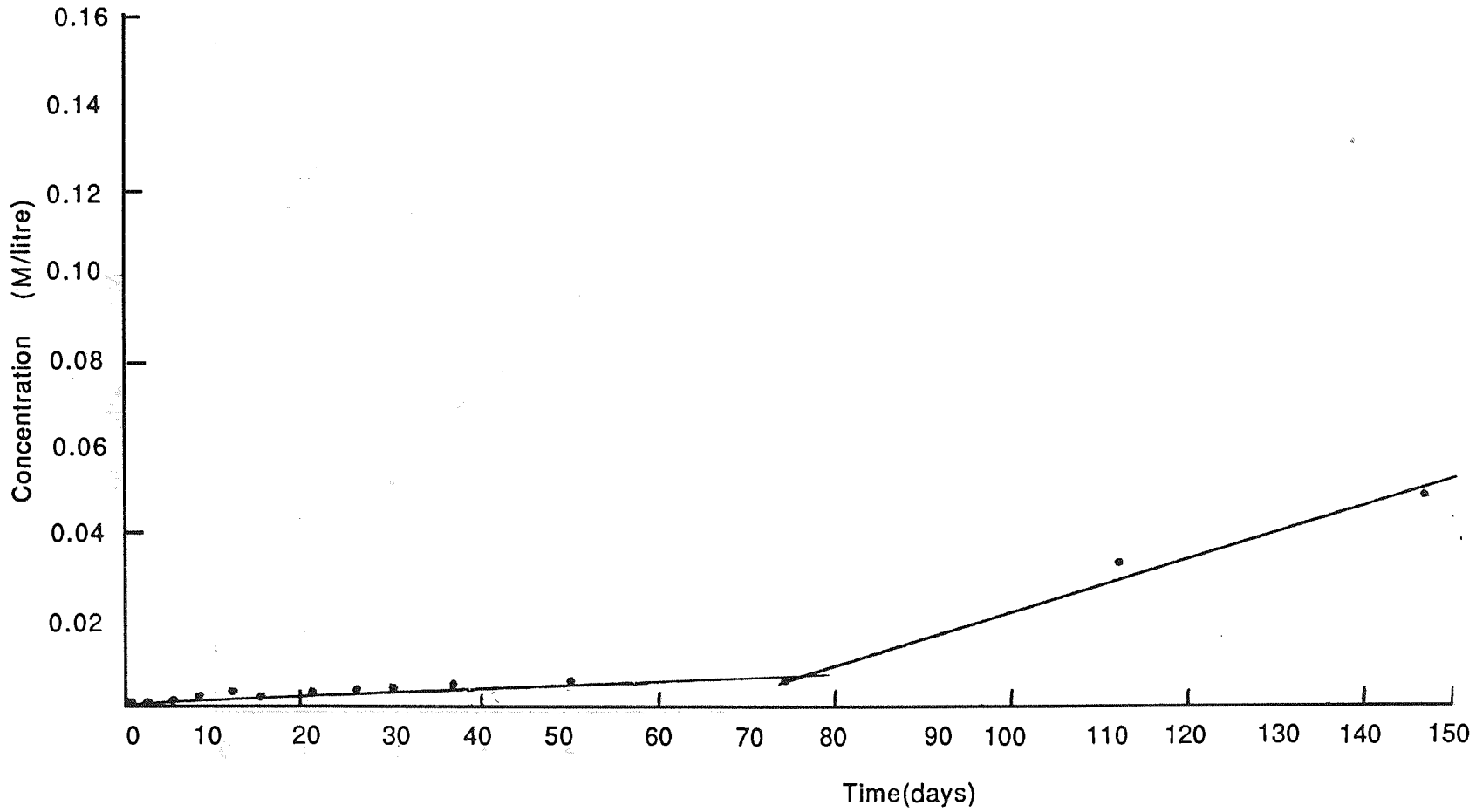

Figure 7.2 Plot of increase of ionic concentration in compartment 2 of the diffusion cell with time for polymer impregnated OPC discs of 0.6 water/cement ratio and cc(1).

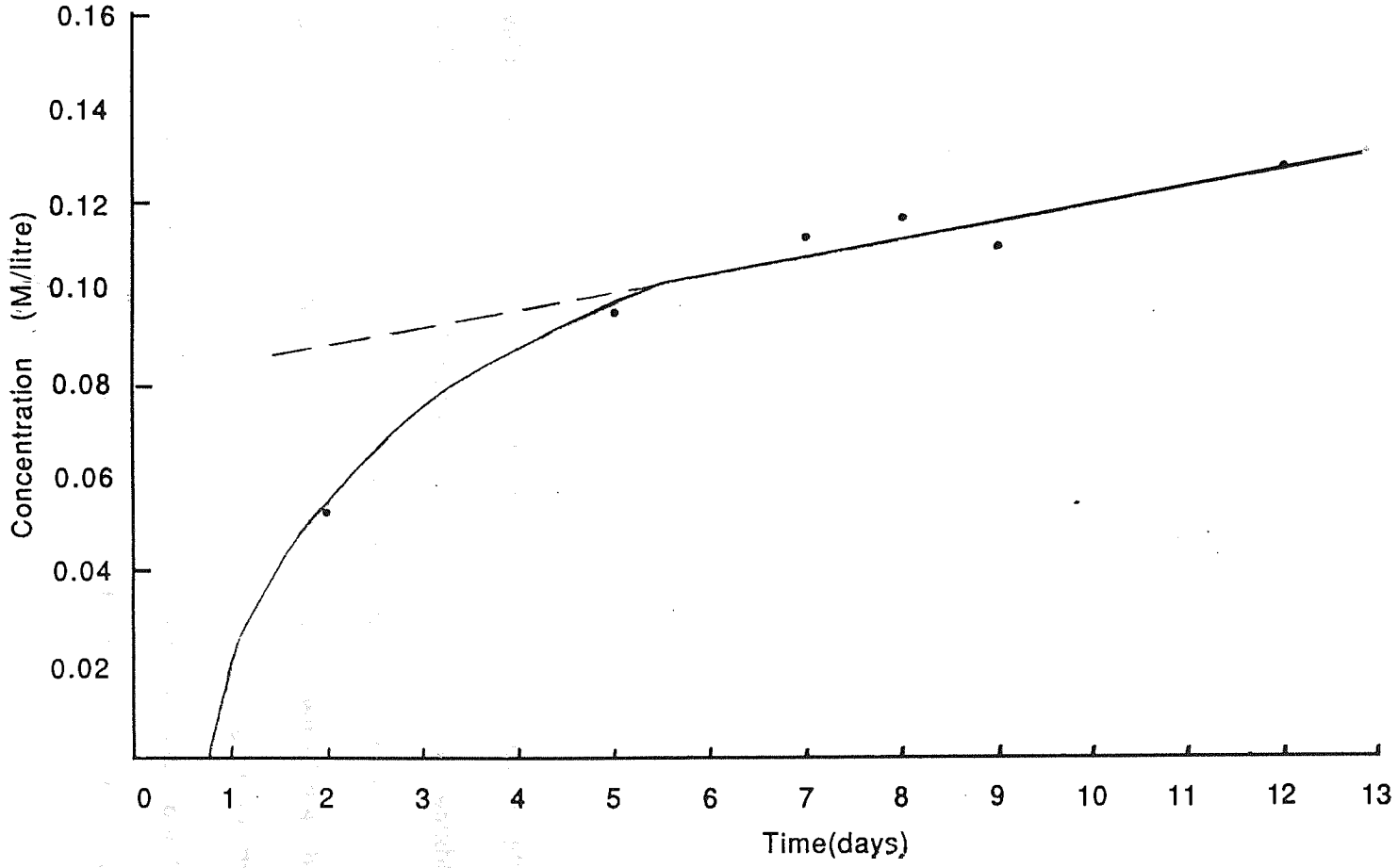

Figure 7.3 Plot of increase of ionic concentration in compartment 2 of the diffusion cell with time for unimpregnated OPC/BFS discs of 0.6 water/cement ratio cured under cc(3).

l = is the thickness of the disc (cm)

C_1= chloride concentration in compartment (1) (M/cm^3)

C_2= chloride concentration in low side (M/cm^3)

For the conditions $t > t_o$, $C_1 >> C_2$ this can be simplified to :-

$$C_2 = \frac{DAC_1}{lV} (t - t_o)$$

Thus D may be calculated from the slope of the rectilinear plot of C_2 versus t :-

$$D = \frac{C_2}{(t - t_o)} \cdot \frac{lV}{C_1 A}$$

Thus the values of D were calculated for 45 disc samples subjected to diffusion test. Normally an induction period, during which diffusion becomes established across the disc is observed (45). In some cases further hydration during the period of diffusion, appears to have caused some slowing down of the chloride migration. This phenomenon was particularly evident in the case of the "badly" cured OPC/BFS cement pastes, figure 7.3. The effective diffusion coefficient values for these specimens were therefore estimated from the earlier part of the curve as will be discussed later.

The increase in concentration in compartment 2 for the impregnated samples was normally very slow and fairly consistent over periods of up to 320 days, figure 7.1, but in some cases for the well cured 0.6 water/cement ratio impregnated OPC

cement pastes after the normal slow increase there was a sudden increase in the diffusion, figure 7.2. In such cases the calculated effective diffusion coefficients were based on the first part of the curve.

The effective diffusivities for the two types of cements OPC and OPC/BFS for both impregnated and unimpregnated samples are given in table 7.1.

In the case of OPC, results were obtained for all conditions i.e. 0.4 and 0.6 water/cement ratio, both for curing condition (1 and 3) except for existing values 0.4 and 0.6 water/cement ratio cc(1)* which were taken from (166). Whereas in the case of OPC/BFS only values for samples of 0.6 water/cement ratio cc(3) were obtained. These were also compared to existing values for unimpregnated samples of cc(1)* (166).

Considering first the case of OPC at 0.4 water/cement ratio for samples of cc(1) and cc(3) it is clear that the average D-value for well cured samples was greatly reduced, compared with badly cured samples. The "badly - impregnated" samples of cc(3) (as explained in chapter 5) show a slightly higher Cl^- diffusion coefficient, than the unimpregnated samples, whereas the samples that were well impregnated with polymer show a much lower Cl^- diffusion even when compared to well cured samples of OPC.

An increased water/cement ratio i.e. 0.6, enabled higher Cl^- diffusion for unimpregnated samples both at cc(1) and cc(3). However this difference was more dramatic for the poorly cured samples than for the well cured ones. As for impregnated samples of both curing conditions at 0.6 water/cement ratio, it can

Cement	W/C ratio	Curing condition	Impregn -ation	Discs						
				1	2	3	4	5	Mean	SD
OPC	0.4	(1) *							2.08	
		(3)	Unimpreg	23.74	31.89	24.90	30.30	32.70	28.71	4.12
		(3)	Badly impreg	41.08	30.39	35.96	39.00	36.62	36.61	4.03
		(3)	well impreg	0.31	0.25	0.33	0.96	0.09	0.39	0.33
OPC	0.6	(1) *							9.89	
		(1)	Unimpreg	6.58	3.95	7.84	7.31	7.57	6.65	1.58
		(1)	Well impreg	1.84	0.61	1.12	0.38	0.24	0.84	0.65
		(3)	Unimpreg	79.60	69.80	75.40	51.90	58.40	67.02	11.61
		(3)	Well impreg	0.16	0.48	0.35	0.74	0.29	0.40	0.22
OPC/BFS	0.6	(1) *							0.97	
		(3)	Unimpreg	103.60	99.90	90.30	96.70	88.20	95.74	6.4
		(3)	well Impreg	0.05	-----	0.45	0.46	0.22	0.30	0.2

* Ref (166)

Table 7.1 Effective diffusivity of chloride ion for polymer impregnated and unimpregnated OPC and OPC/BFS cement pastes at 25°C $(cm^2\ s^{-1}) \times 10^8$.

be seen that Cl^- diffusion was much slower, compared with the unimpregnated samples, particularly for the cc(3) specimens.

Results for blended cements at 0.6 water/cement ratio show that the calculated chloride effective diffusivities of samples cured in cc(1) have exceptionally lower values than samples cured under cc(3). As was the case for OPC, well impregnated OPC/BFS samples showed a substantial reduction in Cl^- effective diffusivity, compared to the unimpregnated samples. Also this value is only slightly lower than that for the unimpregnated samples of cc(1). Comparing the results of Cl^- diffusion between the unimpregnated OPC and OPC/BFS samples at 0.6 water/cement ratio, it can be seen that for samples under cc(1) Cl^- diffusion for OPC was considerably greater than for blended cements (166). Whereas for samples under cc(3) the reverse effect was true. As for impregnated samples for both cements, a very similar value was obtained.

MIP cumulative pore size distribution curves for 0.4 and 0.6 water/cement ratio for OPC cc(3) and OPC/BFS cc(3) for both impregnated and unimpregnated samples before and after subjecting to diffusion were obtained, (figures 7.4 - 7.6).

Considering first the case of OPC 0.4 water/cement ratio for badly impregnated samples, figure 7.4 shows nearly the same pore size distribution value and total volume of pores, showing little effect of the diffusion process on porosity.

Figure 7.5 summarises the MIP results for samples of OPC at 0.6 water/cement ratio cc(3) both in the impregnated and unimpregnated condition. Figure 7.5b shows the way in which the pore size distribution of the pores changes and the total porosity is reduced for impregnated

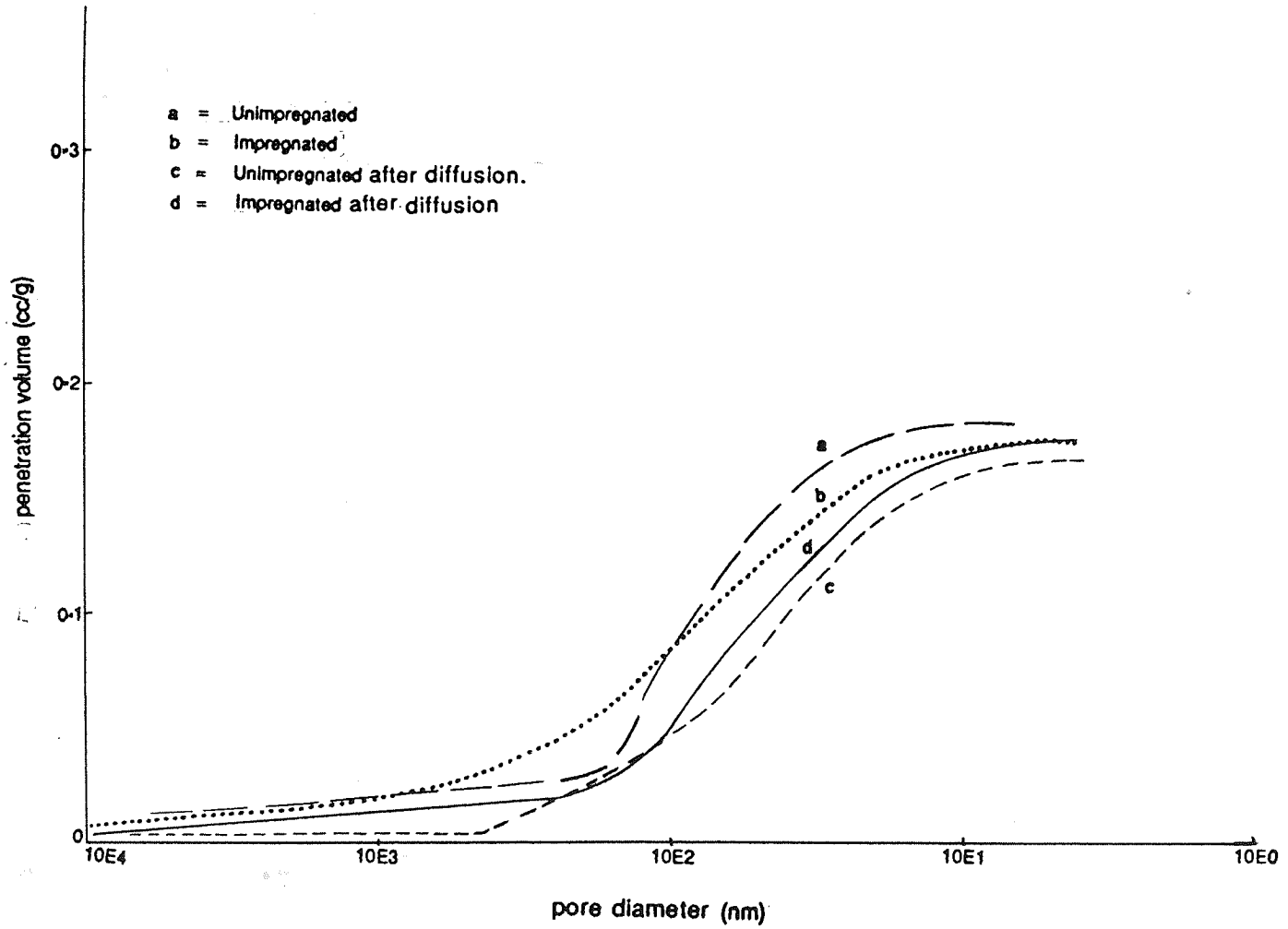

Figure 7.4. Pore size distribution curves of polymer impregnated and unimpregnated OPC discs of 0.4 water/cement ratio cured under cc(3) before and after diffusion.

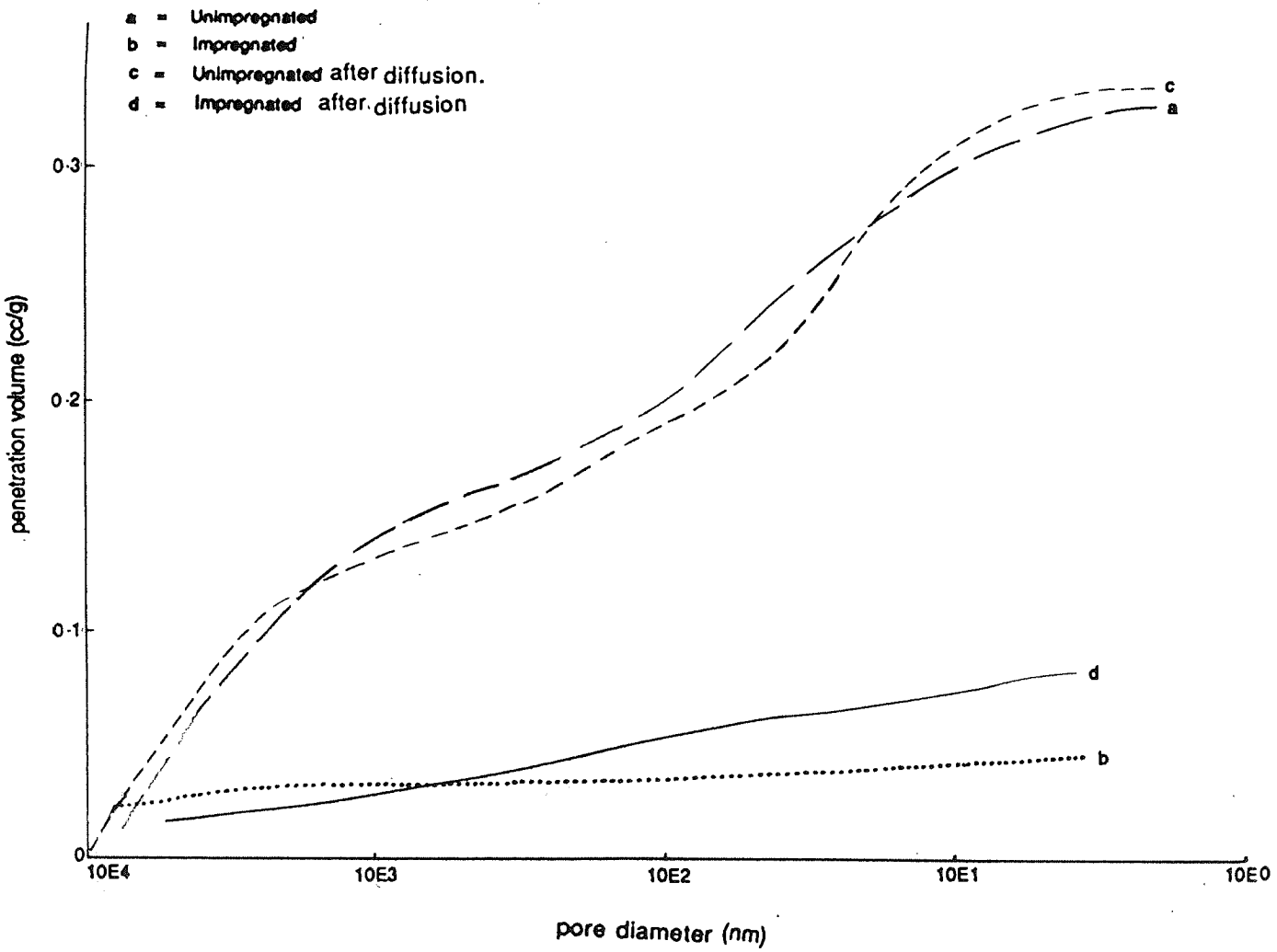

Figure 7.5 Pore size distribution curves of polymer impregnated and unimpregnated OPC discs of 0.6 water/cement ratio cured under cc(3) before and after diffusion.

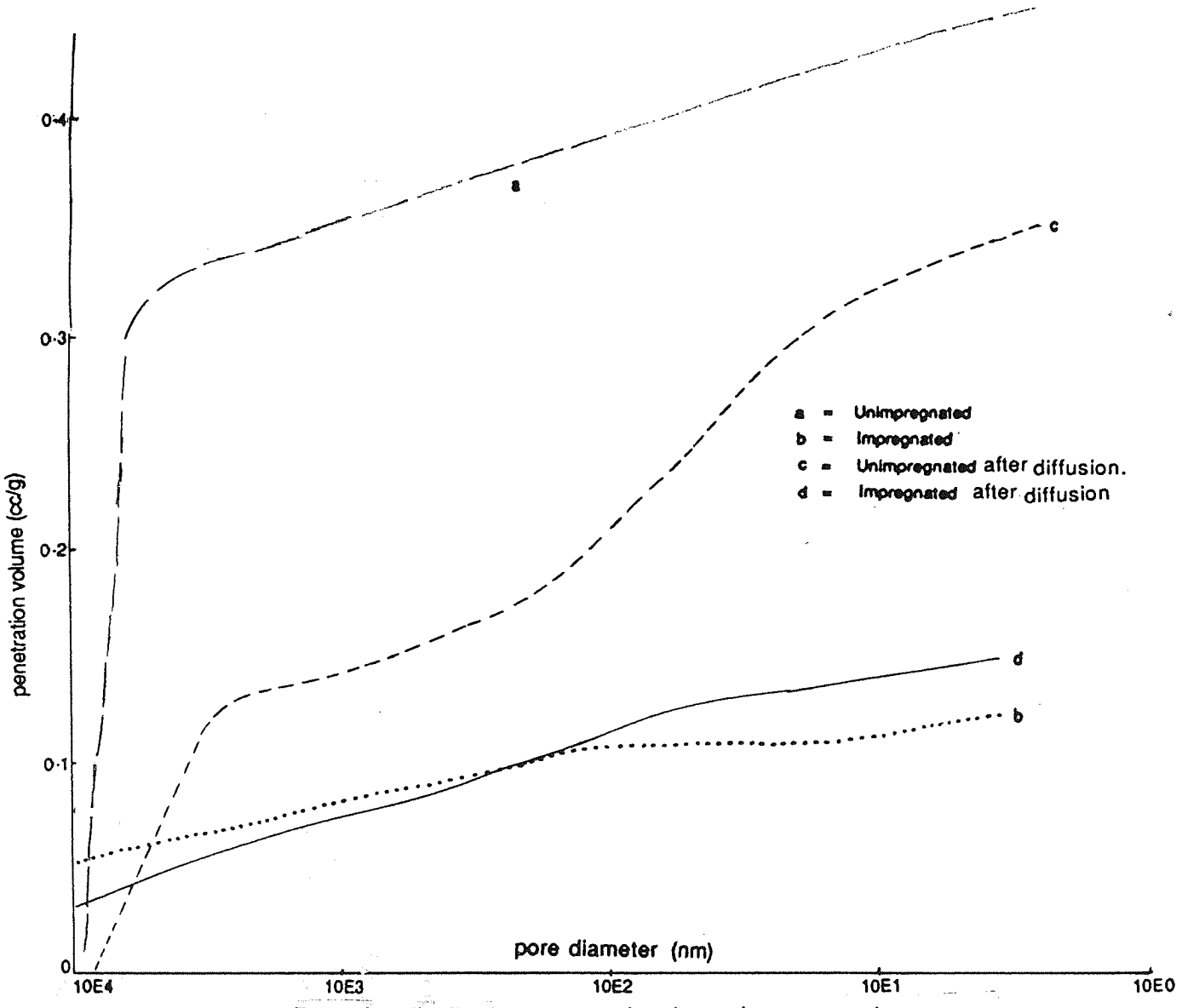

Figure 7.6 Pore size distribution curves of polymer impregnated and unimpregnated OPC/BFS discs of 0.6 water/cement ratio and cc(3) before and after diffusion.

discs compared with figure 7.5a. Both samples were tested before they were subjected to diffusion. As was the case for 0.4 water/cement ratio, there is little difference between figures 7.5a, and 7.5c, and also 7.5b, and 7.5d, before and after subjecting to diffusion.

In a similar manner MIP was carried out for OPC/BFS, figure 7.6, at 0.6 water/cement ratio cc(3). There was a considerable reduction for total pore volume for the unimpregnated condition after diffusion compared with before, i.e. curve a and c. This is caused by the increased curing of the cement pastes while subjected to diffusion. As the porosity decreased, the diffusion of Cl^- was slowed down as can be seen in figure 7.3. Effective diffusion coefficients for these specimens were therefore calculated by taking the gradient of the curve during the early diffusion period.

7.2 DISCUSSION

As shown earlier, well cured samples show less Cl^- diffusion, compared to sample kept under cc(3), but particularly so for the blended cement. The reason for this is mainly due to the higher porosity for poorly cured samples, which encourages the faster diffusion of Cl^- ion from compartment (1) to (2).

The much slower diffusion of chloride in the well cured blended cement cannot however be explained entirely by the porosity. There may also be an increased surface interaction between the diffusing Cl^- ions and the surface of the cement paste particles, as suggested by (52). The observed faster chloride diffusion in the OPC 0.6 water/cement ratio cement pastes compared to 0.4, appears to be mainly due to higher porosity. In the main, polymer impregnation of the samples was shown to decrease the chloride effective diffusivities. the effect was however

less after a length of time for some 0.6 water/cement ratio OPC impregnated samples when chloride diffusion showed a sudden increase, figure 7.2. The reason for the decreased chloride effective diffusivities is not known but may be related to some kind of break down of the polymer with time. The chief reason for the decrease in the chloride effective diffusivities for the polymer impregnated samples is because by impregnating, the porosity of the samples is reduced as shown in table 7.2 -7-3. and figure 7.5 and 7.6 for MIP pore size distribution. Hence it will be far harder for Cl^- ions to diffuse through. For badly impregnated samples of OPC 0.4 water/cement ratio cc(3) the value of diffusion had actually increased by a small margin. By looking at MIP pore size distribution for all cases, figure 7.4 it can be seen that there is little difference among curves, therefore it could well be that by badly impregnating the samples, somehow the interaction between Cl^- ion and cement paste mentioned earlier might have been reduced therefore allowing Cl^- ion to move from one side to the other with less resistance.

7.3 CONCLUSIONS

1. Badly cured OPC and OPC/BFS cements showed higher D-values than well cured ones, because of the increased porosity.

2. Regardless of curing conditions higher water/cement ratio means faster Cl^- diffusion, again due to an increase in porosity.

3. Well impregnated samples showed a substantial reduction in D-values, as pores were filled or blocked by polymer. In a few cases however there could have been some kind of break down of the polymer, allowing an increase in diffusion. For badly impregnated samples there may even have been an increase in diffusivity.

4. Well cured 0.6 water/cement ratio cc(1) OPC/BFS cement, normally showed a slower Cl^- diffusion than either well cured, 0.4 or 0.6 water/cement ratio OPC (68). For the badly cured 0.6 water/cement ratio cc(3) OPC/BFS cement, diffusion was significantly faster than either badly cured 0.4 or 0.6 water cement ratio OPC. This may just be explained by the increased porosity.

Number of Discs			1	2	3	4	5	Mean
Cement	W/C ratio	Curing Conditi - on	% Of polymer loading by weight					
OPC	0.6	1	28.6	25.5	29.8	28.8	27.9	23.4
OPC	0.4	3	15.8	15.4	13.8	15.0	13.1	12.2
OPC	0.6	3	25.1	26.5	28.1	24.8	29.6	22.3
OPC/BFS	0.6	3	22.3	25.8	25.5	24.6	31.4	21.6

Table 7.2 Percentage of polymer loading by weight of the discs for cement pastes at two different water/cement ratios and curing conditions.

Number of Discs			1	2	3	4	5	Mean
Cement	W/C ratio	Curing Conditi - on	% Of volume of pores filled with polymer					
OPC	0.6	1	79.4	70.8	82.8	80.0	77.5	78.1
OPC	0.4	3	77.5	75.5	67.7	73.5	64.2	71.7
OPC	0.6	3	61.5	65.0	68.8	60.8	72.5	65.7
OPC/BFS	0.6	3	46.5	53.8	53.1	51.3	65.4	54.0

Table 7.3 Percentage of volume of pores filled with polymer for cement pastes at two different water/cement ratios and curing conditions.

CHAPTER 8 THE CORROSION BEHAVIOUR OF STEEL EMBEDDED IN HARDENED CEMENT PASTES

8.1 INTRODUCTION

In earlier chapters it was shown that the rate of carbonation and Cl^- ions diffusion in hardened cement pastes, depends on such parameters as type of cement, curing condition, water/cement ratio and also on the degree of polymer loading of the samples.

In chapter 1. section 1.1 it was explained that corrosion of embedded steel can be effected by the presence of Cl^- ion diffusion and carbonation, as the normally passive layer of the steel can depassivate under such conditions.

Experiments were therefore set up to measure the rate of corrosion of steel embedded in a selection of cements exposed to potentialy aggressive environments viz a carbonated inducing environment of 50% RH and 40^{o}C and immersion in 1M NaCl solution in saturated $Ca(OH)_2$, the results are described in this chapter. The preparation of samples used in this part of the work has already been explained in chapter 2. section 2.7 as well as the linear polarisation technique, which is in section 2.7.1.

8.2 RESULTS

Results are presented as plots of I_{corr} versus time and E_{corr} versus time. All values shown are an average of 8 replicates for the NaCl condition or of 6 replicates for the carbonation condition. Plots of E_{corr} versus I_{corr} were also constructed using all individual values and a correlation coefficient was determined for each condition.

I_{corr} and E_{corr} values of parallel duplicate specimens kept in a 100% relative humidity environment, were recorded after about 6~months of exposure.

For polymer impregnated samples the results of percentage of total polymer loading by weight and percentage of total volume of pores being filled with polymer, can be seen in tables 8.1 and 8.2.

8.2.1 Samples Kept At 100% Relative Humidity

All the specimens exposed to 100% relative humidity, impregnated and unimpregnated, as shown in table 8.3 indicated a passive behaviour of low I_{corr} ($< 10^2$ nA/cm^2) and fairly high E_{corr} (> - 200mV) (86) measured after a period of 6 months.

The chief reason for this would appear to be that there are no aggresive agencies to cause the depassivation of the steel bars. The results are in good agreement with visual observation, an example of which can be seen in figure 8.1 and 8.2.

8.2.2 Samples Kept In A Rapid Carbonating Environment

I_{corr} and E_{corr} values for steel embedded in unimpregnated OPC cc(3) kept at 50% relative humidity and 40^{o}C and then exposed to saturated $Ca(OH)_2$ for 24 hours show some corrosion at 120 days. This is most likely to be due to carbonation of the surrounding cement paste. As was shown in chapter 6. table 6.1 at 100 days the depth of carbonation for this particular sample is above 10mm, which is the depth of the embedded steel in this work.

Samples of curing condition (1) showed no corrosion of embedded steel (table 8.4, figures 8.3). This was to be expected from the results of [chapter 6. table 6.1]

Curing conditon	Impregnation	Wt. of sample before impreg (g)	Wt. of sample after impreg (g)	Wt. gain after impreg (g)	% Of polymer loading by wt.	% Of volume of pores filled with polymer
1	Double	174.3	222.9	48.6	27.9	77.5
"	"	176.4	223.5	47.1	26.7	74.2
"	"	178.6	222.7	44.1	24.7	68.6
"	"	175.7	226.5	50.8	28.9	80.3
"	"	173.2	221.3	48.1	27.8	77.2
"	"	174.8	224.1	49.3	28.2	78.3
"	"	175.8	224.6	48.8	27.8	77.2
"	"	172.2	218.1	45.9	26.7	74.2
					The mean values 27.3	75.9
3	Single	169.8	211.6	41.8	24.6	60.3
"	"	169.3	210.2	40.9	24.2	59.3
"	"	172.6	208.2	35.8	20.6	50.5
"	"	167.5	211.5	44.9	26.3	64.5
"	"	170.7	212.0	41.3	24.2	59.3
"	"	171.6	213.8	42.2	24.6	60.3
"	"	169.6	215.7	46.1	27.2	66.7
"	"	172.9	208.8	35.9	20.8	51.0
					The mean values 24.1	59.1

Table 8.1 Percentage of polymer loading by weight and volume of pores filled with polymer, for OPC pastes subjected to single or double impregnation.

Curing conditon	Impregnation	Wt. of sample before impreg (g)	Wt. of sample after impreg (g)	Wt. gain after impreg (g)	% Of polymer loading by wt.	% Of volume of pores filled with polymer
1	Single	189.1	215.5	26.4	14.0	36.5
"	"	180.6	209.3	28.7	15.9	41.4
"	"	183.4	211.6	28.2	15.4	40.1
"	"	182.8	208.9	26.1	14.3	37.2
"	"	182.8	211.6	28.8	15.8	41.2
"	"	181.4	212.0	30.6	16.9	44.0
"	"	181.4	210.1	28.7	15.8	41.1
"	"	176.3	204.5	28.2	16.0	41.7
					The mean values 15.5	40.3
3	"	162.8	206.5	43.7	26.8	55.8
"	"	161.9	204.3	42.4	26.2	54.6
"	"	160.3	200.9	40.6	25.3	52.7
"	"	155.5	199.6	44.1	28.4	59.2
"	"	162.9	203.2	40.3	24.7	51.5
"	"	161.5	203.0	41.5	25.7	53.5
"	"	163.5	198.3	34.8	21.3	44.6
"	"	159.0	200.9	41.9	26.4	55.0
					The mean values 25.6	53.3

Table 8.2 Percentage of polymer loading by weight and volume of pores filled with polymer for OPC/BFS pastes.

Cement	Unimpregn -ated / Im pregnated (imp) / (unimp)	Curing conditions	I_{corr} (nA/cm^2)	I_{corr} mean (nA/cm^2)	E_{corr} (mV)	E_{corr} mean (mV)
OPC	unimp	1	4.127E1	5.961E1	-0.103	-0.151
	unimp	1	7.79E1		-0.199	
	unimp	3	5.688E1	4.472E1	-0.173	-0.177
	unimp	3	3.256E1		-0.181	
	imp	1	-----	-----	-0.378	-0.273
	imp	1	-----		-0.168	
	imp	3	0.832	0.903	-0.169	-0.171
	imp	3	0.974		-0.173	
OPC/BFS	unimp	1	-----	7.054E1	-----	-0.226
	unimp	1	7.054E1		-0.226	
	unimp	3	4.947E1	6.571E1	-0.190	-0.190
	unimp	3	8.195E1		-0.190	
	imp	1	2.948E1	4.149E1	-0.102	-0.099
	imp	1	5.353E1		-0.097	
	imp	3	0.539	0.539	-0.166	-0.210
	imp	3	-----		-0.253	

Table 8.3 Values of I_{corr} and E_{corr} for steel embedded in either polymer impregnated or unimpregnated OPC and OPC/BFS cement pastes kept at 100% RH over a period of about 6 months.

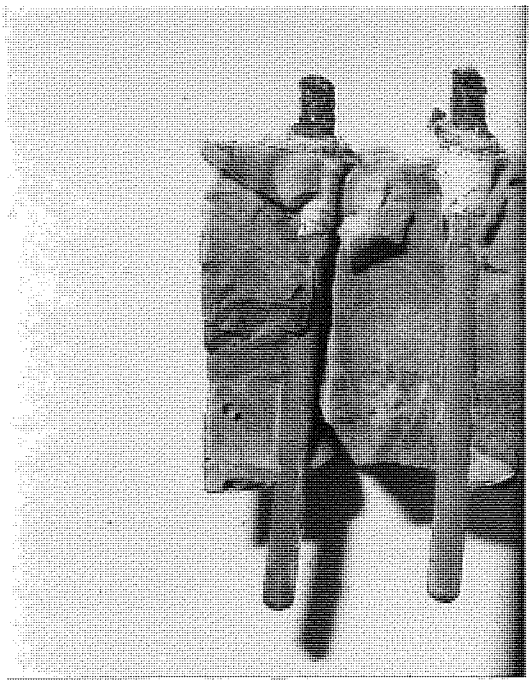

Figure 8.1 Photograph showing no corrosion of steel embedded in OPC paste placed in 100% RH and 25°C over a period of about 6 months.

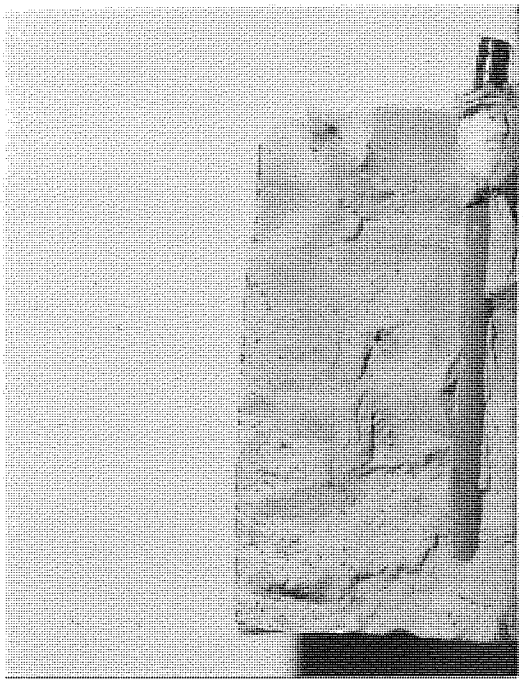

Figure 8.2 Photograph showing no corrosion of steel embedded in OPC/BFS paste placed in 100% RH and 25°C over a period of about 6 months.

which suggested that the depth of carbonation for this particular cement type would be about 6mm even after 160 days, i.e. less than the depth of cover, (at 6 months).

The above results are in good agreement with what was observed under visual observation where an example can be seen in figure 8.4.

No I_{corr} evaluations were possible for the impregnated samples exposed to the carbonating environment, possibly because of the high resistivity of the polymer impregnated cement pastes. E_{corr} values were higher, and always noble (table 8.4 figure 8.3) suggesting no corrosion of the embedded steel. It was demonstrated in chapter 6., that OPC samples of cc(3) which were polymer impregnated and had a high polymer loading, had shown no tendency to carbonate. Although some carbonation was observed for the single impregnated cc(1) samples, (chapter 6. table 6.2), the double impregnation procedure adopted here should have reduced carbonation considerably. Figure 8.5 also supports the evaluation that there was no corrosion of the steel.

As was mentioned in Chapter 2, samples were immersed in saturated $Ca(OH)_2$ solution 24 hours prior to the corrosion measurement. This may not have been the most realistic electrolyte as the pH of the pore solution would have tended to increase, but at the time it was thought the leaching of $Ca(OH)_2$ from within the specimen may have been more detrimental. This wet-dry cycle had immediately encouraged corrosion of the susceptible samples (see for example figute 8.8) so that very high corrosion rates were observed for the steel specimens embedded in OPC/BFS cement pastes of either curing condition, when exposed to the carbonating environment, table 8.5, figure 8.6. This was particularly true for cc(3). By refering to the carbonation chapter, it is obvious that for samples of

Impregnated (Imp) / Unimpregnated (Unimp)	Curing Conditions	13 days		49 days		47 days		118 days		174 days	
		I_{corr} (nA/cm2)	E_{corr} (mv)	I_{corr} (nA/cm2)	E_{corr} (mv)	I_{corr} (nA/cm2)	E_{corr} (mv)	I_{corr} (nA/cm2)	E_{corr} (mv)	I_{corr} (nA/cm2)	E_{corr} (mv)
unimp	1	5.845E1	-0.124	4.648E1	-0.115	3.118E1	-0.0806	4..81E1	-0.115	8.883E1	-0.154
unimp	3	3.238E1	-0.136	5.073E1	-0.171	7.017E1	-0.182	1.650E2	-0.210	3.331E2	-0.284
imp	1	—	-0.219	—	-0.202	—	-0.216	—	-0.219	—	-0.203
imp	3	—	-0.196	—	-0.159	—	-0.179	—	-0.197	—	-0.245

Table 8.4 Values of I_{corr} and E_{corr} with time for steel embedded in polymer impregnated and unimpregnated OPC of 0.6 water/cement ratio cured under cc(1) and cc(3) kept at 50%RH and 40^{o}C.

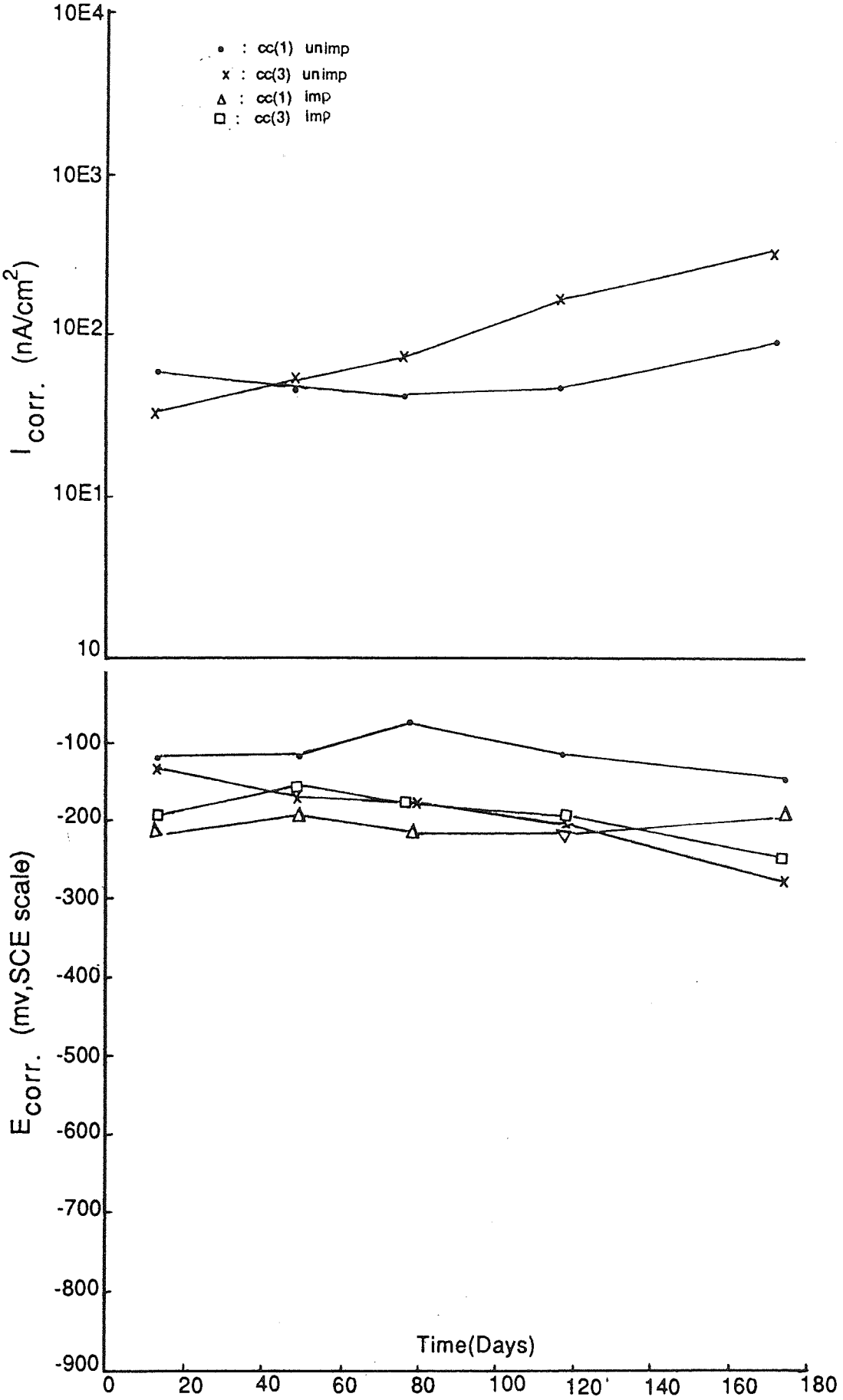

Figure 8.3 Plots of I_{corr} and E_{corr} versus time for steel embedded in polymer impregnated (imp) and unimpregnated (unimp) OPC paste of 0.6 water/cement ratio cured under cc(1) and cc(3) and exposed at 50%RH and 40^{o}C.

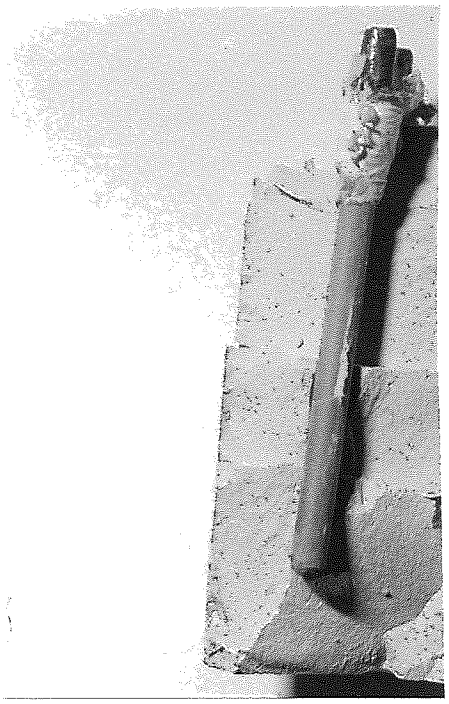

Figure 8.4 Photograph showing no corrosion of steel embedded in OPC paste of 0.6 water/cement ratio cured under cc(1) kept at 50%RH and 40^{o}C.

Figure 8.5 Photograph showing no corrosion of steel embedded in polymer impregnated OPC paste of 0.6 water/cement ratio cured under cc(1) kept at 50%RH and 40^{o}C.

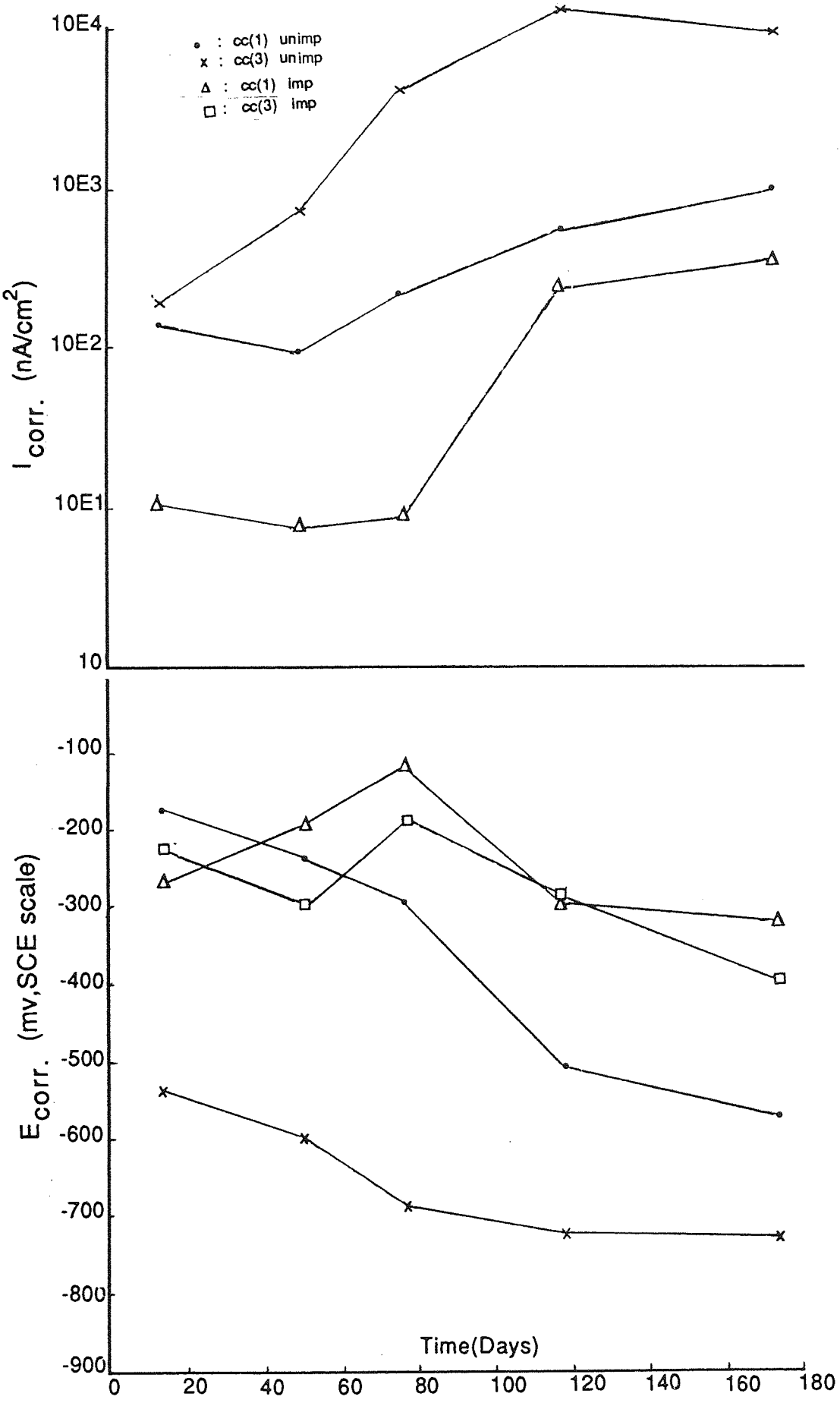

Figure 8.6 Plots of I_{corr} and E_{corr} versus time for steel embedded in polymer impregnated (imp) and unimpregnated (unimp) OPC/BFS pastes of 0.6 water/cement ratio cured under cc(1) and (3) and at 50%RH and 40^{o}C.

Impregnated (Imp) / Unimpregnated (Unimp)	Curing Conditions	14 days		50 days		77 days		118 days		174 days	
		I_{corr} (nA/cm2)	E_{corr} (mv)	I_{corr} (nA/cm2)	E_{corr} (mv)	I_{corr} (nA/cm2)	E_{corr} (mv)	I_{corr} (nA/cm2)	E_{corr} (mv)	I_{corr} (nA/cm2)	E_{corr} (mv)
unimp	1	1.478E2	-0.182	9.362E1	-0.238	2.101E2	-0.302	5.326E2	-0.514	9.535E2	-0.572
unimp	3	1.860E2	-0.537	7.033E2	-0.552	4.013E3	-0.694	1.376E4	-0.719	9.369E3	-0.732
imp	1	1.007E1	-0.269	7.326	-0.199	8.178	-0.119	2.359E2	-0.301	3.416E2	-0.350
imp	3	—	-0.232	—	-0.306	—	-0.186	—	-0.289	—	-0.398

Table 8.5. Values of I_{corr} and E_{corr} with time for steel embedded in polymer impregnated and unimpregnated OPC/BFS of 0.6 water/cement ratio cured under cc(1) and cc(3) kept at 50%RH and 40°C.

cc(3) carbonation reaches the depth at which the steel bars are embedded in a matter of 25 to 40 days, and from then onwards due to the aggresive environment into which steel is subjected the corrosion value increases rapidly. As for the samples of well cured OPC/BFS cc(1) the depth of carbonation does not quite reach the depth of cover, but the uneven progression of the carbonation front as was explained in chapter 2. means that some points of the steel are exposed to carbonated hardened cement paste and figure 8.7, shows this patchy corrosion of the steel quite clearly. Results for the same cement of cc(1) but impregnated (table 8.5 figure 8.6) show that the I_{corr} value was low until 120 days. From then onwards this tended to increase rapidly. This is due to penetration of the carbonation front to the steel surface at 10mm depth. In the carbonation chapter 6. table 6.2, it was shown that at 100 days the depth of carbonation for this sample is about 11mm. Double impregnation, as was mentioned in chapter 5., was not possible, as this led to cracking of the specimens, so protection against carbonation was minimal.

As for cc(3) no I_{corr} values were recorded, because of the high resistivity of the samples. Also as was shown in chapter 6 no carbonation was possible so corrosion was unlikely and again visual examination supported the above results, Figure 8.9.

8.2.3 Samples Kept In A NaCl Solution

The steel specimens embedded in unimpregnated samples of OPC for both cc(1) and cc(3) kept in 1M NaCl solution containing saturated $Ca(OH)_2$ showed a steady increase in corrosion intensity, as can be seen in table 8.6. figure 8.11 to 8.13. Presumably this was due to chloride ions reaching the surface of the steel. Also they do not appear to depend on curing conditions, although the Cl^- diffusion

Figure 8.7 Photograph showing corrosion of steel embedded in OPC/BFS paste of 0.6 water/cement ratio cured under cc(1) kept at 50%RH and 40°C.

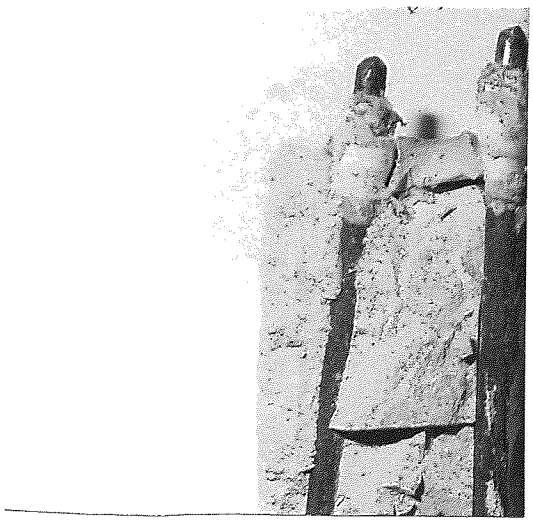

Figure 8.8 Photograph showing severe corrosion of steel embedded in OPC/BFS paste of 0.6 water/cement ratio cured under cc(3) kept at 50%RH and 40°C.

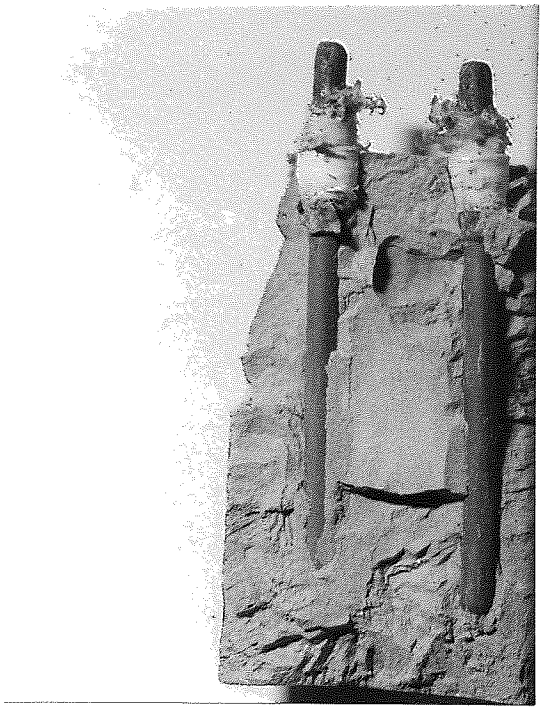

Figure 8.9 Photograph showing no corrosion of steel embedded in polymer impregnated OPC/BFS paste of 0.6 water/cement ratio cured under cc(3) kept at 50%RH and 40^{o}C.

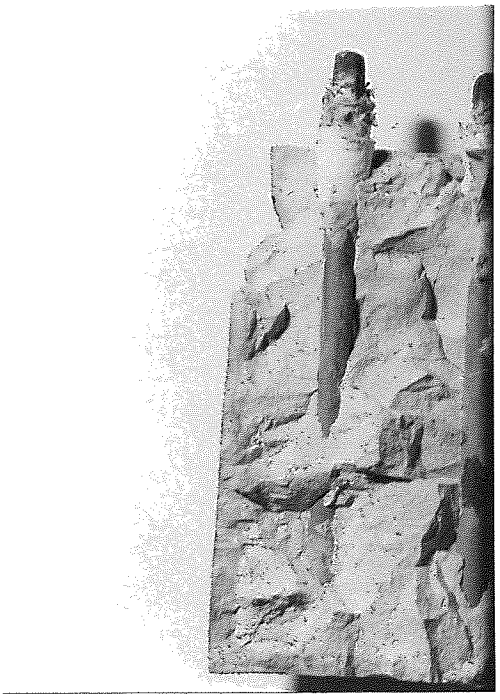

Figure 8.10 Photograph showing corrosion of steel embedded in polymer impregnated OPC/BFS paste of 0.6 water/cement ratio cured under cc(1) kept at 50%RH and 40^{o}C.

Impregnated (Imp) / Unimpregnated (Unimp)	Curing Conditions	9 days		35 days		56 days		84 days		125 days		162 days	
		I_{corr} (nA/cm2)	E_{corr} (mv)	I_{corr} (nA/cm2)	E_{corr} (mv)	I_{corr} (nA/cm2)	E_{corr} (mv)	I_{corr} (nA/cm2)	E_{corr} (mv)	I_{corr} (nA/cm2)	E_{corr} (mv)	I_{corr} (nA/cm2)	E_{corr} (mv)
unimp	1	1.903E2	-0.333	3.793E2	-0.491	6.543E2	-0.514	8.548E2	-0.515	7.143E2	-0.569	2.233E3	-0.530
unimp	3	2.778E2	-0.289	3.548E2	-0.413	2.88E2	-0.428	3.874E2	-0.477	4.808E2	-0.502	8.799E2	-0.524
imp	1	7.580	-0.294	5.568	-0.214	5.748	-0.347	6.536	-0.184	6.53	-0.260	1.829E1	-0.289
imp	3	——	-0.160	3.376	-0.383	2.048	-0.358	5.488E1	-0.378	8.675E1	-0.471	1.493E2	-0.480

Table 8.6 Values of I_{corr} and E_{corr} with time for steel embedded in polymer impregnated and unimpregnated OPC of 0.6 water/cement ratio cured under cc(1) and cc(3) in 1M NaCl solution saturated with $Ca(OH)_2$.

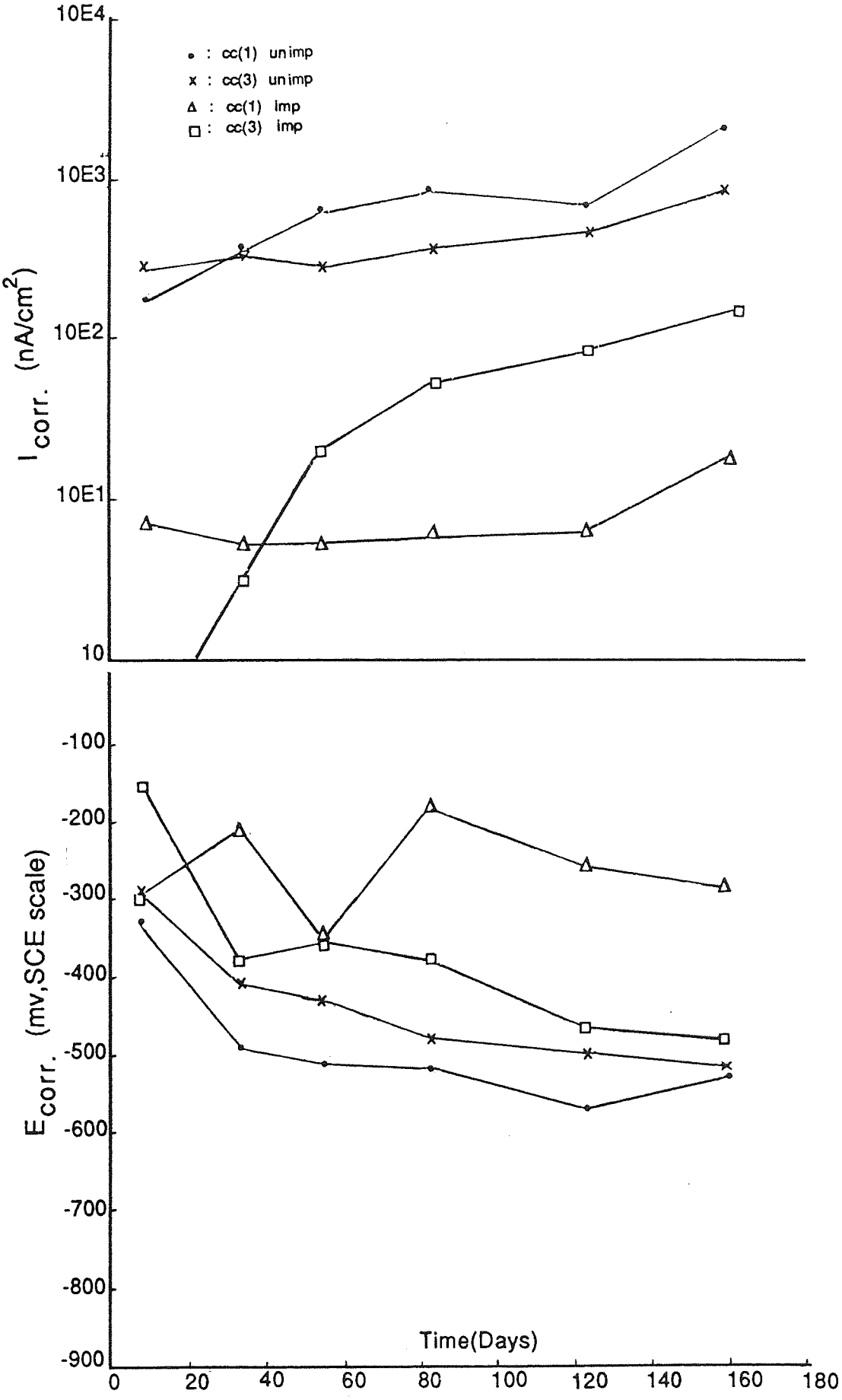

Figure 8.11 Plots of I_{corr} and E_{corr} versus time for steel embedded in polymer impregnated (imp) and unimpregnated (unimp) paste of 0.6 water/cement ratio cured under cc(1) and (3) and exposed to 1M NaCl solution saturated with $Ca(OH)_2$.

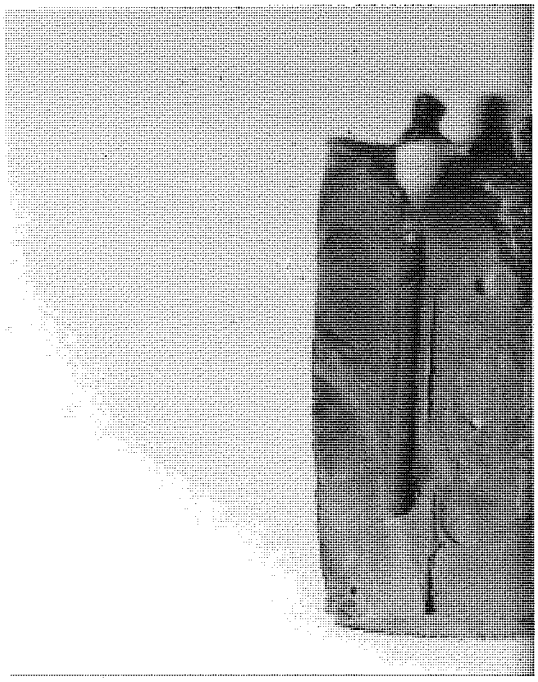

Figure 8.12 Photograph showing corrosion of steel embedded in OPC paste of 0.6 water/cement ratio cured under cc(1) kept in 1M NaCl solution saturated with $Ca(OH)_2$.

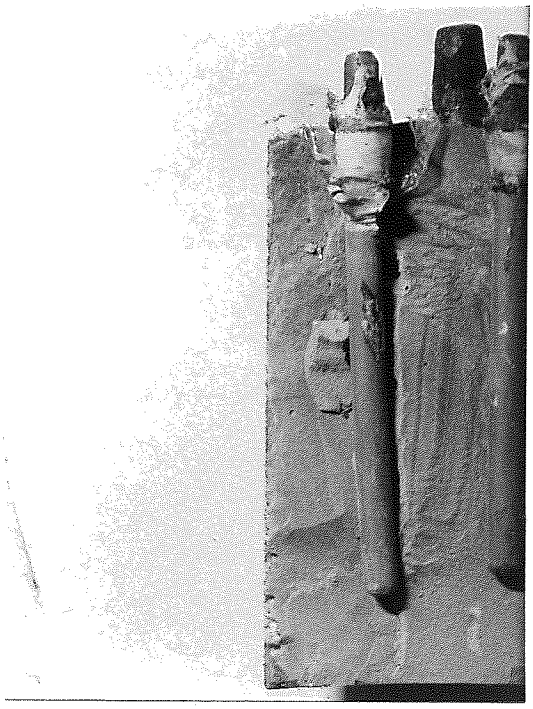

Figure 8.13 Photograph showing corrosion of steel embedded in OPC paste of 0.6 water/cement ratio cured under cc(3) kept in 1M NaCl solution with $Ca(OH)_2$.

coefficient,as shown in chapter 7. table 7.1. is considerably lower for cc(1).

It is however still sufficiently high to allow Cl^- to reach the steel surface fairly rapidly and as OH^- ions diffuse outwards to lower the internal pH, the critical $[Cl^-]/[OH^-]$ ratio for corrosion to occur (167) can be reached with a lower Cl^- concentration. Steel in impregnated OPC where percentage of polymer loading by weight is shown in table 8.1 samples cc(3) showed a low rate of corrosion at the beginning, which rose steadily with time. Corrosion rates were however lower than for either of the unimpregnated conditions, table 8.6. figure 8.11.

In chapter 7. it was shown that the diffusion of Cl^- ions was greatly reduced for the polymer impregnated samples, which explains the delay in the onset of corrosion. Visual observation confirmed some corrosion for this condition (figure 8.15).

The double impregnation of the cc(1) specimens appears to have improved the corrosion resistance of the specimens as no corrosion was detected (figure 8.14) even though their Cl^- diffusion coefficient was no slower than for the cc(3) impregnated specimens figure 8.15, chapter 7. table 7.1.

The I_{corr} and E_{corr} versus time curves for the steel samples embedded in unimpregnated OPC/BFS for cc(3) kept in 1 molar NaCl solution containing saturated $Ca(OH)_2$ can be seen in table 8.7. and figure 8.16; they suggested a relatively high corrosion rate at an early stage, which continued to increase steadily. In chapter 7. it was shown that the value of the Cl^- diffusion is high for this particular condition. Furthermore BFS based cements may not provide a lime rich layer at the steel interface to protect steel as suggested by Page (168).

Figure 8.14 Photograph showing mild corrosion of steel embedded in polymer impregnated OPC paste of 0.6 water/cement ratio cured under cc(1) kept in 1M NaCl solution saturated with $Ca(OH)_2$.

Figure 8.15 Photograph showing some corrosion of steel embedded in polymer impregnated OPC paste of 0.6 water/cement ratio cured under cc(3) kept in 1M NaCl solution saturated with $Ca(OH)_2$.

Impregnated (Imp) / Unimpregnated (Unimp)	Curing Conditions	9 days		35 days		56 days		84 days		125 days		162 days	
		I_{corr} (nA/cm2)	E_{corr} (mv)	I_{corr} (nA/cm2)	E_{corr} (mv)	I_{corr} (nA/cm2)	E_{corr} (mv)	I_{corr} (nA/cm2)	E_{corr} (mv)	I_{corr} (nA/cm2)	E_{corr} (mv)	I_{corr} (nA/cm2)	E_{corr} (mv)
unimp	1	2.184E2	-0.437	8.677E2	-0.587	1.374E3	-0.579	1.964E3	-0.589	1.889E3	-0.582	2.60E3	-0.560
unimp	3	3.476E2	-0.603	4.213E2	-0.548	4.883E2	0.527	1.111E3	-0.579	9.656E2	-0.578	2.427E3	-0.568
imp	1	3.270E2	-0.396	4.743E2	-0.313	4.733E2	-0.363	5.971E2	-0.471	5.975E2	-0.448	3.799E3	-0.455
imp	3	—	-0.170	2.687	-0.412	3.345	-0.535	7.24E1	-0.5778	1.414E2	-0.558	3.642E2	-0.518

Table 8.7 Values of I_{corr} and E_{corr} with time for steel embedded in polymer impregnated and unimpregnated OPC/BFS of 0.6 water/cement ratio cured under cc(1) and cc(3) kept in 1M NaCl solution saturated with $Ca(OH)_2$.

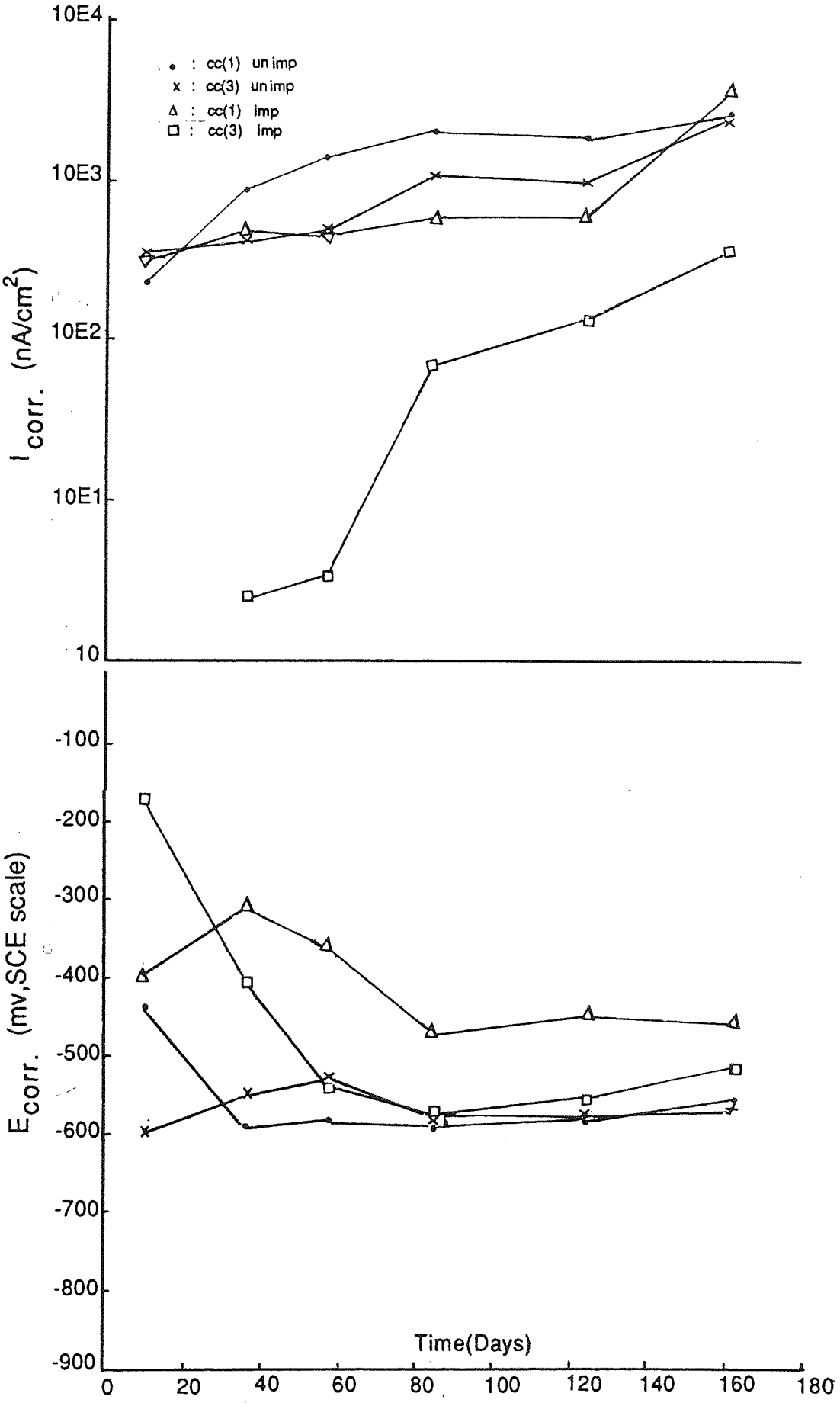

Figure 8.16 Plots of I_{corr} and E_{corr} versus time for steel embedded in polymer impregnated (imp) and unimpregnated (unimp) OPC/BFS pastes of 0.6 water/cement ratio cured under cc(1) and cc(3) and exposed to 1M NaCl solution saturated with $Ca(OH)_2$.

Figure 8.17 Photograph showing severe corrosion of steel embedded in OPC/BFS paste of 0.6 water/cement ratio cured under cc(1) kept in 1M NaCl solution saturated with $Ca(OH)_2$.

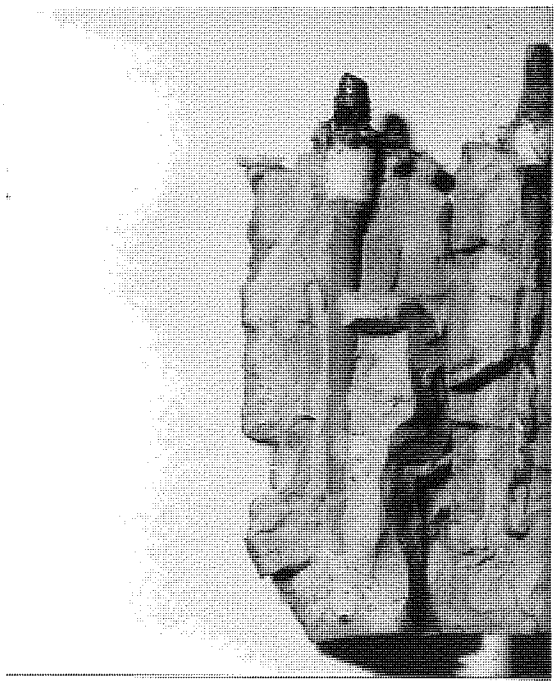

Figure 8.18 Photograph showing severe corrosion of steel embedded in polymer impregnated OPC/BFS paste of 0.6 water/cement ratio cured under cc(1) kept in 1M NaCl solution saturated with $Ca(OH)_2$.

The corrosion value found however for cc(1) was surprisingly high as the rate of chloride diffusion is quite low. This may be related to the absence of lime to act as a buffer, which may then require a lower $[Cl^-]/[OH^-]$ ratio to initiate corrosion figure 8.17. This will be discussed fully later.

Steel in impregnated OPC/BFS samples of cc(1) showed high I_{corr} from early days of testing, figure 8.18. unlike those of cc(3) where initiation of corrosion was delayed. The reason for this is probably due to a poor degree of polymer loading as can be seen in table 8.2 as double impregnation caused cracking. For cc(3) polymer loading was already high only with single impregnation resulting in the better behaviour observed.

8.2.4 The Relationship Between Ecorr And Icorr

Figures 8.19(a-m) show plots of E_{corr} versus I_{corr} for all individual readings and table 8.8 gives the slopes of the lines, and the correlation coefficients for most cases. There is often a Linear relationship with a fairly good correlation coefficient, suggesting anodic control. i.e. as E_{corr} becomes less noble I_{corr} increases, figure 8.19c. (85).

Where there is a combination of a dense structure from high polymer loading and submersion in a solution, normal anodic control is not observed, possibly because of the low availability of oxygen, which can lead to low potential active situations as some points on figures 8.19e, to 8.19m, show where E_{corr} is very low but is associated with a low value of I_{corr}.

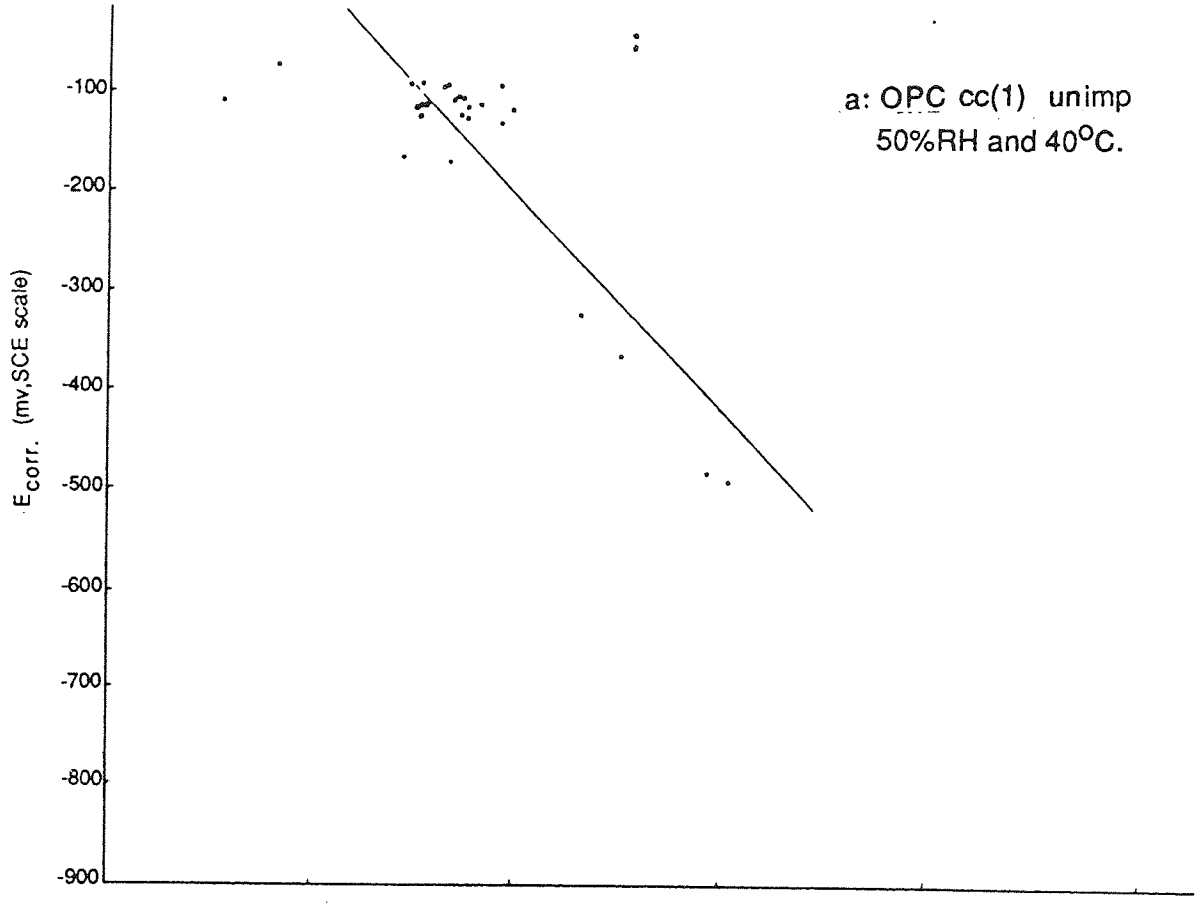

a: OPC cc(1) unimp
50%RH and 40°C.

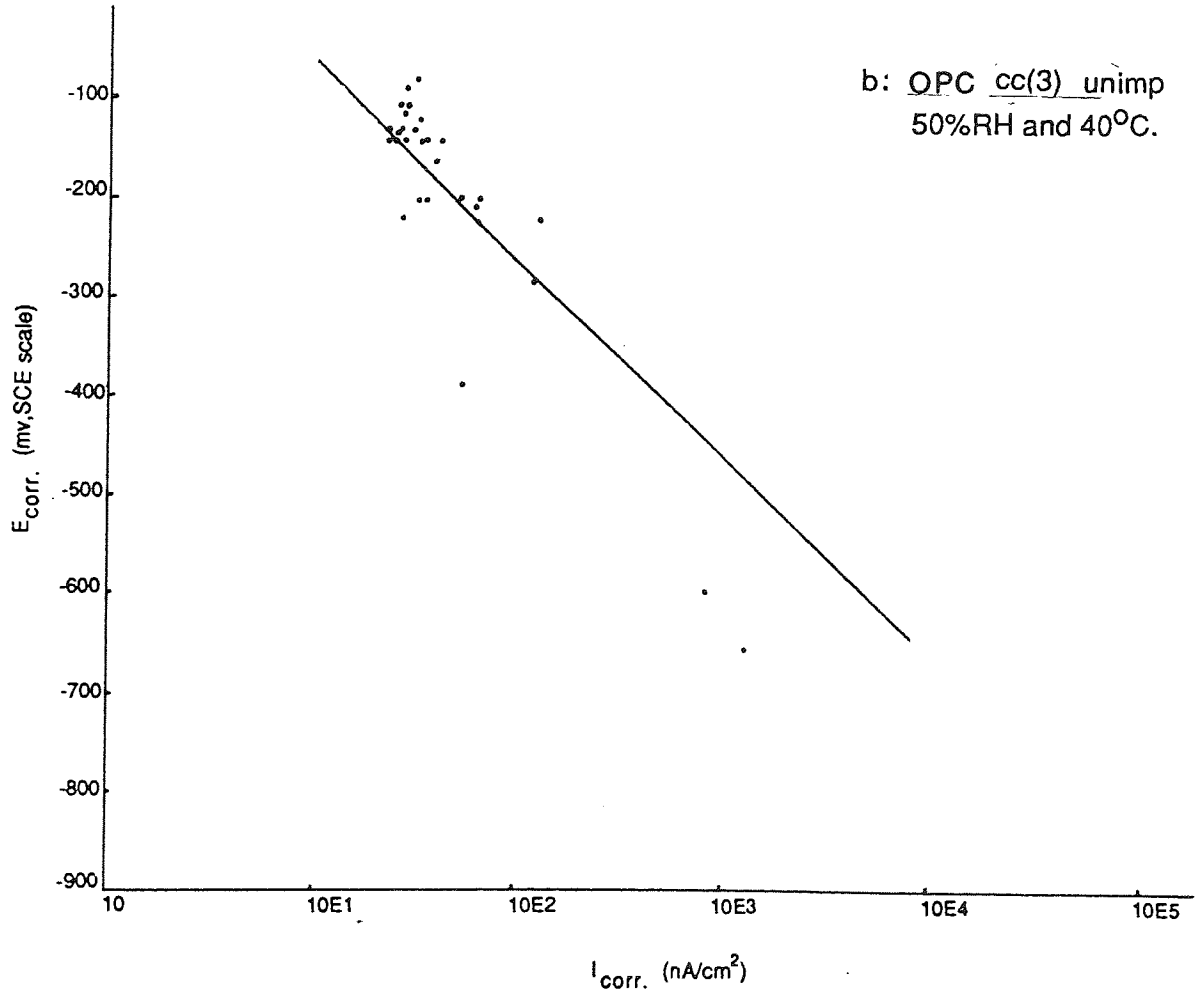

b: OPC cc(3) unimp
50%RH and 40°C.

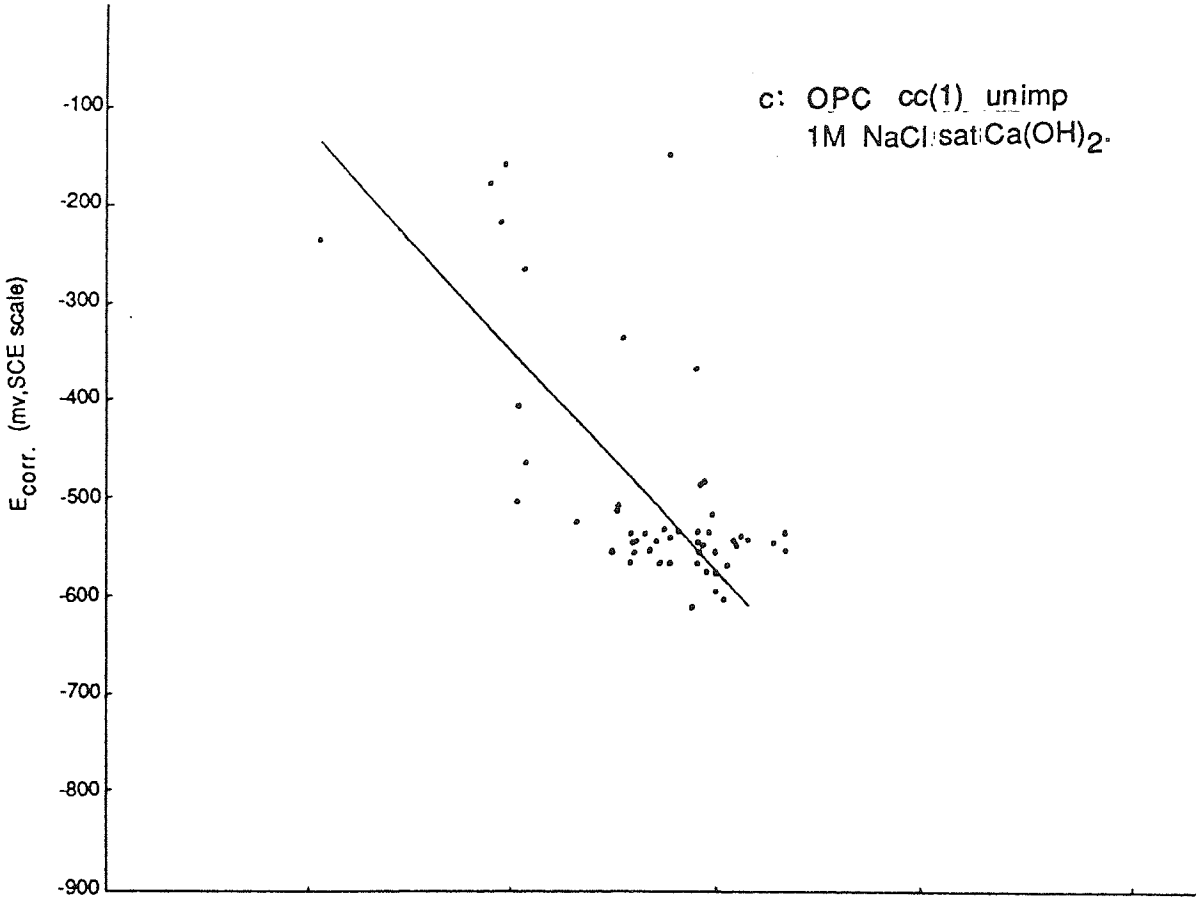
c: OPC cc(1) unimp
1M NaCl sat Ca(OH)2.
-100
-200
-300
-400
-500
-600
-700
-800
-900
Ecorr. (mv,SCE scale)

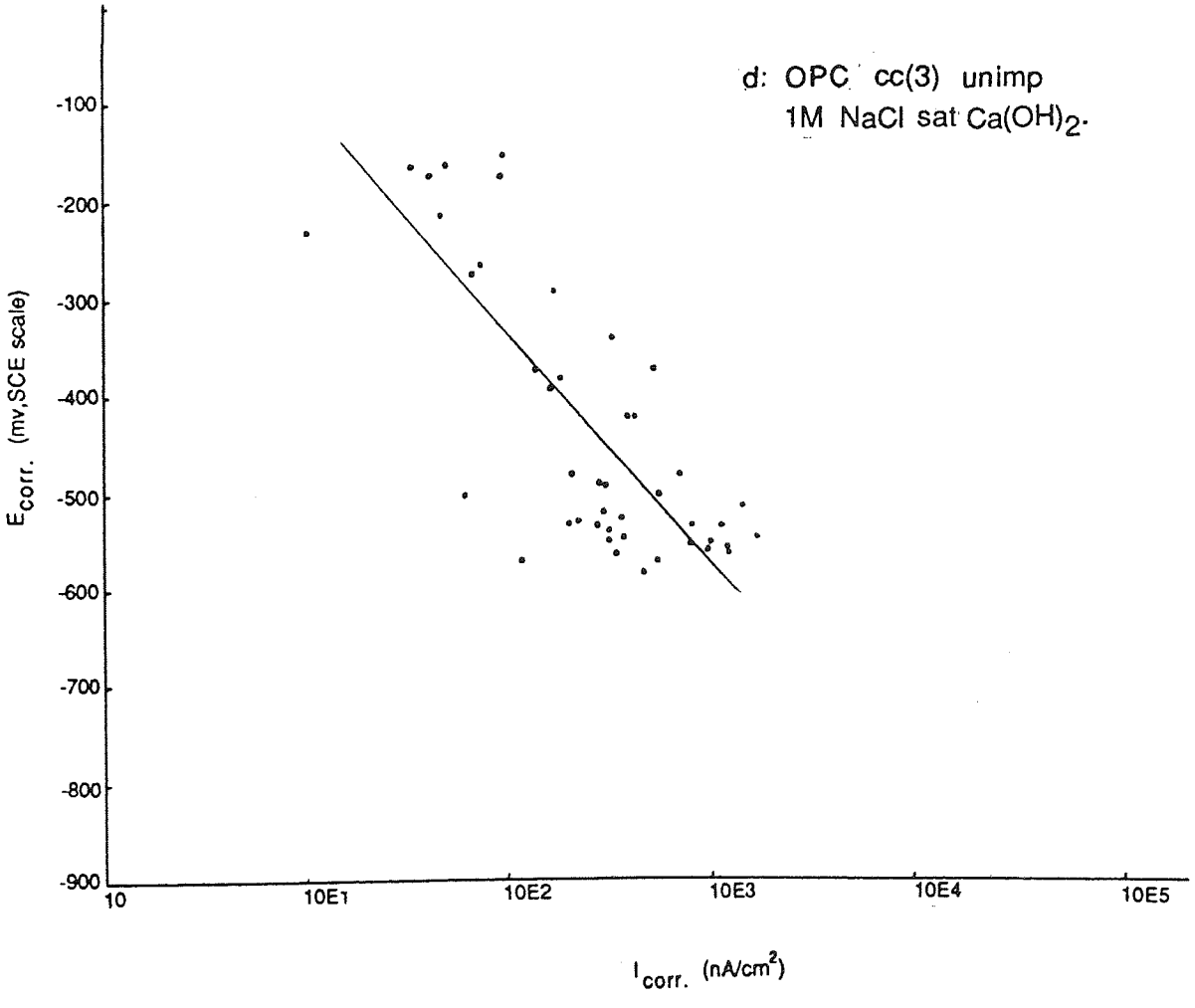
d: OPC cc(3) unimp
1M NaCl sat Ca(OH)2.
-100
-200
-300
-400
-500
-600
-700
-800
-900
Ecorr. (mv,SCE scale)
10
10E1
10E2
10E3
10E4
10E5
Icorr. (nA/cm2)

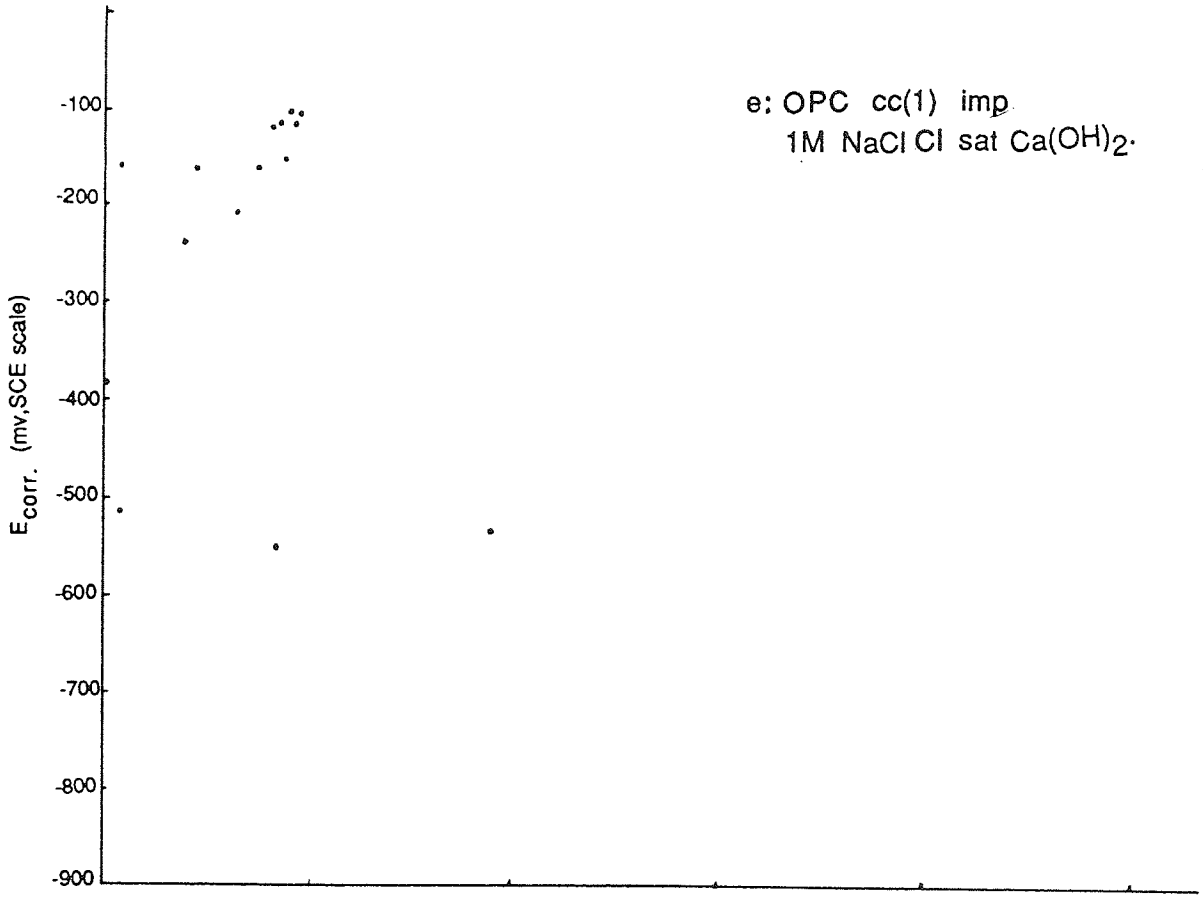
e: OPC cc(1) imp
1M NaCl Cl sat Ca(OH)2.
-100
-200
-300
-400
-500
-600
-700
-800
-900
Ecorr. (mv,SCE scale)

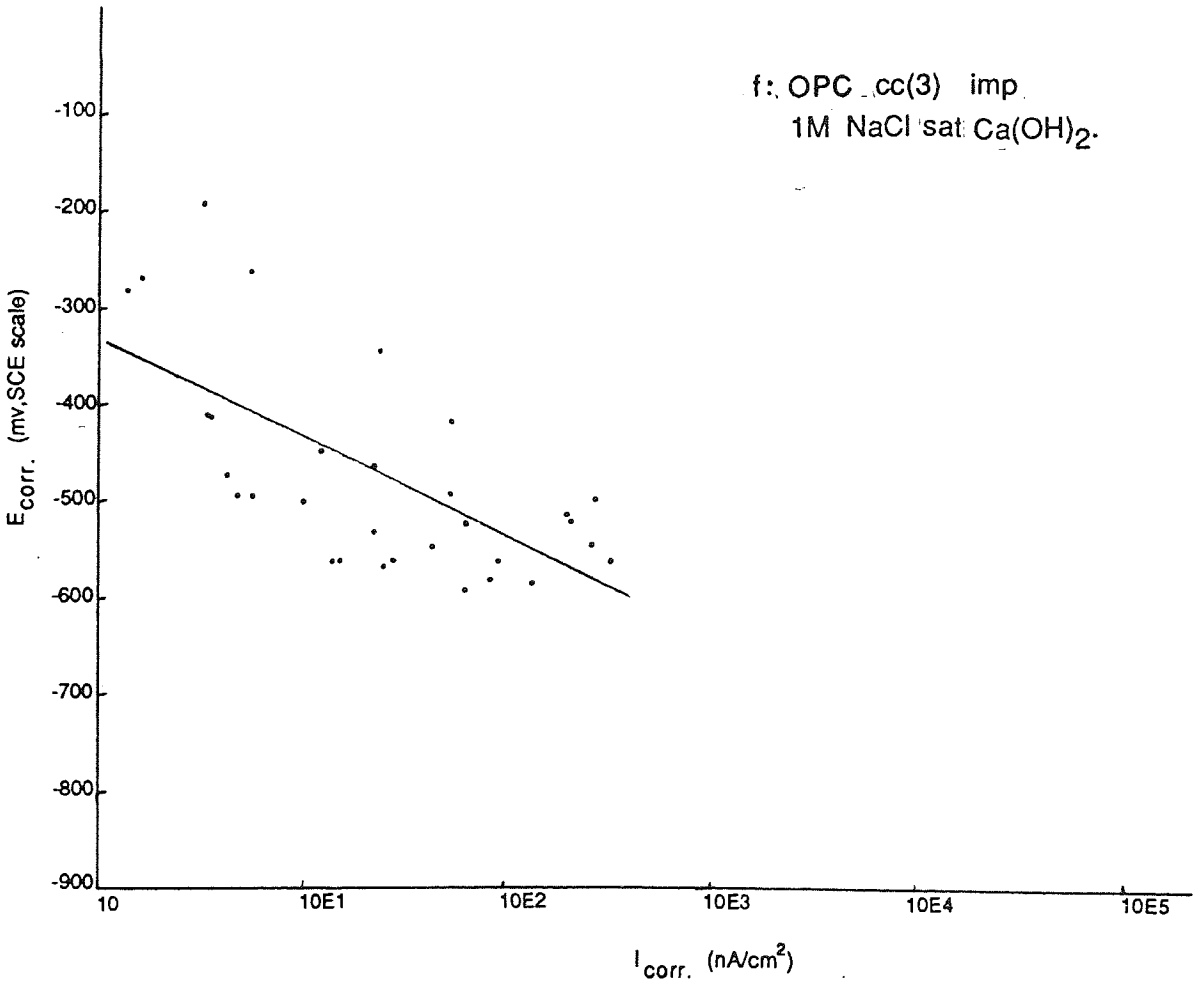
f: OPC cc(3) imp
1M NaCl sat Ca(OH)2.
-100
-200
-300
-400
-500
-600
-700
-800
-900
Ecorr. (mv,SCE scale)
10
10E1
10E2
10E3
10E4
10E5
Icorr. (nA/cm2)

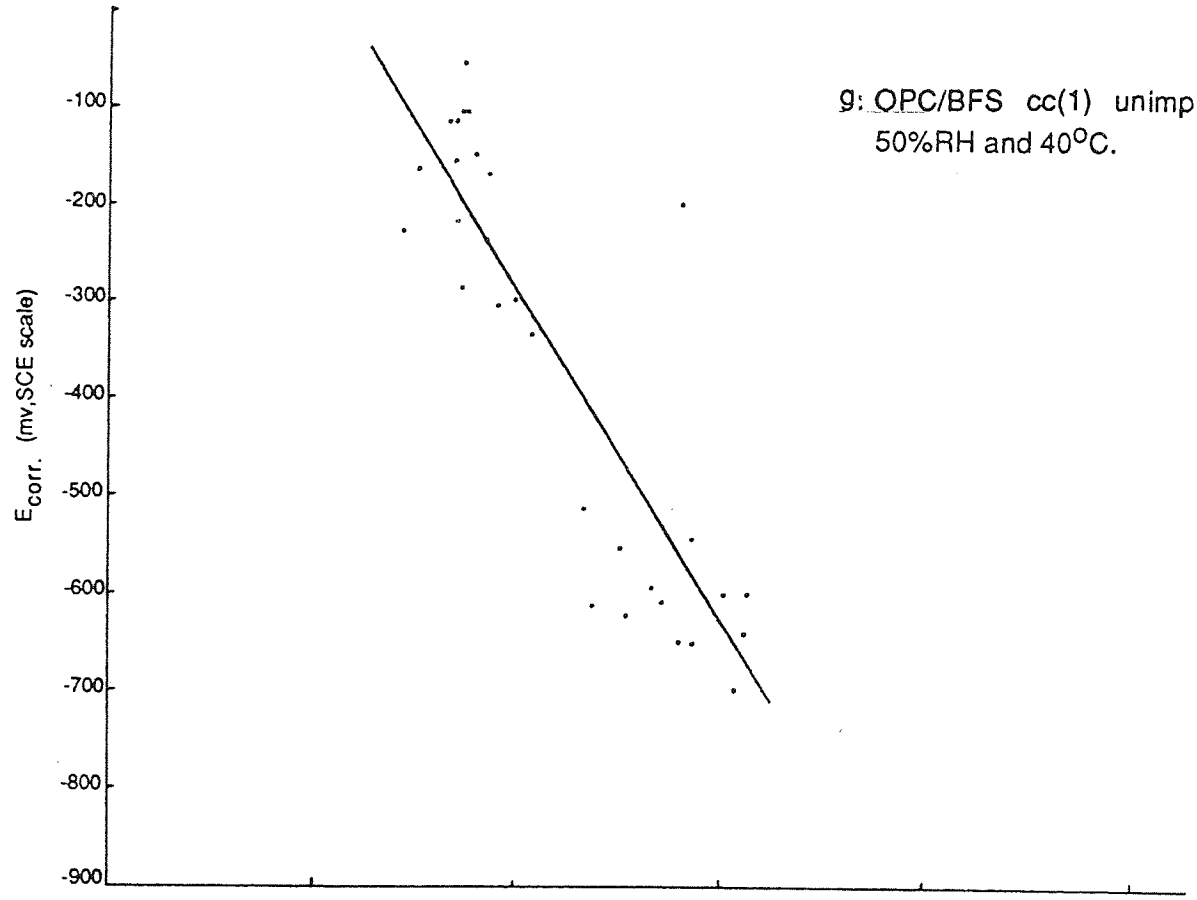

g: OPC/BFS cc(1) unimp 50%RH and 40°C.

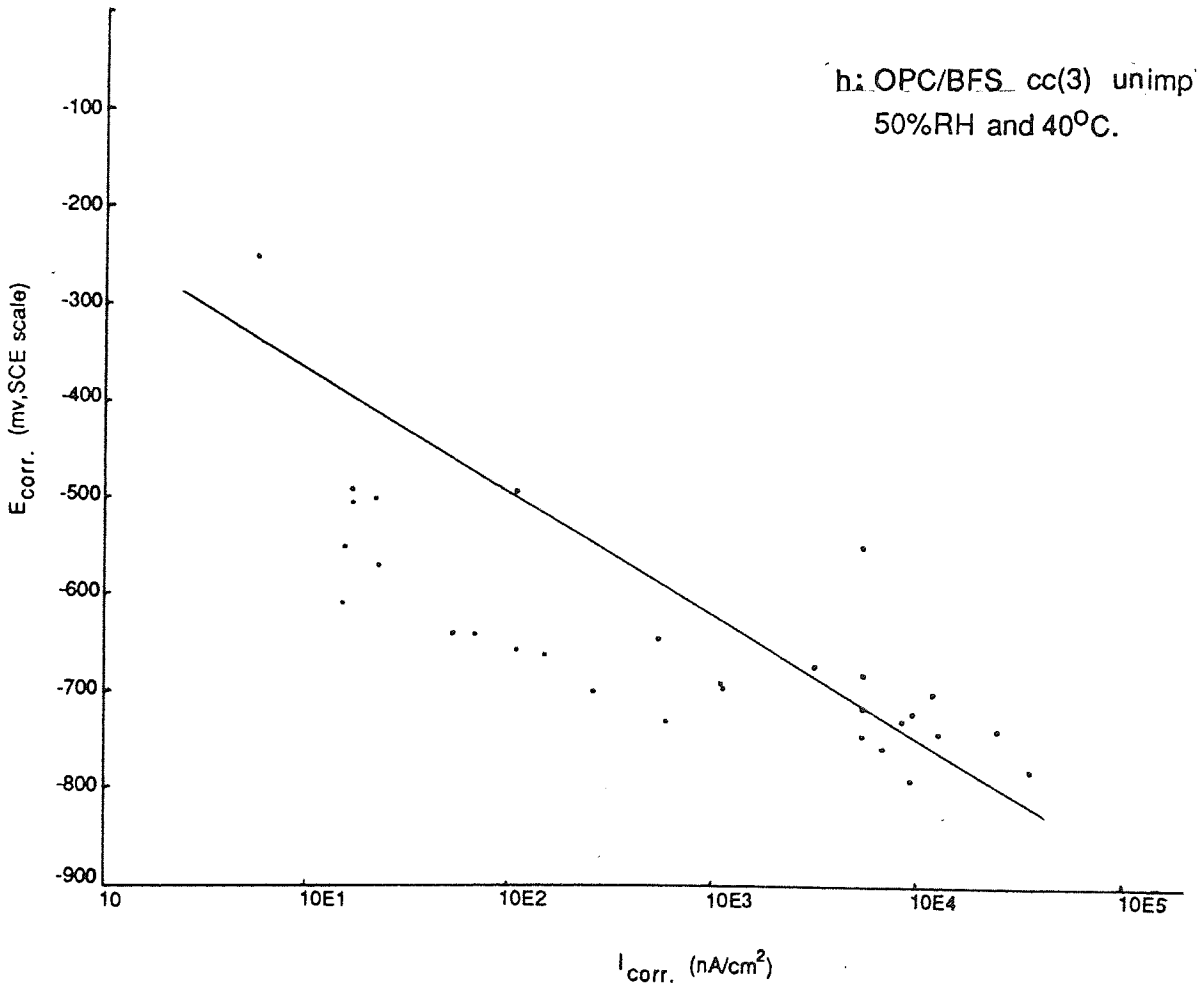

h: OPC/BFS cc(3) unimp 50%RH and 40°C.

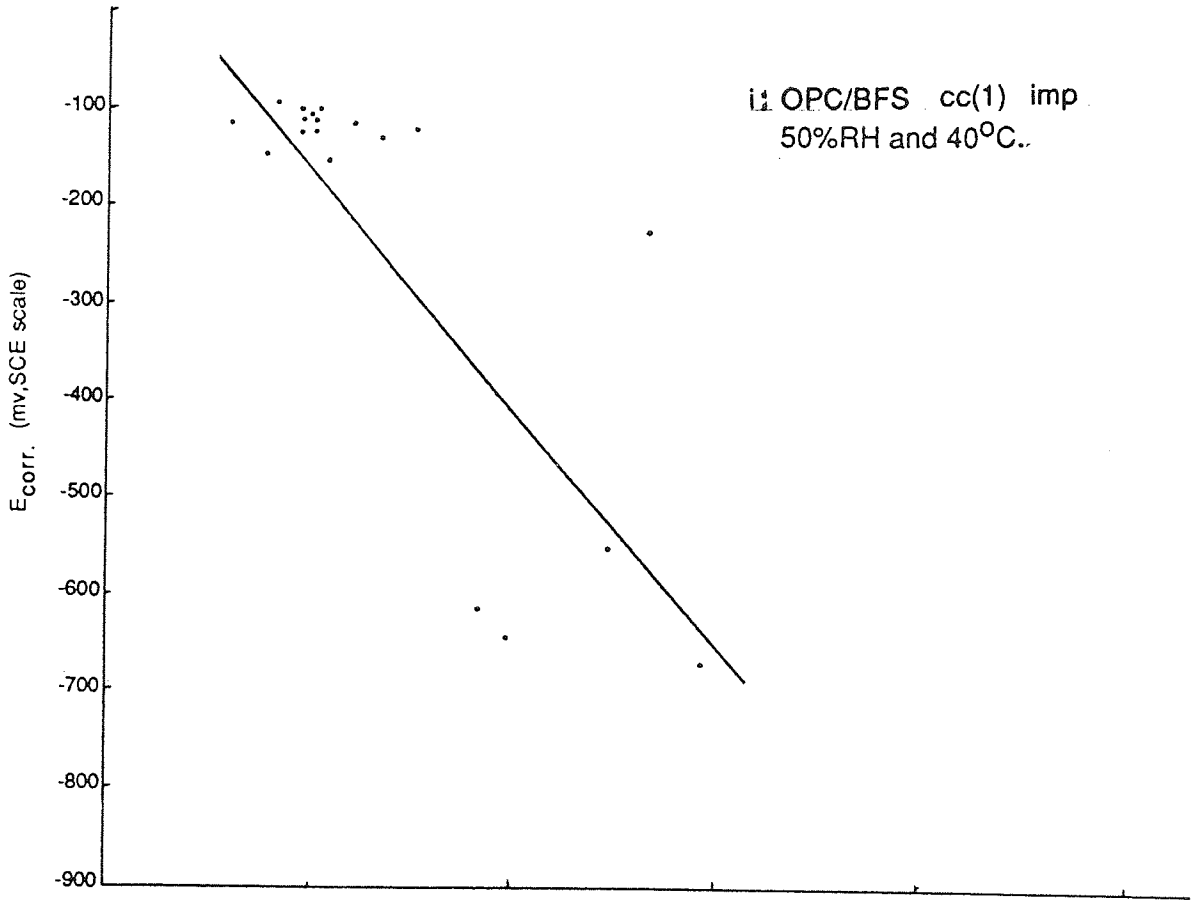
i: OPC/BFS cc(1) imp
50%RH and 40°C.
-100
-200
-300
-400
-500
-600
-700
-800
-900
$E_{corr.}$ (mv,SCE scale)

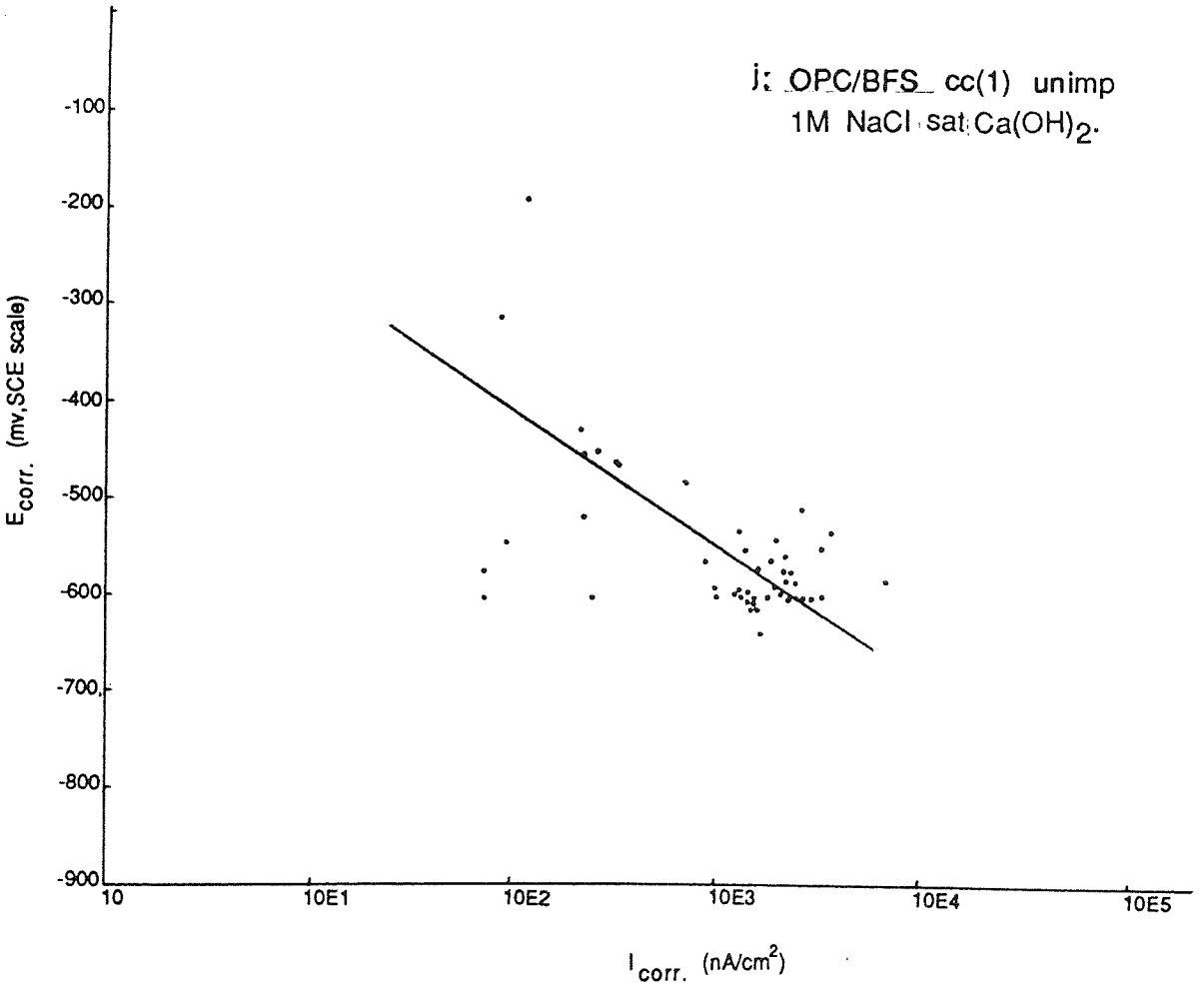
j: OPC/BFS cc(1) unimp
1M NaCl sat $Ca(OH)_2$.
-100
-200
-300
-400
-500
-600
-700
-800
-900
$E_{corr.}$ (mv,SCE scale)
10
10E1
10E2
10E3
10E4
10E5
$I_{corr.}$ (nA/cm^2)

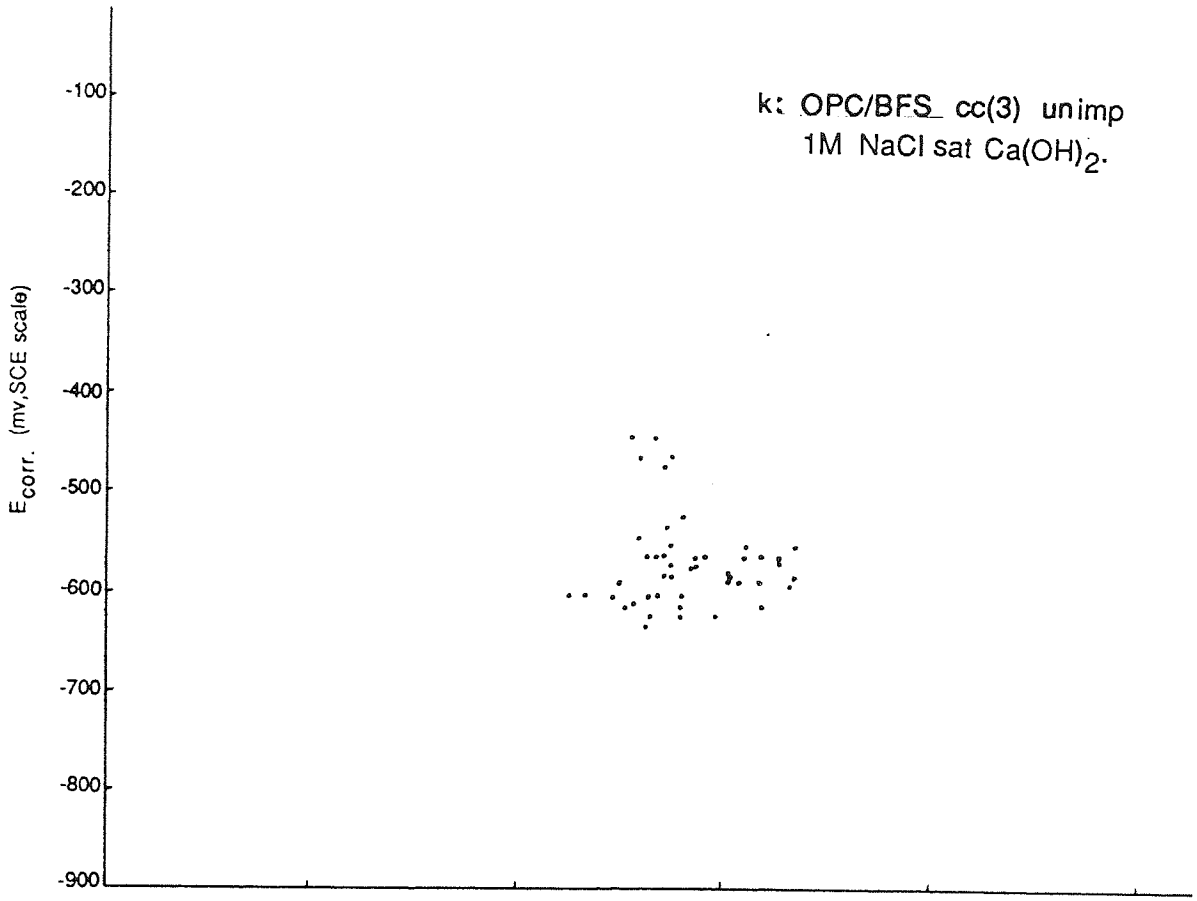
k: OPC/BFS_ cc(3) unimp
1M NaCl sat Ca(OH)2.
-100
-200
-300
-400
-500
-600
-700
-800
-900
Ecorr. (mv,SCE scale)

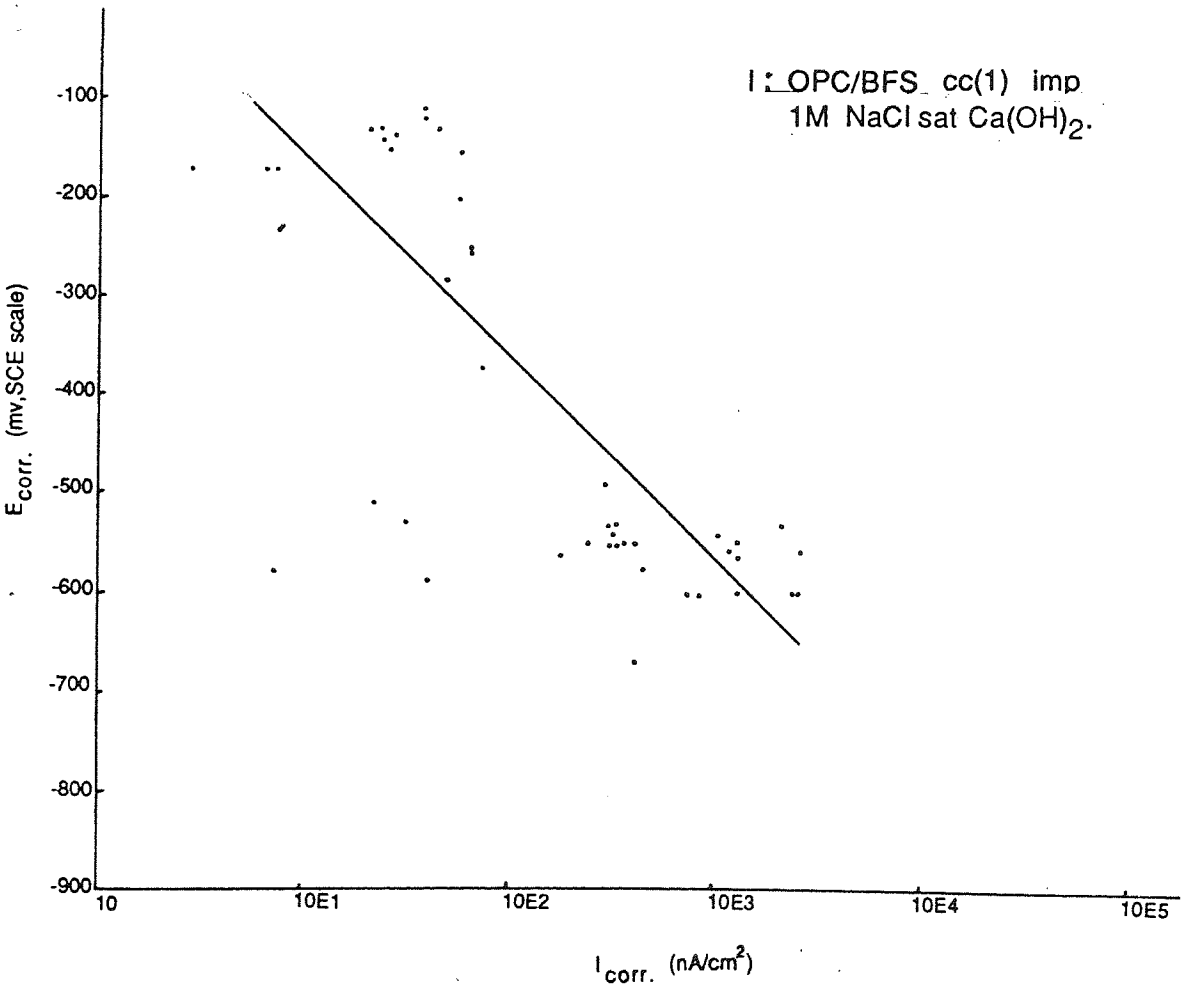
l: OPC/BFS_ cc(1) imp
1M NaCl sat Ca(OH)2.
-100
-200
-300
-400
-500
-600
-700
-800
-900
Ecorr. (mv,SCE scale)
10
10E1
10E2
10E3
10E4
10E5
Icorr. (nA/cm2)

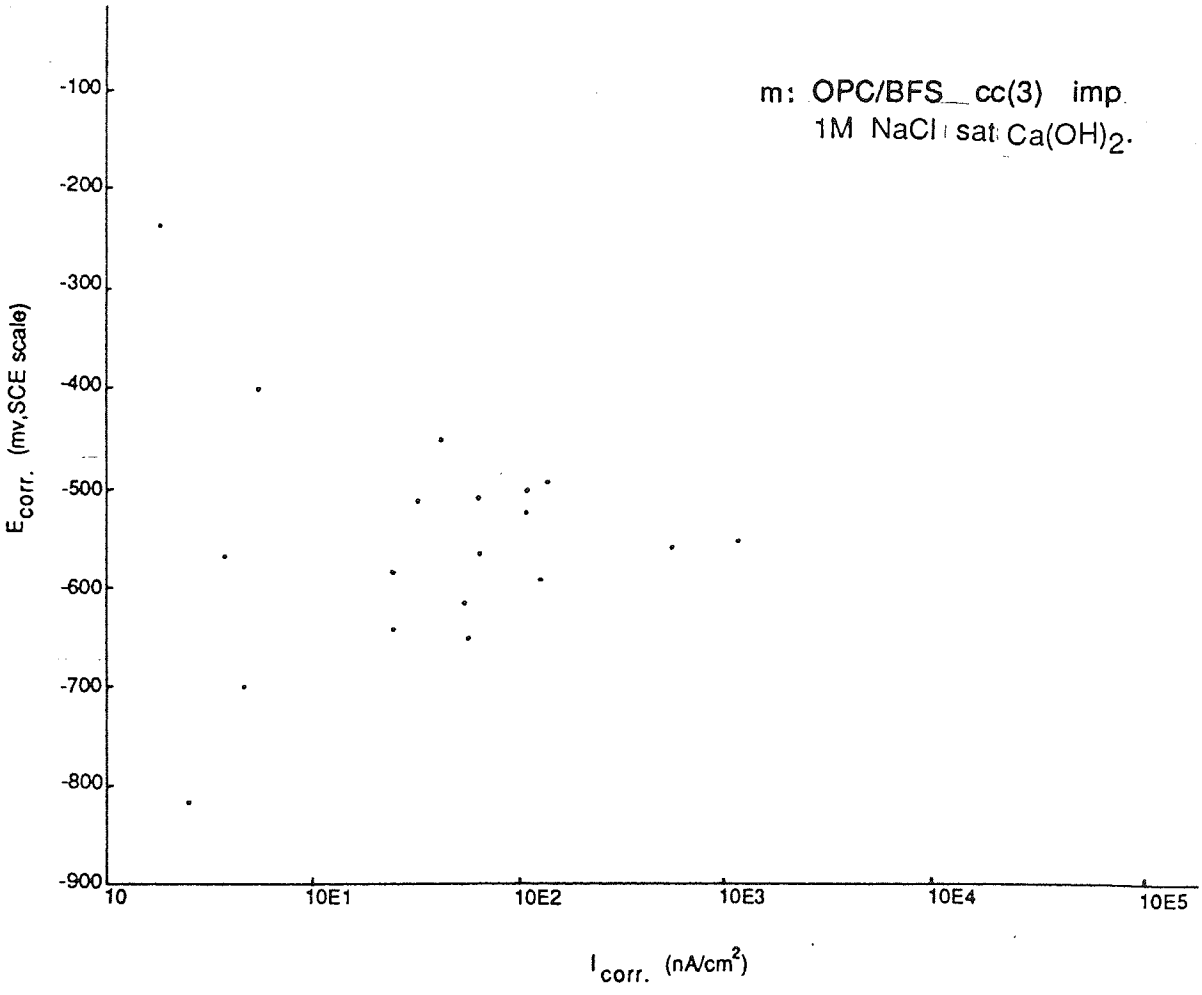

Figure 8.19 Plots of corrosion potential versus log corrosion rate for steel in polymer impregnated and unimpregnated OPC for OPC/BFS pastes of 0.6 water/cement ratio of two different curing conditions and exposed to two environments.

Cement	Environ - ment	Original curing conditions	Unimpreg - nated / Im pregnated (unimp) / (imp)	Pseudo-tafel constant mV/decade	Correlation coefficient
OPC	40°C 50 RH	1	unimp	-217.66	-0.85
		3	unimp	-198.08	-0.83
		1	imp	-----	-----
		3	imp	-----	-----
	1 Mol NaCl sat. $Ca(OH)_2$	1	unimp	-224.93	-0.75
		3	unimp	-238.26	-0.76
		1	imp	-----	-----
		3	imp	-101.98	-0.68
OPC/BFS	40°C 50 RH	1	unimp	-344.4	-0.89
		3	unimp	-126.95	-0.88
		1	imp	-243.76	-0.96
		3	imp	-----	-----
	1 Mol NaCl sat. $Ca(OH)_2$	1	unimp	-138.22	-0.69
		3	unimp	-----	-----
		1	imp	-202.85	-0.79
		3	imp	-38.41	-0.27

Table 8.8 Pseudo-Tafel constants determined from Ecorr verses Icorr plots for impregnated and unimpregnated OPC or OPC/BFS cement pastes of 0.6 W/C ratio and two different curing conditons exposed to two environments.

8.3 DISCUSSION

As was shown in the results polymer impregnation of cements does appear to stop corrosion of the steel from carbonation , provided the polymer loading is high, but is still not very effective for BFS specimens cured under cc(1) where the polymer loading was low.

As was discussed earlier, double impregnation of this cement was not possible as it leads to cracking of the specimens. Similar work must be carried out for specimens which are polymer impregnated to a depth lower than the depth of cover of the steel. This would allow any protection that the $Ca(OH)_2$ present in portland cements normally offers to continue to work whilst having the extra protection of the polymer to delay either the Cl^- or the CO_2 from penetrating the structure. Such a combination may be more desirable and perhaps more realistic in practice.

As the results had shown, exposure of the unimpregnated specimens to a chloride solution had resulted in the eventual corrosion of the embedded steel, as chloride caused its depassivation. As already mentioned, the leaching of sodium and potassium hydroxides from within the cement specimens in these particular experiments would tend to reduce the pH of the internal pore solution to that of saturated $Ca(OH)_2$ i.e. ~ 12.6. If the main parameter for corrosion initiation is a critical ratio of $[Cl^-]/[OH^-]$ as was suggested in the literature (167) then corrosion in this case can occur at lower Cl^- concentrations as OH^- concentration is also lower. This observation may be particularly true for the well cured OPC/BFS cement which although it shows a low diffusion coefficient for Cl^- see chapter 7. corrosion of the embedded steel is observed early on.

The absence of $Ca(OH)_2$ to act as a buffer and as a protective barrier at the steel cement interface for this particular cement (168) also increases the risk of the embedded steel. The present results appear to contradict those of Andrade - Page (169) who had shown that OPC/BFS is no less protective than portland cements. There were however two main differences in these studies. Firstly the chloride source was fixed as that added during mixing so a large proportion could be complexed by cement paste constituents, whereas in the present study the source was from a continuous outside source. Secondly the OH^- concentration of the pore solution of the Andrade - Page study (169) was unaffected and could remain high, whereas that of the present study could have been influenced by leaching of the soluble hydroxides, as already mentioned. Nevertheless results are still surprising because of the short length of time required for the onset of corrosion. i.e. 165 days. This is clearly one area where more research is needed.

Polymer impregnation did not generally stop corrosion altogether, but delayed the onset of corrosion, which is again surprising, as Cl^- diffusion coefficients were shown to be extremely low for these conditions. If the protection offered to the steel by the lime phase is for some reason minimised with polymer impregnation as was mentioned in chapter 6. then the same argument of a lower Cl^- requirement for corrosion may apply here too.

8.4 CONCLUSION

1. Good polymer impregnation of both cements was quite effective at stopping carbonation and preventing corrosion by this route, but was not so successful for the cc(1) BFS based cements with a lower polymer loading where corrosion was at best only delayed.

2. In this particular study, corrosion of steel could not be prevented by blending the cement with BFS, eventhough diffusion experiments suggested that Cl^- penetration was much lower for the well cured BFS cements.

3. Similarly polymer impregnation was not altogether effective at stopping corrosion, possibly because any protection mechanism may have been simply "blocked off" by the polymer allowing even a small amount of Cl^- to cause corrosion.

CHAPTER 9 GENERAL DISCUSSION AND CONCLUSION

9.1 DISCUSSION

An attempt has been made to study the effect of poor curing conditions on the durability of steel in concrete. This is likely to be a problem in Middle Eastern countries, during the hot and mainly dry summer. It has been suggested in the literature that the characteristic behaviour of cement pastes cured under elevated temperature and low relative humidity, substantially differs to those of well cured concrete. In order to evaluate such effects, a study was carried out involving a selection of cements, namely OPC, SRPC, OPC/BFS and OPC/PFA. This involved physicochemical studies on untreated specimens cured in a range of environments aided by scanning electron microscopy. The effect of polymer impregnation on the hardened cement pastes properties was investigated mainly to establish whether carbonation and chloride diffusion rates could be reduced and to what extent steel reinforcement corrosion would be avoided. More specifically, MIP studies were conducted on specimens cured in a range of curing conditions, i.e.

(1) Saturated $Ca(OH)_2$ solution at 20^oC, cc(1)

(2) Saturated $Ca(OH)_2$ solution at 50^oC, cc(2)

(3) Air at 50^oC and 30% relative humidity, cc(3)

Comparing cc(2) with that of cc(1) the former appears to increase the rate of hydration and reduces total porosity but the effects are only noticeable at short times i.e. < 28 days.

When the relative humidity of curing was also altered, a combination of high

temperature and low relative humidity resulted in a coarser pore structure particularly in the case of 0.6 water/cement ratio. A pycnometric technique of measuring porosity had yielded similar results.

SEM studies were then carried out to relate the obtained changes in porosity to morphological changes during the process of hydration. Results were in accord with porosity measurements and showed that badly cured samples always contained greater porosity and had what may be described as an incomplete gel. XRD work was undertaken in conjunction with the SEM studies which revealed differences in the phase transformations during hydration.

In an attempt to find a remedy for the increased porosity of the structures during poor curing, polymer impregnation was carried out, which proved successful for effectively "blocking" the pore network of the poorly cured samples. Well cured hardened cement pastes were shown to be more difficult to impregnate, however, and a second impregnation was necessary.

It was important also to establish how other properties of the cements were altered during polymer impregnation. Differences may have occurred for instance to the chemical nature of the cement hydrates as XRD studies had suggested. Chloride diffusion and carbonation studies also showed, in the main, a reduction in their rates provided a high degree of polymerisation was achieved. A fair prediction would then have been, that polymer impregnation would reduce the risk of corrosion of the steel reinforcements induced by chloride penetration or carbonation. Experimental studies confirmed this, but pointed also to problems when impregnation was for some reason incomplete. In such cases there was no real advantage in polymer impregnation as the detrimental effect of reducing the protective nature of $Ca(OH)_2$ may have countered the reduction in porosity.

Finally the conclusions of the study may be summarised as follows.

9.2 CONCLUSIONS

1) The effect of temperature alone was to generally encourage hydration at an early age (i.e.7 days) e.g. reduce porosity, but at later ages the effect was reduced.

2) High temperature and low relative humidity was shown to delay or diminish the rate of hydration, particularly for BFS blended cements, resulting in more porous structures.

3) Total porosity obtained by MIP compared well with the pycnometric technique. However in the case of impregnated samples there is some evidence to suggest that MIP underestimates the total porosity.

4) Generally speaking, morphological and SEM studies supported the porosity results. OPC/BFS and to some extent OPC cured in a high temperature low relative humidity environment had shown a lower degree of hydration.

5) SEM studies showed that during hydration of OPC a network of fibrous material (C-S-H) gel builds up, this originating from the surface of calcium silicate particles. These fibres eventually interlock to form a compact structure containing hexagonal plate shaped crystals of $Ca(OH)_2$. A similar observation was made for the BFS blended cement but this had shorter fibres developing.

6) Much less $Ca(OH)_2$ was observed in the BFS based hardened cement pastes for both curing conditions.

7) The majority of the pores of badly cured cement pastes of 0.6 water/cement ratio are filled with polymer during impregnation. It was possible to impregnate the whole of the cylindrical specimens.

8) XRD results for impregnated samples showed that the measured intensity for the peaks relating to $Ca(OH)_2$, C_3S, C_2S and C_3A have diminished drastically following polymer impregnation; this may well be due to a chemical reaction between organic monomer and/or catalyst and cement paste. There was however no indication of any formation of a new compound due to such a reaction. Under such circumstances the percentage of polymer loading was very small. However, a second impregnation did lead to very much higher degrees of loading.

9) In all cases well cured specimens showed a lower rate of carbonation than poorly cured ones, probably due to a lower porosity and higher resistance from an increased carbonatable material.

10) The rate of carbonation in all cases was slower for OPC based cements.

11) Badly cured samples i.e cc(3) of all types of impregnated cement pastes, regardless of water/cement ratio result in little or no carbonation.

12) For 0.6 water/cement ratio cc(1) for all types of cements, and for OPC/BFS at 0.4 water/cement ratio cc(1), carbonation after impregnation

was greater than those samples without impregnation.

13) Badly cured cement pastes showed a higher coefficient of Cl^- diffusion than well cured discs. This appears to be related to porosity.

14) Well polymer impregnated samples showed a substantial reduction in the rate of diffusion as pores were filled or blocked with polymer. However there appears to be some breakdown of the polymer after ~ 90 days leading to increased diffusion.

15) Well cured 0.6 water/cement ratio cc(1) OPC/BFS cement, showed a slower Cl^- diffusion than either 0.4 or 0.6 water/cement ratio OPC. For the badly cured 0.6 water/cement ratio cc(3) OPC/BFS cement, diffusion was significantly faster than either 0.4 or 0.6 water/cement ratio OPC.

16) By addition of BFS to OPC the corrosion rate of the embedded steel does not appear to be reduced when the specimens are immersed in a NaCl solution, even though chloride diffusion was shown to be lower for this cement.

17) Polymer impregnation was not entirely effective in stopping corrosion of specimens immersed in a NaCl solution, it just delayed the onset of corrosion.

18) High polymer loading of hardened cement pastes resulted in a complete prevention of corrosion of the embedded steel kept in a carbonating environment. When polymer loading was low, as was the case with the singularly impregnated OPC/BFS specimens, corrosion was only delayed, but not prevented.

9.3 RECOMMENDATIONS FOR FUTURE WORK

It must be emphasised that the present work was carried out on well characterised cement paste specimens produced under laboratory conditions. Results need to be substantiated therefore with field exposure tests which should include concrete specimens.

As it was discussed earlier, polymer impregnation to a depth equal to or greater than the depth of cover, may diminish the protectiveness of the concrete to the embedded steel. Further work is therefore necessary to determine the effect of polymer impregnation to only a small depth. Such a treatment may be beneficial in reducing the ingress of agressive agents, whilst maintaining the protective lime-rich zone around the steel reinforcement.

It appears that the $Ca(OH)_2$ phase of the hardened cement paste is reduced during polymer impregnation, but no clear evidence of reaction was detected. It is of high importance to understand the exact effect of polymer on the chemistry of cement and further work must therefore be carried out. One possible line of study could be to subject cement paste to either monomer or benzoyl peroxide and determine any changes to phase compositions by XRD and DTA or similar techniques.

Furthermore diffusion and carbonation studies could be carried out on such treated specimens, to see whether any small possible chemical or physical changes may alter diffusion characteristics. Diffusion characteristics of the SRPC and PFA based cement pastes should also be looked at in relation to curing condition. Other levels of substitution of the blended cements should also be

looked at. This may help to establish a certain optimum degree of blending for any one type of curing regime

APPENDIX 1 The intrusion of Mercury (a non-wetting liquid) into a spherical pore.

a) The Washburn Equation

In order to encourage mercury to penetrate into a pore of a circular cross-section, it requires an external force, to overcome the surface tension of the liquid (γ).

The opposing force F_o at the entry of liquid is given by :

$$F_o = -\pi d \gamma \cos\theta$$

where

θ = contact angle between mercury and the material

d = the pore diameter

γ = the surface tension of the mercury

The equation which gives the external force, F_a which must be applied to the non-wetting liquid to make it enter the pore is :

$$F_a = \pi \frac{d^2}{4} P$$

At equilibrium, where $F_o = F_a$ P is the applied external pressure,

$$-\pi d \gamma \cos\theta = \pi \frac{d^2}{4} P$$

which gives

$$P = \frac{-4\gamma \cos\theta}{d}$$

b) Example calculation.

Calculation of pore size distribution

From

$$P = \frac{-4\gamma \cos\theta}{d}$$

P = Applied pressure (psi)

d = Pore diameter (nm)

γ = Surface tension of mercury = dynes/cm (474 mJ/m)

θ = The contact angle for oven dried cement paste = (117^{o})

The calculation for pore size distribution curve for a 0.6 water/cement ratio paste, originally cured for 28 days under cc(3) (see figure 3.1 Chapter 3) is as follows :

Weight of sample dried at $105^{o}C$ (W_s) = 4.5465 g

cell factor = 0.000754 cc/count

A = Applied pressure (psi)

B = Penetration counter

C = Corrected counter indication (B-Result of blank run)

D = Pore Diameter (117^{o} contact angle) ($124.9 \times 10^{3} \div A$) nm

(this includes a conversion factor from psi to N/mm^2)

E = Volume of pores of indicated Diameter and larger

C x (cell factor $\div$ W_s) cc/g

The above values are determined for increasing applied pressures and tabulated as follows :

A	B	C	D	E
1	5	5	124.9	0.00083
2	19	19	62.5	0.0032
3	26	26	41.6	0.0043
5	33	33	25.0	0.0055
12	40	40	10.4	0.066
100	825	825	1.25	0.137
150	869	869	0.83	0.144
1200	1227	1227	0.10	0.203
1400	1326	1326	0.09	0.220
1600	1371	1371	0.078	0.227
1800	1420	1420	0.069	0.236
2000	1456	1456	0.062	0.241
2200	1472	1472	0.057	0.244
2400	1496	1496	0.052	0.248
2600	1526	1524	0.048	0.253
2800	1543	1540	0.045	0.255
3000	1567	1563	0.042	0.259
3400	1596	1592	0.037	0.264
3700	1618	1614	0.034	0.268
4000	1641	1637	0.031	0.271
4500	1670	1666	0.028	0.277
5000	1699	1694	0.025	0.281
5500	1725	1720	0.023	0.289
6000	1752	1747	0.021	0.289
6500	1773	1767	0.019	0.293
7000	1794	1788	0.018	0.197
8000	1836	1826	0.016	0.303
9000	1871	1861	0.014	0.309
10000	1902	1891	0.012	0.314
11000	1920	1909	0.011	0.317
12000	1941	1928	0.010	0.320
13000	1955	1940	0.010	0.322
14000	1966	1950	0.009	0.323
16000	1986	1966	0.008	0.326
18000	1998	1974	0.007	0.327
20000	2009	1980	0.006	0.328
24000	2025	1990	0.005	0.330
2800	2036	1994	0.004	0.331
32000	2045	1994	0.004	0.331
36000	2066	2010	0.003	0.333
40000	2077	2011	0.003	0.334
44000	2084	2011	0.003	0.334

A plot of E v's D then produces a pore-size distribution curve as shown in fig. 3.1.

APPENDIX 2 Example calculation of the total porosity of cement paste

a) Calculation of Bulk (Apparent) Density

e.g. For cement paste sample of water/cement ratio 0.4 cc(1) for 28 days.

Mass of dry specimen $= m_s = 2.72$ g

Mass of pycnometer + Hg $= m_a = 247.64$ g

Mass of pycnometer + Hg + specimen $= m_b = 227.84$ g

When specimen present in pycnometer

Mass of pycnometer + Hg $= m_b - m_s = 227.84 - 2.72 = 225.12$ g

Mass of mercury displaced $= m_a - (m_b - m_s) = 247.64 - 225.12$

$= 22.52$ g

$$\text{Volume of mercury displaced} = \frac{m_a - (m_b - m_s)}{\rho_{Hg}} = \frac{22.52}{13.60} = 1.66 \text{ cc}$$

$$\therefore \text{ Bulk Density } (\rho_B) = \frac{m_s \times \rho_{Hg}}{m_a - (m_b - m_s)} = \frac{2.72}{1.66} = 1.64 \text{ g cc}^{-1}$$

Where

ρ_{Hg} = density of Hg = 13.60 g cc^{-1}

b) Calculation of True Density

Let

Mass of empty bottle $= m_1 = 33.40$ g

Mass of bottle + specimen $= m_2 = 38.35$ g

Mass of bottle + paraffin $= m_3 = 77.84$ g

Mass of bottle + paraffin + sample = m_4 = 80.95 g

Mass of specimen = $m_2 - m_1$ = 38.35 - 33.40 = 4.95 g

Mass of paraffin = $m_3 - m_1$ = 77.84 - 33.40 = 44.44 g

Mass of paraffin + specimen = $m_4 - m_1$ = 80.95 -33.40 = 47.55 g

$$\text{Volume of paraffin with no sample} = \frac{m_3 - m_1}{\rho_p} = \frac{44.44}{0.82} = 54.39 \text{ cc}$$

$$\text{Volume of paraffin when specimen added} = \frac{m_4 - m_2}{\rho_p} = \frac{80.95 - 38.35}{0.82} = \frac{42.60}{0.82} = 52.14$$

$$\text{The volume of sample} = \frac{m_3 - m_1}{\rho_p} - \frac{m_4 - m_2}{\rho_p} =$$

$$\frac{m_3 - m_1 - m_4 + m_2}{\rho_p} = \frac{77.84 - 33.40 - 80.95 + 38.35}{0.82} = 2.25 \text{ cc}$$

$$\text{True Density } \rho_T = \frac{\text{Mass of specimen}}{\text{True volume of specimen}} = \rho_T = \frac{(m_2 - m_1) \times \rho_p}{(m_3 - m_1 - m_4 + m_2)}$$

$$\frac{(38.35 - 33.40) \times 0.84}{77.84 - 33.40 - 80.95 + 38.35} = \frac{4.05}{1.39} = 2.20 \text{ g cc}^{-1}$$

c) Calculation of total porosity

For a given mass of specimen let :

V_B be the bulk (or apparent) volume

V_T be the true volume of the solid specimen

$\therefore V_T \rho_T = V_B \rho_B$

Volume of pores $V_p = V_B - V_T$

$$V_p = V_B - \frac{V_B \rho_B}{\rho_T}$$

$$V_p = V_B \left(1 - \frac{\rho_B}{\rho_T} \right)$$

Expressed as percentage of total pore volume

$$V_p = 1 - \frac{\rho_B}{\rho_T} \times 100\%$$

$$V_p = 1 - \frac{1.64}{2.20} \times 100 = 25.39\%$$

For volume of pores (V_p) per unit mass of Dry specimen

$$V_B = V_p + V_T$$

since $$\rho_B = \frac{m_2 - m_1}{V_B} = \frac{(m_2 - m_1)}{V_p + V_T}$$

$$V_p = \frac{m_2 - m_1}{\rho_B} - V_T = \frac{m_2 - m_1}{\rho_B} - \frac{m_3 - m_1 - m_4 + m_2}{\rho_p}$$

$$V_p = \frac{4.95}{1.64} - \frac{1.84}{0.82} = 3.02 - 2.25 = 0.77 \text{ cc}$$

$$\text{The total porosity} = \frac{V_p}{m_2 - m_1} = \frac{0.77}{4.95} = 0.16 \text{ cc g}^{-1}$$

APPENDIX 3 Example of identification of XRD trace.

For carbonated OPC paste, originally cured for 29 days under cc(3) see figure 6.12, the following values for 2θ, d- spacing (based on CuKα = 1.5406 nm) and relative intensity I were determined :

The values of d and I were compared to standard data as shown in the table, to identify the phases. In this case 5 possible phases were identified.

			STANDARD DATA (ref. 136)				
2	d (nm)	I	$Ca(OH)_2$	ß C_2S	C_3S	Vaterite	Calcite
18.1	0.490	30	0.49 (vs)				
21	0.423	5				0.426 (m)	
25	0.356	10				0.358 (s)	
27	0.331	9				0.330 (s)	
28.7	0.311	4	0.311 (m)				
29.5	0.303	12					0.303 (vvs)
30.0	0.298	4			0.296 (m)		
32.3	0.277	10		0.285 (vs)	0.277 (vs)		
32.8	0.273	13		0.273 (m)	0.273 (s)		
34.1	0.263	18	0.263 (vvs)				
47.0	0.193	10	0.193 (ms)			0.193 (w)	
50.0	0.182	8				0.183 (s)	
50.8	0.181	6	0.180 (ms)				

Scale of decreasing related intensities :

vvs, vs, s, ms, m, mv, w, vw, vvw.

Appendix 4

DTA Identification peaks

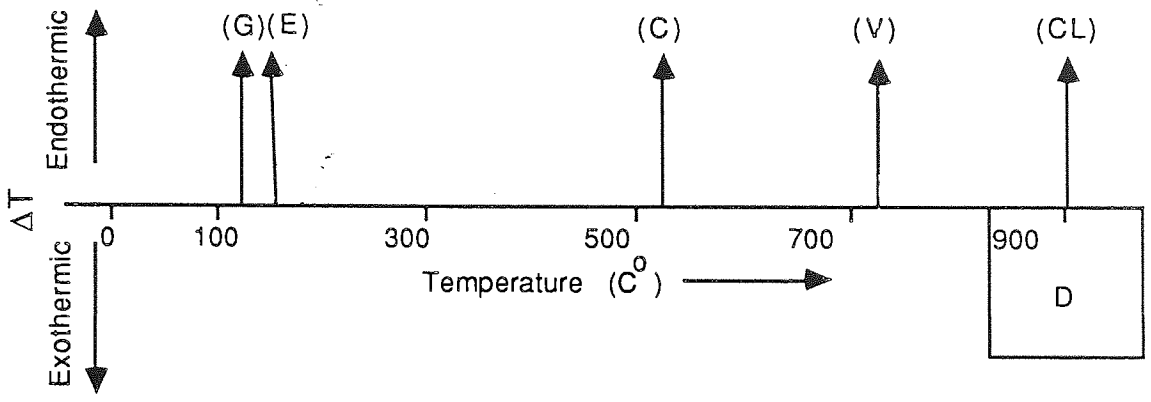

G= C-S-H.gel
E=Calcium Sulphoaluminate Hydrate (Ettringite)
C=Calcium Hydroxide
CL=Calcite (Calcium Carbonate)
V=Vaterite
D=Devitrification of glassy phase

G,E,C and D from reference (137)
CL and V from reference (32)

APPENDIX 5 Chloride Ion Calibration Curve

From the use of the spectrophotometer the absorption values (ABS) can be read-off and then translated into Cl^- concentrations from the following calibration curve constructed from chloride standards.

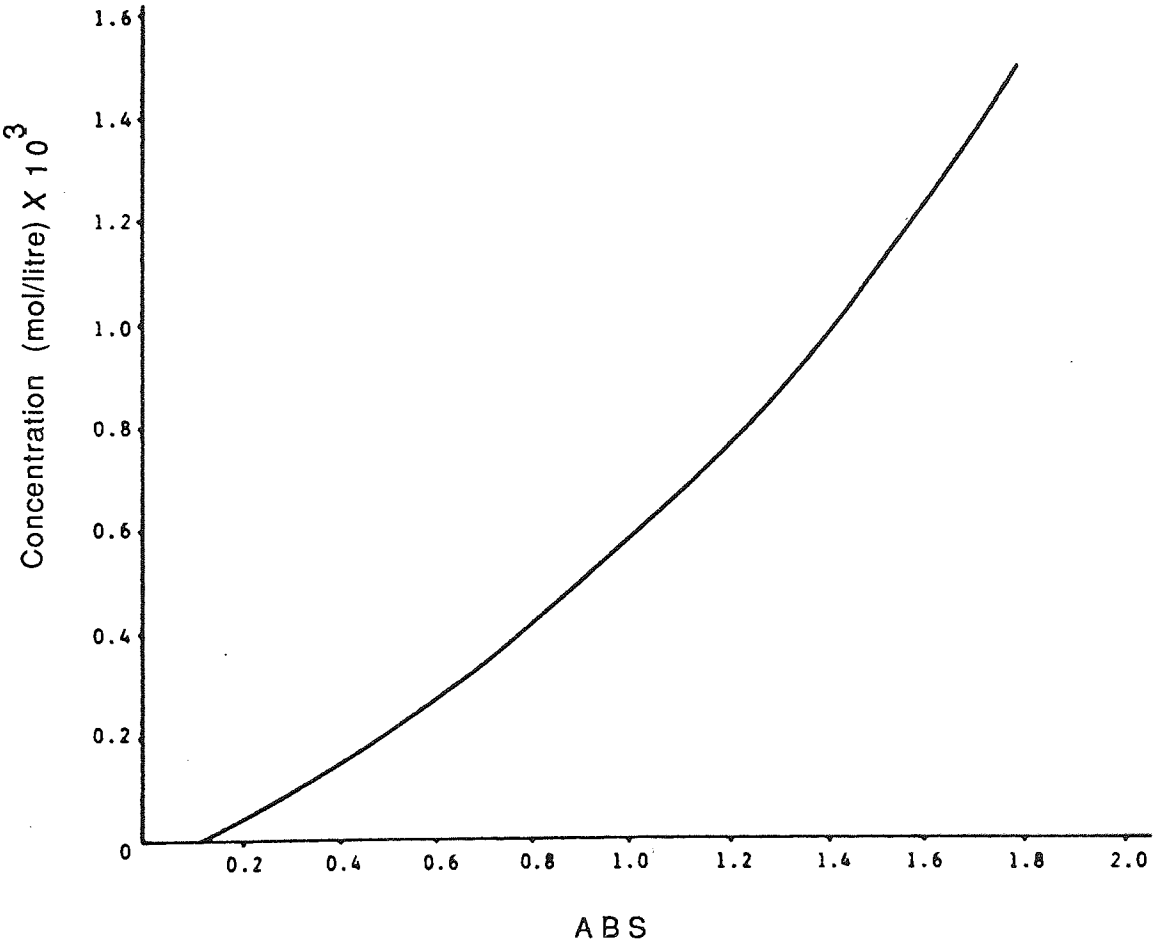

APPENDIX 6 The Cumulative Pore Size Distribution Curves for MIP (Chapter 3).

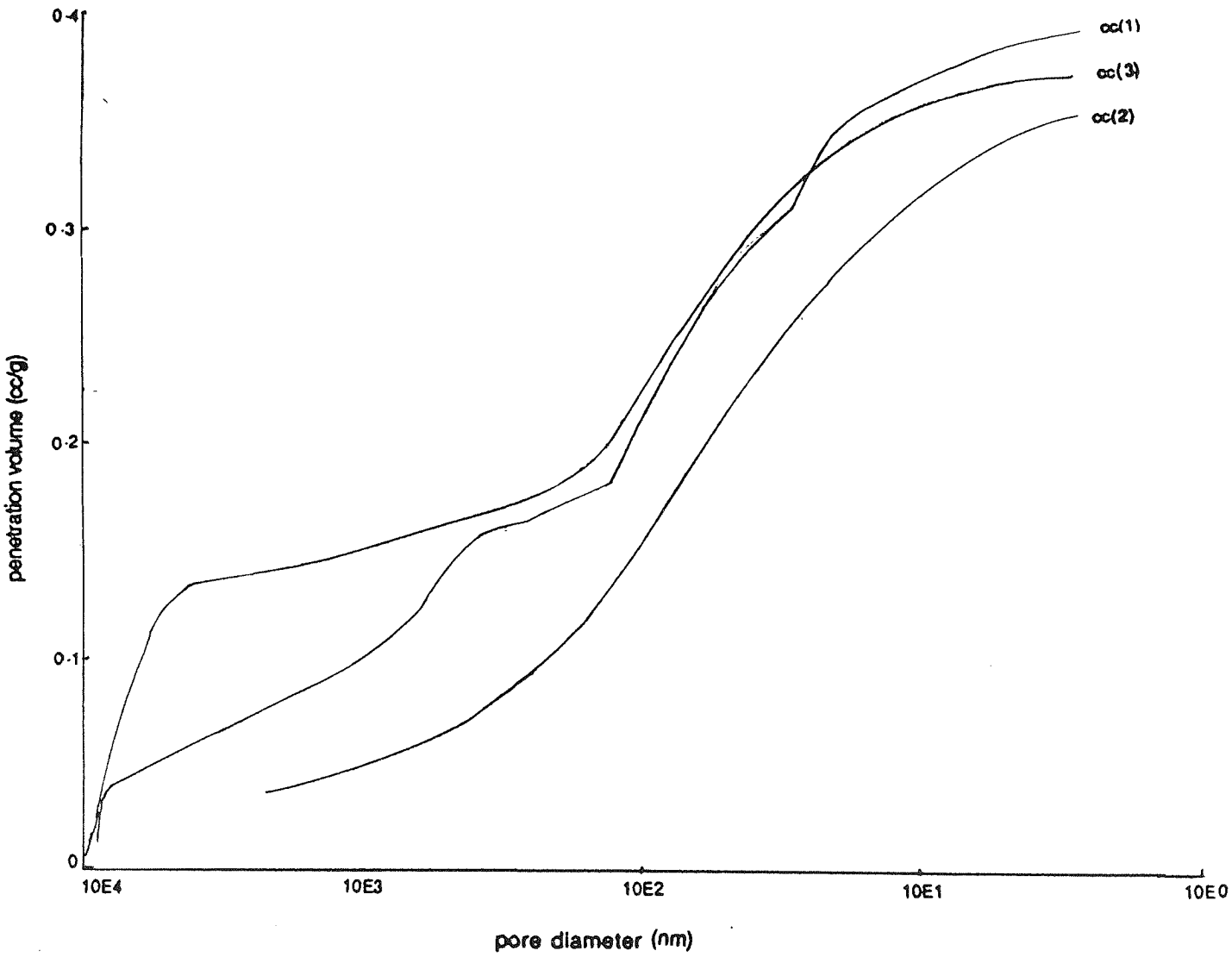

OPC at 7 days 0.6 W/C ratio

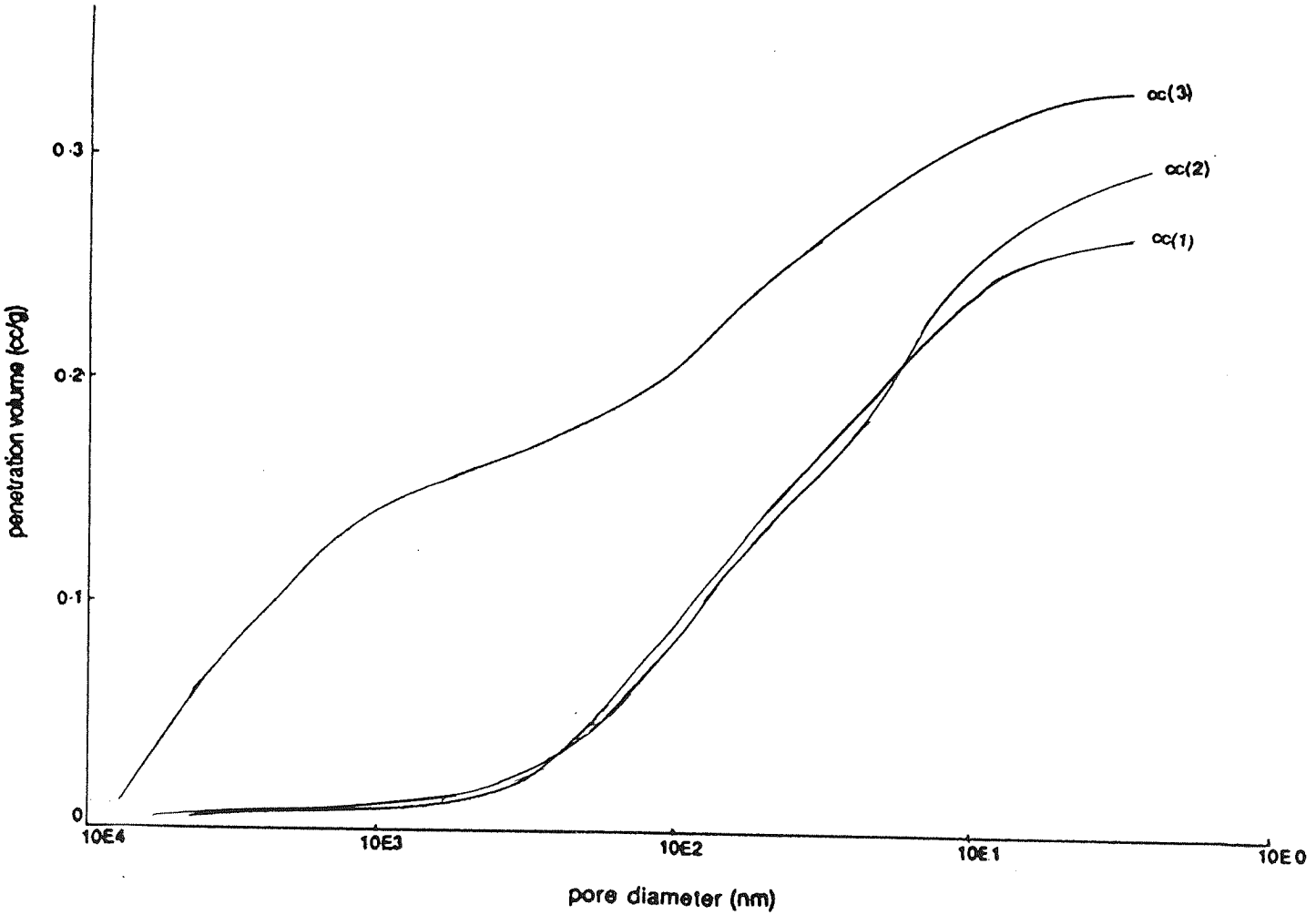

OPC at 28 days 0.6 W/C ratio

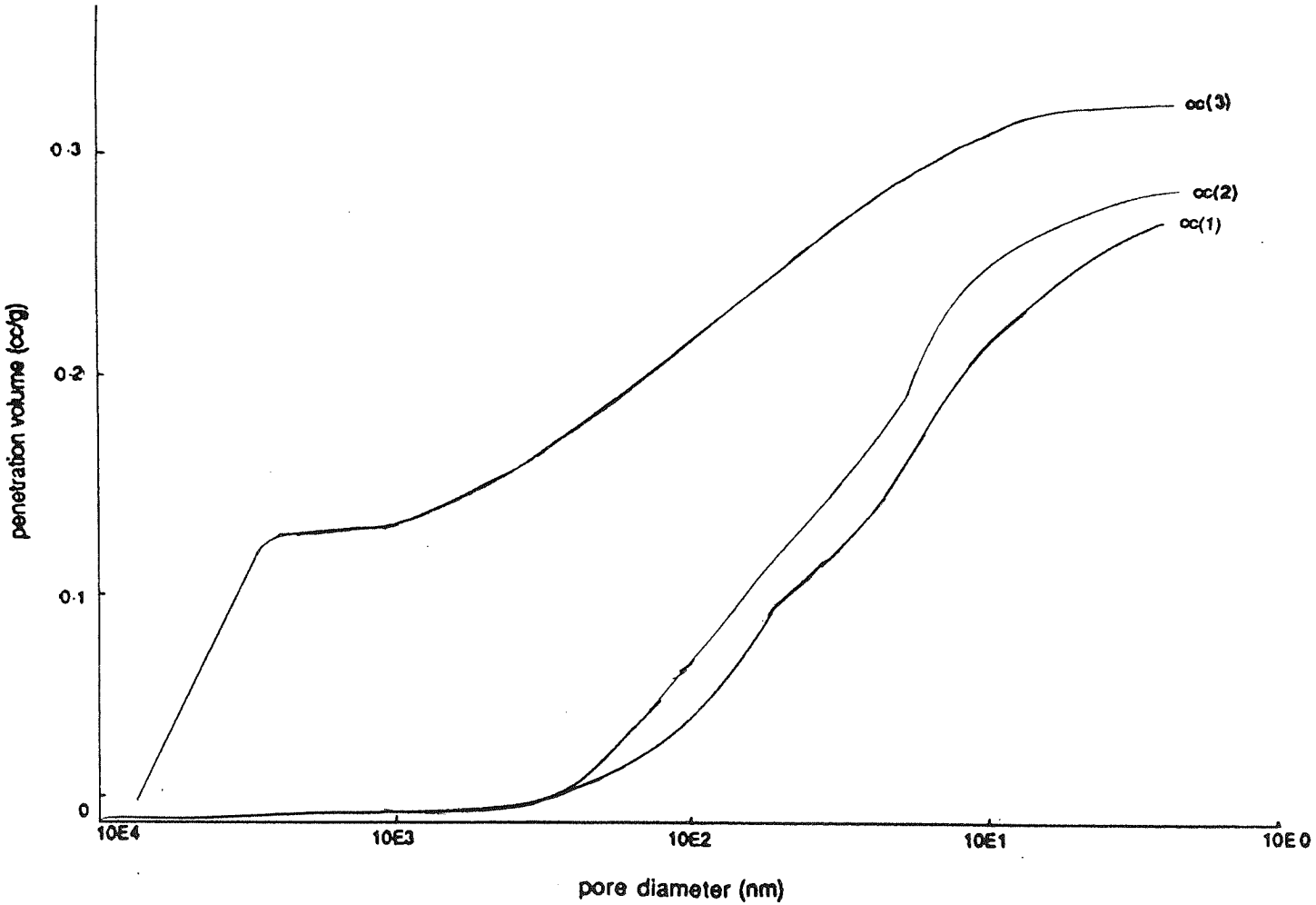

OPC at 60 days 0.6 W/C ratio

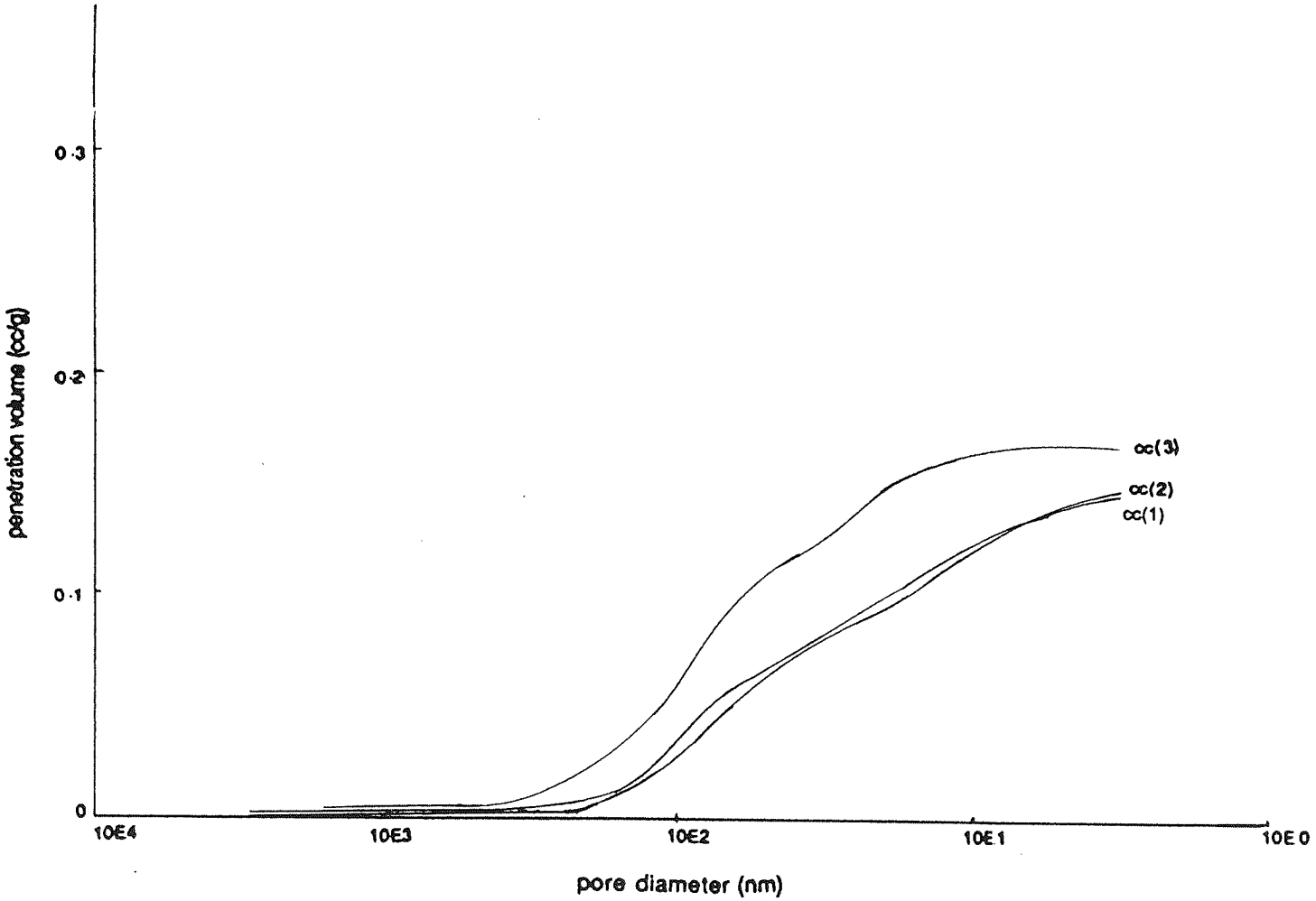

OPC at 28 days 0.4 W/C ratio

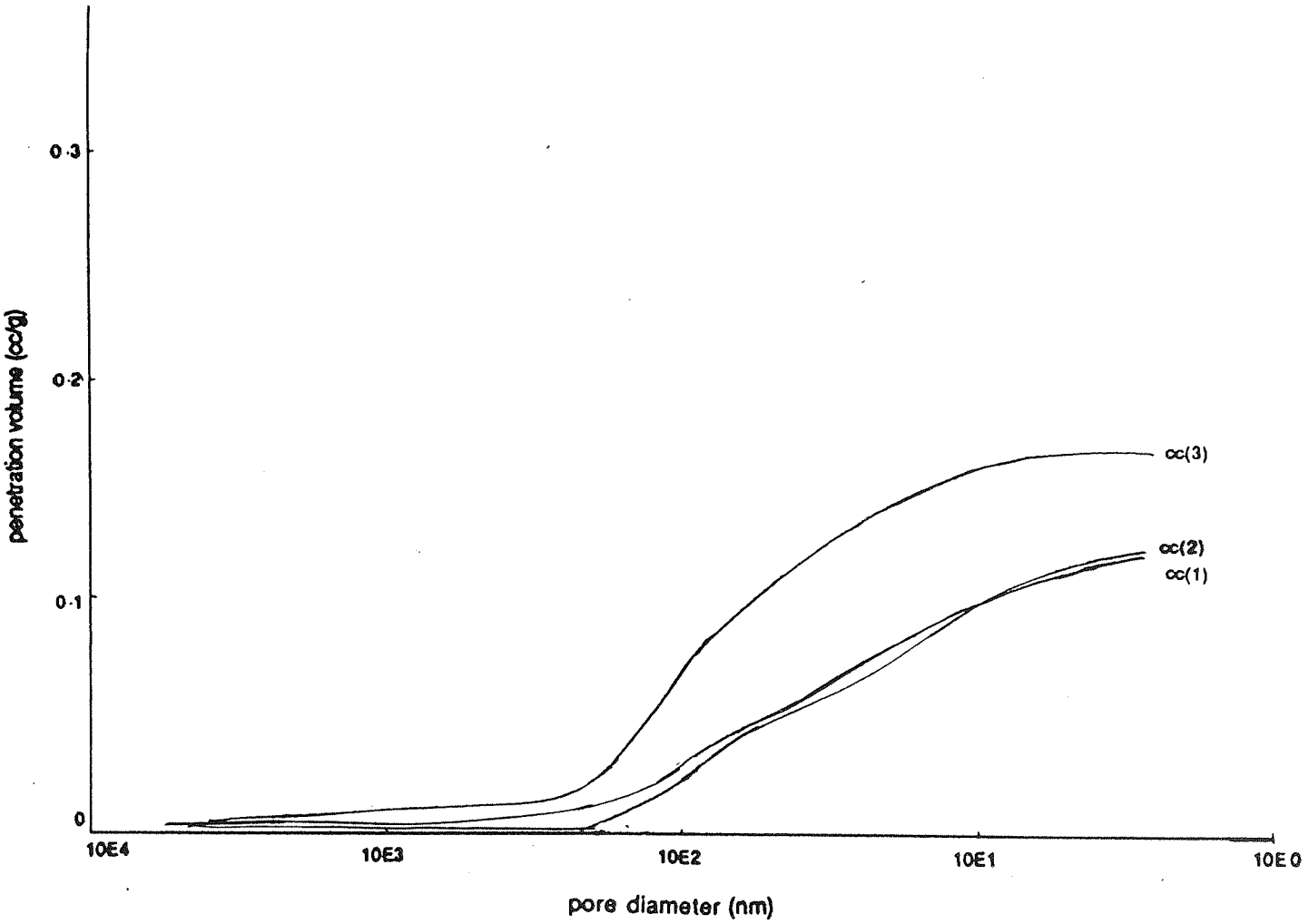

OPC at 60 days 0.4 W/C ratio

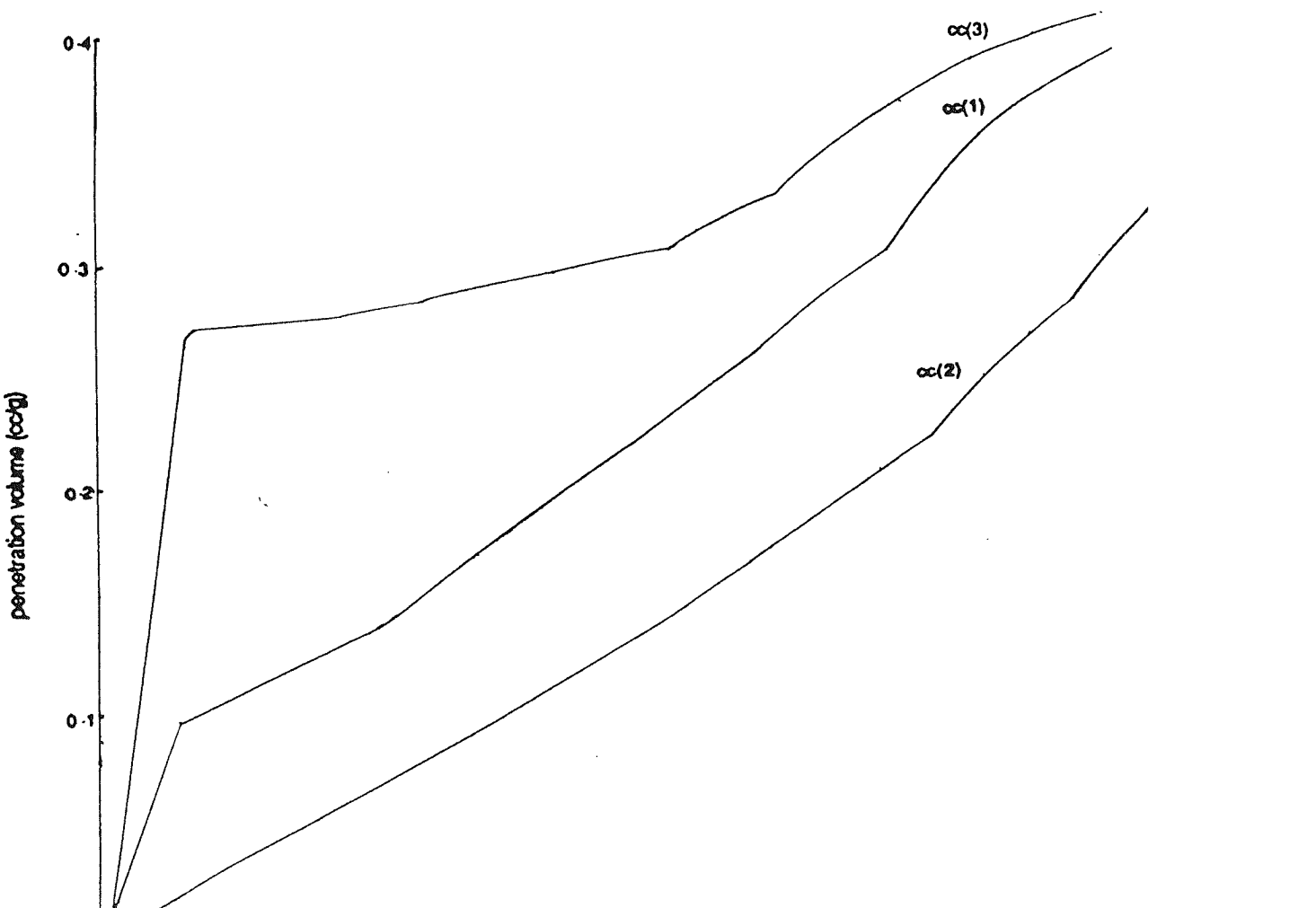

OPC/BFS at 7 days 0.6 W/C ratio

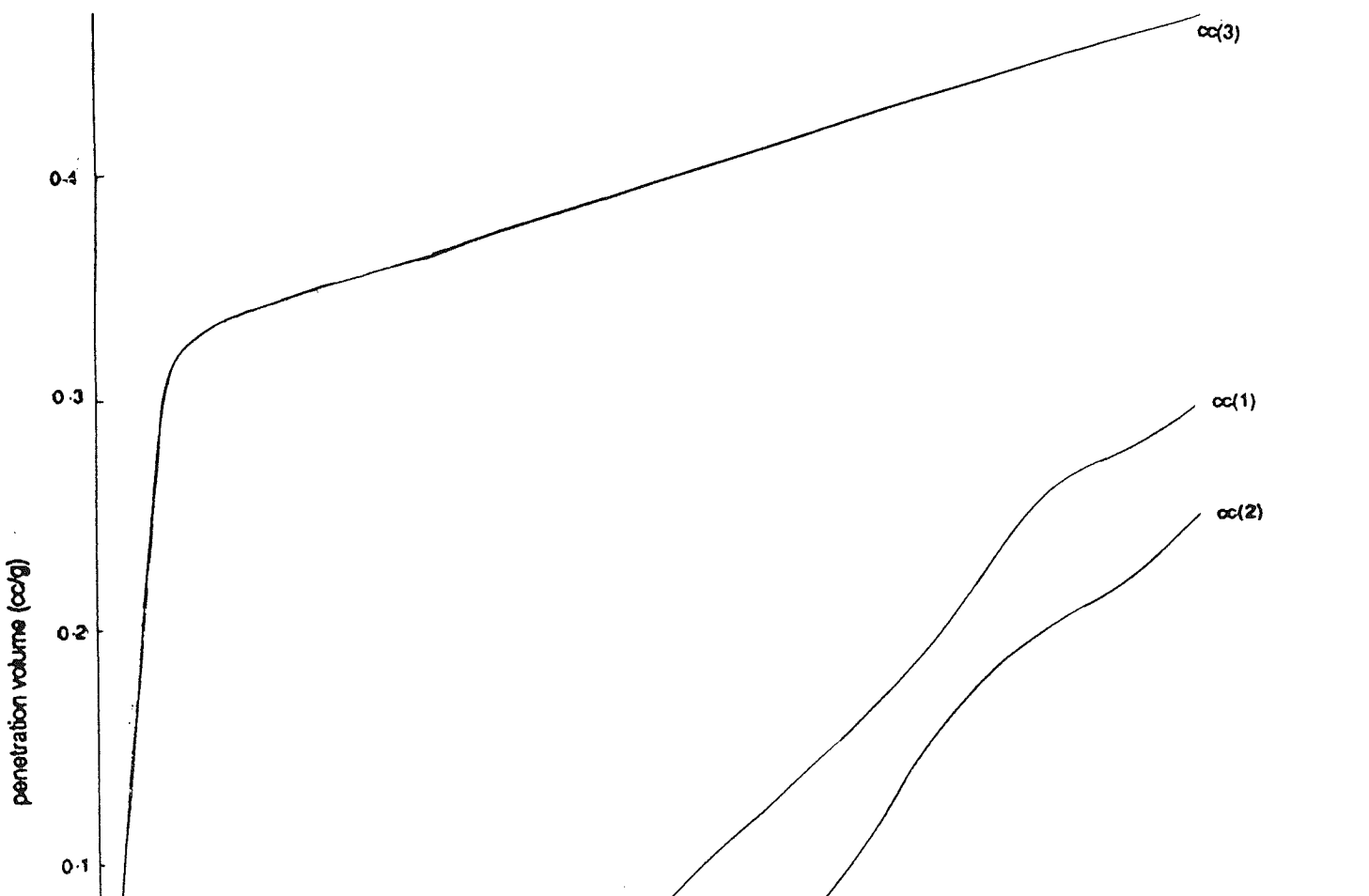

OPC/BFS at 28 days 0.6 W/C ratio

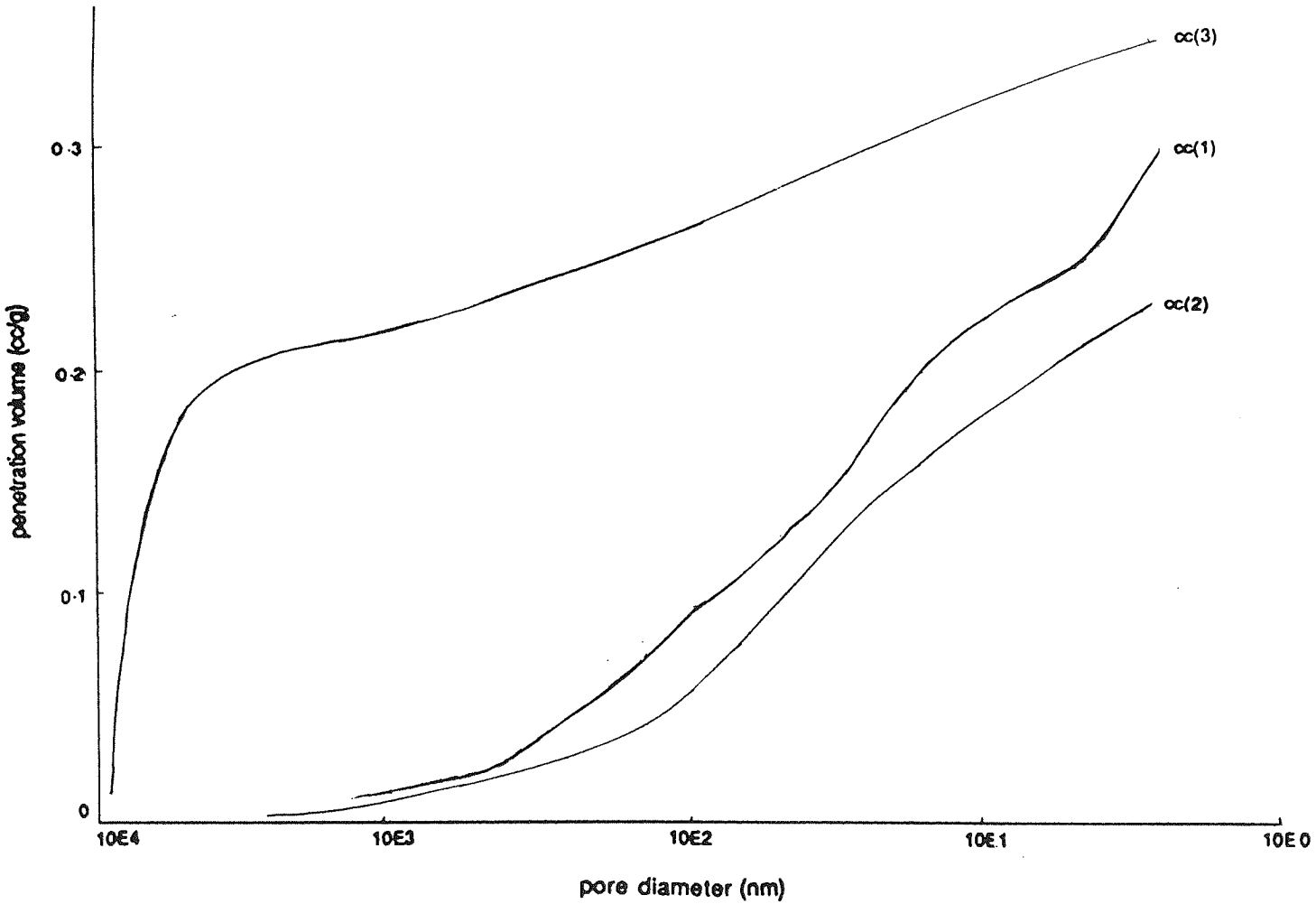

OPC/BFS at 60 days 0.6 W/C ratio

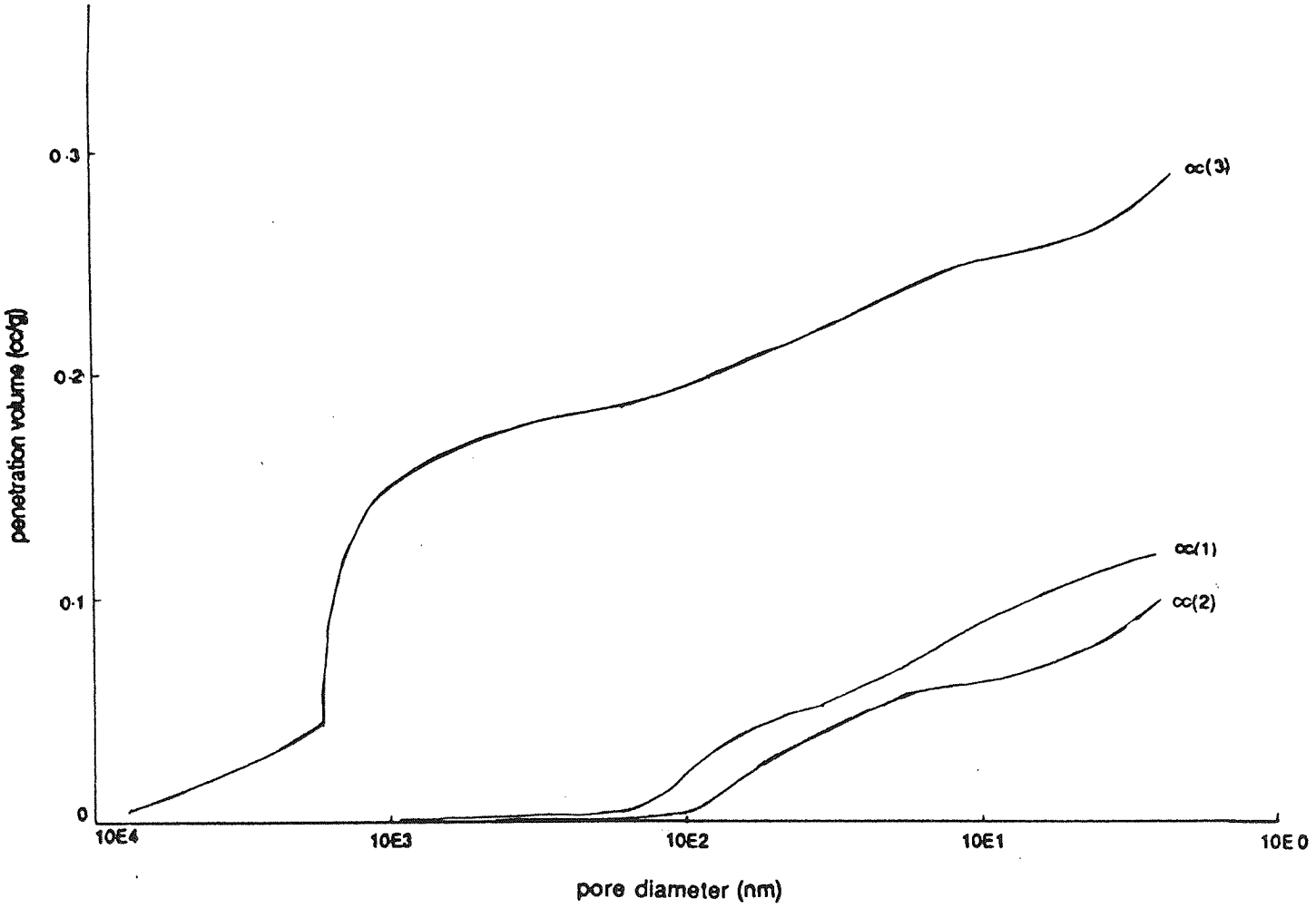

OPC/BFS at 28 days 0.4 W/C ratio

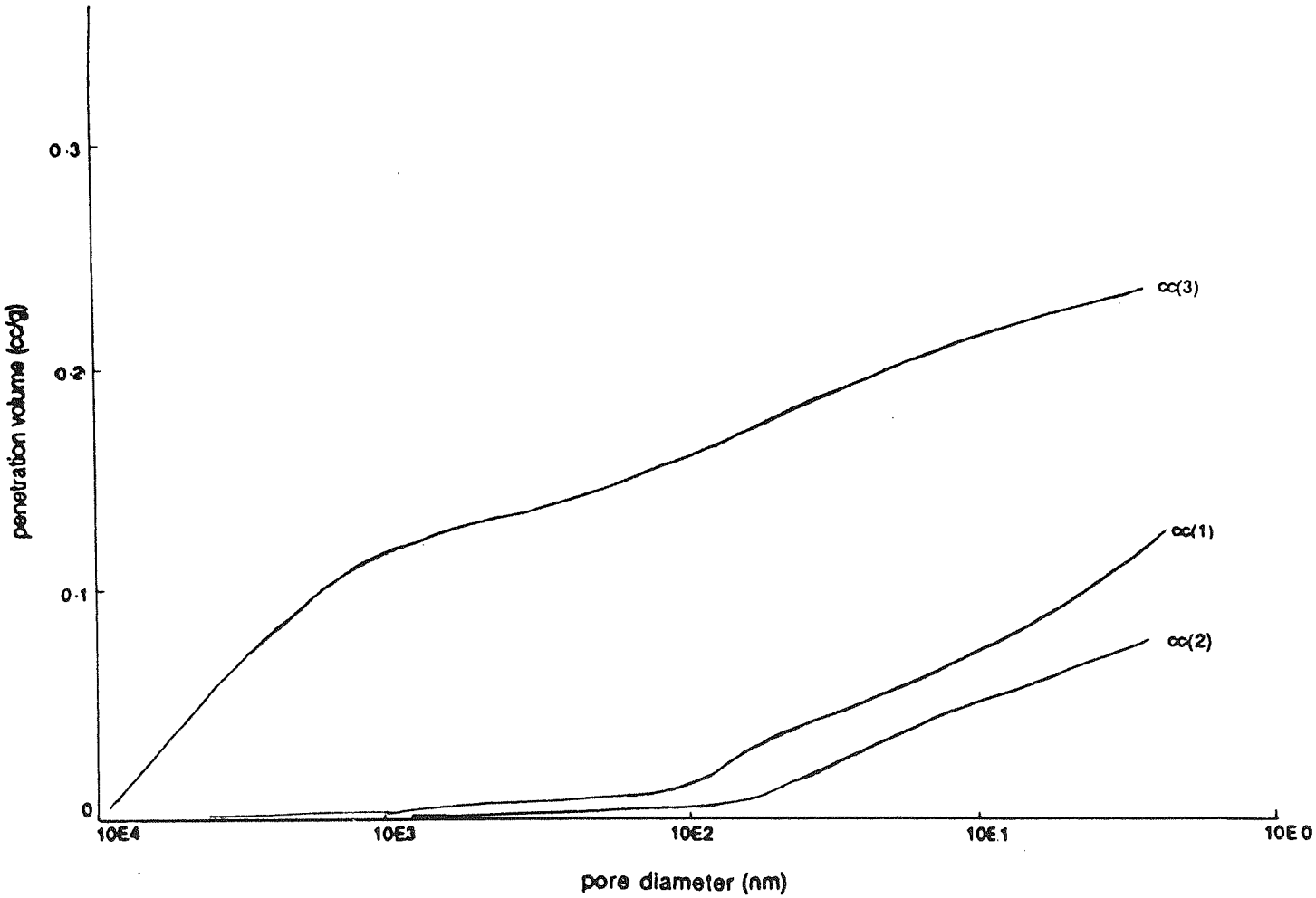

OPC/BFS at 60 days 0.4 W/C ratio

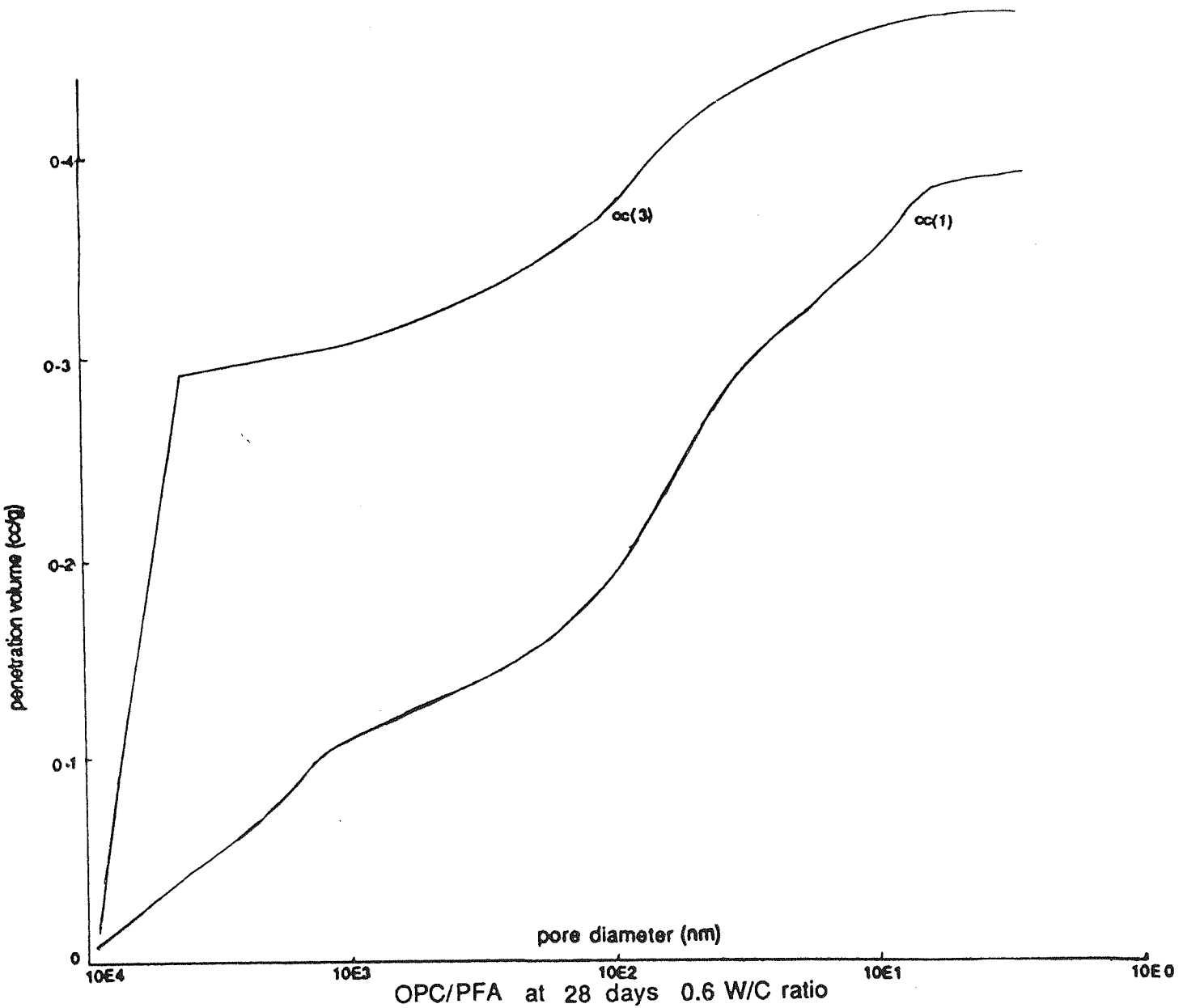

OPC/PFA at 28 days 0.6 W/C ratio

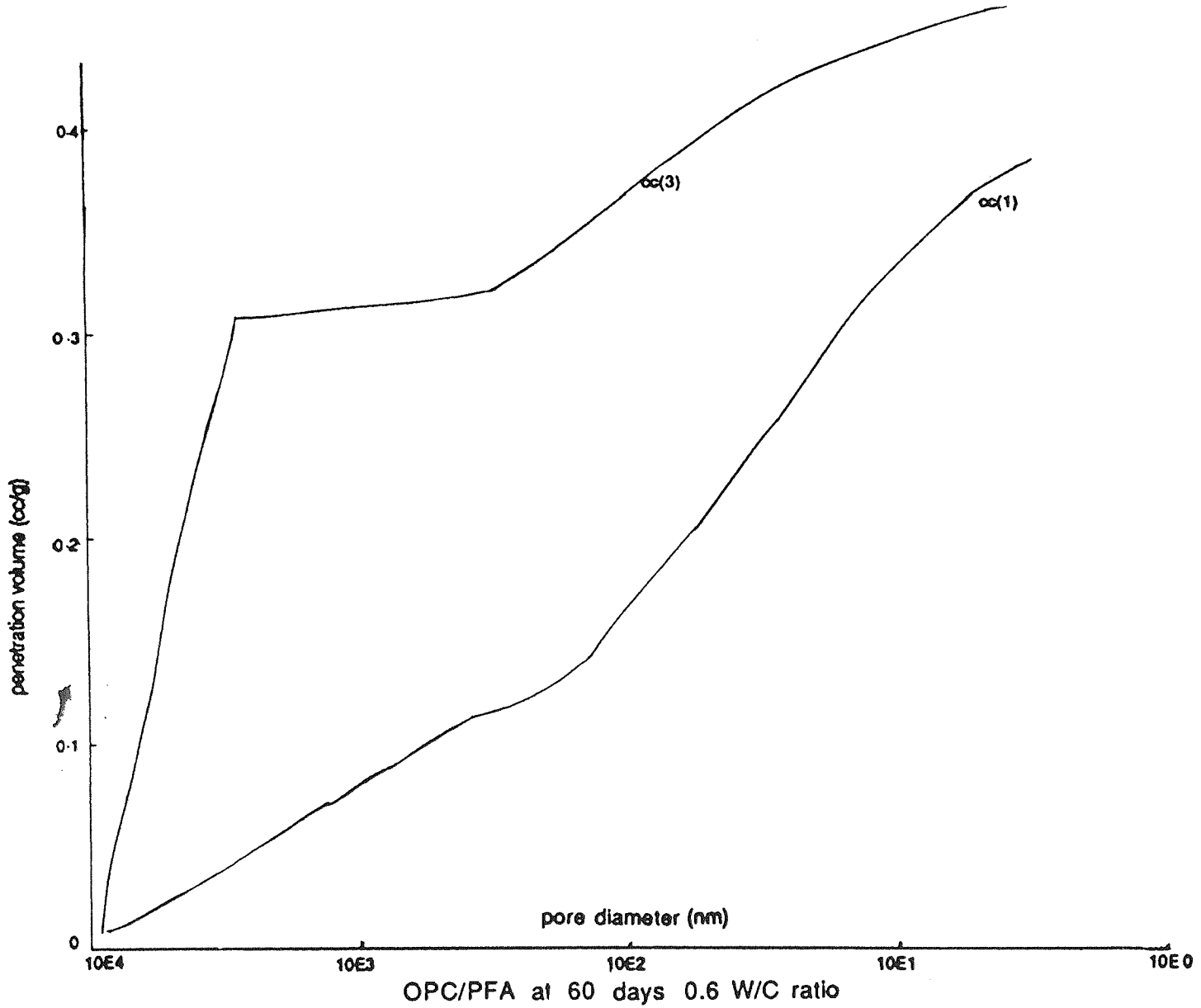

OPC/PFA at 60 days 0.6 W/C ratio

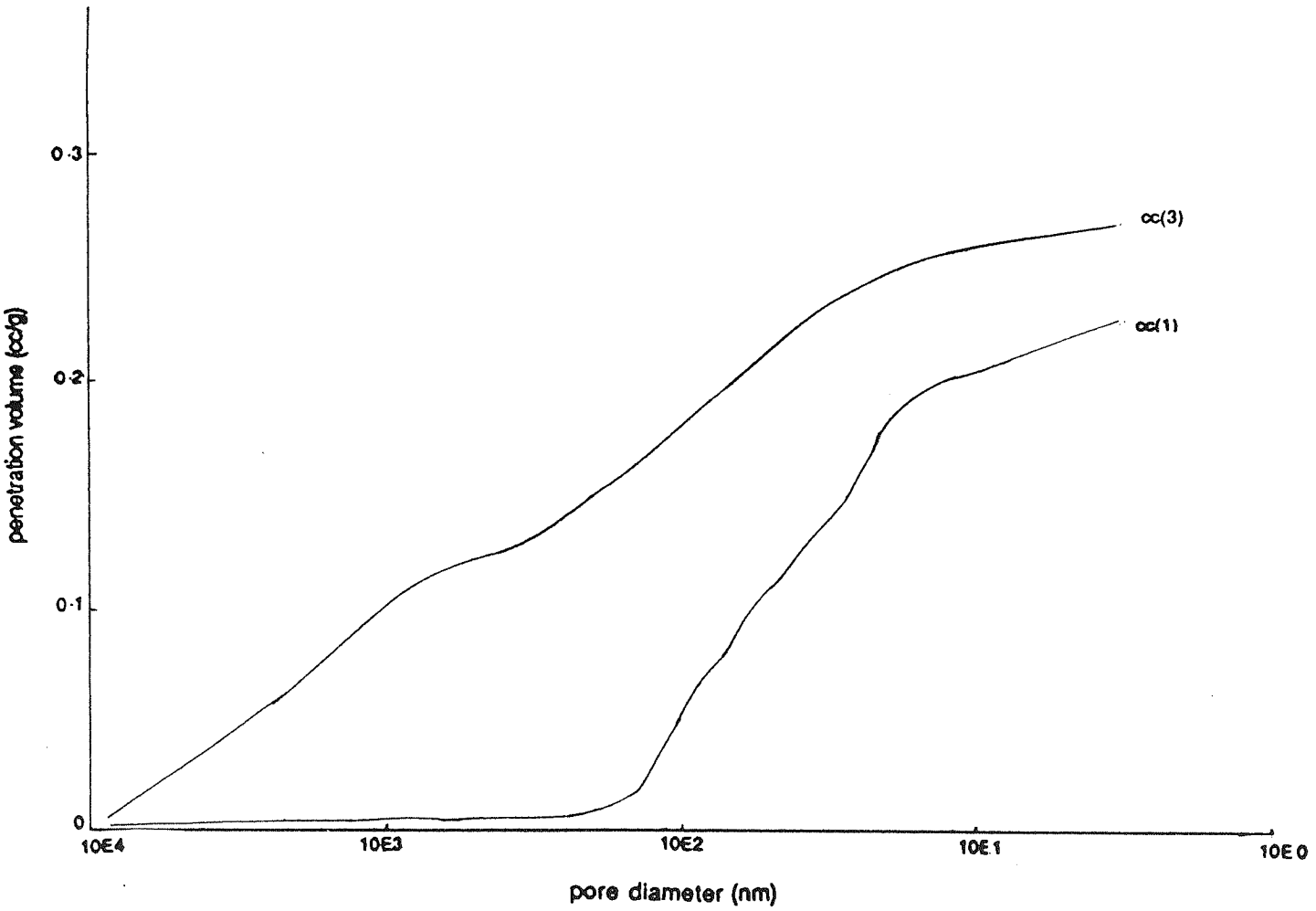

OPC/PFA at 28 days 0.4 W/C ratio

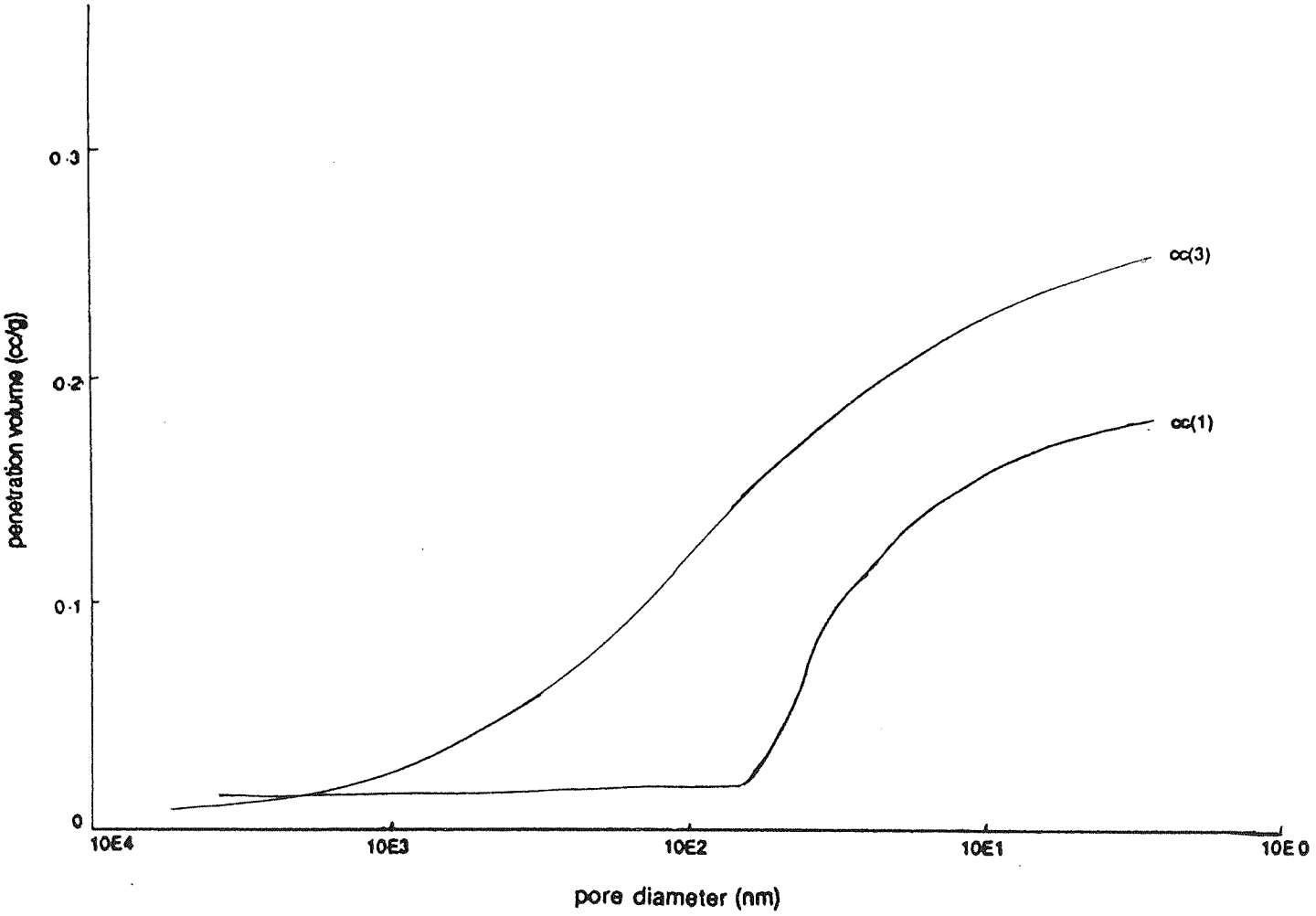

OPC/PFA at 60 days 0.4 W/C ratio

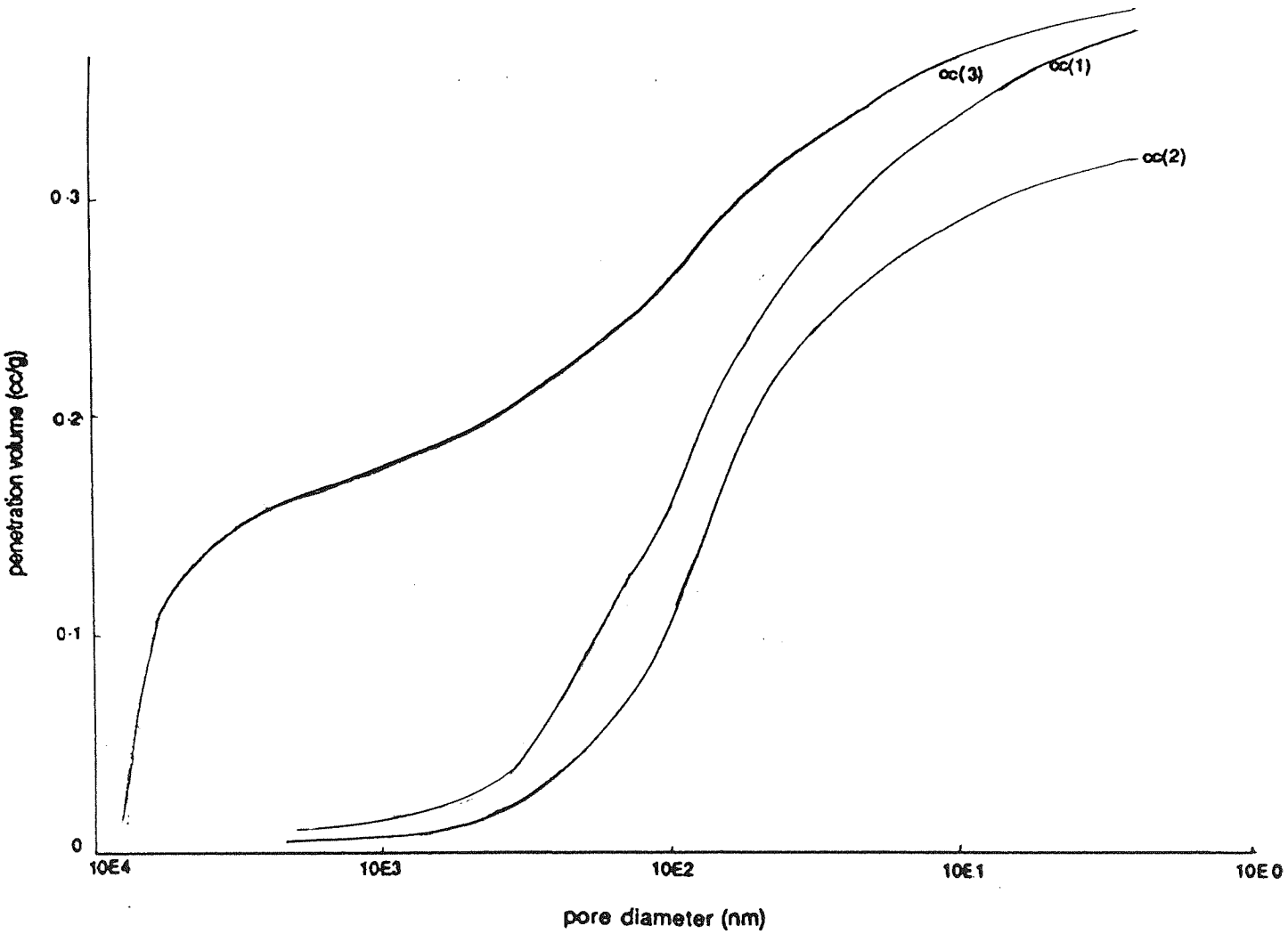

SRPC at 28 days 0.6 W/C ratio

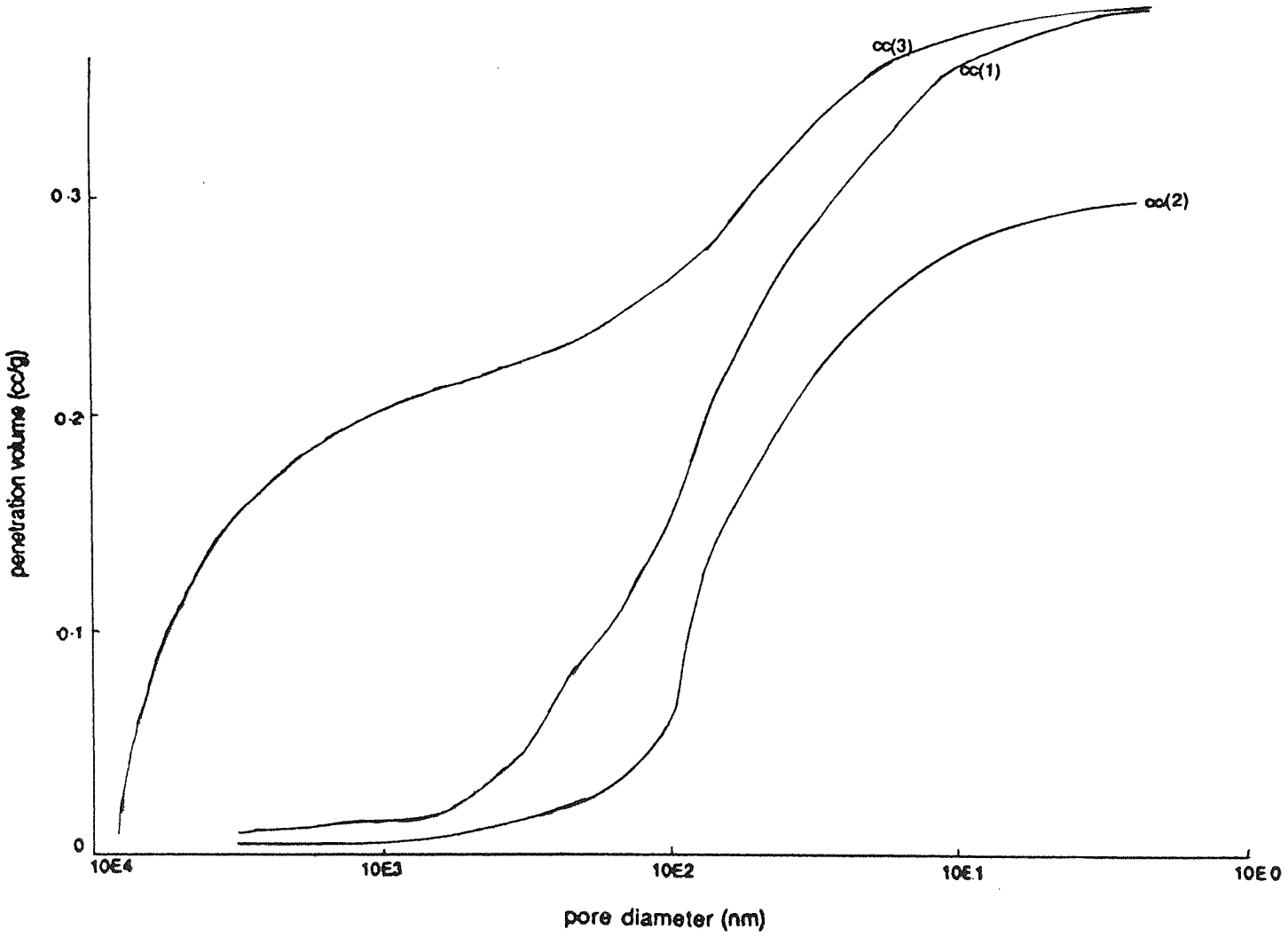

SRPC at 60 days 0.6 W/C ratio

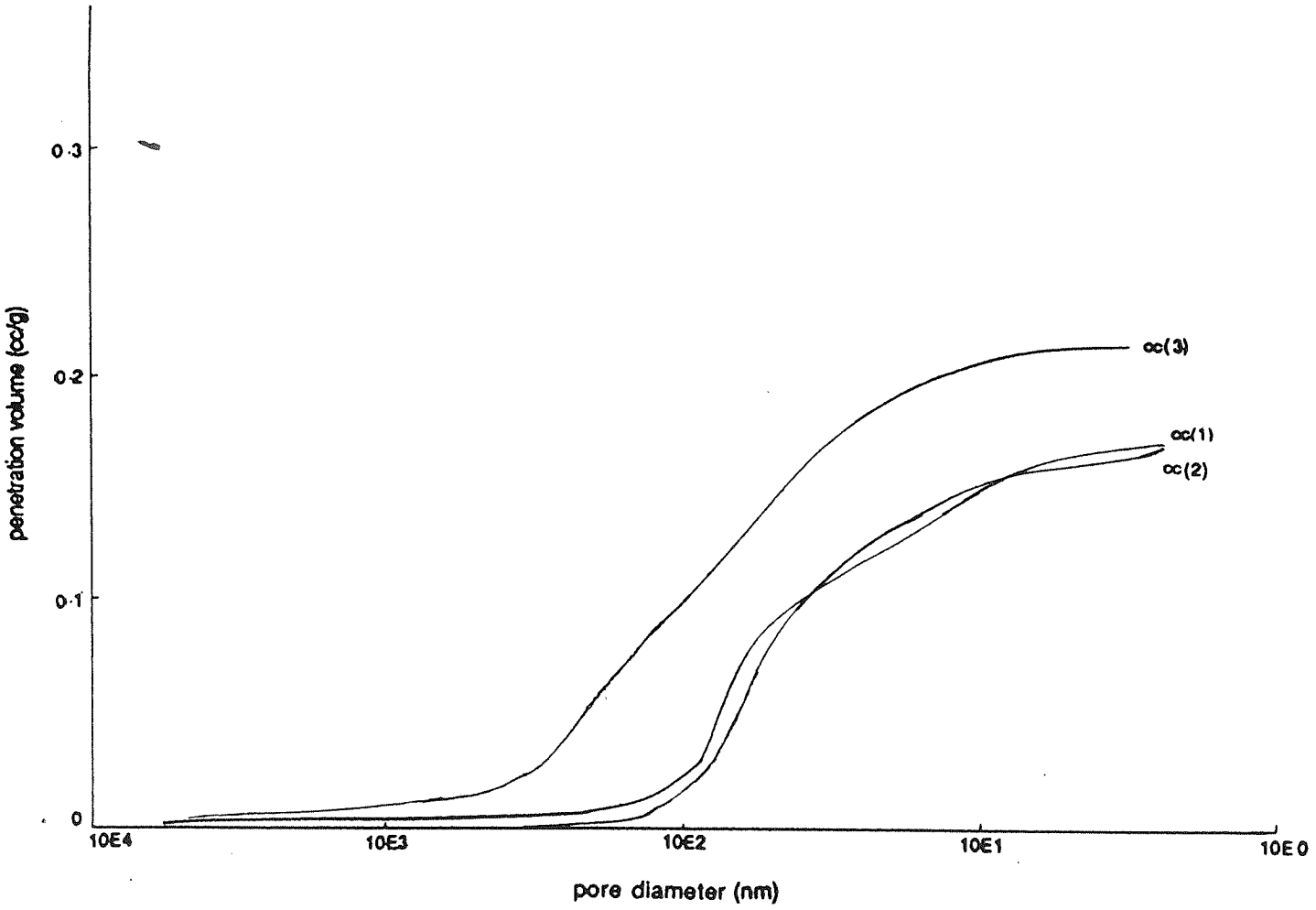

SRPC at 28 days 0.4 W/C ratio

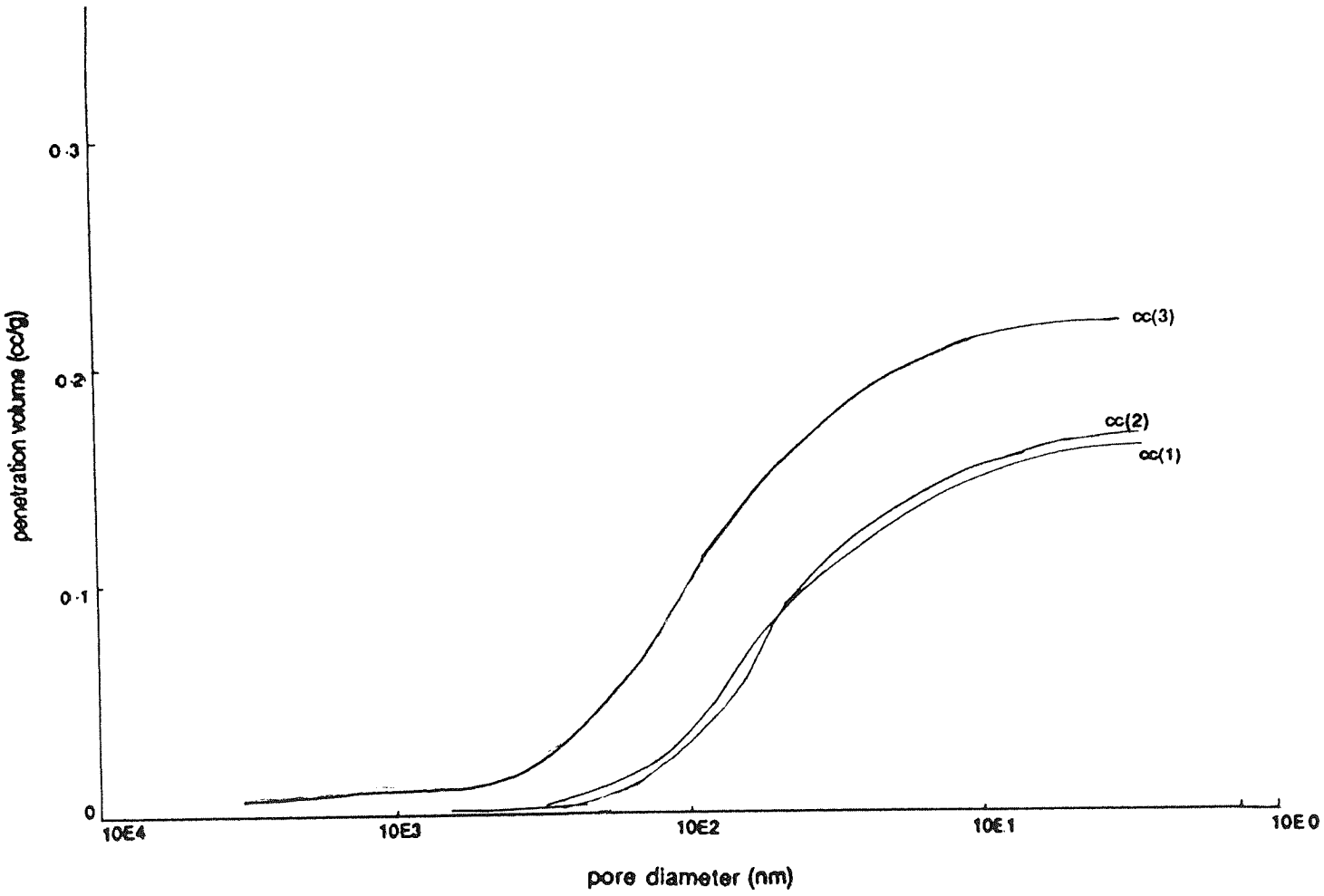

SRPC at 60 days 0.4 W/C ratio

APPENDIX 7 Example calculation of percentage of polymer loading by weight of the sample and percentage of volume of pores filled with polymer.

For OPC paste of 0.6 water/cement ratio originally cured for 28 days under cc(3) and then oven dried at 80-85^{o}C until constant weight.

W_1 = weight of the sample before impregnation = 173.37 g

W_2 = weight of the sample after impregnation = 223.00 g

W_3 = (W_2-W_1) = weight gain after impregnation = 49.63 g

% of polymer loading by weight of the sample = $\frac{100 \times (W_2 - W_1)}{W_1}$ = 28.63

To calculate % volume of pores filled with polymer the following values are required.

The total pore volume measured with pycnometric method for above samples

(V_T) = 0.34 cc/g

Assume the density of polymer is = 1.20 g/cc

then

The % of volume of the polymer within the sample is (P_v) = $\frac{28.63}{1.20}$ = 23.86

Volume of polymer within the sample is (V) = $\frac{23.86}{100}$ = 0.24 cc/g

The percentage of volume of pores filled with polymer =

$\frac{0.24 \times 100}{0.34}$ = 70.18%

APPENDIX 8 Calculation of the carbonation rate constants (K_o and K) and of the depth of Carbonation Lo, related to K_o.

The best fit equation for the relationship between depth of carbonation and time (Chapter 6) was determined by linear regression analysis.

For OPC paste of 0.6 water/cement ratio of originally cured 28 days under cc(3) it was determined as follows :

Values of Σx, Σy, Σx^2, Σxy, Σy^2 and n were calculated. For this example these are as follows :

$\Sigma x = 8.14$ $\quad\quad$ $\Sigma xy = 18.20$

$\Sigma y = 6.00$ $\quad\quad$ $\Sigma y^2 = 20.00$

$\Sigma x^2 = 22.55$ $\quad\quad$ $n = 3$

For the first line (see figure 6.3) need to determine values of a_o and b_o of the best fit equation (170).

$$y = a_o + b_o x$$

$$b_o = \frac{n\Sigma xy - \Sigma x \Sigma y}{n\Sigma x^2 - (\Sigma x)^2}$$

$$\therefore b_o = 4.16 \text{ mm/day}^{1/2}$$

$$\text{and } a_o = \frac{\Sigma y - b\Sigma x}{n} = -9.30 \text{ mm}$$

e.g. best fit equation for the first line :

$$y = 9.30 + 4.16\,x$$

correlation coefficient

$$r_o = \frac{n\Sigma xy - \Sigma x \Sigma y}{\sqrt{[\{n\Sigma x^2 - (\Sigma x)^2\}\{n\Sigma y^2 - (\Sigma y)^2\}]}}$$

$$r_o = 0.999$$

$\Sigma x = 37.23$ $\quad\quad$ $\Sigma xy = 225.78$

$\Sigma y = 45.00$ $\quad\quad$ $\Sigma y^2 = 274.50$

$\Sigma x^2 = 186.08$ $\quad\quad$ $n = 8$

For the second line also need to determine values of a and b of the best fit equation.

$$y = a + bx$$

where

$$b = \frac{n\Sigma xy - \Sigma x \Sigma y}{n\Sigma x^2 - (\Sigma x)^2} = 1.28$$

$$b = 1.28 \quad mm/day^{1/2}$$

and $$a = \frac{\Sigma y - b\Sigma x}{n} = -0.32 \quad mm$$

$\therefore$ best fit equation for the second line $y = -0.32 + 1.28\,x$

correlation coefficient

$r = 0.999$

Calculation of L_o and depth of carbonation at 100 days

$y = a_o + b_o x$ line (1) eq. 1

$y = a + b x$ line (2) eq. 2

(eq.1)xb $by = b a_o + b b_o x$ eq. 3

(eq.2)xb_o $b_o y = b_o a + b_o bx$ eq. 4

Subtract (eq. 4) from (eq.3)

$by - b_o y = ba_o - b_o a$

$y(b - b_o) = ba_o - b_o a$

$$y = \frac{ba_o - b_o a}{b - b_o}$$

At the intersect of the two lines, $y = L_o$

$$\therefore L_o = \frac{[(1.28)x(-9.30)] - [(4.16)x(-0.32)]}{1.28x - 4.16} = 3.65 \text{ mm}$$

Depth of carbonation at 100 days.

$y = a + bx$

where $x = \sqrt{100}$

$y = -0.32 + 1.28 \times 10$

$y = 12.48$ mm

REFERENCES

1. "The Durability of Reinforced Concrete Buildings"
National Building Studies Spec. Rep. No.25
(HMSO, London, 1956)

2. MIDGLEY, H.C., FIGG, J.W. & McLEAN, M.J.
"Durability of concrete in the U.K."
Concrete, Vol. 7. 1, (1973) pp. 24 - 26

3. CROOKS, R.N.
"Cracking of reinforced concrete structures in the Middle East due to corrosion of steel reinforcement"
Society of Chemical Industry Symposium, 2, (1978) pp. 31 - 41

4. FOOKES, P.G. & COLLIS, L.
"Problems in the Middle East"
Concrete, Vol. 9. 7, (1975) pp. 12

5. FOOKES, P.G. & COLLIS, L.
"Aggregates and the Middle East"
Concrete, Vol. 9. 11, (1975) pp. 14

6. FOOKES, P.G. & COLLIS, L.
"Cracking and the Middle East"
Concrete, Vol. 10. 2, (1976) pp. 14

7. VENECANIN, D.
"Influence of temperature on deterioration of concrete in the Middle East"
Concrete, Vol. 11. 8, (1977) pp.31

8. POLLOCK, D.J., KAY, E.A. & FOOKES, P.G.
"Crack mapping for investigation of Middle East concrete"
Concrete, Vol. 15. 5, (1981) pp. 12

9. FOOKES, P.G., POLLOCK, D.J. & KAY, E.A.
"Rates of deterioration"
Concrete, Vol. 9. 9, (1981) pp. 12

10. KAY, E.A., FOOKES, P.G. & POLLOCK, D.J.
"Deterioration related to chloride ingress"
Concrete, Vol. 15. 11, (1981) pp. 22

11. A.C.I. STANDARD 305
"Hot weather concreting"
American Concrete Institute, Detroit. 8, (1977) pp. 313 - 332

12. A.C.I. STANDARD 305
"Recommended practice for hot weather concreting"
American Concrete Institute, Detroit. (1972) pp. 1 - 13

13. NASSER, K.W. & LOHTIA, R.P.
"Mass concrete properties at high temperature"
American Concrete Institute, Detroit. 3, (1971) pp. 180 - 186

14. NEVILLE, A.M.
"Properties of Concrete"
Third Edition, Pub: Pitman Press. (1981) pp. 221 - 224

15. Building Research Establishment
"Building in hot climates"
A selection of overseas building notes, BRE, Pub: BRE News, (1980)

16. MOORFIELD, G.
"Concrete for hot climates"
Concrete, 12, (1982) pp. 14 - 18

17. TATTERSALL, G.H.
"The workability of concrete"
Cement and Concrete Association, A Viewpoint Publication, (1976)

18. NEVILLE, A.M.
"Properties of Concrete"
Third Edition, Pub: Pitman Press. (1981) pp. 100 - 112

19. BIRT, J.C.
"Curing concrete - an appraisal of attitude, practices and Knowledge"
Second Edition. CIRIA, Report 43, 2, (1981) pp. 1 - 33

20. NEVILLE, A.M.
"Properties of Concrete"
Third Edition, Pub: Pitman Press. (1981) pp. 307 - 324

21. Recommended Practice for Curing Concrete
(Proposed ACI Standard)
Journal, American Concrete Institute. 4, (1961) pp. 233 - 243

22. DAIMON, M.
"Mechanism and kinetics of slag cement hydration"
Proceedings, 7th International Congress on the Chemistry of Cement,
(Paris, 1980) Vol. 1. Principal paper 111-2 pp.1 - 9

23. VERBECK, G.J. & HELMUTH, R.A.
"Structures and physical properties of cement paste"
Proceedings, 5th International Symposium on the Chemistry of Cement,
Vol. 3. part 11, (Tokyo 1968) pp. 1 - 13

24. GOTO, S. & ROY, M.
"The effect of water/cement ratio and curing temperature on the permeability of hardened cement paste"
Cement and Concrete Research, Vol. 11. (1981) pp. 575 - 579

25. NEVILLE, A.M.
"Properties of Concrete"
Third Edition. Pub: Pitman Press. (1981) pp. 433 - 440

26. POWERS, T.C., COPELAND, L.E. & MANN, H.M.
"Capillary continuity or discontinuity in cement pastes"
Journal, Portland Cement Assoc. Research and Developement Laboratories,
Vol. 1. No. 2. 5, (1959) pp. 38 - 48

27. NEVILLE, A.M.
"Properties of Concrete"
Third Edition. Pub: Pitman Press. (1981) pp. 391-395

28. ROBERTS, M.H.
"Carbonation of Concrete made with dense natural aggregates"
Building Research Establishment Information Paper. April 1981.

29. SAUMAN, Z.
"Effect of CO_2 on Porous Concrete"
Cement and Concrete Research, Vol. 2, (1972). pp. 541-549.

30. SERGI, G.
"Corrosion of steel in concrete : cement matrix variables"
PhD. Thesis, Aston University. (1986)

31. SMOLCZYK, H.G.
"Physical and chemical phenomena of carbonation"
Carbonation of Concrete - RILEM International Symposium,
Cement and Concrete Association, Theme 1, paper 1. (April 1976).

32. LACH, V. & SAUMAN, Z.
"The determination of $CaCO_3$ modifications in the Carbonated Concrete".
Carbonation of Concrete - RILEM International Symposium,
Cement and Concrete Association, Theme 1, paper 1. (April 1976)

33. SAUMAN, Z.
"Carbonization of porous concrete and its main binding components".
Cement and Concrete Research, Vol. 1, (1971) pp. 645-662.

34. KONDO, R., DAIMON, M. & AKIBA, T.
"Mechanisms and kinetics on carbonation of hardened cement".
5th International Symposium of the Chemistry of Cement
Proc., Vol 111, Supplementary paper 111-116, (Tokyo 1968).pp.
402-409.

35. TUUTTI. K,
"Corrosion of steel in concrete"
Swedish Cement and Concrete Institute S- 100 44- CBI
Forskning Research fo. 4.82 Stockholm (1982).

36. MAYER, A.
"Investigation of the Carbonation of Concrete"
Supplementary Paper 111-52, 5th International Symp.
Chemistry Cem., Proc., Part 3 (Tokyo 1968) pp. 394-401

37. POWERS, T.C.
"A hypothesis on carbonation shrinkage"
Journal of the Portland Cement Association, (Research & Development Labs),
Vol. 4, (1962) pp. 40-50

38. SKALNY, J.P. & BAJZA, A.
"Properties of cement pastes prepared by high pressure compaction"
Journal of the American Concrete Institute, Proc., Vol. 67, (1970) pp. 221-227

39. MANNS, W. & WESCHE, K.
"Variation in strength of mortars made of different cements due to carbonation".
5th International Symposium of the Chemistry of Cement, Proc., Vol 111, Supplementary Paper 111-16 (Tokyo 1968) pp.385-393

40. ROZENTAL, N.K. & ALEKSEEV, S.N.
"Change in concrete porosity during carbonation"
Carbonation of Concrete - RILEM International Symposium;
Cement and Concrete Association, Theme 2, paper 4. (April 1976)

41. PIHLAJAVAARA, S.E.
"Carbonation engineering properties and effects of carbonation on concrete structures - General Report"
Carbonation of Concrete - RILEM International Symposium,
Cement and Concrete Association, Theme 4,paper 1. (April 1976)

42. ALEXANDRE, J.
"Rate of carbonation"
Carbonation of Concrete - RILEM International Symposium,
Cement and Concrete Association, Theme 3, paper 1. (April 1976)

43. PAGE, C.L.
"Barriers to the prediction of service life of metallic materials".
Masters, L.W., Ed., Problems in Service Life Prediction of Building and Construction Materials, NATO advanced Science Institute series: Applied Sciences,
Martinus Nijhoff, E.95, (1985) pp. 59-74.

44. SCHUBERT, P. & EFES, Y.
"The carbonation behaviour of mortar and concrete with jet cement".
Carbonation of Concrete - RILEM International Symposium,
Cement and Concrete Association, Theme 3, paper 5. (April 1976).

45. ALEKSEEV, S.N. & ROZENTAL, N.K.
"The rate of concrete carbonation"
Carbonation of concrete - RILEM International Symposium,
Cement and Concrete Association, Theme 3, paper 6. (April 1976).

46. SMOLCZYK, H.G.
"Explorations to the German longtime - study on the rate of carbonation"
Carbonation of Concrete - RILEM International Symposium,
Cement and Concrete Association, Theme 3, paper 2. (April 1976).

47. VERBECK, G.J. & HELMUTH, R.H.
"Principal paper - structures and physical properties of cement paste"
5th International Symposium of the Chemistry of Cement
Vol 3 Part 3, proc., (Tokyo 1968) pp. 7-8.

48. MILLS, R.H.
"Molecular sieve effect in concrete"
5th International Symposium of the Chemistry of Cement,
Proc., Vol 3, Supplementary Paper 3-46 (Tokyo 1968) pp. 74-85.

49. HAMADA, M.
"Principal paper - Neutralization (Carbonation) of concrete and corrosion of reinforcing steel".
5th International Symposium of the Chemistry of Cement,
Proc., Vol 3, Properties of Cement & Concrete (Tokyo 1968) pp. 343-369.

50. KUMAR, A., ROY, D.M. & HIGGINS, D.D.
"Diffusion through concrete"
Concrete Journal. January 1987 pp. 31-32.

51. BAKKER, R.F.M.
"On the cause of increased resistance of concrete made from blast furnace cement to the alkali-silica reacton and to sulphate corrosion"
Doctoral thesis ,Maastricht,the Netherlands. June,1980.

52. UCHIKAWA , H., UCHIDA, S. & OGAWA, K.
"Diffusion of alkali ions in hardened cement paste"
Review of the 38th General Meeting of the Cement Association of Japan, 10, (1984) pp. 56-59.

53. TAKAGI, T., GOTO, S. & DAIMON, M.
"Diffusion of I^- ion through hardened cement paste"
Review if the 38th General Meeting of the Cement Association of Japan, 14, (1984) pp. 72-75.

54. MIDGLEY, H.G. & ILLSTON, J.M.
"The penetration of chloride into hardened cement pastes"
Cement and Concrete Research. Vol. 14, (1984) pp. 546-558.

55. GOTO, S. & ROY, D.M.
"Diffusion of ions through hardened cement pastes"
Cement and Concrete research. Vol 11, (1981) pp. 751-757.

56. HANSSON, C.M.
"Comments on electrochemical measurements of the rate of corrosion of steel in concrete"
Cement and Concrete Research. Vol 14, (1984) pp. 574-584.

57. HOLDEN, W.R., PAGE, C.L. & SHORT, N.R.
"The influence of chlorides and sulphates on durability of reinforcement in concrete".
Int. Conf. Corr. of Reinforcements in Concrete Construction, A. P. Crane Ed., Soc. of Chem. Industry (London 1983) pp. 143-150.

58. HAUSMAN, D. A.
"Steel Corrosion in Concrete" Materials Protection.
Vol. 6, 11, (1967) pp. 23.

59. PAGE, C.L., & VENNESLAND, Ø
"Pore solution composition and chloride binding capacity of silica fume-cement pastes".
Materiaux et Constructions, Vol 16, 91, (1983) pp. 19-25.

60. LEA, F.M.
"The Chemistry of Cement and Concrete"
Third Edition. Pub: Edward Arnold, 1970. pp 232

61. PAGE, C.L. & TREADAWAY, K.W.
"Aspects of the electrochemistry of steel in concrete"
Nature 297, 5862 (1982) pp. 109-115.

62. CALLEJA, J.
"Durability"
7th Int. Conference on the Chemistry of Cement,
proc.,Vol. 1, VII - 2/I-VII-2/48, Paris France, 1980

63. BROWNE, R.D. & GEOGHEGAN, M.P.
"The Corrosion of marine structures: The present situation".
Symp. Corrosion of Steel Reinforcements in Concrete Construction,
Proc., Society of Chemical Industry, London (1979) pp. 79

64. PAGE, C.L.
"The corrosion of reinforcing steel in concrete; it's causes and control".
Bulletin of the Institute of Corrosion Science and Technology,
Vol. 77 (1979) pp. 2-7

65. JOST, W.
"Diffusion of solids, liquids, gases"
Pub: Academic Press, 1952. pp. 163-164

66. GIRIFALCO, L.A. & WELCH, D.O.
"Point defects and diffusion in strained metals"
Pub: Gordon and Breach, 1967, pp. 1.

67. LAMBERT, P.
"The corrosion and passivation of steel in concrete"
PhD. Thesis, Aston University.
(1983)

68. PAGE, C.L., SHORT, N.R. & EL TARRAS, A.
"Diffusion of chloride ions in hardened cement pastes"
Cement and Concrete Research Vol. 11, 3, (1981) pp. 395-406.

69. KONDO, R., SATAKE, M. & USHIYAMA, H.
"Diffusion of various ions in hardened portland cement "
Cement Association of Japan, 28th General Meeting,
Tokyo (1974) pp. 41-43

70. USHIYAMA, H. & GOTO, S.
"Diffusion of various ions in hardened portland cement paste"
The 6th International Congress on the Chemistry of Cement,
Supplementary Paper, Section 11, 11-3, 4, 5,
Moscow (1974) pp. 331-337

71. SHAW, D.J.
"Introduction to colloid and surface chemistry"
Second Edition. Pub: Butterworth, 1970. pp. 133-166

72. COLLEPARDI, M., MARCIALIS, A. & TURRIZIANI, R.
"The penetration of de-icing agents in cement pastes"
IL Cemento 3, (1972) pp. 143-149.

73. COLLEPARDI, M., MARCIALIS, A. & TURRIZIANI, R.
"The kinetics of penetration of chloride ions into the concrete"
IL Cemento. 4, (1970) pp. 157-163.

74. COLLEPARDI, M., MARCIALIS, A. & TURRIZIANI, R.
"Penetration of chloride ions into cement pastes ans concretes"
Journal of the American Ceramic Society Vol. 55. 10, (1972)
pp. 534-535

75. SPINKS, J.W.T., BALDWIN, H.W. & THORVALDSON, T.
"Tracer Studies of Diffusion in set portland cement"
Canadian Journal of Technology, Vol. 30. (1952) pp. 20-28

76. SIMEONOV, Y., BOZHINOV, G. & BAROVSKY, N.
"Durability of reinforced concrete in Sea Water"
Editor: A.P.Crane. Pub: Ellis Horwood, (1983) Chapter 2. pp. 1

77. LEA, F.M.
"The chemistry of cement and concrete"
Third Edition. Pub: Edward Arnold, (1970) pp553-554

78. BARNEYBACK JUNIOR, R.S. & DIAMOND, S.
"Expression and analysis of pore fluids from hardened cement pastes and mortars"
Cement and Concrete Research, Vol. 11. (1981) pp. 279-285

79. BUILDING RESEARCH ESTABLISHMENT DIGEST
The durability of steel in concrete: Part 1 Mechanism of protection and corrosion.
Department of the Environment. 7, 1982. pp. 1-8

80. GOUDA, V.K.
"Corrosion and corrosion inhibition of reinforcing steel - I . Immersed in alkaline solution"
British Corrosion Journal, 5, (1970) pp. 198-203

81. GOUDA, V.K. & HALAKA, W.Y.
"Corrosion and corrosion inhibition of reinforcing steel - II. Embedded in concrete"
British Corrosion Journal, 5, (1970) pp. 204-208

82. BERMAN, H.M.
"Sodium chloride, corrosion of reinforcing steel, and the pH of Calcium Hydroxide Solution"
A.C.I. Journal, 4, (1975) pp. 150-157

83. POURBAIX, M.
"Atlas of electrochemical equilibria in aqueous solutions"
Pub: Pergamon Press, (1966).

84. GONZALEZ, J.A., ALONSO, C.A. & ANDRADE, C.
"Corrosion rate of reinforcements during accelerated carbonation of mortar made with different types of cement"
Corrosion of Reinforcement in Concrete Construction.
Editor: A.P. Crane. Pub: Ellis Horwood, (1983)
Chapter II. pp. 161-174

85. PAGE, C.L. & HAVDAHL, J.
"Electrochemical monitoring of corrosion of steel in microsilica cement pastes"
Materiaux et Construction. 18, 103, (1985) pp. 41-47

86. VASSIE, P.R.W.
"Evaluation of techniques for investigating the corrosion of steel in concrete"
Transport and Road Research Laboratory supplementary Report Number 397 (1978)

87. ANDRADE, C. & GONZALEZ, J.A.
"Quantitive measurements of corrosion rate of reinforcing steels embedded in concrete using polarization resistance measurements"
British Corrosion Journal 15, 3, (1980). pp. 135-139

88. AMERICAN SOCIETY FOR TESTING AND MATERIALS
"Standard test method for half-cell potential data"
Federal Highway Administration, Washington D.C. (1973)
Report PB - 226 - 053 - 7

89. MIKHAIL, R.S., ABO-ENEIN, S.A., MONSA, A.M. & MARIE, M.S.
"Polymer impregnation of hardened cement pastes of various porosities"
Proceedings of the third International Congress on Polymer in Concrete 5, (1981) pp. 875-887

90. KOSI, V.
"Some properties of poly. (Methyl Methacrylate) impregnated Asbestos - cement materials"
Cement and Concrete Research. Vol. 4. Pub: Pergamon Press (1974) pp. 57-68

91. YULAN, H. & YAPING, X.
"Application of polymer - impregnated concrete in China's Salt Lake Area"
Proceedings of the Third International Congress on polymers in concrete. 5, (1981) pp. 1000-1010

92. KATAWAKI, K., FOWLER, D.W. & PAUL, D.R.
"Effect of depth of polymer impregnation and cracking on corrosion of reinforcing steel"
Proceedings of the Third International Congress on polymer in concrete.
5, (1981) pp. 904-918

93. KING, R.A., DAWSON, J.L. & GEAREY, D.
Proc. Symp. on Corrosion of Steel Reinforcements in Concrete Construction, London,
Soc. Chemical, London (1979) pp 135-143.

94. ROBINSON, R.C.
"Design of reinforced concrete structure for corrosive environments"
Materials Protection and Performance, VOL. 11. 3, (1972) pp.15 - 19

95. MOZER, J.D., BIANCHINI, A.C. & KESTER, C.E.
"Corrosion of reinforcing bars in concrete"
Journal. ACI 8, (1969) pp. 909 - 930

96. CLEAR, K.C.
"Reinforcing Bar Corrosion In Concrete: Effect of Special Treatments"
ACI Publication, SP 49-6, Detroit, (1975) pp. 71 - 82

97. ROBINSON, R.C.
"Cathodic Protection of Steel In Concrete"
ACI Publication, SP 49-7, Detroit, (1975) pp. 83 - 94

98. GRIFFIN, D.F.
"Corrosion Inhibitors for Reinforced Concrete"
ACI Publication, SP 49-8, Detroit, (1975) pp. 95 - 102

99. BACKSTROM, T.E.
"Use of Coatings on Steel Embedded in Concrete"
ACI Publication, SP 49-9, Detroit, (1975) pp. 103 - 113

100. CLIFTON, J.R., BEEGHLY, H.F. & MATHEY, R.G.
"Protecting Reinforcing Bars From Corrosion With Epoxy Coatings"
ACI Publication, SP 49-10, Detroit, (1975) pp. 115 - 132

101. BOYD, W.K. & TRIPLER, A.B.
"Corrosion of reinforcing steel bars in concrete"
Materials Protection and Performance, VOL. 41.10, (1968) pp. 40 - 47

102. BIRD, C.E. & STRAUSS, F.J.
"Metalic Coating for Reinforcing Steel"
Materials Protection and Performance, 7, (1967) pp. 48 - 52

103. BOGUE, R.H.
"Chemistry of Portland Cement"
Pub: Reinhold. New York. (1955)

104. NURSE, P.W.
"Slag cement" - Chapter 13 - "The chemistry of cement"
Vol. 2. Editor, Taylor H.F.W.
Pub: Academic Press (1964) pp. 37-67

105. VERBECK, G.J. & HELMUTH, R.H.
"Principal paper - structures and physical properties of cement paste"
5th International Symposium of the Chemistry of Cement,
Vol III, Part III, proc., (Tokyo 1968) pp. 7-12

106. VERBECK, G.J.
"Pore structure"
American Society for Testing and Materials, Spec. Tech. Pub: 169 -A
(1966) pp. 211

107. OBERHOLSTER, R.E
"Pore structure,Permeability and Diffusivity of Hardened Cement Paste and Concrete in relation to Durability."
8th International Congress on the Chemistry of Cement. Special Reports/Principal Reports Vol. 1,22-27 Sep.1986.
Rio de Janeiro-Brasil pp. 323-335.

108. AUSKERN, A. & HORN, W.
"Capillary porosity in hardened cement paste"
Journal of Testing and Evaluation, JTEVA,
Vol. 1. Part 1. 1, (1973) pp. 74-79

109. WINSLOW, D.N. & DIAMOND, S.
"A Mercury Porosimetry Study of the Evolution of Porosity in Portland Cement"
Journal of Materials, 5, 3, (1970) pp. 564-585

110. NEVILLE, A.M.
"Properties of Concrete"
Third Edition, Pub: Pitman Press (1981) pp. 13-41

111. POWERS, T.C.
"In chemistry of cement"
Proc., 4th Int. Conf. Chemistry of Cement, Washington D.C.
(1960) pp. 577

112. POWERS,T.C and BROWNYARD
Studies of the Physical Properties of Hardened Portland Cement Paste.
J. Amer. Concr. Inst., Vol.18, (1946,1947).Nos. 2 to 8.

113. POWERS, T.C.
"In chemistry of cements"
Chapter 10. Ed. Taylor H.F.W. Pub: Academic Press New York
(1964) pp. 391

114. FELDMAN,R.F & SEREDA,P.G
"A new model for hydated portland cement and its practical implications."
Eng. Jour. (Canada),Vol. 53,(1970), pp. 53-59.

115. DIAMON, M., ABO-EL-ENEIN,S. A ,HOSAKA,G. , GOTO, S & KONDO ,R.
"Pore structure of calcium silicate hydrate in hydrated tricalcium silicate." Jour. Amer. Ceram. Soc.,Vol. 60 , (1977) ,pp 110-114.

116. BRUNAUER , S. ,SKALNY ,J. & ODLDER , I.
"Pore structure and properties of materials .
Proc. RILEM/IUPAC Int. Symp. Pore Structure and Properties of Materials,Paragues,(1973), pp. 3-26.

117. FELDMAN,R.F .
"Sorption and Length-Change Scanning isotherems of methanal and water on hydrated portland cement pastes."
Proceedings fifth International Congress on the Chemistry of Cements,Tokyo, Japan,(1968),pp. 53-66.

118. RAHMAN,A.A
"Characterisation of the porosity of hydrated cement pastes."
British Ceramic Proceedings. No 35. , The chemistry and chemically related properties of cement, (1984) , pp. 249-266.

119. McN. ALFORD, N. & RAHMAN, A.A.
"An assesment of porosity and pore sizes in hardened cement pastes"
Journal of Material Science, Vol. 16. (1981) pp. 3105-3114.

120. DIAMOND, S.
"A critical comparison of Mercury Porosimetry and capillary condensation pore size distribution of Portland cement pastes"
Cement and Concrete Research. Vol. 1. (1971) pp. 531-545.

121. VERBECK, G.J. & HELMUTH, R.H.
"Principal paper - structures and physical properties of cement paste"
5th International Symposium of the Chemistry of Cement
Vol. 3, Part 3, proc., (Tokyo 1968) pp 1-6.

122. DULLIEN, F.A.L.
"Porous media fluid transport and pore structure"
Pub: Academic Press (1979).

123. DIAMOND, S.
"Written Discussion - Mercury porosimetry of cement pastes"
5th Intternational Symposium on the Chemistry of Cement
Proc., (Tokyo 1968) pp. 32-41.

124. CLYDE ORR, J.R.
"Application of mercury penetration to materials analysis"
Powder Technology, Vol. 3. (1969) pp 117-123.

125. WINSLOW, D.N.
"Advance in experimental techniques for mercury intrusion porosimetry"
Surface and Colloid Science, Vol. 13. (1984) pp. 259-282

126. KANEAJI, M., WINSLOW, D.N.
"Cement and Concrete Research - Vol. 10"
(1980) pp. 433 - 441

127. YOUNG, J.F.
"Capillary porosity in hydrated tricalcium silicate paste"
Powder Technology, Vol. 9. (1974) pp. 173 -179

128. MAYER, R.P. & STONE, R.A.
"Mercury porosimetry - Breakthrough pressure for penetration between packed spheres"
Journal of Colloid Science, Vol. 20. (1965) pp. 893 - 911

129. ABDELALIM, A.M.K.
"Strength, Mineralogy and Pore Structure of set high alumina cement pastes"
PhD. Thesis, Aston University. (1980).

130. WASHBURN, E.W.
"Porosity I. Purpose of Investigation. II. Porosity"
Journal of the American Ceramic Society, Vol. 4. (1921) pp. 916 - 922

131. GOOD, R.J.
"The contact angle of mercury on the internal surfaces of porous bodies"
A footnote to D.N. Winslow's review of porosimetry.
Surface and Colloid Science, Vol. 13. (1984) pp. 283 - 287

132. WALSH, D., OTOONI, M.A., TAYLOR.JUN. M.E. & MARCINKOWSKI, M.J.
"Study of portland cement fracture surfaces by scanning electron microscopy techniques"
Journal of Material Science, Vol. 9. (1974) pp. 423 - 429

133. SKALNY, J. & MAYCOCK, J.N.
"Scanning electron microscopy of industrial cement clinkers"
Journal of the American Ceramic Society,Vol. 57. (1974) pp. 253-256.

134. DIAMOND, S.
"Identification of hydrated cement constituents using a scanning electron microscope. Energy dispersive X-ray spectrometer combination"
Cement and Concrete Research, Vol. 2 (1972) pp. 617 - 632

135. BRAGG, L.
"The crystalline state". Volume 1. "A general survey"
Pub: Bell (1949)

136. TAYLOR, H.F.W. (EDITOR)
"The chemistry of cements". Volume 2. Appendix 1.
Pub: Academic Press, (1964) pp. 347 - 404

137. RAMACHANDRAN, V.S.
"Application of thermal analysis in cement chemistry"
Pub: Chemical Publishing Company (1969)

138. AMINABHAVI, T.M.
"Use of polymers in concrete technology"
JMS - REV. Macromol. Chem. Phys., C22 (1), (1982-83) pp. 1 - 55

139. NARAYAN, R.
"Review - Polymer reinforcement of cement systems"
Journal of Materials Science, Vol. 14. (1979) pp. 1525 - 1553

140. ARAKI, K., MAKI, Y., SHINJI, Y., ISHIZAKI, K., MINEGISHI, K. & SUDOH, G.
"Evaluation of PIC-Container for Containment and Disposal of Low and Intermediate Level Radioactive wastes"
3rd International Congress on Polymer in Concrete, Proc., 5, (1981) pp. 987

141. NOSAREV, A.V., ZHIROV, A.S., SHVIDKO, Y.S. & KRASOVSKAYA, T.A.
"Transport Construction Corrosion-Resisting Structure with Polymer Use"
3rd International Congress on Polymer in Concrete, Proc., 5, (1981) pp. 815 - 825

142. FELDMAN, R.F. & BEAUDOIN, J.J.
"Studies of composites by impregnation of porous bodies. 2. Polymethyl Methacrylate in Portland Cement Systems"
Cement and Concrete Research, Vol. 8. (1987) pp. 425 - 432

143. SØRENSEN, E.V. & RADJY, F.
"Monomer Impregnation of hardened cement paste (HCP)"
Cement and Concrete Research, Vol. 2. (1972) pp. 481 - 485

144. FLAJSMAN, F., CAHN, D.S. & PHILLIPS, J.C.
"Polymer-impregnated Fibre-Reinforced Mortars"
Journal of the American Ceramic Society, Vol. 54, No. 3.
3, (1971) pp. 129 - 130

145. MANNING, D.G. & HOPE, B.B.
"The effect of porosity on the compressive strength and elastic modulus of polymer impregnated concrete"
Cement and Concrete Research, Vol. 1. (1971) pp. 631 - 644

146. ZUK, A., WEJCHAN-JUDEK, M. & BALEWSKI, L.
"Devices to improve the technique of preparing PIC"
Cement and Concrete Research. Vol. 14. (1984) pp. 559 - 564

147. VOGEL, A.I.
"A text - book of quantitative inorganic analysis"
Third edition. Pub: Longmans, (1961) pp. 808 - 809

148. ibid. pp. 742

149. STERN, M. & GEARY, A.L.
"A theoretical analysis of the shape of polarisation curves"
Journal of the Electrochemical Society, Vol. 104. (1957) pp. 56 - 63

150. PARKER, K.M.,& ROY.D.M.,
"Porosity , Permeability and amicrostructure of Portland-Blast Furnace-Slag Cement Pastes."
Amer. Ceramic Society Bullitin,Vol. 61, (1982), pp 345.

151. ROY, D.M & IDORN, G.M.
"Hydration,Structure,and Properties of Blast Furnace Slag Cements,Mortars,and Concrete". Jour. of the Amer. Concrete Institute, Proc., Vol. 79,43 , (1982) , pp. 444-457.

152. HALSE ,Y.,JENSEN,H-U.,& PRATT,P.L.
"The effect of the curing temperature on the pozzolanic reaction in fly ash blended cement". 8th international congress on the chemistry of cement.,Vol. IV. 22-27 September (1986),Rio de Janeiro-Brasil, pp 176-182.

153. MARSH, B.K., DAY, R.L. & BONNER, D.G.
"Strength gain and calcium hydroxide depletion in hardened cement pastes containing fly ash"
Magazine of Concrete Research: Vol. 38, 3, (1986).

154. FELDMAN,R.F.,
" Significance of porosity measurements on blended cement performance",proceedinges of the canmet/ACI .First International Conference on the use of fly ash, Silica Fume, Slag and other mineral by -products in concrete SP-79 Montebello, Quebec , Canada (July 31-Agust 5),1983.

155. ROBERT,L.,DAY& MARSH,B.K.,
"Measurement of porosity in blended cement pastes". cement and concrete research. Vol.18(1988).Printed in USA ,pp 63-73.

156. BIRCHALL, J.D., HOWARD, A.J. & BAILEY, J.E.
"On the hydration of portland cements"
Proc., R. Soc. London. A, Vol. 360, (1978) pp. 445 - 453

157. REGOURD, M.
"Structure and behaviour of slag portland cement hydrates"
7th International Congress on the Chemistry of Cement, Proc., (Paris 1980)
Vol. 1. Part 3 -2, pp. 10 - 20

158. MIKHAIL, R. Sh.
"Hardened portland blast-furnace slag cement pastes: 1 Effects of Additives on surface area and on pore structure"
Cement and Concrete Research. Vol. 4. (1974) pp. 807 - 820

159. ROY, D.M. & IDORN, G.M.
"Hydration, Structure and Properties of blast furnace slag cements, mortars and concrete"
A.C.I. Journal, 11-12, (1982) pp. 444 - 457

160. RAMACHANDRAN, V.S.
"Applications of Differential Thermal Analysis in Cement Chemistry"
Pub: Chemical Publishing Company, (1969) pp. 198 - 200

161. RAMACHANDRAN, V.S. & SEREDA, P.J.
"Differential Thermal Studies of Polymethyl Methacrylate - impregnated cement pastes"
Thermochimca Acta, 5, (1973) pp. 443 - 450

162. GEBAUER, J. & COUGGLIN, W.
"Preparation, Properties and Corrosion resistance of composites of cement mortar and organic polymers"
Cement and Concrete Research, Vol. 1. (1971) pp. 187 - 210.

163. PARROTT,L.J.,KILLOH,D.C.,& Patel,R.G.
" Cement hydration under partially saturated curing conditions",8th international congress on the chemistry of cement.Vol. iii.22-27,(September 1986),Rio de janeiro-Brasil,pp. 46-50.

164. PARROTT,L.J.,KILLOH,D.C.
"Prediction of cement hydration",Proc. British Ceramic Society.(September 1984),N.35,pp.41-53.

165. NEVILLE,A.M.
Properties of concrete ",Third edition,Pub: Pitman Press (1981),pp. 308-309.

166. Results obtained through personal communication with Dr N.R. SHORT, Dept. Civil Engineering and Construction, The University of Aston in Birmingham.

167. HAUSMANN, D.A.
"Steel Corrosion in Concrete"
Materials Protection, 11, (1967) pp. 19 - 23

168. PAGE, C.L.
"Mechanism of corrosion protection in reinforced concrete marine structures"
Nature Vol. 258, 12, (1979) pp.514 - 515

169. ANDRADE, C. & PAGE, C.L.
"Pore solution chemistry and corrosion in hydrated cement systems containing chloride salts : a study of cation specific effects"
British Corrosion Journal, Vol. 21. No. 1. (1986) pp. 49 - 53

170. CHATFIELD, C.
"Statistics for technology"
Second Edition. pub: Chapman and Hall, 1978, pp. 166 - 199.